ISSN 2518-1726 (Online),
ISSN 1991-346X (Print)

ҚАЗАҚСТАН РЕСПУБЛИКАСЫ
ҰЛТТЫҚ ҒЫЛЫМ АКАДЕМИЯСЫНЫҢ
Әль-фараби атындағы Қазақ ұлттық университетінің

Х А Б А Р Л А Р Ы

ИЗВЕСТИЯ

НАЦИОНАЛЬНОЙ АКАДЕМИИ НАУК
РЕСПУБЛИКИ КАЗАХСТАН
Казахский национальный университет
имени Аль-фараби

N E W S

OF THE NATIONAL ACADEMY OFSCIENCES
OF THE REPUBLIC OF KAZAKHSTAN
Al-farabi kazakh
national university

SERIES
PHYSICO-MATHEMATICAL

5 (327)

SEPTEMBER-OCTOBER 2019

PUBLISHED SINCE JANUARY 1963

PUBLISHED 6 TIMES A YEAR

ALMATY, NAS RK

«ҚР ҰҒА Хабарлары. Физика-математикалық сериясы».

ISSN 2518-1726 (Online), ISSN 1991-346X (Print)

Меншіктенуші: «Қазақстан Республикасының Ұлттық ғылым академиясы» РҚБ (Алматы қ.)
Қазақстан республикасының Мәдениет пен ақпарат министрлігінің Ақпарат және мұрағат комитетінде 01.06.2006 ж. берілген **№5543-Ж** мерзімдік басылым тіркеуіне қойылу туралы куәлік

Мерзімділігі: жылына 6 рет.
Тиражы: 300 дана.

Редакцияның мекенжайы: 050010, Алматы қ., Шевченко көш., 28, 219 бөл., 220, тел.: 272-13-19, 272-13-18, http://physics-mathematics.kz/index.php/en/archive

---

Типографияның мекенжайы: «Аруна» ЖК, Алматы қ., Муратбаева көш., 75.

«Известия НАН РК. Серия физико-математическая».

ISSN 2518-1726 (Online), ISSN 1991-346X (Print)

Собственник: РОО «Национальная академия наук Республики Казахстан» (г. Алматы)
Свидетельство о постановке на учет периодического печатного издания в Комитете информации и архивов Министерства культуры и информации Республики Казахстан **№5543-Ж**, выданное 01.06.2006 г.

Периодичность: 6 раз в год.
Тираж: 300 экземпляров.

Адрес редакции: 050010, г. Алматы, ул. Шевченко, 28, ком. 219, 220, тел.: 272-13-19, 272-13-18,
http://physics-mathematics.kz/index.php/en/archive

Адрес типографии: ИП «Аруна», г. Алматы, ул. Муратбаева, 75.

News of the National Academy of Sciences of the Republic of Kazakhstan. Physical-mathematical series.

ISSN 2518-1726 (Online), ISSN 1991-346X (Print)

Owner: RPA "National Academy of Sciences of the Republic of Kazakhstan" (Almaty)
The certificate of registration of a periodic printed publication in the Committee of information and archives of the Ministry of culture and information of the Republic of Kazakhstan N 5543-Ж, issued 01.06.2006

Periodicity: 6 times a year
Circulation: 300 copies

Editorial address: 28, Shevchenko str., of. 219, 220, Almaty, 050010, tel. 272-13-19, 272-13-18,
http://physics-mathematics.kz/index.php/en/archive

Address of printing house: ST "Aruna", 75, Muratbayev str, Almaty

N E W S
OF THE NATIONAL ACADEMY OF SCIENCES OF THE REPUBLIC OF KAZAKHSTAN
PHYSICO-MATHEMATICAL SERIES
ISSN 1991-346X **https://doi.org/10.32014/2019.2518-1726.54**
Volume 5, Number 327 (2019), 5 – 10

UDC 524.8

L.M. Chechin[1,2], E.B. Kurmanov[2], T.K. Konysbayev[1]

[1]V.G. Fesenkov Astrophysical Institute “NCSRT” NSA RK, 050020, Observatory 23,
Kamenskoe plato, Almaty, Kazakhstan;
[2]Al-Farabi Kazakh National University, Physics and Technology Department, Almaty, Kazakhstan
chechin-lm@mail.ru, ergaly_90@mail.ru, talgar_777@mail.ru

LIGHT RAYS IN THE EPOCH OF DARK MATTER DOMINATION

Abstract. The cosmological Friedmann model has been generalized for the epoch of dark matter domination. In doing this its equation of state was chosen in the new - non-stationary form. The process of light propagation in such metric was explored and its refractive index was found.

Key words: Friedmann cosmology, dark matter, non-stationary equation of state, Mendeleev – Clapeyron equation, gravitational lenses.

Introduction

One of the actual problems of modern cosmology, as well as particle physics, is understanding the physical properties of dark matter. For this, in particular, the astronomical observations can be used. They demonstrate that dark matter is concentrated mainly around epy large-scale space objects such as galaxies and their clusters, and form the corresponding halos [1,2].

Dark matter is also described in global aspect, since in the substantial structure of the Universe it holds the second place (after dark energy) and amounts to 26.8% [3, 4]. Moreover, it dominates during the period up to six and a half - seven billion years. At a later time, the main role in the Universe evolution takes the cosmic vacuum. The dynamics of light in the era of cosmic vacuum is quite well studied [4]. Therefore, an essentially important problem of modern cosmology is study the process of light propagation at the epoch of dark matter domination.

Talking about the physical properties of dark matter, we will declare about two important aspects of it – the carriers of dark matter and the corresponding equations of state of a medium.

The aim of present article is studying the process of light propagation in the era of domination of dark matter, described by the non-stationary equation of state.

1 Non-stationary equation of state of dark matter

According [5], they are similar to neutrinos and antineutrinos, but should be more massive. Such hypothetical heavy particles (with a mass of order $1.0\,TeV$ and more) are called WIMPs. Their peculiarity is the absence of the effect of annihilation, so that they can appear after freezing at an early time. Therefore, all our calculations can be applied to the gas of WIMPs [6,7].

We emphasize that the equation of state of dark matter was even measured in [7] and found that it corresponds to a medium with vanishingly low pressure, for example, nonrelativistic or relativistic gases.

So, we consider a medium of WIMPs as a relativistic ideal gas described by the Mendeleyev-Clapeyron equation of state. By virtue of thermodynamic equilibrium of such particles with cosmic plasma particles, the approximate condition $T_{DM} \approx T_{BM}$ holds. Therefore, the Mendeleev – Clapeyron equation takes the form

$$P_{DM} = \rho_{DM} \frac{R}{\mu} T_{BM}, \tag{1}$$

with explicit dependency of gas density ρ_{DM}.

For the standard Friedmann cosmological model filled by relativistic gas, the approximate relation linking the temperature of such gas with the age of the Universe holds. It, as shown in [8], is as follows

$$T_{BM} \sim t^{-1/2}. \tag{2}$$

where t - current time. Therefore, it follows from (1) and (2) that the equation of state of an ideal gas takes on the form $P_{DM} = \bar{\omega}_{DM}(t)\rho_{DM} = \rho_{DM} \frac{R}{\mu} T_{BM}(t)$. So, taking into account (2), its state parameter depends on time in the similar way, i.e.

$$\bar{\omega}_{DM}(t) = \frac{R}{\mu} T_{BM}(t) \sim t^{-1/2}. \tag{3}$$

Let us consider the case in which the Universe is filled with real gas, consisting of N molecules and described by the van der Waals equation of state. If the temperature is measured in degrees, then, according to [9], the equation takes the form

$$P_{DM}\left(1 + \nu^2 \frac{\tilde{a}}{P_{DM} V^2}\right)\left(1 - \nu \frac{\tilde{b}}{V}\right) = \rho_{DM} \frac{R}{\mu} T_{BM}, \tag{4}$$

in which $\tilde{a}$ and $\tilde{b}$ are constant quantities describing the properties of WIMP's gas, k is the Boltzmann constant. Recall that the physical meaning of parameter $\tilde{a}$ is in describing the interaction of matter's molecules, parameter $\tilde{b}$ is responsible for accounting their sizes. In addition, here μ is the molar mass of a particular matter, and R is the universal gas constant.

Now our task is to combine (4) with (3) and finding the explicit dependency on time the state parameter of the real gas.

For discussion, we assume that $N\tilde{b}/V << 1$. Such condition describes the real property of WIMP's gas, whose volume is significantly larger than the size of all molecules themselves. In addition, assume that the interaction of molecules is not too large. This corresponds to the situation when the requirement $N^2\tilde{a}/V^2 P_{DM} << 1$ takes the place.

Having in mind these considerations and taking into account the equation of state of an ideal gas (1), we have

$$P_{DM} = \rho_{DM} \frac{R}{\mu}\left(1 - \nu^2 P_{DM}\tilde{a} \Big/ \frac{m^2}{\mu^2} R^2 T_{BM}{}^2\right) T_{BM}. \tag{5}$$

In an ultra-relativistic hot gas – baryonic matter, the pressure is proportional to its temperature in fourth power [10], i.e.

$$P_{DM}(T) = \frac{\pi^2}{90} n(T_{DM}) T_{DM}{}^4 \approx \frac{\pi^2}{90} n(T_{BM}) T_{BM}{}^4, \tag{6}$$

where $n(T_{BM})$ is the effective number of types of particles (bosons and fermions) in different quantum states. Moreover, in realistic theories of elementary particles, as is known, it has an upper limit - $n(T_{BM}) = n_0 \leq 10^4$. So the relation (6) can be rewritten in the form of a power-law function with a constant coefficient $\zeta = \left(\pi^2/90\right) n_0$. Thus,

$$P_{DM}(T) = \zeta T_{BM}{}^4. \tag{7}$$

Applying (7) to (5), we find the state parameter as a function of temperature

$$\omega_{DM}\left(T_{BM}\right)=\bar{\omega}_{DM}\left(T_{BM}\right)+\omega'_{DM}\left(T_{BM}\right)=\frac{R}{\mu}\left(1-v^2\tilde{a}\zeta\,\frac{\mu^2}{m^2R^2}T_{BM}{}^2\right)T_{BM}\ , \tag{8}$$

or as a function of time with two different terms

$$\omega_{DM}\left(t\right)=\begin{matrix}\bar{\omega}_{DM}\left(t\right)\sim t^{-1/2}>0\\ \omega'_{DM}\left(t\right)\sim t^{-3/2}>0\end{matrix}\ . \tag{9}$$

2 The solution of Friedmann equations for the end of domination of dark matter

Recall that the Friedmann equations connect the expansion parameter of the Universe (namely, Hubble parameter $H=\dot{a}/a$) with a density of matter contained in it (evolution equation)

$$\frac{1}{2}\left(\frac{da}{dt}\right)^2-\frac{4\pi G}{3}\rho\left(t\right)a^2=0, \tag{10}$$

and their time with a similar expression,

$$\dot{\rho}+3\frac{\dot{a}}{a}\left(\rho+P\right)=\dot{\rho}+3\frac{\dot{a}}{a}\rho\left(1+\omega\left(t\right)\right)=0, \tag{11}$$

represented the law of energy conservation.

However, the question arises here: is it possible to use a non-static medium in Friedmann's static equations? For example the medium with non-stationary equation of state.

According to Tolman [11] with reference to Lemetre's research, the non-static spherical interval differs from the static case by the presence of mixed terms in the energy-momentum tensor of the gravitating medium. In the general case, they correspond to the appearance of transverse waves related with radial mass flows. How this conclusion relates with properties of the gas of WIMPs considering by us?

We emphasize once again that they represent massive particles, a priori moving with velocity much lower than the velocity of light, i.e. $v_{WIMP}<<c$. This factor gives possibility to neglect the flows of matter in the gas of WIMPs and, therefore, to confidently use the proposed energy-momentum tensor to study the cold (ideal) dark matter.

So, we pass directly to the solution of the Friedmann equations. In our case, based on expressions (9), we will operate with the non-stationary equation of state in the form $P/\rho\sim\left(t/t_{DM}\right)^n$ where t_{DM} - the time of the end of domination of dark matter. Substituting it into (11), and putting $t>t_{DM}$, $\xi>1$ anyone can find a solution in the following representation

$$\ln\rho/\rho_0=-3H_0t_{DM}\left(1-\frac{1}{\xi^2}\right)\xi\approx-3H_0t_{DM}\cdot\xi\,,$$
$$\rho\left(t\right)/\rho_0\approx\exp\left(-3t/t_{DM}\right)\ . \tag{12}$$

So, it follows that the density of dark matter even with the non-stationary equation of state decreases with time during the evolution of the Universe.Then the evolutionary Friedmann equation takes on the form

$$\frac{\dot{a}}{a}=\sqrt{\frac{8\pi G}{3}}\sqrt{\rho\left(t\right)} \tag{13}$$

with the standard expression of the Hubble parameter. But in contrast to the main vacuum model of the Universe$\left(p=-\rho\right)$, the density of a substance consideration depends on time.

Introducing (12) into (13), we obtain

$$\frac{\dot{a}}{a} = \chi \exp\left(-\frac{3}{2}t/t_{DM}\right), \tag{14}$$

where $\chi = \sqrt{\frac{8\pi G}{3}}$. Thus, an additive to the Hubble parameter is expressed as follows

$$\Delta H \propto \exp\left(-\frac{3}{2}t/t_{DM}\right). \tag{15}$$

An analysis of this expression shows that find additive (15), in contrast to the purely vacuum model of the Universe, decreases with time. But despite the one-sidedness of model constructed by us, the full expression of Hubble constant, under considering the overall substances, especially the cosmic vacuum, will increase. Moreover, as shown above

$$a(t)/a_0 = \exp\left(\chi t_{DM}\left(-\frac{2}{3}\exp\left(-\frac{3}{2}t/t_{DM}\right)\right)\right), \tag{16}$$

where a_0 - some constant quantity.

One of such models, a homogeneous and isotropic flat Universe filled with non-relativistic matter and a scalar field with potential, can provide not only accelerated, but also slowed down the expansion of the Universe.

3 On the theory of gravitational lenses in the Universe with a domination of dark matter

Gravitational lenses are massive galaxies or clusters of galaxies that act as a collecting object when light is refracted in their gravitational field.

Although today more than 400 such lenses are known, it is believed that at photographing review of the sky (for example, in the Sloan Digital review [12]) they were captured significantly more, but many of them have not yet been identified.

One of the very distant galaxies in the Universe is MACS0647-JD, located 13.3 billion light-years from us. We see its how it was about 420 million years after the Big Bang. A very important factor in its discovery is that it has changed significantly under the influence of the intermediate galaxy MACSJ0647 +7015 (gravitational lens) at a distance of about five billion light-years.

Another example is the discovery of the supernova PS1-10afx. It originated in the galaxy about nine billion light-years ago, which also makes it one of the farthest type Ia supernovae.

Recently [13] galaxy (J1000 0221) with a pronounced effect of gravitational lensing was discovered. This galaxy is extremely distant and giving four images. One more distant IRC 0218 lens was discovered by researchers from the Keck Observatory, but it has a double images.

The amount of images in the gravitational lens is theoretically can calculate, using algebraic aberration equations. Its justification is given in the monograph [14], and application to some gravitational lenses was proposed in [15,16]. The amount of images is determined by the order of such an equation. Besides, in [17] gives an overview of some theoretical researches of gravitational lensing, including the results of local research.

In general, dark matter can produce a refractive index which differs from vacuum. Its presence, as noted in [18], is described by frequency-dependent effects at the propagation and attenuation of light. Other characteristics of light propagation in the Universe have been considered in [19].

So, we write the standard expression for the Friedman metric –

$$ds^2 = c^2dt^2 - a^2(t)\left[dr^2 + r^2\left(d\theta^2 + \sin^2\theta d\varphi^2\right)\right], \tag{17}$$

from which it is easy to obtain the law of light propagation and its corresponding velocity in the medium. For simplicity, we'll consider the movement of light along the radial component, so that $\theta = const, \varphi = const$. Therefore, the velocity of light propagation in our case is $\upsilon = dr/dt = c/a(t)$.

The corresponding variable refractive index referred to it, as follows from (16) in the approximation t/t_{DM} , will be described by a quasi-constant quantity

$$n\left(t_{DM}\right)=\sqrt{\frac{8\pi G}{3}}\left(1-\frac{2}{3}\right)t_{DM}\,. \tag{18}$$

Further, it is important to pay attention to the following possible cosmological effect. For time $\Delta t \approx \frac{1}{3}t_{DM}\left[1-\left(\frac{\rho_v}{\rho_0}\right)^{1/2}\right]$, $\rho_v<\rho_0$, $t_{DM}<t_{Un}$ the vacuum expansion the vacuum expansion of the Universe will be equal to its deceleration under the influence of non-stationary dark matter. So the light will move almost in empty space. Therefore, in the specified period of time astronomer must detect the radiation splash from galaxies. But such the splash, as it easy to see, will be determined as time t_{DM} and density ρ_0 by these poorly defined quantities.

Conclusion

We constructed a model of the Friedmann Universe with a non-stationary equation of state. It is shown that the density of dark matter decreases with time, and the addition to the Hubble constant increases with time. But this result does not violate the general conclusion about the evolution of the Universe (its expansion) with all the set of matter included in it. The refractive index of our model was calculated, which turned out to be a constant value. The refractive index of our model was calculated, which turned out to be a constant value (more precisely, depending on the era of the end of domination of dark matter) and a possible burst effect of incoming radiation was predicted.

Acknowledgments

The authors (T.K. and L.Ch.) express their sincere gratitude to "NCSRT" NSA RK for supporting this work in the framework of financing the scientific project AP 05134454 "Evolution of perturbations in the density of dark matter in the very early Universe" under the budget program 217 "Development of science", subprogram 102 "Grant financing of scientific research", priority - information, telecommunications and space technologies, scientific research in the field of natural sciences ", The Republic of Kazakhstan.

Author (E.K.) expresses sincere gratitude to his supervisor Corresponding Member of the National Academy of Sciences of the Republic of Kazakhstan, Doctor of Physical and Mathematical Sciences, Professor L.M. Chechin for his assistance in writing articles.

УДК 524.8

Л.М.Чечин[1,2], Е.Б. Курманов[2], Т.К. Конысбаев[1]

[1]В.Г. Фесенков атындағы Астрофизикалық институт "ҰҒЗТО" ҚР ҚАӨМ АҒК, 050020 Обсерватория 23, Алматы, Қазақстан

[2]Физика-техникалық факультет, Әл-Фараби атындағы. Қазақ Ұлттық Университеті, Алматы, Қазақстан; Обсерватория 23, Алматы, Қазақстан

ҚАРАҢҒЫ МАТЕРИЯНЫҢ ҮСТЕМ БОЛУ ДӘУІРІНДЕГІ ЖАРЫҚ СӘУЛЕЛЕРІ

Аннотация. Қараңғы материяның үстемдік ету дәуіріне жалпыланған Фридманның космологиялық моделі қарастырылды. Оның үстіне оның күй теңдеуі жаңа - стационарлық емес формада таңдалды. Осындай метрикада жарықтың таралу процесі зерттелді және оның сыну көрсеткіші табылды.

Түйін сөздер: Фридман космологиясы, қараңғы материя, стационар емес күй теңдеуі, Менделеев – Клапейрон теңдеуі, гравитациялық линзалар.

УДК 524.8

Л.М. Чечин[1,2], Е.Б. Курманов[2], Т.К. Конысбаев[1]

[1]Астрофизический институт В.Г. Фесенкова НЦКИТ (МЦРИАП) РК, 050020,
Обсерватория 23, Каменское плато, Алматы, Казахстан;
[2]Казахский национальный университет имени аль-Фараби,
Физико-технический факультет, Алматы, Казахстан

ЛУЧИ СВЕТА В ЭПОХУ ДОМИНИРОВАНИЯ ТЕМНОЙ МАТЕРИИ

Аннотация. Рассмотрена космологическая модель Фридмана, обобщенная на эпоху доминирования темной материи. При этом ее уравнение состояния выбрано в новой - нестационарной форме. Исследован процесс распространения света в такой метрике, найден ее показатель преломления.

Ключевые слова: космология Фридмана, темная материя, нестационарное уравнение состояния, уравнение Менделеева – Клапейрона, гравитационные линзы.

Information about authors:

Chechin L.M. - Doctor of physical-mathematical science, professor, corresponding member of NAS RK, Chief Researcher, Fesenkov Astrophysical Institute “NCSRT” NSA RK, al-Farabi Kazakh National University. The author formulated the problem statement, checked the calculations. E-mail.ru: chechin-lm@mail.ru;

Kurmanov E.B. – PhD student at Faculty of Physics and Technology, Al-Farabi Kazakh National University. The author carried out calculations for solving the Friedmann equations with a variable equation of state of dark matter. E-mail.ru: ergaly_90@mail.ru;

Konysbayev T.K. – junior researcher, Fesenkov Astrophysical Institute “NCSRT” NSA RK, Master of Science (Astronomy), Author conducted a review of gravitational lenses. E-mail.ru: talgar_777@mail.ru

REFERENCES

[1] Bertone G., Hooper D. Silk J. Particle dark matter: evidence, candidates and constraints, Phys. Rep. 405, DOI: 10.1016/j.physrep.2004.08.031

[2] Iocco F., Pato M., Bertone G. (2011) Dark Matter distribution in the Milky Way: microlensing and dynamical constraints, JCAP11 029, DOI: 10.1088/1475-7516/2011/11/029

[3] Byrd G.G., A.D.Chernin, M.J.Valtonen. (2007) Cosmology. Foundations, and frontiers. M. URSS

[4] P. A. R. Ade et al. Planck Collaboration. (2013) Planck 2013 results. I. Overview of products and scientific results, Astronomy and Astrophysics J., V.1303, DOI: 10.1051/0004-6361/201321529

[5] Green A.M., Hofmann S., Schwarz D.J., MNRAS, 353, L23–L27 (2004). DOI: 10.1111/j.1365-2966.2004.08232.x

[6] Chechin L.M., Kairatkyzy D., Konysbayev T.K. (2018) Toward a theory of the evolution of perturbations of the dark matter density in the very early universe, R. Phys. J., Vol. 61, No. 5, DOI 10.1007/s11182-018-1472-9

[7] Amangeldyieva A., Kairatkyzy D., Konysbayev T.K. (2018) On the nonstationary parameter of the state for dark matter, V. 6, No. 322, 44-48 https://doi.org/10.32014/2018.2518-1726.16

[8] Dolgov A.D., Sazhin M.V., Zeldovich Ya.B. (1990) Basics of Modern Cosmology, Editions Frontiers, ISBN-10: 2863320734

[9] Landau L.D., Lifshitz E.M. (1980) Statistical Physics, Butterworth-Heinemann, London ISBN 10: 0750633727

[10] Linde A. D., (1990) Elementary Particle Physics and Inflationary Cosmology, CRC Press, Boca Raton ISBN-10: 3718604906

[11] Tolman R. (1974) Relativity, thermodynamics and cosmology, Nauka (in Russian).

[12] http://www.astronet.ru/db/msg/1202878/index.html

[13] A. van der Wel , G. van der Ven , M. Maseda , et al. (2018) Astrophysical J. Letters Discovery of a quadruple lens in candels with a record lens redshift z = 1.53 DOI: 10.1088/2041-8205/777/1/L17

[14] Blioh P.V., Minakov A.A. (1989) Gravitational lenses [Gravitacionnye linzy], Kiev, Nauka, P. 41(in Russian)

[15] Chechin L.M., Avkhunbaeva G.M., (2013) Two component gravitational lens, Rus. Phys. J., No. 56, P. 30 – 35. (in Russian)

[16] Chechin L.M., Kairatkyzy D. (2014) Differential aberration equation in gravitational optics [Differencial'noe aberracionnoe uravnenie v gravitacionnoj optike], No 3, Reports of NAS RK, (in Russian)

[17] Chechin L.M., Kurmanov E.B. (2019) On the new direction in the theory of gravitational lensing [O novom napravlenii v teorii gravitacionnogo linzirovanija], No.1(68), Rec. Cont. Phys. DOI: 10.26577/RCPh-2019-1-1115

[18] Gardner S., Latimer D.C. (2010) Dark Matter Constraints from a Cosmic Index of Refraction DOI: 10.1103/PhysRevD.82.063506

[19] Linder, E. V. (1989) Light propagation through gravitationally perturbed Friedmann universes Thesis Stanford Univ., CA.

N E W S
OF THE NATIONAL ACADEMY OF SCIENCES OF THE REPUBLIC OF KAZAKHSTAN
PHYSICO-MATHEMATICAL SERIES
ISSN 1991-346X **https://doi.org/10.32014/2019.2518-1726.55**
Volume 5, Number 327 (2019), 11 – 18

UDC 524.834

S.R. Myrzakul, K. Yerzhanov, D. Zh. Kenzhalin, K.R. Myrzakulov

Department of General & Theoretical Physics,
L.N. GumilyovEurasian National University, Nur-Sultan, Kazakhstan
yerzhanovkk@gmail.com, dzh.kenzhalin@gmail.com, krmyrzakulov@gmail.com

TELEPARALLEL DARK ENERGY MODEL WITH FERMIONIC FIELD FOR BIANCHI TYPE I SPACETIME

Abstract. The search for constituents that can explain the periods of accelerating expansion of the Universe is a fundamental topic in cosmology. In the present work, we consider a model with a fermionic field that is non-minimally coupled to gravity in the framework of teleparallel gravity for Bianchi type I spacetime. Here we determined form the point-like Lagrangian and obtained the corresponding field equations. In order to determine forms of the coupling and potential function of fermionic field for the considered model, we use Noether symmetry approach. In modern cosmology, we often used this approach to determine the unknown function and obtain exact cosmological solutions for considered model. For our model, we obtained of the coupling and fermionic field functions as $F = F_0 \Psi$ and $V = V_0 \psi$. Then, we put these solutions to the field equations, we got the equation depend only on the functions A, B and C. After some mathematical calculations, we found exact solutions for these functions as de Sitter solutions. Finally, we determined the equation of state parameter is equal to -1. In cosmology this solution gives us dark energy model and which can describes the late-time epoch of the evolution our universe. Thus, here the fermion fields play the role of dark energy.

Key words. Teleparallel dark energy, Bianchi Type I Model, fermionic field,Noethersymmetry approach.

Introduction

In modern cosmology, teleparallel gravity is used to describe the evolution of the universe. For the first time teleparallel theory of gravity (theory of gravity with teleparallelism) was proposed by Einstein. Due to the specific nature of parallel transfers, any calibration theory, including these transformations, will differ in many respects from conventional internal calibration models, and the most significant is the presence of a field tetrad.

On the other hand, field tetrads can be used to determine the linear connectivity of Weizenbock, which is a connectivity defined by torsion but not by the curvature of space. The tetrad field can also be naturally used to introduce a Riemann metric in terms of which the Levi-Civita connectivity can be constructed.

It is important to note that torsion and curvature are connectivity properties and different connectedness can be defined on the same space. Thus, the presence of a nontrivial tetrad field in gauge theory induces both a tele-parallel and a Riemannian structure in space-time. The first obligation of Weizenbock connectivity, the second connectivity Levi-Civita. Due to the universality of the gravitational interaction, it is possible to link these geometric structures in the theory of gravity.Previously, it was considered in [1,2].Cosmological solutions were obtained within the framework of the theory of the tele-parallel of gravity and the Friedman-Robertson-Walker(FRW) metric.The anisotropic model of the Universe for the Bianchi I metric in the framework of the theory of the teleparallel of gravity was considered in the works [3,4].

In modern cosmology, scalar and vector fields, as well as their modifications, such as k -essence, f -essence, g –essence, are used as matter fields. Here we consider fermion fields in the framework of the tele-parallel gravity theory for an anisotropic Bianchi type I. universe.Earlier, cosmological models with fermion fields in the framework of GR for the FRW metric were considered in [5-8]. Also, within the framework of the teleparallel of gravity, models for the FRWmetric were considered in [9].

The paper is organized as follows. In Section 2, we present action and equation of motion for this model. The geometrical Noether point symmetries and their connections to the $F(\Psi)$ model is discussed in section 3. Section 4 is analytical solutions for those $F(\Psi)$ models which admit Noether point symmetries.Finally, we draw our main conclusions in section 5.

Actionandequationofmotion

In this theory, the action is given in the following form

$$S=\int d^4xe\left\{F(\Psi)T+\frac{i}{2}\Big[\bar{\psi}\Gamma^{\mu}\left(\overleftarrow{\partial_{\mu}}-\Omega_{\mu}\right)\psi-\bar{\psi}\left(\overrightarrow{\partial_{\mu}}+\Omega_{\mu}\right)\Gamma^{\mu}\psi\Big]-V(\Psi)\right\}, \quad (1)$$

where $e=det(e^a_\mu)$, e^a_μ is a tetrad (vierbein) basis, T is a torsion scalar, and ψ and $\bar{\psi}=\psi^{\dagger}\gamma^0$ denote the spinor field and its adjoint, with the dagger representing complex conjugation. $F(\Psi)$ and $V(\Psi)$ are generic functions, representing the coupling with gravity and the self-interaction potential of the fermionic field, respectively. In our study, for simplicity, weassume that $F(\Psi)$ and $V(\Psi)$ depend only on functions of the bilinear $\Psi=\bar{\psi}\psi$. In the above action, furthermore, Ω_μ is the spin connection $\Omega_\mu=-\frac{1}{4}g_{\sigma\nu}\left[\Gamma^{\nu}_{\mu\lambda}-e^{\nu}_{b}\partial_{\mu}e^{b}_{\lambda}\right]\Gamma^{\sigma}\Gamma^{\lambda}$ with $\Gamma^{\nu}_{\mu\lambda}$ denoting the standard Levi-Civita connection and $\Gamma^{\mu}=e^{\mu}_{a}\gamma^{a}$. The Γ^{μ} are Dirac matrices.

Together with the action (1), the FRW metric is considered

$$ds^2=dt^2-a^2(t)\left(dx^2+dy^2+dz^2\right),$$

where $a(t)$ is the scale factor of the Universe. Here and then the dot above the letter denotes the derivative in time. This metric describes four-dimensional planar, homogeneous, and isotropic space-time.

In our model we will define field equations for action (1) and Bianchi metrics of type I

$$ds^2=dt^2-A^2(t)dx^2-B^2(t)dy^2-C^2(t)dz^2, \quad (2)$$

where

$$e=\sqrt{-g}=ABC, T=-2\left(\frac{\dot{A}\dot{B}}{AB}+\frac{\dot{A}\dot{C}}{AC}+\frac{\dot{C}\dot{B}}{CB}\right), Y=\frac{i}{2}\left(\bar{\psi}\gamma^0\dot{\psi}-\dot{\bar{\psi}}\gamma^0\psi\right).$$

The Lagrange function for metric (3) can be written as

$$L=2FC\dot{A}\dot{B}+2FB\dot{A}\dot{C}+2FA\dot{C}\dot{B}-\frac{i}{2}ABC\left(\bar{\psi}\gamma^0\dot{\psi}-\dot{\bar{\psi}}\gamma^0\psi\right)+ABCV, \quad (3)$$

Next, we will use the Euler-Lagrange equations and the zero energy condition to determine the field equations:

$$\frac{\dot{A}\dot{B}}{AB}+\frac{\dot{A}\dot{C}}{AC}+\frac{\dot{C}\dot{B}}{CB}=\frac{1}{2F}\rho_f, \tag{4}$$

$$\frac{\ddot{B}}{B}+\frac{\ddot{C}}{C}+\frac{\dot{B}\dot{C}}{BC}+\frac{\dot{F}}{F}\left(\frac{\dot{B}}{B}+\frac{\dot{C}}{C}\right)=-\frac{1}{2F}p_f, \tag{5}$$

$$\frac{\ddot{A}}{A}+\frac{\ddot{C}}{C}+\frac{\dot{A}\dot{C}}{AC}+\frac{\dot{F}}{F}\left(\frac{\dot{A}}{A}+\frac{\dot{C}}{C}\right)=-\frac{1}{2F}p_f, \tag{6}$$

$$\frac{\ddot{A}}{A}+\frac{\ddot{B}}{B}+\frac{\dot{A}\dot{B}}{AB}+\frac{\dot{F}}{F}\left(\frac{\dot{A}}{A}+\frac{\dot{B}}{B}\right)=-\frac{1}{2F}p_f, \tag{7}$$

$$\dot{\psi}+\frac{1}{2}\left(\frac{\dot{A}}{A}+\frac{\dot{B}}{B}+\frac{\dot{C}}{C}\right)\psi+iV'\psi\gamma^0+2i\left(\frac{\dot{A}\dot{B}}{AB}+\frac{\dot{A}\dot{C}}{AC}+\frac{\dot{C}\dot{B}}{CB}\right)F'\psi\gamma^0=0, \tag{8}$$

$$\dot{\bar{\psi}}+\frac{1}{2}\left(\frac{\dot{A}}{A}+\frac{\dot{B}}{B}+\frac{\dot{C}}{C}\right)\bar{\psi}-iV'\bar{\psi}\gamma^0-2i\left(\frac{\dot{A}\dot{B}}{AB}+\frac{\dot{A}\dot{C}}{AC}+\frac{\dot{C}\dot{B}}{CB}\right)F'\bar{\psi}\gamma^0=0, \tag{9}$$

where $\rho_f=V$ is the energy density and $p_f=\frac{i}{2}\left(\bar{\psi}\gamma^0\dot{\psi}-\dot{\bar{\psi}}\gamma^0\psi\right)-V$ is the pressure of the fluid.

Thus, we obtained the field equations for the anisotropic Universe model in the framework of the theory of body parallel to gravity, where fermionic fields were considered as matter fields. In the following we will investigate various cosmological aspects of these equations.

TheNoethersymmetryapproach

To solve the systems of field equations (4)-(9) we use the Noether symmetry. This approach means that the lie derivative of the point Lagrangian from the vector field X is zero

$$XL=0. \tag{10}$$

The field vector has the form

$$X=\alpha\frac{\partial}{\partial A}+\beta\frac{\partial}{\partial B}+\gamma\frac{\partial}{\partial C}+\eta_j\frac{\partial}{\partial\psi_j}+\chi_j\frac{\partial}{\partial\psi_j^\dagger}+\dot{\alpha}\frac{\partial}{\partial\dot{A}}+\dot{\beta}\frac{\partial}{\partial\dot{B}}+ \\ +\dot{\gamma}\frac{\partial}{\partial\dot{C}}+\dot{\eta}_j\frac{\partial}{\partial\dot{\psi}_j}+\dot{\chi}_j\frac{\partial}{\partial\dot{\psi}_j^\dagger}, \tag{11}$$

where

$$\begin{aligned}
\dot{\alpha} &= \frac{\partial\alpha}{\partial A}\dot{A}+\frac{\partial\alpha}{\partial B}\dot{B}+\frac{\partial\alpha}{\partial C}\dot{C}+\sum_{j=0}^{3}\left(\frac{\partial\alpha}{\partial\psi_j}\dot{\psi}_j+\frac{\partial\alpha}{\partial\psi_j^{\dagger}}\dot{\psi}_j^{\dagger}\right),\\
\dot{\beta} &= \frac{\partial\beta}{\partial A}\dot{A}+\frac{\partial\beta}{\partial B}\dot{B}+\frac{\partial\beta}{\partial C}\dot{C}+\sum_{j=0}^{3}\left(\frac{\partial\beta}{\partial\psi_j}\dot{\psi}_j+\frac{\partial\beta}{\partial\psi_j^{\dagger}}\dot{\psi}_j^{\dagger}\right),\\
\dot{\gamma} &= \frac{\partial\gamma}{\partial A}\dot{A}+\frac{\partial\gamma}{\partial B}\dot{B}+\frac{\partial\gamma}{\partial C}\dot{C}+\sum_{j=0}^{3}\left(\frac{\partial\gamma}{\partial\psi_j}\dot{\psi}_j+\frac{\partial\gamma}{\partial\psi_j^{\dagger}}\dot{\psi}_j^{\dagger}\right),\\
\dot{\eta}_i &= \frac{\partial\eta_i}{\partial A}\dot{A}+\frac{\partial\eta_i}{\partial B}\dot{B}+\frac{\partial\eta_i}{\partial C}\dot{C}+\sum_{j=0}^{3}\left(\frac{\partial\eta_i}{\partial\psi_j}\dot{\psi}_j+\frac{\partial\eta_i}{\partial\psi_j^{\dagger}}\dot{\psi}_j^{\dagger}\right),\\
\dot{\chi}_i &= \frac{\partial\chi_i}{\partial A}\dot{A}+\frac{\partial\chi_i}{\partial B}\dot{B}+\frac{\partial\chi_i}{\partial C}\dot{C}+\sum_{j=0}^{3}\left(\frac{\partial\chi_i}{\partial\psi_j}\dot{\psi}_j+\frac{\partial\chi_i}{\partial\psi_j^{\dagger}}\dot{\psi}_j^{\dagger}\right).
\end{aligned} \tag{12}$$

By collecting all the terms of equation (12) with coefficients $\dot{A}^2,\dot{B}^2,\dot{C}^2,\dot{A}\dot{B},\dot{A}\dot{C},\dot{B}\dot{C},\dot{A}\dot{\psi},\dot{B}\dot{\psi},\dot{C}\dot{\psi},\dot{A}\dot{\psi}^{\dagger},\dot{B}\dot{\psi}^{\dagger},\dot{C}\dot{\psi}^{\dagger},\dot{A},\dot{B},\dot{C}$ and equating them to zero, we obtain the following system of differential equations:

$$C\frac{\partial\beta}{\partial A}+B\frac{\partial\gamma}{\partial A}=0, \tag{13}$$

$$C\frac{\partial\alpha}{\partial B}+A\frac{\partial\gamma}{\partial B}=0, \tag{14}$$

$$B\frac{\partial\alpha}{\partial C}+A\frac{\partial\beta}{\partial C}=0, \tag{15}$$

$$\gamma+C\frac{\partial\alpha}{\partial A}+C\frac{\partial\beta}{\partial B}+B\frac{\partial\gamma}{\partial B}+A\frac{\partial\gamma}{\partial A}+C\frac{F'}{F}\sum_{i=0}^{3}\left(\varepsilon_i\eta_i\psi_i^{\dagger}+\varepsilon_i\chi_i\psi_i\right)=0, \tag{16}$$

$$\beta+B\frac{\partial\alpha}{\partial A}+C\frac{\partial\beta}{\partial C}+A\frac{\partial\beta}{\partial A}+B\frac{\partial\gamma}{\partial C}+B\frac{F'}{F}\sum_{i=0}^{3}\left(\varepsilon_i\eta_i\psi_i^{\dagger}+\varepsilon_i\chi_i\psi_i\right)=0, \tag{17}$$

$$\alpha+C\frac{\partial\alpha}{\partial C}+B\frac{\partial\alpha}{\partial B}+A\frac{\partial\beta}{\partial B}+A\frac{\partial\gamma}{\partial C}+A\frac{F'}{F}\sum_{i=0}^{3}\left(\varepsilon_i\eta_i\psi_i^{\dagger}+\varepsilon_i\chi_i\psi_i\right)=0, \tag{18}$$

$$C\frac{\partial\beta}{\partial\psi_j}+B\frac{\partial\gamma}{\partial\psi_j}=0,\ C\frac{\partial\alpha}{\partial\psi_j}+A\frac{\partial\gamma}{\partial\psi_j}=0,\ B\frac{\partial\alpha}{\partial\psi_j}+A\frac{\partial\beta}{\partial\psi_j}=0, \tag{19}$$

$$C\frac{\partial\beta}{\partial\psi_j^\dagger}+B\frac{\partial\gamma}{\partial\psi_j^\dagger}=0,\;\; C\frac{\partial\alpha}{\partial\psi_j^\dagger}+A\frac{\partial\gamma}{\partial\psi_j^\dagger}=0,\;\; B\frac{\partial\alpha}{\partial\psi_j^\dagger}+A\frac{\partial\beta}{\partial\psi_j^\dagger}=0, \tag{20}$$

$$\sum_{i=0}^{3}\left(\frac{\partial\eta_j}{\partial A}\psi_i^\dagger-\frac{\partial\chi_j}{\partial A}\psi_i\right)=0,\;\; \sum_{i=0}^{3}\left(\frac{\partial\eta_j}{\partial B}\psi_i^\dagger-\frac{\partial\chi_j}{\partial B}\psi_i\right)=0,$$
$$\sum_{i=0}^{3}\left(\frac{\partial\eta_j}{\partial C}\psi_i^\dagger-\frac{\partial\chi_j}{\partial C}\psi_i\right)=0, \tag{21}$$

$$\alpha BC\psi_j^\dagger+\beta AC\psi_j^\dagger+\gamma AB\psi_j^\dagger+ABC\chi_j+ABC\sum_{i=0}^{3}\left(\frac{\partial\eta_j}{\partial\psi_j}\psi_i^\dagger-\frac{\partial\chi_j}{\partial\psi_j}\psi_i\right)=0, \tag{22}$$

$$\alpha BC\psi_j+\beta AC\psi_j+\gamma AB\psi_j+ABC\eta_j-ABC\sum_{i=0}^{3}\left(\frac{\partial\eta_j}{\partial\psi_j^\dagger}\psi_i^\dagger-\frac{\partial\chi_j}{\partial\psi_j^\dagger}\psi_i\right)=0, \tag{23}$$

$$\left(\alpha BC+\beta AC+\gamma AB\right)+ABC\frac{V'}{V}\sum_{i=0}^{3}\left(\varepsilon_i\eta_i\psi_i^\dagger+\varepsilon_i\chi_i\psi_i\right)=0. \tag{24}$$

Next, we will look for the solution in the following form

$$\alpha=N(A),\beta=N(A)\cdot M(B),\gamma=N(A)\cdot L(C), \tag{25}$$

and

$$\eta_j=N(A)\cdot Q(\psi_j),\chi_j=N(A)\cdot P(\psi_j^\dagger). \tag{26}$$

From equation (22):

$$M=-\frac{B}{C}L. \tag{27}$$

Equations (23) and (24), if $L=C, M=-B$ will look like this:

$$A\frac{\partial N}{\partial A}+A^2\frac{\partial N}{\partial A}-N=0, \tag{28}$$

accordingly we get the following equation

$$N(A)=\frac{C_1A}{A+1}, \tag{29}$$

To obtain a solution, we will consider the following form Q and P:

$$Q=-\left(\frac{1}{2}A^{-1}+\varepsilon_j\eta_0\right)\psi_j,\;\; P=-\left(\frac{1}{2}A^{-1}-\varepsilon_j\eta_0\right)\psi_j^\dagger, \tag{30}$$

then

$$V = V_0 u, \tag{31}$$

$$F = F_0 u. \tag{32}$$

Substituting the last equation in the equation of motion (2), we find the value of T:

$$T = -\frac{V_0}{F_0} = const.$$

Exact cosmological solutions

Solutions will be sought in the form of de Sitter:

$$A = e^{\lambda_1 t},\ B = e^{\lambda_2 t},\ C = e^{\lambda_3 t},$$

we know that $\lambda = \lambda_1 = \lambda_2 = \lambda_3$, then from the equation of motion (5) we can determine the values $\lambda = \mp\sqrt{\frac{V_0}{6F_0}}$, then energy density and pressur given as

$$\rho = \mp\sqrt{\frac{V_0}{2F_0}},\ p = -3H^2 = -\frac{V_0}{2F_0}. \tag{33}$$

The equation of state parameter will look like this:

$$\omega = \frac{p}{\rho} = -1. \tag{34}$$

From equations (9) and (10) we obtain the following equation:

$$\dot{\Psi} + \left(\frac{\dot{A}}{A} + \frac{\dot{B}}{B} + \frac{\dot{C}}{C}\right)\Psi = 0, \tag{35}$$

and integrationgives

$$\Psi = \frac{\dot{\Psi}_0}{(ABC)^3}.$$

Conclusion

In this paper, we considered a model with a fermion field that is not minimally related to gravity within the framework of teleparallel gravity for Bianchi I type space-time. Here we defined the form of a point Lagrangian and obtained the corresponding field equations. To determine the bond forms and the potential function of the fermion field for the model under consideration, the Noether symmetry approach was used. For our model, we obtained of the coupling and fermionic field functionsas $F = F_0\Psi$ and $V = V_0\psi$ .Then, we put these solutions to the field equations, we got the equation depend only on the functions A, B and C. After some mathematical calculations, we found the exact solutions for these functions as de Sitter solutions. We also determined that the equation of the state parameter is equal -1.In cosmology, this solution gives us a model of dark energy, which can describe the late epoch of evolution of our Universe. Thus, here the fermion fields play the role of dark energy.

Ш.Р. Мырзақұл, К.К.Ержанов, Д.Ж. Кенжалин, К.Р. Мырзакулов

Жалпы және теориялық физика кафедрасы, Л.Н. Гумилев атындағы
Еуразия ұлттық университеті, Нұр-Сұлтан, Қазақстан

БЬЯНКИІКЕҢІСТІК-УАҚЫТЫНДА ФЕРМИОНДЫ ӨРІСІ БАР КҮҢГІРТ ЭНЕРГИЯНЫҢ ТЕЛЕПАРАЛЛЕЛЬ МОДЕЛІ ҮШІН НЕТЕР СИММЕТРИЯ ӘДІСІ

Аннотация. Әлемнің үдемелі ұлғаюының табиғатын түсіндіре құрамды бөліктерді іздеуі космологияның іргелі тақырыбы болып табылады.Қарастырылып отырған жұмыста Бьянки I метрикасы үшін телепараллель гравитация аясында гравитациямен минималды емес әрекеттесетін фермионды өрістің моделы зерттеледі.Бұл жұмыста біз нүктелік лагранжианның түрін анықтадық. Қарастырылыр отырған модель үшін фермионды өрістің потенциалының және байланыс функциясының түрін анықтауда Нетер симметриясы әдісін пайдаландық. Қазіргі таңда космологияда аталған әдісті – зерттеліп отырған модель үшін белгісіз функцияны анықтауға және нақты космологиялық шешімдерді алуда жиі қолданады. Өзіміздің моделіміз үшін фермионды өрістің байланыс функциясын алдық. Содан кейін алыған шешімдерді өріс теңдеулеріне қойып, A, B және C функцияларына ғана тәуелді теңдеуі аламыз. Математикалық есептеулерден соң осы функциялар үшін де-Ситтер түріндегі нақты шешімдерді таптық. Нәтижесінде күй теңдеуінің мәні – 1 екенідігін анықтадық. Космологияда бұл шешім күңгірт энергияның моделін береді және біздің Әлем эволюциясының кеш дәуірін сипаттай алады. Сонымен біздің жұмысымызда анықталғаны – фермионды өрістер күңгірт энергияның рөлін ойнайды.

Түйін сөздер.Телепараллельді күңгірт энергия, Бьянки I типті моделі, фермионды өріс, Нетер симметрия әдісі.

УДК 524.834

Ш.Р. Мырзақұл, К.К.Ержанов, Д.Ж. Кенжалин, К.Р. Мырзакулов

Кафедра общей и теоретической физики, Евразийский национальный университет
имени Л.Н. Гумилева, Нур-Султан, Казахстан

ПОДХОД НЕТЕРОВОЙ СИММЕТРИИ В ТЕЛЕПАРАЛЛЕЛЬНОЙ МОДЕЛИ ТЕМНОЙ ЭНЕРГИИ С ФЕРМИОННЫМ ПОЛЕМ ДЛЯ ПРОСТРАНСТВА-ВРЕМЕНИ ТИПА I БЬЯНКИ

Аннотация. Поиск составных частей, которые могут объяснить периоды ускоряющегося расширения Вселенной является фундаментальной темой космологии. В настоящей работе рассматривается модель с фермионным полем, не минимально связанным с гравитацией в рамках телепараллельной гравитации для пространства-времени типа Бьянки I. Здесь мы определили форму точечного лагранжиана и получили соответствующие уравнения поля. Для определения форм связи и потенциальной функции фермионного поля для рассматриваемой модели используется подход симметрии Нетер. В современной космологии часто используется этот подход для определения неизвестной функции и получения точных космологических решений для рассматриваемой модели. Для нашей модели мы получили функции связи и фермионного поля. Затем мыподставляя эти решения в уравнения поля, мы получаем уравнение, зависящее только от функций A, B и C. После некоторых математических вычислений мы нашли точные решения для этих функций как решения де Ситтера. Наконец, мы определили, что уравнение параметра состояния равно -1. В космологии это решение дает нам модель темной энергии, которая может описать позднюю эпоху эволюции нашей Вселенной. Таким образом, здесь фермионные поля играют роль темной энергии.

Ключевые слова: телепараллельная темная энергия, модель Бьянки типа I, фермионное поле, подход симметрии Нетер.

Information about authors:

Myrzakul S.R. – PhD,candidate of physical and mathematical Sciences, associate professor, Department of General & Theoretical Physics, L.N. Gumilyov Eurasian National University, Nur-Sultan, Kazakhstan, srmyrzakul@gmail.com;

Yerzhanov K.K. – PhD, candidate of physical and mathematical Sciences, associate professor, Department of General & Theoretical Physics, L.N. Gumilyov Eurasian National University, Nur-Sultan, Kazakhstan, yerzhanovkk@gmail.com, https://orcid.org/0000-0003-0732-2080;

Kenzhalin D. Zh. – second year doctoral student, Department of General & Theoretical Physics, L.N. Gumilyov Eurasian National University, Nur-Sultan, Kazakhstan, dzh.kenzhalin@gmail.com;

MyrzakulovK.R. – candidate of physical and mathematical Sciences, associate professor, Department of General & Theoretical Physics, L.N. Gumilyov Eurasian National University, Nur-Sultan, Kazakhstan, krmyrzakulov@gmail.com

REFERENCES

[1] Cai Y-F., Capozziello S., De Laurentis M., Saridakis E.N. F(T) teleparallel gravity and cosmology//Reports on Progress in Physics. Vol.79, 2016. P. 106901https://doi.org/10.1088/0034-4885/79/10/106901.

[2] Myrzakulov R. Accelerating universe from F(T) gravity // The European Physical Journal C. Vol.71, 2011. P.1752.https://doi.org/10.1140/epjc/s10052-011-1752-9.

[3] Adnan A., Mubasher J., Myrzakulov R. Noether gauge symmetry for Bianchi type I model in F(T) gravity // Physica Scripta. Vol.88, №2. 2013. P.5003. https://doi.org/10.1088/0031-8949/88/02/025003.

[4] Rodrigues M. E.,Houndjo M. J. S., Saez-Gomez D., Rahaman F. Anisotropic Universe Models in F(T) Gravity // Phys. Rev. D. Vol.86, 2012. P. 104059 https://doi.org/10.1103/PhysRevD.86.104059.

[5] De Souza Rudinei C., Kremer G.M. Noether symmetry for non-minimally coupled fermion fields // Classical and Quantum Gravity. Vol. 25, №22. 2008. P.5006 https://doi.org/10.1088/0264-9381/28/12/125006.

[6] Grams G., De Souza RudineiC.,Kremer G. M. Fermion field as inflaton, dark energy and dark matter // General Relativity and Quantum Cosmology. Vol.31, № 18. 2014. P.5008. https://doi.org/10.1088/0264-9381/31/18/185008.

[7]Myrzakul S.R., Belisarova F.B., Myrzakul T.R., MyrzakulovK.R.Noether symmetry approach in $f-$essence cosmology with scalar-fermion interaction// N e w sof the National Academy of Sciences of the Republic of Kazakhstan.Physico-mathematical series. Vol. 5, № 315. 2017. P. 163 – 171 ISSN 1991-346X.

[8]Myrzakul S.R., Belisarova F.B., Myrzakul T.R., MyrzakulovK.R.Dynamics of $f-$essence in frame of the Starobinsky model // N e w sof the National Academy of Sciences of the Republic of Kazakhstan. Physico-mathematical series. Vol. 5, № 315. 2017. P. 143 – 148. ISSN 1991-346X.

[9] Kucukakca Y. Teleparallel dark energy model with a fermionic field via Noether symmetry // The European Physical Journal C. Vol.74, №10. 2014. P.3086. https://doi.org/ 10.1140/epjc/s10052-014-3086-x.

N E W S
OF THE NATIONAL ACADEMY OF SCIENCES OF THE REPUBLIC OF KAZAKHSTAN
PHYSICO-MATHEMATICAL SERIES
ISSN 1991-346X **https://doi.org/10.32014/2019.2518-1726.56**
Volume 5, Number 327 (2019), 19 – 39

UDK 517.929

A.Sh. Shaldanbayev[1], S.M. Shalenova[2], M.B. Ivanova[3], A.A. Shaldanbayeva[4]

[1]Silkway International University, Shymkent, Kazakhstan;
[2]Yessenov University; Aktau, Kazakhstan;
[3]South Kazakhstan medical Academy, Shymkent, Kazakhstan;
[4]Regional social-innovative University, Shymkent, Kazakhstan
shaldanbaev51@mail.ru, salima_shalenova@mail.ru, marina-iv@mail.ru, altima_a@mail.ru

ON SPECTRAL PROPERTIES OF A BOUNDARY VALUE PROBLEM OF THE FIRST ORDER EQUATION WITH DEVIATING ARGUMENT

Abstract. In this paper, we study spectral properties of a boundary value problem of a first order differential equation with constant coefficients and deviating argument; the deviation is present at the highest term of the equation, and it cannot be transferred to the lower terms of the equation without an additional condition. By spectral properties, we mean completeness and basic properties of a system of eigenfunctions and associated functions of a boundary value problem, as well as Volterra properties.

Keywords: equation with deviating argument, completeness, basic property, Volterra property, Gaal's formula, Lidsky's theorem, Sturm – Liouville operator, Riesz basis.

1. Introduction. The first works on the theory of differential equations with involution are found in the scientific literature of the nineteenth century. This is the extensive work of Babbage [1] from 1816. The work consists of several parts. Algebraic and transcendental equations with involution, integral and differential equations containing an involution are considered. At present, mathematicians from many countries are studying differential equations with involution. The reference devoted to the study of differential equations with involution is quite extensive. An extensive bibliography contains monographs by D. Przevorska-Rolevicz [2], J. Wiener [3]. Jack K. Hale Sjoerd M. Verduyn Lunel [4].

Partial differential equations with involution arise in mathematical models of population dynamics, ecology and physiology. A series of papers by S. Busenberg [6], J.M. Cushing [7-8] and others, devoted to mathematical modeling in population theory (biology), suggest the need for deep research on the analytical theory of differential equations with involution. In the work of J. Wiener [3, p. 264], attempts were made to apply the method of variable separation to partial differential equations with involution. In this case, solution is sought as a series in eigenfunctions. Conditions on existence of unbounded solutions of the considered problems are obtained, as well as the condition for a series to diverge in terms of eigenfunctions. Among the studies of recent years we can note the work of W.Watkins [9-10], which deals with solvability of one-dimensional differential equations with involution, and A.P. Khromov and his followers [11–12], which consider questions of solvability of integral and partial differential equations with involution.

Method of variable separation for solving partial differential equations is based on the spectral theory of one-dimensional differential operators. Spectral theory of self-adjoint and non-self-adjoint ordinary differential operators, which originated in depths of the equations of mathematical physics and began with classical works of Sturm, Liouville, Steklov and others, has received a fairly complete development over the past century. Spectral theory of self-adjoint ordinary differential operators is almost complete. In the field of spectral theory of non-self-adjoint ordinary differential operators, substantial results on completeness and basicity of eigenfunctions and associated functions are obtained by M.V. Keldysh [13], V.A. Il'in [14-19], M. Otelbaev [20], A.A. Shkalikov [21], Radzievsky [22] and many other mathematicians.

Theory of basicity of systems of eigenfunctions and associated functions of non-self-adjoint ordinary differential operators, proposed by V.A. Ilyin, received rapid development. Review papers [23-24] give a fairly complete picture of development of the basicity theory by V.A. Il'in.

Compared with the spectral theory of ordinary differential operators, the spectral theory of one-dimensional differential operators with involution is in its infancy. Apparently, the first works on the spectral theory of one-dimensional differential operators with involution were carried out on initiative of T.Sh. Kalmenov [25-29] in the past decade of this century. These studies were continued in the cycle of works by M.A. Sadybekov and A.M. Sarsenby [30-35]. Over the past decade, interest of researchers to differential equations with involutions has noticeably increased, as evidenced by the publications [36–52]. The bases theory is described in [54–55] in detail.

In this paper we continue the studies begun in [28], a brief summary of this paper was announced in [53].

Formulation of the problem. We investigate the boundary value problem

$$Ly = ay'(x) + by'(1-x) = \lambda y(x), x \in (0,1), \tag{1.1}$$

$$\alpha y(0) + \beta y(1) = 0, \tag{1.2}$$

where a, b, α, β are arbitrary, previously known constants, and λ is a spectral parameter, $y(x)$ is a desired function from the class $C^1(0,1) \cap C[0,1]$.

Let operator P be defined by the following formula

$$Py(x) = ay(x) + by(1-x),$$

then

$$P^{-1}v(x) = \frac{(aI - bS)v(x)}{a^2 - b^2},$$

where $Sv(x) = v(1-x)$, I is unit operator.

Indeed,

$$PP^{-1}v(x) = (aI + bS)\frac{(aI - bS)v(x)}{a^2 - b^2} =$$
$$= \frac{a^2 I - abS + baS - b^2 S^2}{a^2 - b^2} = \frac{(a^2 - b^2)I}{a^2 - b^2} = I.$$

Consequently, if $a^2 - b^2 \neq 0$, then the problem (1.1) - (1.2) takes the following form:

$$Ly = P\frac{d}{dx}y(x) = f(x), x \in (0,1),$$
$$\alpha y(0) + \beta y(1) = 0.$$

$$\begin{cases} y'(x) = \lambda P^{-1} y(x), \\ \alpha y(0) + \beta y(1) = 0; \end{cases} \begin{cases} y'(x) = \lambda \dfrac{aI - bS}{a^2 - b^2} y(x), \\ \alpha y(0) + \beta y(1) = 0. \end{cases}$$

It is a generalized spectral problem.

Let $Qy(x) = ay(x) + by(1-x)$, then

$$Q^{-1}v(x) = \frac{(aI - bS)v(x)}{\alpha^2 - \beta^2}.$$

Supposing $Qy(x) = z(x)$, we have

$$y(x) = Q^{-1}z(x) = \frac{aI - bS}{\alpha^2 - \beta^2} z(x) = \frac{\alpha z(x) - \beta z(1-x)}{\alpha^2 - \beta^2},$$

$$y'(x) = \frac{\alpha z'(x) + \beta z'(1-x)}{\alpha^2 - \beta^2} = \frac{Qz'(x)}{\alpha^2 - \beta^2};$$

Then our problem takes the following form:

$$\frac{Qz'(x)}{\alpha^2 - \beta^2} = \lambda \frac{aI - bS}{a^2 - b^2} Q^{-1} z(x), => \ Qz'(x) = \lambda \frac{\alpha^2 - \beta^2}{a^2 - b^2} Q^{-1} z(x),$$
$$Qz'(x) = \lambda(\alpha^2 - \beta^2) P^{-1} Q^{-1} z(x),$$

$$\begin{cases} z'(x) = \lambda(\alpha^2 - \beta^2) Q^{-1} P^{-1} Q^{-1} z(x), \\ \qquad z(0) = 0. \end{cases} \quad (1.3), (1.4)$$

It is a generalized spectral Cauchy problem.

Remark 1.1. If $(\alpha^2 - \beta^2)(a^2 - b^2) \neq 0$, then the problem (1.1)-(1.2) is equivalent to the generalized spectral Cauchy problem (1.3)-(1.4).

2. Research Methods.

2.1. Solvability. If $y_n(x) = \sin n\pi x$, then

$$y_n(1-x) = (-1)^{n+1} y_n(x), y_{2m}(1-x) = -y_{2m}(x),$$
$$y_{2m-1}(x) = y_{2m-1}(1-x);$$

moreover $y_n(0) = 0, y_n(1) = 0$.

a) $y_{2m}(1-x) + y_{2m}(x) = 0, => y'_{2m}(x) - y'_{2m}(1-x) = 0$;

б) $y_{2m-1}(x) - y_{2m-1}(x) = 0, => y'_{2m-1}(x) + y'_{2m-1}(x) = 0$.

Lemma 2.1. If $Ly_0 = 0, y_0(x) \not\equiv 0$, then

$$(a^2 - b^2)(\alpha + \beta) = 0. \ (2.1)$$

Proof. From the equation (1.1) we have

$$\begin{cases} ay'(x) + by'(1-x) = 0, \\ by'(x) + ay'(1-x) = 0; \end{cases} =>$$

a) or $a^2 - b^2 = 0$, and $y'(x) \not\equiv 0$;

б) or $a^2 - b^2 \neq 0$, and $y'(x) \equiv 0$.

If $a = b \neq 0$, then the problem has the form

$$\begin{cases} y'(x) + y'(1-x) = 0, \\ \alpha y(0) + \beta y(1) = 0. \end{cases}$$

Functions $y_{2m-1}(x) = \sin(2m-1)\pi x, m = 1,2, \dots$ are solutions of this problem, therefore, in this case the point $\lambda_0 = 0$ is an infinitely multiple eigenvalue of the boundary value problem (1.1)-(1.2).

If $b = -a \neq 0$, then the boundary value problem (1.1)-(1.2) takes the following form

$$\begin{cases} y'(x) - y'(1-x) = 0, \\ \alpha y(0) + \beta y(1) = 0. \end{cases}$$

Solution of this problem is the following functions

$$y_{2m}(x) = \sin 2m\pi x, m = 1,2, \dots$$

therefore, also in this case the point $\lambda_0 = 0$ is infinitely multiple eigenvalue of the boundary value problem (1.1) - (1.2).

If $a^2 - b^2 \neq 0$, then $y'(x) \equiv 0, y(x) = C - const; =>$
$$\alpha \cdot C + \beta \cdot C = 0, (\alpha + \beta) \cdot C = 0, => \ \alpha + \beta = 0,$$

since $C \neq 0$.

Let $(a^2 - b^2)(\alpha + \beta) = 0$, then

a) or $\alpha + \beta = 0$, or $\alpha + \beta \neq 0$, then $a^2 - b^2 = 0$.

If $\alpha+\beta=0$, then the function $y_0(x)=C-const$ is an eigenfunction and $\lambda_0=0$ is an eigenvalue.

If $a^2-b^2=0$, then as we have already noted, in the case $a=b$ the functions $y_{2m-1}(x)=\sin(2m-1)\pi x, m=1,2,\ldots$ are eigenfunctions, and $\lambda_0=0$ is eigenvalue of the infinitely multiple. In the case $b=-a$ the functions $y_{2m}(x)=\sin 2m\pi x$ are eigenfunctions, and $\lambda_0=0$ is infinitely multiple eigenvalue.

Lemma 2.2. Operator L is invertible if and only if

$$(a^2-b^2)(\alpha+\beta)\neq 0, \tag{2.2}$$

where

$$Ly=ay'(x)+by'(1-x), \tag{1.1}$$

$$\alpha y(0)+\beta y(1)=0. \tag{1.2}$$

Proof. If $(a^2-b^2)(\alpha+\beta)=0$, then in the case $a^2-b^2=0$, $\lambda_0=0$ is eigenvalue, thus the operator L is not invertible, and in the case $a^2-b^2\neq 0$, $\lambda_0=0$ is a simple eigenvalue, therefore the operator L is again non-invertible.

Inversely, if operator L is non-invertible, then there exists a function $D_0(x)\not\equiv 0$ such that $Ly_0=0$, then due to Lemma 2.1, we have the equality (2.1).

2.2. About inverse operator.

$$Ly=ay'(x)+by'(1-x)=f(x), x\in(0,1), \tag{1.1}$$

$$\alpha y(0)+\beta y(1)=0, |\alpha|+|\beta|\neq 0. \tag{1.2}$$

Let $Tu(x)=au(x)+bu(1-x)=(aI+bS)u(x)$,
where $Su(x)=u(1-x)$, then

$$T^{-1}v(x)=\frac{aI-bS}{\alpha^2-\beta^2}v(x).$$

Indeed,

$$TT^{-1}v(x)=(aI+bS)\frac{(aI-bS)v(x)}{a^2-b^2}=\frac{(a^2I-abS+baS-b^2S^2)}{a^2-b^2}v(x)=v(x).$$

The problem (1.1)-(1.2) takes the following form

$$\begin{cases} T\dfrac{d}{dx}y(x)=f(x), x\in(0,1), \\ \alpha y(0)+\beta y(1)=0. \end{cases}$$

Consequently,

$$y'(x)=T^{-1}f(x), =>$$

$$y(x)=y(0)+\int_0^x T^{-1}f(t)dt, y(1)-y(x)=\int_x^1 T^{-1}f(t)dt,$$

$$y(x)=y(1)-\int_x^1 T^{-1}f(t)dt, \ =>$$

$$(\alpha+\beta)y(x)=\alpha\int_0^x T^{-1}f(t)dt-\beta\int_x^1 T^{-1}f(t)dt,$$

$$y(x) = L^{-1}f(x) = \frac{\alpha}{\alpha+\beta}\int_0^x T^{-1}f(t)dt - \frac{\beta}{\alpha+\beta}\int_x^1 T^{-1}f(t)dt =$$

$$= \frac{\alpha}{\alpha+\beta}\int_0^1 \theta(x-t)T^{-1}f(t)dt - \frac{\beta}{\alpha+\beta}\int_0^1 и(x-t)T^{-1}f(t)dt =$$

$$= \int_0^1 \frac{\alpha\theta(x-t) - \beta\theta(t-x)}{\alpha+\beta}T^{-1}f(t)dt =$$

$$= \int_0^1 \frac{\alpha\theta(t-x) - \beta\theta(t-x)}{\alpha+\beta}\cdot\frac{af(t) - bf(1-t)}{a^2-b^2}dt =$$

$$= \frac{a}{(a^2-b^2)(\alpha+\beta)}\int_0^1 [\alpha\theta(x-t) - \beta\theta(t-x)]f(t)dt -$$

$$- \frac{b}{(a^2-b^2)(\alpha+\beta)}\int_0^1 [\alpha\theta(x-t) - \beta\theta(t-x)]f(t)dt =$$

$$\frac{a}{(a^2-b^2)(\alpha+\beta)}\int_0^1 [\alpha\theta(x-t) - \beta\theta(t-x)]f(t)dt -$$

$$- \frac{b}{(a^2-b^2)(\alpha+\beta)}\int_0^1 [\alpha\theta(x-1+t) - \beta\theta(1-t-x)]f(t)dt =$$

$$= \int_0^1 \frac{a[\alpha\theta(x-t) - \beta\theta(t-x)] - b[\alpha\theta(x-1+t) - \beta\theta(1-t-x)]}{(a^2-b^2)(\alpha+\beta)}\cdot$$

$$\cdot f(t)dt = \int_0^1 K(x,t)f(t)dt,$$

where

$$K(x,t) = \frac{a[\alpha\theta(x-t) - \beta\theta(t-x)] - b[\alpha\theta(x-1+t) - \beta\theta(1-t-x)]}{(a^2-b^2)(\alpha+\beta)}.$$

We have proved the following theorem.

Lemma 2.3. If

$$(a^2-b^2)(\alpha+\beta) \neq 0$$

then the inverse operator L^{-1} exists and has the form

$$y(x) = L^{-1}f(x) = \int_0^1 K(x,t)f(t)dt,$$

where

$$K(x,t) = \frac{a[\alpha\theta(x-t) - \beta\theta(t-x)] - b[\alpha\theta(x-1+t) - \beta\theta(1-t-x)]}{(a^2-b^2)(\alpha+\beta)}.$$

2.3. Criteria about Volterra property.

We consider the following boundary value problem

$$Ly = ay'(x) + by'(1-x) = f(x), x \in (0,1), \tag{1.1}$$

$$\alpha y(0) + \beta y(1) = 0, \quad (1.2)$$

in the space $L^2(0,1)$, where a, b, α, β are arbitrary complex constants, satisfying the condition

$$(|a| + |b|)(|\alpha| + |\beta|) \neq 0, b \neq 0 \quad (2.1)$$

$f(x)$ is a continuous function on the segment [0,1], $y(x)$ is a unknown, continuously differentiable function.

Definition 2.1. If the boundary value problem

$$Ly = ay'(x) + by'(1-x) - \lambda y(x) = 0, \quad (1.1)$$

$$\alpha y(0) + \beta y(1) = 0, \quad (1.2)$$

has only trivial solution at any complex λ, then it is called Volterra.

Theorem 2.1. Boundary value problem (1.1) - (1.2) is Volterra if and only if

1) $(a^2 - b^2)(\alpha^2 - \beta^2) \neq 0$; (2.2)
2) $b(\alpha^2 + \beta^2) + 2\alpha\beta a = 0$. (2.3)

Proof.

a) Necessity. Let boundary value problem (1.1) - (1.2) be Volterra, then $(a^2 - b^2)(\alpha + \beta) \neq 0$, otherwise $\lambda_0 = 0$ is eigenvalue, which contradicts the Volterra property of the boundary value problem (1.1) - (1.2). If the condition $(a^2 - b^2)(\alpha + \beta) \neq 0$ holds, then there exists inverse operator L^{-1}, which has the form

$$L^{-1}f(x) = \int_0^1 K(x,t)f(t)dt,$$

where

$$K(x,t) = \frac{a[\alpha\theta(x-t) - \beta\theta(t-x)] - b[\alpha\theta(x-1+t) - \beta\theta(1-t-x)]}{(a^2 - b^2)(\alpha + \beta)}.$$

If the operator L does not any nonzero eigenvalues, then the operator L^{-1} also does not have nonzero eigenvalues, consequently, kernel operator $(L^{-1})^2$ does not have nonzero eigenvalues. Then, by the Lidsky theorem [59], we get

$$SpL^{-2} = 0.$$

Now we calculate the left part of this formula

$$L^{-2}f(x) = \int_0^1 K^2(x,t)f(t)dt,$$

where

$$K^2(x,t) = \int_0^1 K(x,\xi)K(\xi,t)d\xi.$$

It is known that (by the Gaal theorem) [60]

$$SpL^{-2} = \int_0^1 K^2(x,x)\,dx,$$

thus

$$SpL^{-2} = \int_0^1 \int_0^1 K(x,\xi)K(\xi,t)d\xi dx.$$

It remains to calculate this double integral:

$$K(x,\xi)K(\xi,t) = ?$$

$$K(x,\xi)=\frac{a[\alpha\theta(x-\xi)-\beta\,\text{绎}(\xi-x)]-b[\alpha\theta(x-1+\xi)-\beta\theta(1-\xi-x)]}{(a^2-b^2)(\alpha+\beta)}=\frac{K[1]-K[2]}{(a^2-b^2)(\alpha+\beta)};$$

$$K(\xi,x)=\frac{a[\alpha\theta(\xi-x)-\beta\theta(x-\xi)]-b[\alpha\theta(\xi-1+x)-\beta\theta(1-x-\xi)]}{(a^2-b^2)(\alpha+\beta)}=\frac{K[3]-K[2]}{(a^2-b^2)(\alpha+\beta)}.$$

$$K[1]\cdot K[3]=-\alpha\beta\theta(x-\xi)-\beta\alpha\theta(\xi-x)=-\alpha\beta[\theta(x-\xi)+\theta(\xi-x)]=-\alpha\beta;$$

$$K[1]\cdot K[2]=\alpha^2\theta(x-\xi)\cdot\theta(x+\xi-1)-\alpha\beta\theta(x-\xi)\theta(1-x-\xi)-$$
$$-\beta\alpha\theta(\xi-x)\theta(x+\xi-1)+\beta^2\theta(\xi-x)\cdot\theta(1-x-\xi);$$

$$K[2]\cdot K[3]=\alpha^2\theta(x+\xi-1)\cdot\theta(\xi-x)-\alpha\beta\theta(x+\xi-1)\theta(x-\xi)-$$
$$-\beta\alpha\theta(1-x-\xi)\theta(\xi-x)+\beta^2\theta(1-x-\xi)\cdot\theta(x-\xi);$$

$$K[2]\cdot K[2]=\alpha^2\theta(x+\xi-1)+\beta^2\theta(1-x-\xi);$$

Consequently,

$$K(x,\xi)=\frac{aK[1]-bK[2]}{(a^2-b^2)(\alpha+\beta)},K(\xi,x)=\frac{aK[3]-bK[2]}{(a^2-b^2)(\alpha+\beta)},$$

$$K(x,\xi)\cdot K(\xi,x)=\frac{a^2K[1]\cdot K[3]-abK[1]\cdot K[2]-baK[2]\cdot K[3]+b^2K^2[2]}{(a^2-b^2)(\alpha+\beta)}=$$

$$=a^2(-\alpha\beta)-ab[\alpha^2\theta(x-\xi)\cdot\theta(x+\xi-1)-\alpha\beta\theta(x-\xi)\theta(1-x-\xi)-$$

$$-\beta\alpha\theta(\xi-x)\theta(x+\xi-1)+\beta^2\theta(\xi-x)\cdot\theta(1-x-\xi)]-$$

$$-ba[\alpha^2\theta(x+\xi-1)\cdot\theta(\xi-x)-\alpha\beta\theta(x+\xi-1)\theta(x-\xi)-$$

$$-\beta\alpha\theta(1-x-\xi)\theta(\xi-x)+\beta^2\theta(1-x-\xi)\cdot\theta(x-\xi)]+$$

$$+b^2[\alpha^2\theta(x+\xi-1)+\beta^2\theta(1-x-\xi)]\,/\,(a^2-b^2)(\alpha+\beta)^2;$$

We calculate the following integrals:

1) $\int_0^1\int_0^1 \text{и}(x-\xi)\theta(x+\xi-1)d\xi dx=\left|\begin{matrix}x-\xi>0,\\ x+\xi-1>0,\end{matrix}\ => x>\xi>1-x\right|$

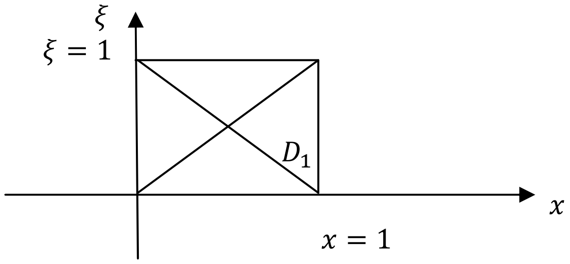

$$=\iint_{D_1}d\xi dx=\frac{1}{4};$$

2) $\int_0^1 \int_0^1 \theta(x-\xi)\theta(1-x-\xi)d\xi dx = \left| \begin{matrix} x-\xi>0, \\ 1-x-\xi>0, \end{matrix} \;\Rightarrow\; \begin{matrix} x>\xi, \\ 1-\xi>x>\xi, \end{matrix} \right|$

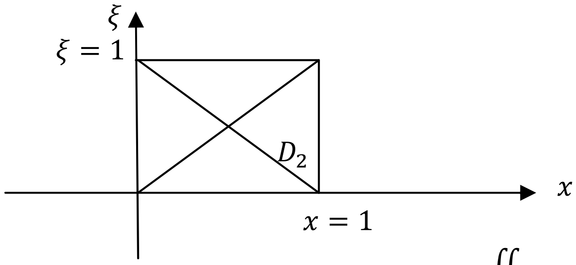

$$= \iint_{D_2} d\xi dx = \frac{1}{4};$$

3) $\int_0^1 \int_0^1 \theta(\xi-x)\theta(x+\xi-1)d\xi dx = \left| \begin{matrix} \xi-x>0, \\ x+\xi-1>0, \end{matrix} \;\Rightarrow\; \begin{matrix} \xi>x, \\ \xi>1-x, \end{matrix} \right|$

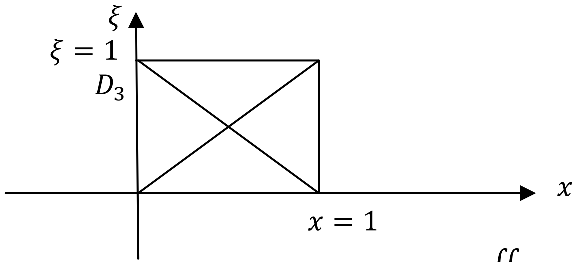

$$= \iint_{D_3} d\xi dx = \frac{1}{4};$$

4) $\int_0^1 \int_0^1 \theta(\xi-x)\theta(1-x-\xi)d\xi dx = \left| \begin{matrix} x-\xi>0, \\ 1-x-\xi>0, \end{matrix} \right|$

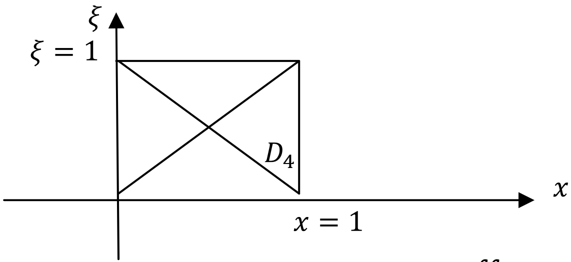

$$= \iint_{D_4} d\xi dx = \frac{1}{4};$$

5) $\int_0^1 \int_0^1 [\alpha^2\theta(x+\xi-1) + \beta^2\theta(1-x-\xi)]d\,\xi dx = ?$

$$\int_0^1\int_0^1 \alpha^2\theta(x+\xi-1)d\xi dx = \int_0^1 dx \int_{1-x}^{x} \alpha^2 d\xi = \int_0^1 (1-1+x)\alpha^2 dx =$$

$$= \alpha^2 \int_0^1 x dx = \alpha^2 \left.\frac{x^2}{2}\right|_0^1 = \frac{\alpha^2}{2};$$

$$\int_0^1\int_0^1 \beta^2\theta(1-x-\xi)dxd\xi = \beta^2 \int_0^1 dx \int_0^{1-x} d\xi = \beta^2 \int_0^1 (1-x)dx =$$

$$= \beta^2 \left.\left(x-\frac{x^2}{2}\right)\right|_0^1 = \beta^2\left(1-\frac{1}{2}\right) = \frac{\beta^2}{2};$$

$$SpL^{-2}=\int_0^1\int_0^1 K(x,\xi)K(\xi,t)d\xi dx=$$

$$=\frac{a^2(-\alpha\beta)-\frac{ab}{4}(\alpha^2-\alpha\beta-\beta\alpha+\beta^2)-\frac{ba}{4}(\alpha^2-\alpha\beta-\beta\alpha+\beta^2)+b^2\frac{\alpha^2+\beta^2}{2}}{(a^2-b^2)^2(\alpha+\beta)^2}$$

$$=\frac{-2\alpha\beta a^2-ab(\alpha-\beta)^2+b^2(\alpha^2+\beta^2)}{2(a^2-b^2)^2(\alpha+\beta)^2}=$$

$$=\frac{-2\alpha\beta a^2-ab\alpha^2+2\alpha\beta ab-ab\beta^2+b^2\alpha^2+b^2\beta^2}{2(a^2-b^2)^2(\alpha+\beta)^2}=$$

$$=\frac{[\alpha^2(b^2-ab)+\beta^2(b^2-ab)+2\alpha\beta ab-2\alpha\beta a^2]}{2(a^2-b^2)^2(\alpha+\beta)^2}=$$

$$=\frac{(b^2-ab)(\alpha^2+\beta^2)+2\alpha\beta(ab-a^2)}{2(a^2-b^2)^2(\alpha+\beta)^2}=$$

$$=\frac{b(b-a)(\alpha^2+\beta^2)+2\alpha\beta a(b-a)}{2(a^2-b^2)^2(\alpha+\beta)^2}=$$

$$=\frac{(b-a)[b(\alpha^2+\beta^2)+2\alpha\beta a]}{2(a^2-b^2)^2(\alpha+\beta)^2}=0.$$

Since $b-a\neq 0$, then $b(\alpha^2+\beta^2)+2\alpha\beta a=0$, thus the necessity of the second condition is proved.

If $\beta=-\alpha$, then $b\cdot 2\alpha^2-2\alpha^2\cdot a=2\alpha^2(b-a)=0$, since $\alpha\neq 0$, therefore $b-a=0$, it is impossible, thus $\beta\neq-\alpha$ or $\beta+\alpha\neq 0$.

Similarly, if $\beta=\alpha$, then $b\cdot 2\alpha^2+2\alpha^2\cdot a=0, 2\alpha^2(b+a)=0$, since $\alpha\neq 0$, then $b+a=0$, it is impossible, therefore $\beta-\alpha\neq 0$. Earlier we showed that $(a^2-b^2)(\alpha+\beta)\neq 0$, due to the last condition, we have $(a^2-b^2)(\alpha^2-\beta^2)\neq 0$, t.e. we get the inequality (4.2).

б) Sufficiency.

Let $(a^2-b^2)(\alpha^2-\beta^2)\neq 0$ and $b(\alpha^2+\beta^2)+2\alpha\beta a=0$. From the equation (1.1) we have

$$T\frac{d}{dx}y(x)=\lambda y(x), y'(x)=\lambda T^{-1}y(x),$$

$$y'(x)=\lambda\frac{aI-bS}{a^2-b^2}y(x).$$

Differentiating this equation, we obtain

$$y''(x)=\lambda\frac{ay'+by'(1-x)}{a^2-b^2}=\lambda\frac{aI+bS}{a^2-b^2}y'(x)=$$

$$=\lambda^2\frac{aI+bS}{a^2-b^2}\cdot\frac{aI-bS}{a^2-b^2}=\frac{\lambda^2}{a^2-b^2}y(x).$$

Lemma 2.4. If $\lambda\neq 0$ is a eigenvalue of the boundary value problem

$$ay'(x)+by'(1-x)=\lambda y(x), x\in(0,1), \tag{1.1}$$

$$\alpha y(0)+\beta y(1)=0, \tag{1.2}$$

where $b\neq 0, |\alpha|+|\beta|\neq 0, a^2-b^2\neq 0$, then the quantity

$$\mu^2=\frac{\lambda^2}{a^2-b^2} \tag{2.4}$$

is eigenvalue of the Sturm - Liouville operator

$$y''(x)=\mu^2 y(x), x\in(0,1), \tag{2.5}$$

$$\begin{cases} \alpha y(0) + \beta y(1) = 0, \\ \alpha[ay'(0) + by'(1)] + \beta[ay'(1) + by'(0)] = 0, \end{cases} \tag{2.6}$$

Corollary 2.1. If the Sturm - Liouville problem (2.5)-(2.6) does not have nonzero eigenvalues, then the problem (1.1)-(1.2) also does not them.

Boundary value problem (2.5)-(2.6) does not eigenvalues if and only if

$$\Delta_{24} = 0, \Delta_{14} + \Delta_{32} = 0, \Delta_{13} = 0,$$

where Δ_{ij} are minors of the matrix

$$\begin{pmatrix} \alpha & 0 & \beta & 0 \\ 0 & \alpha a + \beta b & 0 & \alpha b + \beta a \end{pmatrix}.$$

It is obvious that

$$\Delta_{24} = 0, \Delta_{14} = \alpha(\alpha b + \beta a), \Delta_{23} = -\beta(\alpha a + \beta / b), \Delta_{13} = 0.$$

Moreover,

$$\Delta_{14} + \Delta_{32} = \alpha(\alpha b + \beta a) + \beta(\alpha a + \beta b) =$$
$$= \alpha^2 b + \alpha\beta a + \beta\alpha a + \beta^2 b = b(\alpha^2 + \beta^2) + 2\alpha\beta a = 0.$$

Consequently, the problem (4.5) - (4.6) is Volterra, i.e. does not have eigenvalues on all complex plane, thus the problem (1.1) - (1.2) also does not have nonzero eigenvalues.

Remark 2.1.

Other proof of sufficiency.

If $\alpha^2 - \beta^2 \neq 0$ and $a^2 - b^2 \neq 0$, then our boundary value problem is equivalent to the generalized Cauchy problem

$$\begin{cases} z'(x) = \lambda(\alpha^2 - \beta^2)Q^{-1}P^{-1}Q^{-1}z(x), \\ z(0) = 0; \end{cases} \qquad (2.7), (2.8)$$

where

$$Pu(x) = au(x) + bu(1-x) = (aI + bS)u(x),$$

$$Qu(x) = \alpha u(x) + \beta u(1-x) = (\alpha I + \beta S)u(x),$$

$$Q^{-1} = \frac{\alpha I - \beta S}{\alpha^2 - \beta^2}, P^{-1} = \frac{aI - bS}{a^2 - b^2},$$

$$P^{-1}Q^{-1} = \frac{aI - bS}{a^2 - b^2} \cdot \frac{\alpha I - \beta S}{\alpha^2 - \beta^2} = \frac{a\alpha I - a\beta S - b\alpha S + b\beta S}{(a^2 - b^2)(\alpha^2 - \beta^2)} =$$

$$= \frac{a\alpha I - (a\beta + b\alpha)S + b\beta S}{(a^2 - b^2)(\alpha^2 - \beta^2)} = \frac{(a\alpha + b\beta)I - (a\beta + b\alpha)S}{(a^2 - b^2)(\alpha^2 - \beta^2)};$$

$$Q^{-1}P^{-1}Q^{-1} = \frac{\alpha I - \beta S}{\alpha^2 - \beta^2} \cdot \frac{(a\alpha + b\beta)I - (a\beta + b\alpha)S}{(a^2 - b^2)(\alpha^2 - \beta^2)} =$$

$$= \frac{\alpha(a\alpha + b\beta)I + \beta(a\beta + b\alpha)I - \alpha(a\beta + b\alpha)S - \beta(a\alpha + b\beta)S}{(a^2 - b^2)(\alpha^2 - \beta^2)^2} =$$

$$= \frac{(\alpha^2 a + \alpha\beta b + \beta^2 a + \alpha\beta b)I - (a\alpha\beta + \alpha^2 b + \beta\alpha a + \beta^2 b)S}{(a^2 - b^2)(\alpha^2 - \beta^2)^2} =$$

$$= \frac{[a(\alpha^2 + \beta^2) + 2\alpha\beta b]I - [b(\alpha^2 + \beta^2) + 2\alpha\beta a]S}{(a^2 - b^2)(\alpha^2 - \beta^2)^2}.$$

Consequently, Cauchy problem (2.7) - (2.8) takes the following form

$$\begin{cases} z'(x) = \lambda \dfrac{[a(\alpha^2+\beta^2)+2\alpha\beta b]}{(a^2-b^2)(\alpha^2-\beta^2)} z(x), \\ z(0) = 0; \end{cases}$$

It is obvious that this Cauchy problem has only trivial solution at any value of λ.

Remark 2.2. This proof prompted us that $\alpha^2 - \beta^2 \neq 0$. The fact is that we did not check the conditions

1) $(a^2-b^2)(\alpha+\beta) \neq 0$,

2) $b(\alpha^2+\beta^2) + 2\alpha\beta a = 0$

on compatibility.

From the second condition when $\beta = \alpha$, we have

$$b \cdot 2\alpha^2 + 2\alpha^2 \cdot a = 0, 2\alpha^2(b+a) = 0.$$

If $\alpha = 0$, then $\beta = 0$, which is not acceptable therefore $b + a = 0$, and this contradicts the first condition, therefore в $\neq \alpha$ or $\beta - \alpha \neq 0$. And the final look of the Volterra is

1) $(a^2-b^2)(\alpha^2-\beta^2) \neq 0$,

2) $b(\alpha^2+\beta^2) + 2\alpha\beta a = 0$.

2.4. On basis property.

Lemma 2.5. If

a) $(a^2-b^2)(\alpha^2-\beta^2) \neq 0$,

б) function $y(x, \pm\lambda)$ is eigenfunction for the boundary value problem

$$ay'(x) + by'(1-x) = \pm\lambda y(x), x \in (0,1), \quad (2.9)$$

$$\alpha y(0) + \beta y(1) = 0, \quad (2.10)$$

where $|\alpha| + |\beta| \neq 0$, then it is eigenfunction for the Sturm - Liouville boundary value problem

$$y''(x) = \mu^2 y(x), x \in (0,1), \quad (2.11)$$

$$\begin{cases} \alpha y(0) + \beta y(1) = 0, \\ (a\alpha + b\beta)y'(0) + (a\beta + b\alpha)y'(1) = 0, \end{cases} \quad (2.12)$$

where

$$\mu^2 = \frac{\lambda^2}{b^2-a^2}. \quad (2.13)$$

Inversely, if the quantity $\mu^2 = \frac{\lambda^2}{b^2-a^2}$ is eigenvalue of the Sturm - Liouville boundary value problem

$$y''(x) = \mu^2 y(x), x \in (0,1), \quad (2.11)$$

$$\begin{cases} \alpha y(0) + \beta y(1) = 0, \\ (a\alpha + b\beta)y'(0) + (a\beta + b\alpha)y'(1) = 0, \end{cases} \quad (2.12)$$

Then the function $y(x)$ is eigenfunction for the boundary value problem

$$ay'(x) + by'(1-x) = \pm\lambda y(x), \quad (2.9)$$

$$\alpha y(0) + \beta y(1) = 0, \quad (2.10)$$

Proof. Suppose that (2.9) - (2.10) holds. Then, assuming

$$Tu(x) = au(x) + bu(1-x) = (aI + bS)u(x),$$
$$Su(x) = u(1-x)$$

we have

$$Ty'(x) = \pm\lambda y(x),$$

$$y'(x) = \pm\lambda T^{-1}y(x) = \pm\lambda\frac{aI - bS}{a^2 - b^2}y(x),$$

$$y''(x) = \pm\lambda\frac{ay'(x) + by'(1-x)}{a^2 - b^2} = \pm\lambda\frac{aI + bS}{a^2 - b^2}y'(x) =$$

$$= \frac{\pm\lambda}{a^2 - b^2}Ty'(x) = \frac{\lambda^2}{a^2 - b^2}y(x),$$

consequently,

$$-y''(x) = \frac{\lambda^2}{b^2 - a^2}y(x).$$

Further, from the equation (2.9) due to the boundary condition (2.10), we obtain

$$\alpha[ay'(0) + by'(1)] + \beta[ay'(1) + by'(0)] = \pm\lambda[\alpha y(0) + \beta y(1)] = 0.$$

Therefore, the second boundary condition has the form

$$(a\alpha + b\beta)y'(0) + (a\beta + b\alpha)y'(1) = 0.$$

Inversely, let function $y(x,\mu)$ be a eigenfunction of the Sturm – Liouville boundary value problem

$$y''(x) = \mu^2 y(x), x \in (0,1), \tag{2.11}$$

$$\begin{cases} \alpha y(0) + \beta y(1) = 0, \\ (a\alpha + b\beta)y'(0) + (a\beta + b\alpha)y'(1) = 0, \end{cases} \tag{2.12}$$

where

$$\mu^2 = \frac{\lambda^2}{b^2 - a^2}. \tag{2.13}$$

We find a eigenfunction, corresponding to the eigenvalue μ^2.

General solution of the equation (2.11) has the form

$$y(x,\mu) = Ae^{i\mu x} + Be^{-i\mu x},$$

where A, B are arbitrary constants. Putting this expansion into the boundary condition (2.12), we receive a system of homogeneous equations for unknowns A, B.

$$\alpha\,,(0) + \beta y(1) = \alpha(A + B\ ) + \beta\left(Ae^{i\mu} + Be^{-i\mu}\right) =$$

$$= A\left(\alpha + \beta e^{i\mu}\right) + B\left(\alpha + \beta e^{-i\mu}\right) = 0;$$

$$y'(x,\mu) = i\mu\left(Ae^{i\mu x} - Be^{-i\mu x}\right), y'(0) = i\mu(A - B),$$

$$y'(1) = i\mu\left(Ae^{i\mu} - Be^{-i\mu}\right),$$

$$(a\alpha + b\beta)i\mu(A - B) + (a\beta + b\alpha)i\mu\left(Ae^{i\mu} - Be^{-i\mu}\right) = 0, i\mu \neq 0;$$

$$(A - B)(a\alpha + b\beta) + (a\beta + b\alpha)\left(Ae^{i\mu} - Be^{-i\mu}\right) = 0,$$

$$A\left[a\alpha + b\beta + (a\beta + b\alpha)e^{i\mu}\right] + B\left[-a\alpha - b\beta - (a\beta + b\alpha)e^{-i\mu}\right] = 0,$$

$$\begin{cases} A\left(\alpha + \beta e^{i\mu}\right) + B\left(\alpha + \beta e^{-i\mu}\right) = 0, \\ A\left[a\alpha + b\beta + (a\beta + b\alpha)e^{i\mu}\right] + B\left[-a\alpha - b\beta - (a\beta + b\alpha)e^{-i\mu}\right] = 0. \end{cases}$$

We calculate determinant of this system of equations

$$\Delta(\mu) = \begin{vmatrix} \alpha + \beta e^{i\mu} & \alpha + \beta e^{-i\mu} \\ a\alpha + b\beta + (a\beta + b\alpha)e^{i\mu} & -a\alpha - b\beta - (a\beta + b\alpha)e^{-i\mu} \end{vmatrix} =$$

$$= -\left(\alpha + \beta e^{i\mu}\right)\left[a\alpha + b\beta + (a\beta + b\alpha)e^{-i\mu}\right] -$$

$$-\left(\alpha + \beta e^{-i\mu}\right)\left[a\alpha + b\beta + (a\beta + b\alpha)e^{i\mu}\right] = 0. \; (2.14)$$

Transforming this expression, we get

$$\Delta(\mu) = -\left[\alpha(a\alpha + b\beta) + \alpha(a\beta + b\alpha)e^{-i\mu} + \beta(a\alpha + b\beta)e^{i\mu} + \beta(a\beta + b\alpha) + \right.$$

$$\left. +\alpha(a\alpha + b\beta) + \alpha(a\beta + b\alpha)e^{i\mu} + \beta(a\alpha + b\beta)e^{-i\mu} + \beta(a\beta + b\alpha)\right] =$$

$$= -\{2\alpha(a\alpha + b\beta) + 2\beta(a\beta + b\alpha) + [\alpha(a\beta + b\alpha) + \beta(a\alpha + b\beta)]e^{-i\mu} +$$

$$+[\alpha(a\beta + b\alpha) + \beta(a\alpha + b\beta)]e^{i\mu}\} =$$

$$= -\{2\alpha^2 a + 2\alpha\beta b + 2\beta^2 a + 2\alpha\beta b +$$

$$+[\alpha(a\beta + b\alpha) + \beta(a\alpha + b\beta)]\left(e^{i\mu} + e^{-i\mu}\right)\} =$$

$$= -2[(\alpha^2 + \beta^2)a + 2\alpha\beta b + (\alpha\beta a + b\alpha^2 + \beta\alpha a + b\beta^2)\cos\mu] =$$

$$= -2\{a(\alpha^2 + \beta^2) + 2\alpha\beta b + [b(\alpha^2 + \beta^2) + 2\alpha\beta a]\cos\mu\}.$$

Remark 2.3. If

1) $b(\alpha^2 + \beta^2) + 2\alpha\beta a = 0$;
2) $a(\alpha^2 + \beta^2) + 2\alpha\beta b \neq 0$

then $\Delta(\mu) \neq 0$, i.e. the problem is Volterra.

In this case:

$$2) - 1) = (\text{б}^2 + \beta^2)(a - b) + 2\alpha\beta(b - a) = (a - b)(\alpha - \beta)^2 \neq 0,$$

$$2) + 1) = (\alpha^2 + \beta^2)(a + b) + 2\alpha\beta(b + a) = (a + b)(\alpha + \beta)^2 \neq 0.$$

Therefore, $(a^2 - b^2)(\alpha^2 - \beta^2)^2 \neq 0$, that coincides with the first condition of Volterra property, see (2.2).

Supposing $b(\text{б}^2 + \beta^2) + 2\alpha\beta a \neq 0$, from the equation $\Delta(\mu) = 0$ we have

$$\cos\mu = -\frac{a(\alpha^2 + \beta^2) + 2\alpha\beta b}{b(\alpha^2 + \beta^2) + 2\alpha\beta a},$$

$$\mu = \pm arccos\left[-\frac{a(\alpha^2 + \beta^2) + 2\alpha\beta b}{b(\alpha^2 + \beta^2) + 2\alpha\beta a}\right] + 2n\pi, n = 0, \pm 1, \pm 2, \ldots$$

We investigate multiplicity of eigenvalues

$$\dot{\Delta}(\mu) = 2[b(\alpha^2 + \beta^2) + 2\alpha\beta a]\sin\mu.$$

If $\dot{\Delta}(\mu) = 0$, then $\sin\mu = 0, \cos\mu = \pm 1$. Thus

$$-\frac{a(\alpha^2 + \beta^2) + 2\alpha\beta b}{b(\alpha^2 + \beta^2) + 2\alpha\beta a} = \pm 1.$$

a) If
$a(\alpha^2 + \beta^2) + 2\alpha\beta b = b(\alpha^2 + \beta^2) + 2\alpha\beta a$, then

$$(a - b)(\alpha^2 + \beta^2) + 2\alpha\beta(b - a) = (a - b)(\alpha^2 + \beta^2 - 2\alpha\beta) =$$

$$= (a - b)(\alpha - \beta)^2 = 0;$$

б) If

$$a(\alpha^2+\beta^2)+2\alpha\beta b=-b(\alpha^2+\beta^2)-2\alpha\beta a,$$

$$(\alpha^2+\beta^2)(a+b)+2\alpha\beta(b+a)=(a+b)(\alpha^2+\beta^2+2\alpha\beta)=$$

$$=(a+b)(\alpha+\beta)^2=0.$$

In oue case, $(a^2-b^2)(\alpha^2-\beta^2)\neq 0$, therefore $\dot{\Delta}(\mu)\neq 0$ and the Sturm - Liouville problem does not have associated functions.

Supposing,

$$A=K(\alpha+\beta e^{-i\mu}), B=(-\alpha-\beta e^{i\mu})K,$$

where K is arbitrary constant, we obtain (find) eigenfunctions of the Sturm – Liouville boundary value problem

$$y(x,\mu)=K(\alpha+\beta e^{-i\mu})e^{i\mu x}-K(\alpha+\beta e^{i\mu})e^{-i\mu x}.$$

Then

$$y'(x,\mu)=K\left[i\mu(\alpha+\beta e^{-i\mu})e^{i\mu x}+i\mu(\alpha+\beta e^{i\mu})e^{-i\mu x}\right],$$

$$y'(1-x,\mu)=K\left[i\mu(\alpha+\beta e^{-i\mu})e^{i\mu(1-x)}+i\mu(\alpha+\beta e^{i\mu})e^{-i\text{м}(1-x)}\right]=$$

$$=K\left[i\mu(\alpha e^{i\mu}+\beta)e^{-i\mu x}+i\mu(\alpha e^{-i\mu}+\beta)e^{i\mu x}\right];$$

$$ay'+by'(1-x)=i\mu K\{\left[a(\alpha+\beta e^{-i\mu})+b(\alpha e^{-i\mu}+\beta)\right]e^{i\mu x}+$$

$$+\left[a(\alpha+\beta e^{i\mu})+b(\alpha e^{i\mu}+\beta)\right]e^{-i\mu x}\}.$$

Further, from the equality $\Delta(\text{м})=0$ it follows that rows of this determinant (2.14) are linear dependent, therefore we have

$$a\alpha+a\beta e^{-i\mu}+b\alpha e^{-i\mu}+b\beta=$$

$$=a\alpha+b\beta+(a\beta+b\alpha)e^{-i\mu}=-C(\alpha+\beta e^{-i\mu}), \quad (2.15)$$

$$a\alpha+a\beta e^{i\mu}+b\alpha e^{i\mu}+b\beta=$$

$$=a\alpha+b\beta+(a\text{в}+b\alpha)e^{i\mu}=C(\alpha+\beta e^{i\mu}), \quad (2.16)$$

Consequently,

$$ay'+by'(1-x)=i\mu K\cdot C\left[-(\alpha+\beta e^{-i\mu})e^{i\mu x}+(\alpha+\beta e^{i\mu})e^{-i\mu x}\right]=$$

$$=i\mu K\cdot C\left[(\alpha+\beta e^{-i\mu})e^{i\mu x}-(\alpha+\beta e^{i\mu})e^{-i\mu x}\right]=$$

$$=-i\mu\cdot Cy(x,\mu)=-\tfrac{\lambda}{\sqrt{a^2-b^2}}Cy(x,\mu). \quad (2.17)$$

Calculate the constant C. If we sum up formulas (2.15) and (2.16), then we get

$$2(a\alpha+b\beta)+(a\beta+b\alpha)(e^{i\mu}+e^{-i\mu})=C(e^{i\mu}-e^{-i\mu})\cdot\beta,=>$$

$$a\alpha+b\beta+(a\beta+b\alpha)\cos\mu=C\cdot\beta i\sin\mu.$$

Subtracting the formula (2.15) from (2.16), we have

$$(a\beta+b\alpha)(e^{i\mu}-e^{-i\mu})=C\left[2\alpha+\beta(e^{i\mu}+e^{-i\mu})\right],=>$$

$$i(a\beta+b\alpha)\sin\mu=C[\alpha+\beta\cos\mu];$$

Consequently,

$$C=\frac{i(a\beta+b\alpha)\sin\mu}{\alpha+\beta\cos\mu}=\frac{a\alpha+b\beta+(a\beta+b\alpha)\cos\mu}{i\beta\sin\mu};$$

In our situation

$$\cos\mu=-\frac{a(\alpha^2+\beta^2)+2\alpha\beta b}{b(\alpha^2+\beta^2)+2\alpha\beta a},$$

Thus

$$\alpha + \beta\cos\mu = \alpha - \frac{a\beta(\alpha^2+\beta^2)+2\alpha\beta^2 b}{b(\alpha^2+\beta^2)+2\alpha\beta a} =$$

$$= \frac{\alpha b(\alpha^2+\beta^2)+2\alpha^2\beta a - a\beta(\alpha^2+\beta^2)-2\alpha\beta^2 b}{b(\alpha^2+\beta^2)+2\alpha\beta a} =$$

$$= \frac{(\alpha^2+\beta^2)(\alpha b - a\beta)+2\alpha\beta(\alpha a-\beta b)}{b(\alpha^2+\beta^2)+2\alpha\beta a} =$$

$$= \frac{b[\alpha(\alpha^2+\beta^2)-2\alpha\beta^2]+a[-\beta(\alpha^2+\beta^2)+2\alpha^2\beta]}{b(\alpha^2+\beta^2)+2\alpha\beta a} =$$

$$= \frac{b\alpha(\alpha^2-\beta^2)+a\beta(\alpha^2-\beta^2)}{b(\alpha^2+\beta^2)+2\alpha\beta a} = \frac{(\alpha^2-\beta^2)(b\alpha+a\beta)}{b(\alpha^2+\beta^2)+2\alpha\beta a};$$

$$\sin\mu = \pm\sqrt{1-\frac{[a(\alpha^2+\beta^2)+2\alpha\beta b]^2}{[b(\alpha^2+\beta^2)+2\alpha\beta a]^2}} = \frac{\pm\sqrt{b^2-a^2}(\alpha^2-\beta^2)}{b(\alpha^2+\beta^2)+2\alpha\beta a};$$

$$C = \frac{\pm i(a\beta+b\alpha)\sqrt{b^2-a^2}(\alpha^2-\beta^2)}{b(\alpha^2+\beta^2)+2\alpha\beta a} : \frac{(б^2-\beta^2)(b\alpha+a\beta)}{b(\alpha^2+\beta^2)+2\alpha\beta a} =$$

$$= \pm i\sqrt{b^2-a^2} = \pm\sqrt{a^2-b^2}.$$

Putting this expression into the formula (2.17), we have

$$ay'(x)+by'(1-x) = \mp\lambda y(x,\mu),$$

which was required to prove.

Problem. Prove that the system of eigenfunctions of the Sturm - Liouville boundary value problem is basis

$$-y''(x) = \mu^2 y(x), x\in(0,1), \tag{2.11}$$

$$\begin{cases} \alpha y(0)+\beta y(1) = 0, \\ (a\alpha+b\beta)y'(0)+(a\beta+b\alpha)y'(1) = 0, \end{cases} \tag{2.12}$$

where $(\alpha^2-\beta^2)(a^2-b^2)\neq 0$, by the Kesselman - Mikhailov Test [57-58].

Solution. Boundary matrix of the boundary value problem (2.11) - (2.12) has the form

$$\begin{pmatrix} \alpha & 0 & \beta & 0 \\ 0 & \alpha a+b\beta & 0 & a\beta+b\alpha \end{pmatrix}.$$

We calculate minors of this matrix

$$\Delta_{12} = \alpha(\alpha a+b\beta), \Delta_{13} = 0, \Delta_{14} = \alpha(a\beta+b\alpha),$$

$$\Delta_{23} = -\beta(\alpha a+\beta b), \Delta_{24} = 0, \Delta_{34} = \beta(a\beta+b\alpha);$$

Hence,

$$\Delta_{14}+\Delta_{32} = \alpha(a\beta+b\alpha)+\beta(\alpha a+\beta b) =$$

$$= b(\alpha^2+\beta^2)+2\alpha\beta a \neq 0,$$

otherwise the problem is Volterra.

First we check the Birkhoff regularity condition [54]; for this, we rearrange rows of the boundary matrix

$$\begin{pmatrix} a_0 & a_1 & b_0 & b_1 \\ 0 & \alpha a + b\beta & 0 & a\beta + b\alpha \\ \alpha & 0 & \beta & 0 \\ c_0 & c_1 & d_0 & d_1 \end{pmatrix}$$

1) $a_1 d_1 - b_1 c_1 = 0,$
2) $a_1 d_1 - b_1 c_1 = 0, |a_1| + |b_1| = |\alpha a + b\beta| + |a\beta + b\alpha| > 0,$

$$b_1 c_0 + a_1 d_0 = \alpha(a\text{в} + b\alpha) + \beta(\alpha a + \beta b) = b(\alpha^2 + \beta^2) + 2\alpha\beta a \neq 0,$$

3) $a_1 = b_1 = c_1 = d_1 = 0, a_0 d_0 - b_0 c_0 \neq 0.$

It is obvious that in our case conditions 1) and 3) coincide, only condition 2) remains.

If $|a_1| + |b_1| = 0$, then $a_1 = 0$ and $b_1 = 0$. Then we get

$$\begin{cases} \alpha a + b\beta = 0, \\ a\beta + b\alpha = 0. \end{cases}$$

Since $|a| + |b| \neq 0$, then $\alpha^2 - \beta^2 = 0$; similarly from the condition $|\alpha| + |\beta| \neq 0$ we have that $a^2 - b^2 = 0$, which is not possible by our condition. Consequently, our boundary value problems (2.12) are regular by the second part of the Birkhoff condition [56].

The Kesselman condition [57] is

$$\Delta_{14}^2 + \Delta_{32}^2 - \Delta_{12}^2 - \Delta_{34}^2 \neq 0.$$

In our case,

$$\Delta_{14}^2 + \Delta_{32}^2 = \alpha^2(a\beta + b\alpha)^2 + \beta^2(\alpha a + \text{в}b)^2,$$

$$\Delta_{12}^2 = \alpha^2(\alpha a + \beta b)^2, \Delta_{34}^2 = \beta^2(a\beta + b\alpha)^2, =>$$

$$\Delta_{14}^2 + \Delta_{32}^2 - \Delta_{12}^2 - \Delta_{34}^2 = (\alpha^2 - \beta^2)(a\beta + b\alpha)^2 + (\beta^2 - \alpha^2(\alpha a + \beta b)^2) =$$

$$= (\alpha^2 - \beta^2)[(a\beta + b\alpha)^2 - (\alpha a + \beta b)^2] =$$

$$= (\alpha^2 - \beta^2)[(a\beta + b\alpha - \alpha a - \beta b)(a\beta + b\alpha + \alpha a + \beta b)] =$$

$$= (\alpha^2 - \beta^2)[a(\beta - \alpha) + b(\alpha - \beta)][\text{б}(a + b) + \beta(a + b)] =$$

$$= (\alpha^2 - \beta^2)(\alpha - \beta)(b - a)(a + b)(\alpha + \beta) =$$

$$= (\alpha^2 - \beta^2)(\alpha^2 - \beta^2)(b^2 - a^2) = (\alpha^2 - \beta^2)^2(b^2 - a^2) \neq 0.$$

Consequently, the eigenfunctions of the Sturm – Liouville boundary value problem (2.11) - (2.12) form a Riesz basis in the space $L^2(0,1)$.

Theorem 2.2. If

a) $(\alpha^2 - \beta^2)(a^2 - b^2) \neq 0,$

b) $b(\alpha^2 + \beta^2) + 2\alpha\beta a \neq 0,$

then eigenfunctions of the bpundary value probelm

$$ay'(x) + by'(1 - x) = \lambda y(x), x \in (0,1), \tag{1.1}$$

$$\alpha y(0) + \beta y(1) = 0, \tag{1.2}$$

form a Riesz basis in the space $L^2(0,1)$.

Remark 2.5.

If $a = 0, b = 1$, then the boundary value problem (1.1)-(1.2) takes the form

$$y'(1 - x) = \lambda y(x), x \in (0,1),$$

$$\alpha y(0)+\beta y(1)=0.$$

Thus the conditions a) and b) of Theorem 2.2. are transformed as follows:

a)′ $\alpha^2-\beta^2\neq 0,$

b)′ $\alpha^2+\beta^2\neq 0$

or $(\alpha^2-\beta^2)(\alpha^2+\beta^2)\neq 0$, or $\alpha^4-\beta^4\neq 0$, that coincides with the results of [28].

3. Research Results

We consider in the space $L^2(0,1)$ the following boundary value problem

$$Ly=ay'(x)+by'(1-x)=\lambda y(x), x\in(0,1), \quad (1.1)$$

$$\alpha y(0)+\beta y(1)=0, \quad (1.2)$$

where a,b,α,β are arbitrary, previously known constants, and λ is a spectral parameter, $y(x)$ is a desired function from the class $C^1(0,1)\cap C[0,1]$, and we formulate the obtained results.

Theorem 3.1. The boundary value problem (1.1) - (1.2) is Volterra if and only if

1) $(a^2-b^2)(\alpha^2-\beta^2)\neq 0$; (2.2)
2) $b(\alpha^2+\beta^2)+2\alpha\beta a=0$. (2.3)

Theorem 3.2. If

a) $(\alpha^2-\beta^2)(a^2-b^2)\neq 0,$
б) $b(\alpha^2+\beta^2)+2\alpha\beta a\neq 0;$

then eigenfunctions of the boundary value problem

$$ay'(x)+by'(1-x)=\lambda y(x), x\in(0,1), \quad (1.1)$$

$$\alpha y(0)+\beta y(1)=0, \quad (1.2)$$

form a Riesz basis in the space $L^2(0,1)$.

4. Discussion of Results.

Remark 4.1. If

$$\begin{cases} b(\alpha^2+\beta^2)+2\alpha\beta a=0, \\ b2\alpha\beta+(\alpha^2+\beta^2)a=0, \end{cases}$$

then $(\alpha^2+\beta^2)^2-4\alpha^2\beta^2=0$, i.e.

$$(\alpha^2+\beta^2)^2-4\alpha^2\beta^2=(\alpha^2+\beta^2-2\alpha\beta)(\alpha^2+\beta^2+2\alpha\beta)=(\alpha-\beta)^2(\alpha+\beta)^2$$
$$=(\alpha^2-\beta^2)^2=0.$$

Remark 4.2.

a) If $C=-\sqrt{a^2-b^2}.$, then from the formula (2.15) we have

$$a\alpha+b\beta+(a\beta+b\alpha)e^{-i\mu}=\sqrt{a^2-b^2}.\left(\alpha+\beta e^{-i\mu}\right),$$

$$a\alpha+b\beta+(a\beta+b\alpha)e^{-i\mu}=\beta\sqrt{a^2-b^2}e^{-i\mu}+\alpha\sqrt{a^2-b^2},$$

$$\left(a\beta+b\alpha-\beta\sqrt{a^2-b^2}\right)e^{-i\mu}=\alpha\sqrt{a^2-b^2}-a\alpha-b\beta,$$

$$e^{-i\mu}=\frac{б\sqrt{a^2-b^2}-a\alpha-b\beta}{a\beta+b\alpha-\beta\sqrt{a^2-b^2}},$$

and from the formula (2.16) we have

$$e^{i\mu}=\frac{-\alpha\sqrt{a^2-b^2}-a\alpha-b\beta}{a\beta+b\alpha+\beta\sqrt{a^2-b^2}},=>$$

consequently, $e^{-i\mu}\cdot e^{i\mu}=1$.

б) If $C=\sqrt{a^2-b^2}.$, then from the formula (2.15) we have

$$a\alpha+b\beta+(a\beta+b\alpha)e^{-i\mu}=-\sqrt{a^2-b^2}.\left(\alpha+\beta e^{-i\mu}\right),$$

$$a\alpha+b\beta+(a\beta+b\alpha)e^{-i\mu}=-\beta\sqrt{a^2-b^2}e^{-i\mu}-\alpha\sqrt{a^2-b^2},$$

$$\left(a\beta+b\alpha+\beta\sqrt{a^2-b^2}\right)e^{-i\mu}=-\alpha\sqrt{a^2-b^2}-a\alpha-b\beta,$$

$$e^{-i\mu}=-\frac{\alpha\sqrt{a^2-b^2}+a\alpha+b\beta}{a\beta+b\alpha+\beta\sqrt{a^2-b^2}}.$$

5. Findings. Operator corresponding to this boundary value problem is not semi-bounded; therefore, variational methods are not suitable to study such problems, and this is a distinctive feature of this problem. In our opinion, such operators can be used to construct non-local transformation operators, and apply them to study spectral properties of operator sheaves.

ӘОЖ 517.929

А.Ш.Шалданбаев[1], С.М.Шаленова[2], М.Б.Иванова[3], А.А.Шалданбаева[4]

[1]Халықаралық Silkway университеті, Шымкент қ., Казақстан;
[2]Ш. Есенов атындағы Каспий мемлекеттік технологиялар мен инжиниринг университеті, Ақтау қ., Қазақстан;
[3]Оңтүстік Қазақстан медициналық академиясы, Шымкент қ., Казақстан;
[4]Аймақтық әлеуметтік-инновациялық университеті, Шымкент қ., Казақстан;

АРГУМЕНТІ АУЫТҚЫҒАН БІРІНШІ РЕТТІ ДИФФЕРЕНЦИАЛДЫҚ ТЕҢДЕУДІҢ ШЕКАРАЛЫҚ ЕСЕБІНІҢ СПЕКТРӘЛДІК ҚАСИЕТТЕРІ ТУРАЛЫ

Аннотация. Бұл еңбекте Аргументі ауытқыған бірінші ретті дифференциалдық теңдеудің шекаралық есебінің спектрәлдік қасиеттері зерттелді. Бір айта кетері, ауытқу теңдеудің үлкен ретті туындыларында кездеседі және оны қосымша шарттарсыз төменгі ретті мүшелерге ауыстыруға болмайды. Спектрәлді қасиеттер ретінде, біз оның меншікті векторлары мен оларға еншілес векторлар системасының толымдылығы мен базистігін таныймыз, сонымен бірге осы қасиеттер қатарына оның вөлтерлігін де жатқызамыз.

Түйін сөздер: аргументі ауытқыған теңдеу, толымдылық, базистік, вөлтерлік, Гаалдың формуласы, Лидскийдің теоремасы, Штурм –Лиувиллдің операторы, Рисстің базисі.

УДК 517.929

А.Ш.Шалданбаев[1], С.М.Шаленова[2], М.Б.Иванова[3], А.А.Шалданбаева[4]

[1]Международный университет Silkway, г. Шымкент, Казахстан;
[2]Каспийский государственный университет технологий и инжиниринга им. Ш.Есенова, г.Актау, Казахстан;
[3]Южно-Казахстанская медицинская академия, г. Шымкент, Казахстан;
[4]Региональный социально-инновационный университет, г. Шымкент, Казахстан.

О СПЕКТРАЛЬНЫХ СВОЙСТВАХ КРАЕВОЙ ЗАДАЧИ УРАВНЕНИЯ ПЕРВОГО ПОРЯДКА С ОТКЛОНЯЮЩИМСЯ АРГУМЕНТОМ

Аннотация. В данной работе изучены спектральные свойства краевой задачи дифференциального уравнения первого порядка с постоянными коэффициентами и отклоняющимся аргументом, при этом отклонение присутствует при старшем члене уравнения, и его нельзя перебрасывать без дополнительного условия на младшие члены уравнения. Под спектральными свойствами мы имеем в виду полноту и базисность системы собственных и присоединенных функций краевой задачи, а также вольтерровость.

Ключевые слова: уравнение с отклоняющимся аргументом, полнота, базисность, вольтерровость, формула Гаала, теорема Лидского, оператор Штурма - Лиувилля, базис Рисса.

Information about authors:
Shaldanbayev A.Sh. – doctor of physico-mathematical Sciences, associate Professor, head of the center for mathematical modeling, «Silkway» International University, Shymkent; http://orcid.org/0000-0002-7577-8402;
Shalenova S.M. - Yessenov University; Aktau; https://orcid.org/0000-0002-1378-3310;
Ivanova M.B. - South Kazakhstan medical Academy, Shymkent; https://orcid.org/0000-0001-6548-0699;
Shaldanbayeva A.A. - "Regional Social-Innovative University", Shymkent; https://orcid.org/0000-0003-2667-3097

REFERENCES

[1] Babbage C. An essay towards the calculus of calculus of functions, Part II., Philos Trans. Roy. Soc. London.106. p :179-256. London, 1816

[2] Przevorska- Rolewicz D. Equations with transformed argument an Algebraic approach. Warszawa. 1973. 354 p.

[3] Wiener J. Generalized solutions of functional differential equations, Singapore, World Sci. p:160-215, Singapore, 1993.

[4] Jack K. Hale Sjoerd M.,Verduyn Lunel, Introduction to Functional Differential Equations, Springer Science+Business Media, LLC, 1993.

[5] Cabada A., Tojo F.A.F. Differential Equations with Involutions. N.Y.: Atlantis Press, 2015.

[6] Busenberg S. Stability and Hopf Bifurcation for a Population Delay Model with Diffusion Effects//Journal of Differential Equations. 1996. 124, Article No 0003.-p. 80-107

[7] Cushing J.M. Bifurcation of Periodic Oscillations Due to Delays in Single Species Growth Models// J. Math. Biology.-1978. 6.p. 145-161

[8] Cushing J.M. Bifurcation of Periodic Solutions of Integro-differential Systems with Applications to time Delay Models in Population Dynamics//SIAM J. Appl. Math. December, 1977. Vol.33, No4.

[9] Watkins W., Modified Wiener equations. Int. J. Math. Math. Sci.Vol-27. p: 347-356. 2001.

[10] Watkins W.T., Asymptotic properties of differential equations with involutions. Int. J. Pure Appl. Math. Vol 44. p: 485-492, 2008.

[11] Burlutskaya M.Sh., Khromov A.P., Justification of Fourier method in mixed problems with involution. // Izv. Sarat. un-ty. New Ser. Maths. Mechanics. Informatics.-2011. vol.11, №4. p. 3-12.

[12] Burlutskaya M.Sh., Khromov A.P., Fourier method in mixed problem for a first-order partial differential equation with involution // Zh. Computed. Math and math. Ph. 2011. vol.51, №12. p. 2233-2246.

[13] Keldysh M.V., On completeness of eigenfunctions of some classes of non-self-adjoint linear operators // Success of Math Sciences. 1967. vol. 26, No. 4 (160). p. 15-41.

[14] Il'in V. A., Existence of a reduced system of eigen and associated functions for Xa non-self-adjoint ordinary differential operator // Number theory, mathematical analysis and their applications, Trudy Math. Inst. Steklov. 1976. 142. p. 148–155.

[15] Il'in V.A. Necessary and sufficient conditions for basis property and equal convergence with trigonometric series of spectral expansions, 1 // Differential Equations. 1980. vol. 16, № 5. p. 771-794.

[16] Il'in V.A. Necessary and sufficient conditions for basis property and equal convergence with trigonometric series of spectral expansions, 2 // Differential Equations. 1980. vol. 16, № 6. p. 980-1009.

[17] Il'in V.A. Necessary and sufficient conditions for basis property in L_2 and equal convergence with trigonometric series of spectral expansions and expansions in exponential systems // DAN SSSR. 1983. vol. 273, No. 4. p. 784-793.

[18] Il'in V.A. On unconditional basis property of systems of eigenfunctions and associated functions of a second-order differential operator on a closed interval // DAN SSSR. 1983. vol. 273, No. 5. p. 1048-1053.

[19] Il'in V.A. On relationship between type of boundary conditions and properties of basis property and equal convergence with trigonometric series of expansions of a non-self-adjoint differential operator by root functions // Differential Equations. 1994. V. 30, № 9. p. 1516-1529.

[20] Otelbaev M. Estimates for S-numbers and completeness condition for a system of root vectors of a non-self-adjoint Sturm-Liouville operator, Math. Notes, 1979, Vol. 25, No. 3, p. 409-418.

[21] Shkalikov A.A. Boundary value problems for ordinary differential equations with a parameter in boundary conditions // Trudy Sem. by I.G.Petrovsky. 1983. Vol. 9. p. 190-229.

[22] Gomilko A.M., Radzievsky G.V. Basis properties of eigenfunctions of a regular boundary value problem for a vector functional differential equation // Differential Equations. 1991. vol. 27, No.3. p. 385-395.

[23] Il'in V.A., Kritskov L. V. Properties of spectral expansions corresponding to non-self-adjoint differential operators // J. Math. Sci. (NY). 2003. 116, N 5. P. 3489–3550.

[24] Il'in V.A., Kritskov L.V. Properties of spectral expansions corresponding to non-self-adjoint operators, Functional analysis. Results of science and technology. Ser .: Rec.math. and its app. Them.view, M: VINITI, 2006, vol.96, p.5-105.

[25] Ibraimkulov A.M. On spectral properties of boundary value problem for an equation with deviating argument. News of AS KazSSR, ser. of ph. math. 1988. №3. p.22-25.

[26] Shaldanbayev A.Sh., Akhmetova S.T., On completeness of eigenvectors of the Cauchy problem. // Republican scientific journal "Science and Education of the SK" No.27, 2002. p. 58-62.

[27] Akhmetova S.T., On Bitsadze-Samarskii Problem for the Wave Equation, Mathematical Journal, Almaty. 2003, Vol. 3. №2 (8), p.15-18.

[28] Kalmenov T.Sh., Akhmetova S.T., Shaldanbayev A.Sh. To spectral theory of equations with deviating argument, Mathematical Journal, Almaty.2004.vol. 4, No. 3. P. 41-48.

[29] Shaldanbaev A.Sh. Criteria for Volterra property of differential operator of the first order with deviating argument, Bulletin of Karaganda University, "Mathematics" series, № 3 (47) / 2007, p.39-43.

[30] Sadybekov M.A., Sarsenbi A.M. Unconditional convergence of spectral expansions associated with a second-order differential equation with deviating argument. // Bulletin of KazNU. 2006. №2 (49) . p.48-54.

[31] Sadybekov M.A., Sarsenbi A.M. Solution of main spectral problems of all boundary value problems for a single differential equation of the first order with deviating argument. // Uzbek Mathematical Journal. 2007. №3. p.88-94.

[32] Sadybekov M.A., Sarsenbi A.M. On notion of regularity of boundary value problems for a second order differential equation with deviating argument. // Mathematical journal. 2007. vol.7, №1 (23). p. 82-88

[33] Sadybekov M.A., Sarsenbi A.M. Criterion for basis property of a system of the eigenfunctions of a multiple differentiation operator with involution. // Differential equations - 2012. vol.48, No. 8. p. 1126-1132

[34] Kopzhasarova A.A, Sarsenbi A.M. Basis Properties of Eigenfunctions of Second-Order Differential Operators with Involution//Abstract and Applied Analysis. 2012. Volume 2012, Article ID 576843. 6 pages doi:10.1155/2012/576843.

[35] Kopzhassarova A. A., Lukashov A. L., Sarsenbi A. M. Spectral properties of non-self-adjoint perturbations for a spectral problem with involution // Abstr. Appl. Anal. 2012. p. 1–5.

[36] Sarsenbi A.M., Tengaeva A.A. On basis properties of root functions of two generalized eigenvalue problems// Differential Equations.-2012.- vol. 48, no. 2.- p. 306–308

[37] Imanbaeva A.B., Kopzhasarova A.A., Shaldanbaev A.Sh., Asymptotic expansion of solution of a singularly perturbed Cauchy problem for a system of ordinary differential equations with constant coefficients.\\ "News of NAS RK. Physics and Mathematics Series, 2017, No. 5, 112-127.

[38] Kopzhasarova A.A., Shaldanbaev A.Sh., Imanbaeva A.B. Solution of singularly perturbed Cauchy problem by the similarity method. "News of NAS RK. Physics and Mathematics Series, 2017, no 5, p.127-134.

[39] Amir Sh. Shaldanbayev, Manat T. Shomanbayeva ,Solution of singularly perturbed Cauchy problem for ordinary differential equation of second order with constant coefficients by Fourier method ,Citation: AIP Conference Proceedings 1880, 040017 (2017); doi: 10.1063/1.5000633 View online: http://dx.doi.org/10.1063/1.5000633 View Table of Contents: http://aip.scitation.org/toc/apc/1880/1 Published by the American Institute of Physics.

[40] Akulbaev M.I., Beisebaeva A., Shaldanbaev A. Sh. On periodic solution of the Goursat problem for a wave equation of a special form with variable coefficients (in English), News of NAS RK. Physical and mathematical Series. № 1. 2018, p.34-50.

[41] Shaldanbaeva A. A., Akylbayev M.I., Shaldanbaev A. Sh., Beisebaeva A.Zh., The spectral decomposition of cauchy problem's solution for laplace equation, News of the National Academy of Sciences of the Republic of Kazakhstan Physico-mathematical Series, Issn 1991-346X. https://doi.org/10.32014/2018.2518-1726.10 Volume 5, Number 321 (2018), 75–87.

[42] Shaldanbayev A.Sh., Shaldanbayeva A.A., Shaldanbay B.A., On projectional orthogonal basis of a linear non-self - adjoint operator, News of the national academy of sciences of the republic of Kazakhstan Physico-mathematical series7,Issn 1991-346X https://doi.org/10.32014/2019.2518-1726.15 Volume 2, Number 324 (2019), 79 – 89.

[43] Akylbayev M.I., Shaldanbayev A.Sh., Orazov I., Beysebayeva A.. About single operator method of solution of a singularly perturbed Cauchy problem for an ordinary differential equation n – order, News of the national academy of sciences of the republic of Kazakhstan Physical-mathematical series, Issn 1991-346X https://doi.org/10.32014/2019.2518-1726.8,Volume 2, Number 324 (2019), 17 – 36.

[44] Ashyralyev A., Sarsenbi A. M. Well-posedness of an elliptic equations with an involution // EJDE. 2015. 284. P. 1–8.

[45] Kritskov L. V., Sarsenbi A. M. Spectral properties of a nonlocal problem for the differential equation with involution // Differ. Equ. 2015. 51, N 8. P. 984– 990.

[46] Kurdyumov V. P. On Riesz bases of eigenfunction of 2-nd order differential operator with involution and integral boundary conditions // Izv. Saratov Univ. (N.S.), Ser. Math. Mech. Inform. 2015. 15, N 4. P. 392–405.

[47] Kirane M., Al-Salti N. Inverse problems for a nonlocal wave equation with an involution perturbation // J. Nonlinear Sci. Appl. 2016. 9. P. 1243–1251.

[48] Baranetskij Ya. O., Kolyasa L. I., Boundary value problem for second order differentialoperator equation with involution, Vestnik Nath.University, “Lvovskaya polytech”,“Phys.-math.science”, № 871, 2017, p. 20–26.

[49] Kritskov L.V., Sarsenbi A.M.,Equiconvergence property for spectral expansions related to perturbations of the operator $-u''(-x)$ with initial data, Filomat, 2018,том 32, № 3, p. 1069-1078.

[50] Kritskov L.V., Sadybekov M.A., Sarsenbi A.M., Nonlocal spectral problem for a second-order differential operator with an involution // Bulletin of Karaganda University -MATHEMATICS, 2018 № 3 (91), p. 53-60.

[51] Kritskov L.V., Sadybekov M.A., Sarsenbi A.M., Properties in L_p of root functions for a nonlocal problem with involution, Turkish Journal of Mathematics, Scientific and Technical research Council of Turkey - TUBITAK/Turkiye Bilimsel ve Teknik Arastirma Kurumu (Turkey), 2019, vol. 43, p. 393-401.

[52] Vladykina V.E., Shkalikov A.A., Spectral Properties of Ordinary Differential Operators with Involution, Dokl. Akad. Nauk, 2019, Vol. 484, No. 1, p. 12–17.

[53] Shaldanbaev A.Sh., Kulazhanov G.S. On spectral properties of one model operator with deviating argument // International Conference VEKUA-100, Novosibirsk 2007.

[54] Bari N.K. Biorthogonal systems and bases in the Hilbert space, // Uch.zap.MGU. 1951. vol.4, Issue.148. p. 69-106.

[55] Gokhberg I.T., Krein M.G. Introduction to the theory of linear non-self-adjoint operators in a Hilbert space, M: Nauka, 1965, 448 p.

[56] Naimark M.A. Linear Differential Operators. M .: Science, 1969. 528 p.

[57] Kesselman G.M. On unconditional convergence of expansions in eigen functions of some differential operators. // News of univ. Math. 1964. № 2 (39). p. 82-93.

[58] Mikhailov V.P. On Riesz bases in $L_2(0,1)$. // DAN USSR. 1962. vol. 144, № 5. p. 981-984.

[59] Lidsky V.B. Non-self-adjoint operators having a trace. DAN USSR, 1959, vol.125. No.3, p. 485-488.

[60] Brislawn C., Kernels of trace class operators. // American Mathematical Society, V.104, № 4, 1988, p. 1181-1190.

N E W S
OF THE NATIONAL ACADEMY OF SCIENCES OF THE REPUBLIC OF KAZAKHSTAN
PHYSICO-MATHEMATICAL SERIES
ISSN 1991-346X **https://doi.org/10.32014/2019.2518-1726.57**
Volume 5, Number 327 (2019), 40 – 50

МРНТИ: 41.29.21; 41.29.25
UDK 524

D. Kairatkyzy

Al-Farabi Kazakh National University, “V.G. Fesenkov Astrophysical Institute”,
JSC “national Center of Space Research and Technology”, Aerospace Committee
of the MDAI of the Republic of Kazakhstan
kairatkyzy_dina90@mail.ru

INVESTIGATION OF THE DISTRIBUTION OF DARK MATTER IN THE GALACTIC STRUCTURE

Abstract. We investigate the formation of disk-bulge-halo systems by including the basic components in the theory of the formation of galaxy. The purpose of this article is to investigate the distribution of dark matter in the Galactic structure and examine the impact of subhalo on the halo and the disk components to be included in one simple scenario of the formation of the galaxy. We investigate several important characteristics of galaxies, such as coordinates, position, velocity and masses, to form a stable component of the galaxy. We search for the parameters and physical processes that determine the subhalo-halo ratio, and thus largely explain the origin of the collision or other obstacles through the galactic halo. The spread over the radial velocities of the halo, combined with the spread of obstacles in the distances from the center of the galaxy, may explain the observed spread over the properties of the disk and the bulge. The paper uses data from Auriga_proper_unit - a data file of the main galaxies in Aurig-6 before free run. The units of data length used in Gadget2, such as coordinates and density, are converted from Mpc to kpc and also include star_age.

Key words: dark matter (DM), radial velocity, Galactocentric coordinate system.

I. Introduction

One of the most compelling puzzles in present day astronomy is the question how galaxies formed. In particular, we need to understand the wide variety of sizes, masses and morphologies of galaxies observed, as well as their coordinates, position, velocity and masses. The main morphological parameter that sets the classification of galaxies in the (revised) Hubble diagram is the disk-to-bulge ratio. Disk dominated systems such as spirals are believed to have formed by cooling of the baryonic matter inside a virialized dark halo. As the gas cools, its specific angular velocity is conserved, and the amount of angular velocity of the dark halo thus determines the size of the disk [1].

We envision an inside-out formation scenario for the bulge. It is assumed that the bulge forms out of the low-angular velocity material in the halo, which cools and tries to settle into a small, compact disk. Such disks are however unstable, and we assume here that this instability, coupled with the continuous supply of new layers of baryonic matter that cool and collapse, forms the bulge. This inside-out bulge formation is self-regulated in that the bulge grows until it is massive enough to allow the remaining gas to form a stable disk component. We do not describe the bulge formation in any detail but merely use empirical relations of the characteristic structural parameters of bulges and ellipticals to describe the end result of the formation process as a realistic galaxy. We use this simple formation scenario to investigate the predicted disk-to-bulge ratios and disk scale-lengths as a function of the halo angular velocity, and as a function of formation redshift and cosmology.

II Observational results

In this paper we use data from Auriga_proper_unit - a data file of the main galaxies in Aurig-6 before free run. The units of data length used in Gadget2, such as coordinates and density, are converted from Mpc to kpc and also include star_age. Snapshot_000 is the initial condition of collision simulation, snapshot_029 is a snapshot when the distance between the satellite is about 10 kpc, snapshot 032 is a snapshot when the distance to the satellite is about 5 kpc, and snapshot when the distance to the satellite is about 1 kpc.

In each snapshot file, there are 6 types of particles: gas (type 0), dark matter (type 1), disk (type 2), bulge (type 3), star (type 4; also include wind particles) and black hole (type 5). Gas particles only exist in the host galaxy. Dark matter particles exist in both the host and the satellite: those from the host with particle ID <= 2701512 and the satellite with particle ID > 2701512. Disk and bulge particles only exist in the satellite – they together form its stellar component. Star particles and black hole particle only exist in the host. In total, there are 667454 gas particles, 2371259 dark matter particles (2034059 in the host and 337200 in the satellite), 100000 disk particles, 25999 bulge particles, 1575406 star particles and 1 black hole.

The snapshot files only contain the coordinates, the velocities, the particle IDs, the potentials and the masses (solar mass), and for gas particles, the densities and several other parameters. The units of these data are the same as Illustris, with Hubble parameter h=0.6777. If you want to read the stellar age, metallicity or other fields of particles from the host galaxy provided by Auriga, please refer to the file 'Auriga_proper_units.hdf5'. Note that in this file, I have changed the unit of length of all the data fields that also exist in the snapshot files to kpc/h, while other data fields are unchanged, because this file is used as an initial condition file for my simulation. So when you use it, be careful of the units. For your convenience, here is a free software that can read and display data stored in hdf5 files: https://www.hdfgroup.org/downloads/hdfview/.

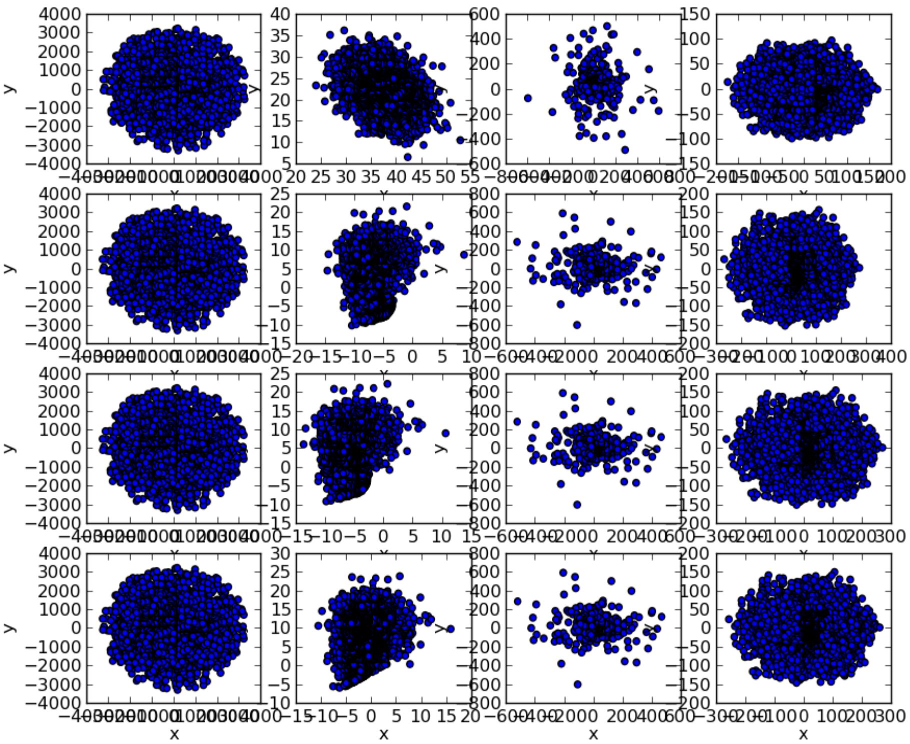

Figure 1 - Distribution of stars in the horizontal coordinate plane. The panels are for stars in our sample located at initial conditions of collision simulation, satellite data from the disk about 1kpc, 5kpc and 10 kpc. a) The first column represents two-dimensional histogram in bins of $D_x = 0.1kpc$ and $D_y = 0.1kpc$ for halo, with the darkness being proportional to the number of counts.; b) The second column represents plane coloured as a two-dimensional histogram of disk; c) same as for bulge; d) but for subhalo

Figure 1 shows the distribution of particles with respect to the center of the Galaxy for the he units of data length used in Gadget2. Snapshot_000 is the initial condition of collision simulation, snapshot_029 is a snapshot when the distance between the satellite is about 10 kpc, snapshot 032 is a snapshot when the distance to the satellite is about 5 kpc, and snapshot when the distance to the satellite is about 1 kpc. In which orbital evolution and masses are consistent with previous models. This model can reproduce the observed location and the LA reasonably well and shows bifurcated structures, which appears to be consistent with observations.

III Distances and Geometry

Remind that galactic coordinates system this is the system with origin placed on the Sun and extended through the center of Galaxy. Its plane coincides with the plane of Galaxy dick [2]. In disk. In doing this, its latitude b is measured from galaxies plane to an object and takes magnitudes from −90˚ up to +90˚. Galactic longitude l is measured at the Galaxy plane from the baseline connected the Sun and galactic center up to the baseline connected the Sun and object. Counting directs to the same way that the right ascension in the second equatorial coordinates. Therefore the galactic longitude puts i limits from 0 ˚ up to 360˚. The position of object in galactic coordinates describes by matrix expression

$$x = r\cos\alpha\cos\delta$$
$$y = r\sin\alpha\cos\delta$$
$$z = r\sin\delta$$

The longitude-velocity distribution (Figs. 1b and 2b) is approximately sinusoidal and that of the latitude-velocity distribution (Figs. 1c and 2c) follows a cosine law. In consequence, the radial velocity momentum distribution of the LMCs can be represented by the following formula:

$$L_x = y \cdot v_z + z \cdot v_y$$
$$L_y = x \cdot v_z + z \cdot v_x$$
$$L_z = x \cdot v_y + y \cdot v_x$$

We assume that we start with a 3D position in the ICRS reference frame: a Right Ascension, Declination, and heliocentric distance (α, β, r). We can convert this to a Cartesian position using the standard transformation from Cartesian to spherical coordinates:

$$r = \sqrt{x^2 + y^2 + z^2}$$

where $v_r \approx 200 - 230 km/\sec$. This distribution law admits a simple interpretation (or “inversion”), namely: it reflects a roughly uniform flow of HVCs that comes approximately from galactic coordinates $l_0 = 90^0$ and $b_0 = 0^0$ and that encloses the whole Galaxy. If $v_{\odot}$ and v_r are the velocities of the Sun and of the LMC flow with respect to the Galactic center respectively, the radial velocities of the LMCs with respect to the LSR are given by

$$v_r = \frac{x \cdot v_x + y \cdot v_y + z \cdot v_z}{r}$$

This model is therefore one of the successful models in the present study. The physical properties can be well reproduced by the present models, as long as we adopt the velocity type. However, models with the velocity type cannot reproduce well the observed locations. The physical properties in models with different velocity types are briefly discussed in Figure 2.

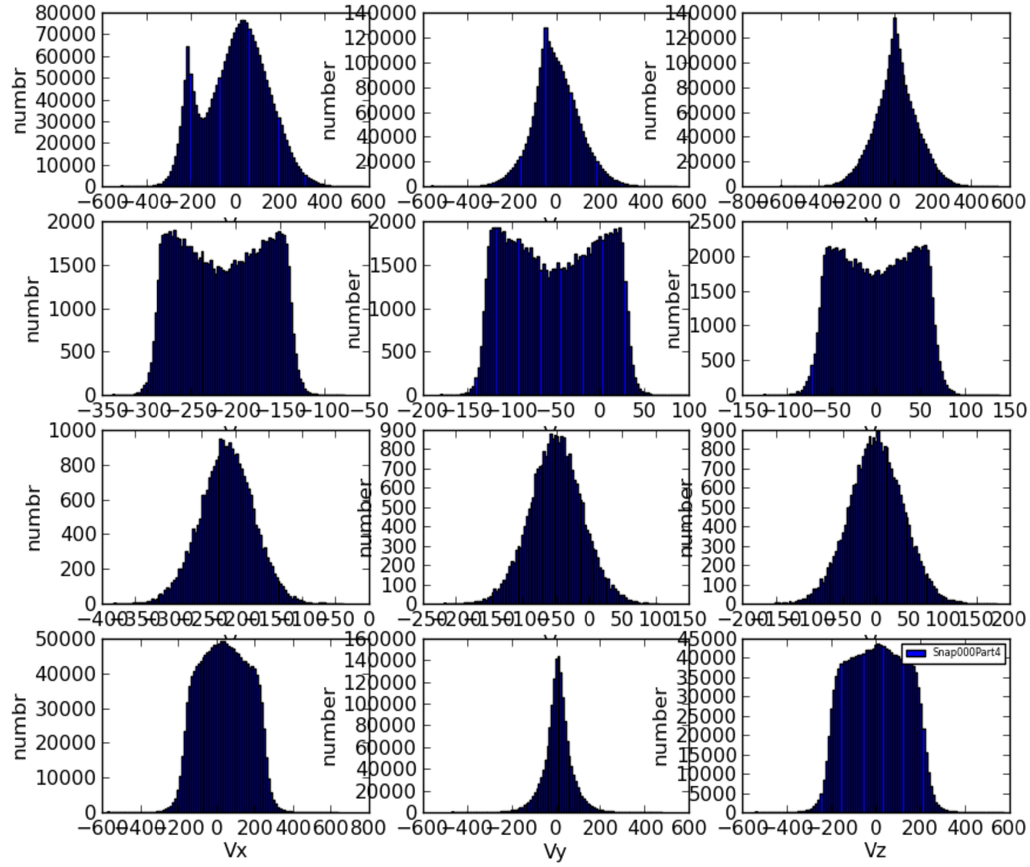

Figure 2 - Distribution of velocity in the horizontal coordinate plane. The panels are for stars in our sample located at the satellite data from the disk about 1kpc, from left to right is velocity in v_x, v_y, v_z coordinate direction, from top to bottom stellar halo, disk, bulge and dark halo

IV Observational results

We explore the parameter space in terms of the coordinates, position, velocity and masses, and the bar pattern speed. Besides, we run control simulations without satellite for both 2-d and 3-d configurations. All simulations were run for 8-12 kpc from the sun, an order of magnitude longer than the satellite merger timescale. The models are listed in Table 1, showing also the amount of mass that reaches the inner 8 kpc (a generous definition of the central region).

Figure 6 shows the distribution of the star velocity in the horizontal coordinate plane for the its units of data length used in Gadget2. Snapshot_000 is the initial condition of collision simulation, snapshot_029 is a snapshot when the distance between the satellite is about 10 kpc, snapshot 032 is a snapshot when the distance to the satellite is about 5 kpc, and snapshot when the distance to the satellite is about 1 kpc. In which orbital evolution and masses are consistent with previous models. This model can reproduce the observed location and the LA reasonably well and shows bifurcated structures, which appears to be consistent with observations.

From the parameter astrometric solution and line-of-sight velocities of these particles, we derived distances (as $1/\varpi$), positions and velocities in the cylindrical Galactic reference frame, that is ($R, \varphi, Z, V_R, V_\varphi, V_Z$). For convenience, we took φ positive in the direction of Galactic rotation and with origin at the line Sun-Galactic Centre. For these transformations, we adopted a vertical distance of the Sun above the plane of 8 kpc, a distance of the Sun to the Galactic centre of 8.34 kpc and a circular velocity at the Sun radius of $V_c\left(R_\odot\right) = 240\ km \cdot s^{-1}$. We assumed a peculiar velocity of the Sun with respect of the Local Standard of Rest of $\left(U_\odot, V_\odot, W_\odot\right) = \left(11.1, 12.24, 7.25\right)\ km \cdot s^{-1}$. Our choice of values give

$\left(V_c\left(R_\odot\right)+V_\odot\right)/R_\odot=30.2km\cdot s^{-1}kpc^{-1}$, which is compatible with the reflex motion of galaxy. To derive the uncertainties in these coordinates, we propagate the full covariance matrix. The median errors in the V_R, V_φ, V_Z velocities are 1.4, 1.5, and $1.0km\cdot s^{-1}$, respectively, and 80% of dark matter particles have errors smaller than 3.3, 3.7, $2.2km\cdot s^{-1}$ in these velocities. The positions in the Cartesian coordinates X-Y and X-Z of the sample are shown in Extended Data Fig.1.

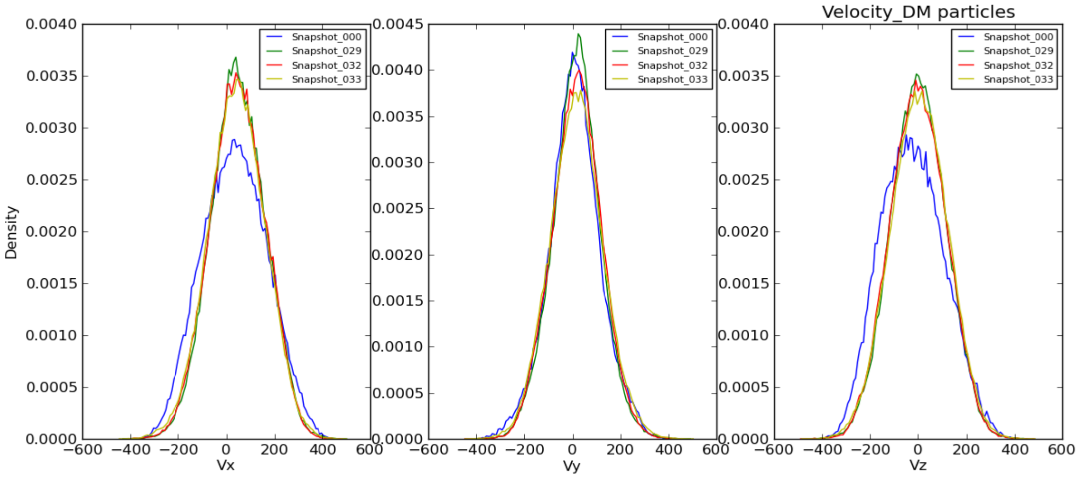

Figure 12 - Distribution of radial velocities (v_x, v_y, v_z) of the dark matter particles within 5 kpc of the sun in various snapshots with the center of the main galaxy as the coordinate system. The position of the sun is x=8kpc

Given an initial distribution of stars $Z\left(t=0\right)$ and $V_Z\left(t=0\right)$, the vertical amplitudes of the orbits can be derived through the conservation of energy and using the fact that at the vertical turn-around point of the orbit $\left(V_Z=0\right)$, the (vertical) kinetic energy is null. Assuming that stars follow a simple harmonic oscillation (but with different frequencies), the movement of the stars with time is described by Eq. (3) where the initial phase of the stars $\varphi 0\equiv\varphi\left(t=0\right)$ is obtained from the initial distribution of Z and V_Z and the corresponding amplitudes.

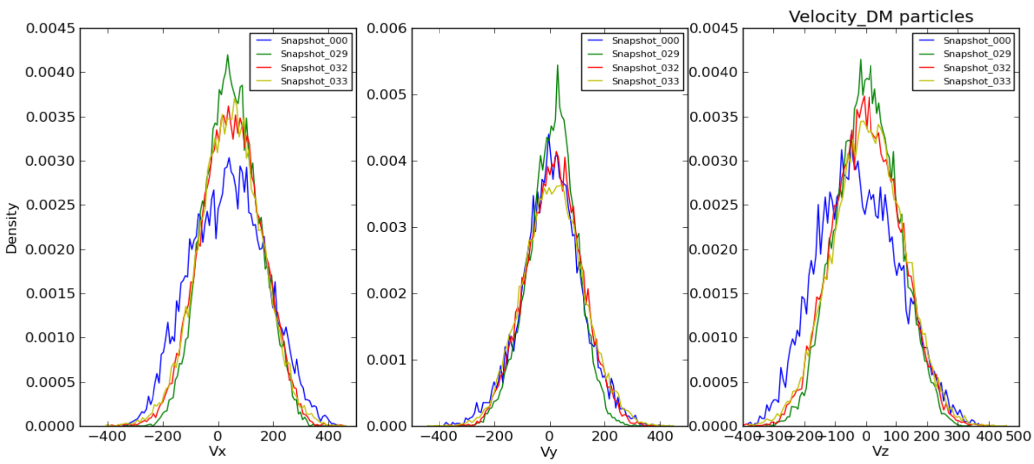

Figure 13 - Distribution of radial velocities (v_x, v_y, v_z) of the dark matter particles within 2 kpc of the sun in various snapshots with the center of the main galaxy as the coordinate system

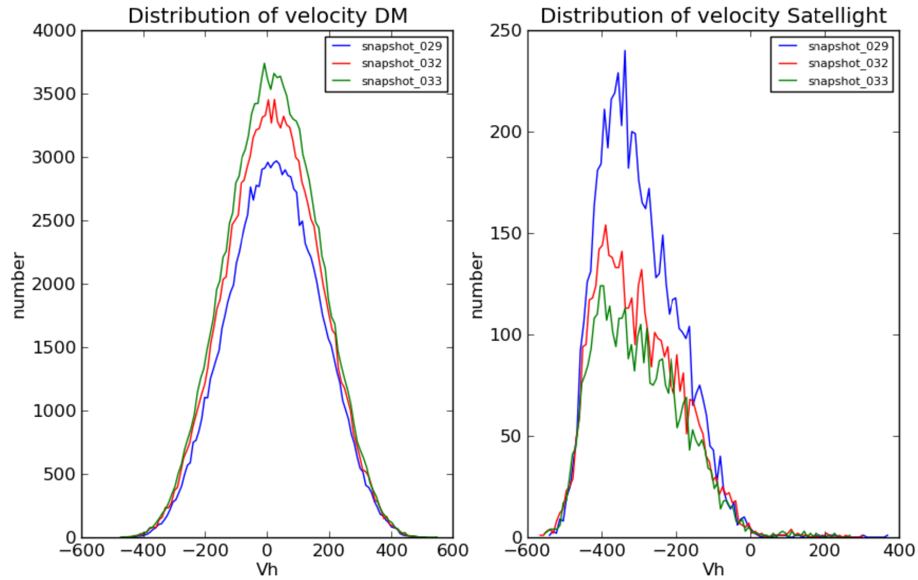

Figure 14 - Distribution of heliocentric velocities (v_h) obtained for the solar reflex motion using the circular motion of the LSR at the Sun and Sun's peculiar velocity of the satellite and dark matter and satellite particles within 2 kpc of the sun in various snapshots with the center of the main galaxy as the coordinate system

For part of our study, we selected from our sample the 2371259 dark matter particles located in the solar Galactic cylindrical ring, that is with Galactocentric radius $8.24 < R < 8.44\ kpc$ (dotted lines in Extended Data Fig.2). For this selection, the median errors in the V_R, V_φ, V_Z velocities are 0.5, 0.8, and $0.6\ km \cdot s^{-1}$, respectively, and 80% of dark matter particles have errors smaller than in these velocities 1.1, 2.0, 1.3 $km \cdot s^{-1}$. We note that the velocity uncertainties are significantly smaller than the sizes of the substructures detected and that, together with the number of dark matter particles in our samples, this is what made possible their detection. Although there are some correlations between the astrometric Gaia observables, these are not responsible for the correlations and substructure seen in our phase space plots. This is because the particles in our sample are distributed through all sky directions, and the phase space coordinates come from combinations of astrometric measurements and radial velocities, in different contributions depending on the direction on the sky. Besides, the astrometric correlations for our sample are small (smaller than 0.2 in their absolute value for more than 50% of dark matter particles) and this, combined with the small errors, makes their contribution nonsignificant.

Alternatively, we used the mode of the posterior distribution and a prior of an exponentially decreasing density of dark matter particles with a scale length of 8 kpc from the center of the Milky Way. We found the differences between this distance determination and the inverse of the parallax are between -2% and 0.6% for 90% of the 6,376,803 dark matter particles for the different snapshots. Therefore, the difference in velocity presented here is in the change of v_y and v_z. We can see that in the initial condition of snapshot_000, the dark matter particles move according to the original trajectory, but when the satellite passes through the galaxies, the velocity of the dark matter particles in the snapshot-029, snapshot-032 and snapshot-033 changes subtly. When observing the running trajectory on the side of the v_x, we cannot observe the large parallax error due to the deviation of the line of sight direction, but for velocity v_y, v_z due to the longitudinal observation, when the satellite passes through the galaxies, we can find the radial velocity of dark matter particles has changed. For these dark matter particles, the estimator of the parallax inverse will produce a non-physical distance.

V. Models for the vertical phase mixing of dark matter density

We first reproduced the spiral shape observed in the $Z - V_Z$ plane with the Gaia DR2 data by using a simple toy model. Often the classic harmonic oscillator is employed to describe the vertical movement of dark matter particles in galaxy disks under the epicyclic theory. However, in this approximation, which is valid only for very small amplitude orbits for which the potential changes little vertically, stars have the same vertical oscillatory frequency ν and there is no phase mixing, unless orbits at different guiding radius, thus with different frequencies, are considered [3]. Instead, we used an anharmonic oscillator with the potential. We took the coefficients $\alpha_0, \alpha_1, \alpha_2$ corresponding to the expansion for small Z, derived elsewhere, with values of $a = 6.5kpc,\ b = 0.26kpc,\ M = 10^{11} M_{\odot}$. These coefficients α depend on Galactocentric radius R.

The phase space evolution described above is shown in the top row of Extended Data Fig.3. Initially, the particles followed a Gaussian distribution in $Z(t=0)$ and $V_Z(t=0)$ with mean and dispersion of $-0.1kpc$ and $0.04kpc$, and $-2km \cdot s^{-1}$ and $1km \cdot s^{-1}$, respectively. We located all particles at the same Galactocentric radius $R = 8.5kpc$, and thus, they all move under the same functional form of the vertical potential. The initial conditions are shown in Extended Data Fig. 3a, where we colour-coded the particles according to their period. Following Eq. (3), each star follows a clockwise rotation in the $Z - V_Z$ plane. However, they do it at a different angular speed: stars with smaller period located at the closer distances from the mid-plane $(Z = 0)$ revolve faster than those located at the largest distances from the mid-plane. The whole range of frequencies is what creates, therefore, the spiral shape. Extended Data Fig.3b shows the evolution of the system for three initial phases of the time evolution when the spiral shape begins to form. Extended Data Fig.3c shows the spiral shape after $1000Myr$ of evolution.

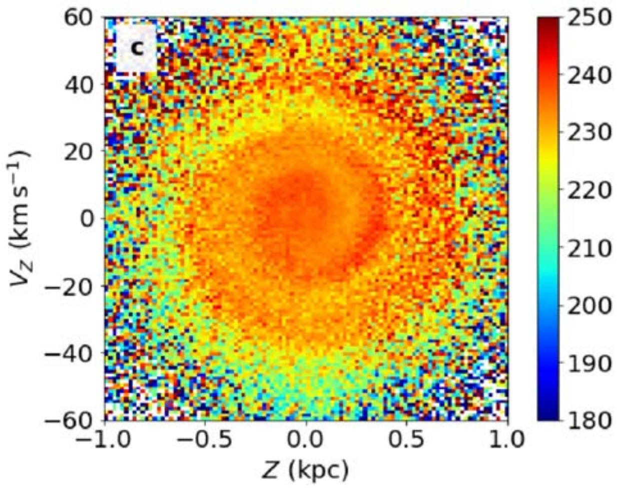

Figure 7 - Distribution of stars in the horizontal coordinate plane within 2 kpc of the sun. The panels are for stars in our sample located at initial conditions of collision simulation, satellite data from the disk about 10kpc and 1 kpc. a) The first column represents two-dimensional histogram in bins of $D_x = 0.1kpc$ and $D_y = 0.1kpc$ for halo, with the darkness being proportional to the number of counts.; b) The second column represents plane coloured as a two-dimensional histogram of disk

In the Gaia data, we do not see a thin spiral but a thick one, with many of the stars in the volume participating in it [4]. A similar effect was reached with our toy model when we included particles at different radius for which the vertical potential changes and the range of amplitudes/frequencies also changes. In Extended Data Fig.3 (bottom row) we let the same system evolve as in the top row but starting with initial radius following a skewed normal distribution, which creates a density decreasing with radius as in galaxy disks, with skewness of 10, location parameter of $8.4kpc$ and scale parameter of $0.2kpc$. The spiral structure is now thickened similarly to the data, with higher density of stars at the leading edge of the spiral.

To estimate the time of the phase mixing event from the spiral seen in the Gaia data (Fig.1) using Eq. (4), we needed to locate two consecutive turns of the spiral and estimate their vertical frequencies from their amplitudes and mean radius. For this, we used Extended Data Fig.5 which has been colour coded as a function of median guiding radius. This was approximated as $R_g \sim \frac{V_\varphi R_{\odot}}{V_c\left(R_{\odot}\right)}$, under the hypothesis of a flat rotation curve, where we used the values of $R_{\odot} = 8.34kpc$ and $V_c\left(R_{\odot}\right) = 240km \cdot s^{-1}$ assumed in the coordinate transformation of the data. In this panel we see that the density gradient across the spiral shape is created by stars with different guiding radius that arrive at the solar neighbourhood due to their different amplitudes of (horizontal) radial oscillation.

Applying this method to several streams at a variety of Galactocentric distances and orientations with respect to the Galactic disk would allow us to build a comprehensive map of the distribution of DM in the halo – its shape, density profile, and orientation [5]. In the last few years evidence for dSph galaxy tidal tails has been discovered around Milky Way satellites at very large Galactic radii, and other distant streams are known. With SIM Lite, such distant streams can be used to trace the Galactic mass distribution as far out as the virial radius with an unprecedented level of detail and accuracy. This would provide the very first, accurate three-dimensional observational assessment of the shape and extent of a galactic-scale DM halo.

We can begin to understand their spatial distribution and kinematics in stratified formation scenarios as satellite galaxies traverse the main cluster of galaxies in association with the ability to cause tidal flows in the CDR clumps [6]. The global effect has been proposed that re-ionization in this era strongly influences the initial motion trajectory of dark matter particles, directly reaching the tidal flow of a larger mass scale, equivalent to the scale of the Magellanic Cloud [7]. Therefore, the dark matter particle composition and globular clusters of our protogalaxies are distributed in the center of the cluster of galaxies. Since the dark matter particles are too hot to cool efficiently, thousands of similar mass halos are generated during the movement of the original running track. This situation can explain the problem of uneven distribution of dark matter particles caused by satellite galaxies crossing the main galaxies, observing the uneven distribution of density among the thousands of DM substructures visible in Figure 8 at the center of the main galaxies.

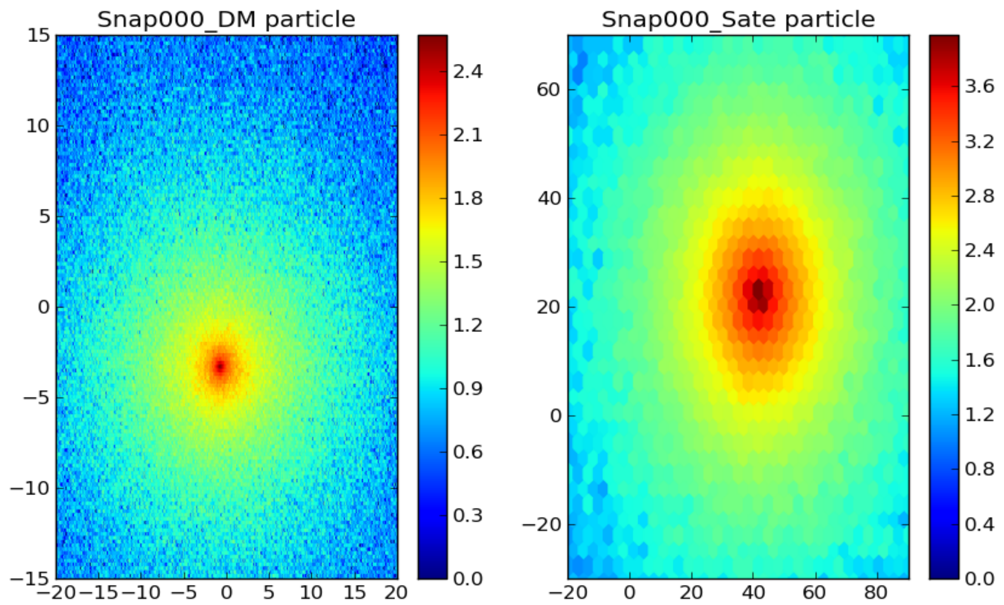

Figure 8 - The density distribution of projections in the Z direction drawn by the particle ID to distinguish the two galaxies (satellite particles and dark matter particles for snapshot_000). The density unit is $(kpc/h)^{-2}$

Most of the rare, luminous protogalaxies rapidly merge together, their stellar contents and DM becoming smoothly distributed and forming the Galactic stellar and dark halo (Figure 4-8). The metal-poor globular clusters and old halo stars formed in these early Milky Way structures become tracers of this early evolutionary phase, centrally concentrated and naturally reproducing the observed steep number density fall off with radius. The most outlying substructures fall in late and survive to the present day as our familiar satellite galaxies. The observed radial velocity dispersion profile and the local radial velocity anisotropy of Milky Way halo stars are successfully reproduced in this model, but only with full three-dimensional orbits can we be assured that the orbital shapes are truly consistent with predictions.

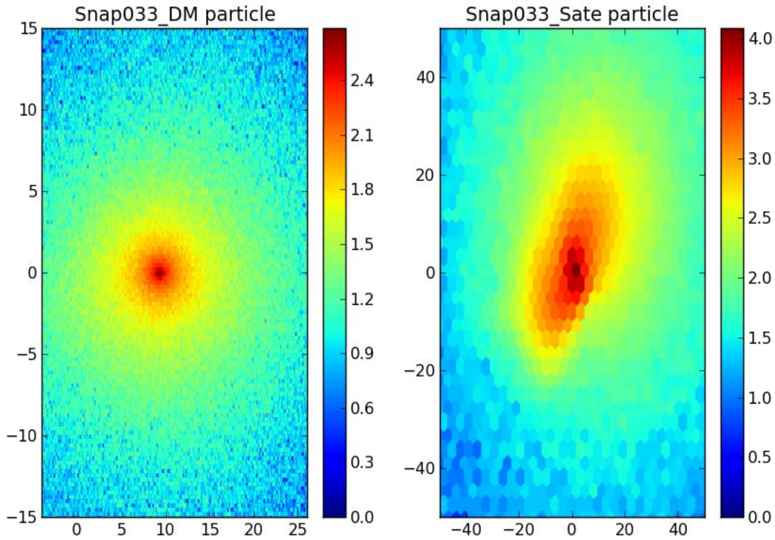

Figure 9 - The density distribution of projections in the Z direction drawn by the particle ID to distinguish the two galaxies (satellite particles and dark matter particles for snapshot_033). The density unit is $(kpc/h)^{-2}$

Determining the nature of the DM that surrounds galaxies and overwhelms the gravitational force from visible matter constitutes a fundamental task of modern astrophysics [8]. CDM particles are characterized by low initial velocity dispersion and high phase space density, resulting from a relatively heavy particle mass. After the satellite galaxies cross the main galaxies, they cause tidal currents in the center of the total cluster due to external shocks, which affect the distribution of dark matter particles, with steep density cusps at the center. In cosmologies with a somewhat lighter DM particle there are reduced phase space densities and higher velocity dispersions. These alternative models, broadly classified as warm DM, produce more constant density cores in galactic halos. In this sense, by precisely measuring the shape of the central DM density profile (characterized by the logarithm of the slope there), one places important constraints on the primordial phase space density of DM, which in turn bears on such microphysical properties of the DM particle as its mass and details of its formation mechanism.

Based on measured mass-to-light ratios, dwarf spheroidal (dSph) galaxies occupy the least massive known DM halos in the Universe. Dwarf spheroidals are also unique among all classes of galaxies in their ability to probe the particle nature of DM, because phase space cores resulting from the properties of the DM particle are expected to be most prominent in these small halos. In recent years, the measurement of line-of-sight velocities for upwards of a thousand stars in several dSphs has allowed for a precise determination of their masses. However, despite the great progress made in estimating masses of these systems, determining the logarithmic slope of their central density profile, and thus the nature of the DM contained within, remains elusive.

VI. Conclusion

Most of the stars in our Galaxy including our Sun move in a disk-like component and give the Milky Way its characteristic appearance on the night sky. As in all fields in science, motions can be used to reveal the under lying forces, and in the case of disk stars they provide important diagnostics on the structure and history of the Galaxy. But because of the challenges involved in measuring stellar motions, samples have so far remained limited in their number of stars, precision and spatial extent. This has changed dramatically with the second Data Release of the Gaia mission which has just become available. Here we report that the phase space distribution of stars in the disk of the Milky Way is full of substructure with a variety of morphologies never observed before, namely snail shells and ridges when spatial and velocity coordinates are combined. The nature of these new substructures implies that the disk is phase mixing from an out of equilibrium state, and that it is strongly affected by the Galactic bar and/or spiral structure.

The ability of Auriga_proper_unit - by used in Gadget2 to make μ as measurements of the positions of faint stars is unmatched among all planned missions. Tis simulation method will be able to probe accurately the three-dimensional stellar phase space distribution around the outskirts of our own Galaxy, within a nearby sample of dwarf galaxies, and in other Local Group systems – and these are the only galaxies in the Universe for which such data will be available. These measurements provide unique windows on some key astrophysical problems, from galaxy formation and the structure of DM halos, to the nature of DM itself.

The work was carried out within the framework of Project No. AP05134454 "Evolution of the perturbations in the density of dark matter in a very early Universe", financed by the JSC "National Center for Space Research and Technology", Aerospace Committee of the MDAI of the Republic of Kazakhstan.

Author express their gratitude to professor Yougang Wang from National Astronomical Observatories of Chinese Academy of Sciences for the problem forwarding and the permanent supporting for its solving.

Д. Қайратқызы

Әл-Фараби атындағы ҚазҰУ, «В.Г. Фесенков атындағы Астрофизика Институты», «Ұлттық ғарыштық зерттеулер мен технологиялар орталығы»АҚ, Қазақстан Республикасы ММАИ аэроғарыштық комитеті

ГАЛАЛТИКАЛЫҚ ҚҰРЫЛЫМЫНДАҒЫ ҚАРАҢҒЫ МАТЕРИЯНЫҢ ТАРАЛУЫН ЗЕРТТЕУ

Аннотация. Галактиканың қалыптасу теориясындағы негізгі компоненттерді қосу арқылы дискілік-гало-гало жүйелерінің қалыптасуын зерттейміз. Бұл мақаланың мақсаты галактик құрылымында қараңғы материяның таралуын зерттеу және негізгі галоға субгалонның әсерін, сонымен қатар галактиканың қалыптасуының қарапайым сценарийіне енетін диск компоненттерін зерттеу болып табылады. Галактиканың тұрақты компоненттерін қалыптастыру үшін координаттар, орналасу, жылдамдықтар және массалар сияқты галактикалардың бірнеше маңызды сипаттамаларын зерттейміз. Субгало-гало қатынасын анықтайтын параметрлер мен физикалық процестерді іздейміз, осылайша галактикалық гало арқылы соқтығысудың немесе басқа кедергілердің пайда болуын айтарлықтай түсіндіреміз. Галактиканың орталығынан қашықтықта кедергілер таралуымен біріктірілген субгалосының радиалды жылдамдықтары бойынша таралуы дискінің қасиеттері мен қабынуының байқалған таралуын түсіндіре алады. Бұл құжатта Auriga_proper_unit - Aurig-6 негізгі галактикалардың деректер файлы еркін айналымнан бұрын қолданады. Gadget2-де координаттар мен тығыздық сияқты қолданылатын деректер ұзындығының бірліктері, мпк-дан кпк-ға дейін өзгертіледі және жұлдыз_жасын қамтиды.

Түйін сөздер: қара материя (DM), радиалды жылдамдық, Галактоцентрический координат жүйесі

Д. Кайраткызы

Казахский национальный университет им. Аль-Фараби, «Атрофизический институт им. В.Г. Фесенкова», АО «Национальный центр космических исследований и технологий», Аэрокосмический комитет МДАИ Республики Казахстан

ИССЛЕДОВАНИЕ РАСПРЕДЕЛЕНИЯ ТЕМНОЙ МАТЕРИИ В ГАЛАКТИЧЕСКОЙ СТРУКТУРЕ

Аннотация. Мы исследуем образование систем диск-балж-гало путем включения основных компонентов в теорию образования галактики. Цель этой статьи - исследовать распределение темной материи в структуре Галактики и изучить влияние субгало на гало и компоненты диска, которые должны быть включены в один простой сценарий формирования галактики. Мы исследуем нескольких важных

характеристик галактик, таких как координаты, положение, скорость и массы, чтобы сформировать стабильности компоненты галактики. Мы ищем параметры и физические процессы, которые определяют отношение субгало-гало, и, таким образом, в значительной степени объясняют происхождение столкновения или других препятствий через галактическое гало. Разброс по лучевым скоростям гало в сочетании с разбросом препятствий на расстояниях от центра галактики может объяснить наблюдаемый разброс по свойствам диска и выпуклости. В работе используются данные из Auriga_proper_unit - файла данных о главных галактиках в Auriga-6 до свободного запуска. Единицы длины данных, используемые в Gadget2, такие как координаты и плотность, конвертируются из Mpc в kpc и также включают star_age.

Ключевые слова: темная материя (ДМ), лучевая скорость, галактоцентрическая система координат.

Information about the authors:

Kairatkyzy D. - Master of Natural Science in “Astronomy”, PhD - doctoral student in the specialty "Physics and Astronomy". Senior Lecturer of the Department of Solid State Physics and Nonlinear Physics of the Physical-Technical Faculty of the al-Farabi Kazakh National University. An expert in the field of modern cosmology, specializing in the problems of formation and evolution of the Universe. She has more than 20 publications, including articles in the journal “Reports of the National Academy of Sciences of Kazakhstan”, made 8 reports at republican conferences. Orcid code: 0000-0002-9543-8464

REFERENCES

[1] Luri X. et al. Distances from parallaxes: on the proper use of astrometric data. Astron. Astrophys. (2018).

[2] Chen B. et al. Stellar Population Studies with the SDSS. I. The Vertical Distribution of Stars in the Milky Way. Astrophys. J. 553, 184–197 (2001). DOI 10.1086/320647.

[3] Reid M.J. et al. Trigonometric Parallaxes of High Mass Star Forming Regions: The Structure and Kinematics of the Milky Way. Astrophys. J. 783, 130 (2014). DOI 10.1088/0004-637X/783/2/130. 1401.5377.

[4] Schonrich R. Galactic rotation and solar motion from stellar kinematics. Mon. Not. R. Astron. Soc. 427, 274–287 (2012). DOI 10.1111/j.1365-2966.2012.21631.x. 1207.3079.

[5] Reid M.J. Brunthaler A. The Proper Motion of Sagittarius A*. II. The Mass of Sagittarius A*. Astrophys. J. 616, 872–884 (2004). DOI 10.1086/424960. arXiv:astro-ph/0408107.

[6] Lindegren L. et al. Gaia Data Release 2: The astrometric solution. ArXiv e-prints (2018). 1804. 09366.

[7] Taylor M.B. Starlink Table/VOTable Processing Software. In Shopbell, P., Britton, M. & Ebert, R. (eds.) Astronomical Data Analysis Software and Systems XIV, vol. 347 of Astronomical Society of the Pacific Conference Series, 29 (2005).

[8] Astraatmadja T. L., Bailer-Jones C.A. Estimating Distances from Parallaxes. II. Performance of Bayesian Distance Estimators on a Gaia-like Catalogue. Astrophys. J. 832, 137 (2016). DOI 10.3847/0004-637X/832/2/137. 1609.03424.

N E W S
OF THE NATIONAL ACADEMY OF SCIENCES OF THE REPUBLIC OF KAZAKHSTAN
PHYSICO-MATHEMATICAL SERIES
ISSN 1991-346X **https://doi.org/10.32014/2019.2518-1726.58**
Volume 5, Number 327 (2019), 51 – 58

K.B. Jakupov

Institute of mathematics and mathematical modeling, Almaty, Kazakhstan.
Kazak National University named after Al-Farabi
jakupovKB@mail.ru

FALSIFICATIONS OF THE ENERGY BALANCE EQUATION, PUASSON ADIABATS AND LAPLACE SOUND SPEED

Abstract. The falsity of the energy balance equation with a specific heat capacity coefficient at constant pressure, the fake Poisson adiabat, and the fake Laplace formula of adiabatic sound velocity are established. Universal formulas of adiabatic ideal gas and sound velocity are proposed and substantiated. Bibl.10.

Keywords: equation, sound, heat capacity, adiabat, isobaric.

1. Falsifications of the heat equation with specific coefficient of heat capacity at constant pressure

Scalar product of the equation of dynamics

$$\rho\frac{d\mathbf{v}}{dt} = \rho\mathbf{F} + \frac{\partial \mathbf{p}_x}{\partial x} + \frac{\partial \mathbf{p}_y}{\partial y} + \frac{\partial \mathbf{p}_z}{\partial z} + \mathbf{f}$$

on speed gives kinetic energy equation

$$\rho\frac{d\mathbf{v}}{dt}\cdot\mathbf{v} = \rho\mathbf{F}\cdot\mathbf{v} + \frac{\partial \mathbf{p}_x}{\partial x}\cdot\mathbf{v} + \frac{\partial \mathbf{p}_y}{\partial y}\cdot\mathbf{v} + \frac{\partial \mathbf{p}_z}{\partial z}\cdot\mathbf{v} + \mathbf{f}\cdot\mathbf{v}, \tag{1.1}$$

which is part of the energy balance equation

$$\rho\frac{d}{dt}(E+|\mathbf{v}|^2/2) = \rho\mathbf{F}\cdot\mathbf{v}+\mathbf{f}\cdot\mathbf{v}+\frac{\partial}{\partial x}\mathbf{p}_x\cdot\mathbf{v}+\frac{\partial}{\partial y}\mathbf{p}_y\cdot\mathbf{v}+\frac{\partial}{\partial z}\mathbf{p}_z\cdot\mathbf{v}-\nabla\cdot\mathbf{q}+\rho Q,$$

as can be seen from the following:

$$\rho\frac{dE}{dt}+\rho\frac{d\mathbf{v}}{dt}\cdot\mathbf{v} = \rho\mathbf{F}\cdot\mathbf{v}+\mathbf{f}\cdot\mathbf{v}+\frac{\partial \mathbf{p}_x}{\partial x}\cdot\mathbf{v}+\mathbf{p}_x\cdot\frac{\partial \mathbf{v}}{\partial x}+\frac{\partial \mathbf{p}_y}{\partial x}\cdot\mathbf{v}+\mathbf{p}_y\cdot\frac{\partial \mathbf{v}}{\partial y}+$$
$$+\frac{\partial \mathbf{p}_z}{\partial z}\cdot\mathbf{v}+\mathbf{p}_z\cdot\frac{\partial \mathbf{v}}{\partial z}-\nabla\cdot\mathbf{q}+\rho Q$$

The abbreviation for (1.1) leads to the equation

$$\rho\frac{dE}{dt} = \mathbf{p}_x\cdot\frac{\partial \mathbf{v}}{\partial x}+\mathbf{p}_y\cdot\frac{\partial \mathbf{v}}{\partial y}+\mathbf{p}_z\cdot\frac{\partial \mathbf{v}}{\partial z}-\nabla\cdot\mathbf{q}+\rho Q$$

from which for the internal energy $dE = c_v dT$ and according to the Fourier law $\mathbf{q} = -\lambda\nabla T$ we obtain various representations of the heat equation, respectively, to the stress tensors.

With asymmetric stress tensor for Newton's law of friction:

$$\rho c_v \frac{dT}{dt} = \nabla \cdot \left(\lambda \nabla T\right) - p\nabla \cdot \mathbf{v} + \mu \sum_{i=1}^{3}\sum_{j=1}^{3}(\frac{\partial v_i}{\partial x_j})^2 + \rho Q$$

with an asymmetric tensor of the Jakupov [9-10] friction law:

$$\rho c_v \frac{dT}{dt} = \nabla \cdot \left(\lambda \nabla T\right) - p\nabla \cdot \mathbf{v} + \sum_{j=1}^{3}\sum_{i=1}^{3} \frac{\alpha\mu}{m_i^{m_i-1}} \frac{\partial v_i^{m_i}}{\partial x_j}\frac{\partial v_i}{\partial x_j} + \rho Q,\ \alpha = 1(\frac{cek}{м})^{m_i-1}$$

and the heat equation with the symmetric Stokes stress tensor [1-8]:

$$\rho c_v \frac{dT}{dt} = \nabla \cdot (\lambda \nabla T) - p\nabla \cdot \mathbf{v} + \frac{\mu}{2}\sum_{i=1}^{3}\sum_{j=1}^{3}(\frac{\partial v_i}{\partial x_j} + \frac{\partial v_j}{\partial x_i})^2 - \frac{2}{3}\mu(\nabla \cdot \mathbf{v})^2, \qquad (1.2)$$

which is false due to the falseness of the Stokes stress tensor [9-10].

Let us pay attention to the fact that these equations include the coefficient C_v of the specific heat capacity of a gas with a constant volume, according to the 1st law of thermodynamics.

In addition to the fact that the heat conduction equation is fake according to the Stokes friction law, the tendency to transform into an equation with the specific heat coefficient of gas C_p at constant pressure [1–9] is well known.

Specifically, Lykov (see [3] p. 32) gives the following equation:

$$\rho c_p \frac{dT}{dt} - \frac{dp}{dt} = \lambda \nabla^2 T + \frac{\mu}{2}\sum_{i=1}^{3}\sum_{j=1}^{3}(\frac{\partial v_i}{\partial x_j} + \frac{\partial v_j}{\partial x_i})^2 - \frac{2}{3}\mu(\nabla \cdot \mathbf{v})^2 \qquad (1.3)$$

For the derivation, the universal gas constant and the Clapeyron-Mendeleev state equation are used

$$c_p - c_v = R,\ \ p = \rho RT \qquad (1.4)$$

Using (1.4) in the error equation (1.2), substitutions are made

$$c_v T = (c_p - R)T = c_p T - RT = c_p T - \frac{p}{\rho},$$

$$\rho c_v \frac{dT}{dt} = \rho(c_p \frac{dT}{dt} - \frac{d}{dt}\frac{p}{\rho}) = \rho[c_p \frac{dT}{dt} - \frac{1}{\rho^2}(\rho\frac{dp}{dt} - p\frac{d\rho}{dt})] =$$

$$= \rho c_p \frac{dT}{dt} - \frac{dp}{dt} + \frac{p}{\rho}\frac{d\rho}{dt}$$

where by the continuity equation $\frac{1}{\rho}\frac{d\rho}{dt} = -\nabla \cdot \mathbf{v}$. Therefore

$$\rho c_v \frac{dT}{dt} = \rho c_p \frac{dT}{dt} - \frac{dp}{dt} + \frac{p}{\rho}\frac{d\rho}{dt} = \rho c_p \frac{dT}{dt} - \frac{dp}{dt} - p\nabla \cdot \mathbf{v}$$

Substitution in the equation (1.2) gives

$$\rho c_p \frac{dT}{dt} - \frac{dp}{dt} - p\nabla \cdot \mathbf{v} = \nabla \cdot (\lambda \nabla T) - p\nabla \cdot \mathbf{v} + \frac{\mu}{2}\sum_{i=1}^{3}\sum_{j=1}^{3}(\frac{\partial v_i}{\partial x_j} + \frac{\partial v_j}{\partial x_i})^2 - \frac{2}{3}\mu(\nabla \cdot \mathbf{v})^2$$

After contractions and rearrangements, the equation is obtained

$$\rho c_p \frac{dT}{dt} = \nabla\cdot(\lambda\nabla T) + \frac{dp}{dt} + \frac{\mu}{2}\sum_{i=1}^{3}\sum_{j=1}^{3}\left(\frac{\partial v_i}{\partial x_j} + \frac{\partial v_j}{\partial x_i}\right)^2 - \frac{2}{3}\mu(\nabla\cdot\mathbf{v})^2 \tag{1.5}$$

For constant thermal conductivity coefficient $\lambda = const$ equation (1.5) goes over to the Lykov equation (1.3).

Theorem. The equation of heat conduction with the coefficient of specific heat capacity of gas at constant pressure

$$\rho c_p \frac{dT}{dt} = \nabla\cdot(\lambda\nabla T) + \frac{dp}{dt} + \frac{\mu}{2}\sum_{i=1}^{3}\sum_{j=1}^{3}\left(\frac{\partial v_i}{\partial x_j} + \frac{\partial v_j}{\partial x_i}\right)^2 - \frac{2}{3}\mu(\nabla\cdot\mathbf{v})^2$$

is fake in flows with variable pressure, as formula C_p - Cv = is valid only for constant pressure p = const.

Evidence. The 1st law of thermodynamics is attracted [7]:

$$d'Q = dE + pdV \tag{1.6}$$

In an ideal gas $dE = c_v dT$, c_v is the coefficient of specific heat of gas at a constant volume. Between the specific volume V and the density of the gas there is a connection $V = \frac{1}{\rho}$, $dV = d(\frac{1}{\rho})$.

Therefore, the 1st law is used in the form [1]:

$$d'Q = c_v dT + pd(\frac{1}{\rho}),\ d'Q = c_v dT + pd(\frac{RT}{p}) \tag{1.7}$$

Let the heat be supplied to the gas at a constant volume of $V = const$. Since $dV = 0$ in this case it follows from (1.6) $d'Q = dE = c_v dT$.

Let heat be supplied to gas $d'Q = c_p dT$ with constant pressure $p = const$.

The 1st law of thermodynamics (1.7) is converted to the form

$$c_p dT = c_v dT + pd(\frac{RT}{p}),\ (c_p - c_v)dT = p\frac{pd(RT) - RTdp}{p^2},$$

$$(c_p - c_v)dT = RdT - RT\frac{dp}{p},\ \ p = \rho RT$$

Dividing the last equality by dT we obtain the following formula for a universal gas constant:

$$R = c_p - c_v + \frac{1}{\rho}\frac{dp}{dT}, \tag{1.8}$$

At constant pressure $p = const,\ dp = 0$ from (1.8) we get the formula widely used in gas dynamics [1-9]:

$$R = c_p - c_v \tag{1.9}$$

By virtue of (1.8) in non-isobaric gas flows with variable pressure $p \neq \text{const}$, $dp \neq 0$, there will always be inequality $R \neq c_p - c_v$!

This axiom is also evident from the 1st law of thermodynamics

$$d'Q = c_v dT + pd(\frac{RT}{p}),\ d'Q = c_v dT + p\frac{pd(RT) - RTdp}{p^2},$$

$$d'Q = c_v dT + RdT - RT\frac{dp}{p},\ d'Q = c_v dT + RdT - \frac{1}{\rho}dp$$

For universal constant gas, dividing the last expression on the temperature differential, we get the formula

$$R = \frac{d'Q}{dT} - c_v + \frac{1}{\rho}\frac{dp}{dT} \tag{1.10}$$

It is obvious, by virtue of equality (1.10), that in non-isobaric flows of gas with variable pressure $p \neq \text{const},\ dp \neq 0$, inequality

$$R \neq c_p - c_v\,!$$

Consequently, the heat conduction equation with a coefficient C_p of the specific heat of a gas at constant pressure is false, since it is obtained for connection Cp - $C\nu = R$, which does not hold for variable pressure $p \neq const.$

What was required to prove.

2. Falsifications of Poisson adiabat

In the dynamics of an ideal gas, a false heat equation (1.5) for enthalpy $h = c_p T,\ \lambda \equiv 0,\ \mu \equiv 0$ takes the form (see [1] p. 115):

$$\rho c_p \frac{dT}{dt} = \frac{dp}{dt},\ \rho\frac{dh}{dt} = \frac{dp}{dt}, \tag{2.1}$$

therefore, it is also false.

Reducing the differential in time gives the connection

$$dp = \rho c_p dT \tag{2.2}$$

From the fake equation (2.2), converted to Form $\frac{dp}{\rho} = c_p dT$, again using $R = c_p - c_v$, which is valid only for constant pressure, the Poisson adiabat is displayed (see Loitsyansky [1] p.115):

$$\frac{dp}{\rho} = c_p dT = \frac{c_p}{R}d(RT) = \frac{c_p}{c_p - c_v}d(\frac{p}{\rho}),\ \frac{dp}{\rho} = k\frac{d\rho}{\rho},\ \frac{p}{p_0} = (\frac{\rho}{\rho_0})^k, k = \frac{c_p}{c_v}$$

Calculate the pressure differential using the Clapeyron-Mendeleev equation of state $p = R\rho T$:

$$dp = \rho RdT + TRd\rho$$

Similarly, assuming in this ratio $R = c_p - c_v$, just used to derive the Poisson adiabat, we get the true value of the pressure differential

$$dp = \rho(c_p - c_v)dT + TRd\rho,$$

whose transformed expression

$$dp = \rho c_p dT - \rho c_v dT + TRd\rho,\ \frac{dp}{dt} = \rho\frac{dh}{dt} - \rho c_v\frac{dT}{dt} + TR\frac{d\rho}{dt} \tag{2.3}$$

does not coincide with the differential (2.2) and equation (2.1) !!!

The difference between (2.2) and (2.3) is not equal to zero:

$$-\rho c_v dT + TRd\rho \neq 0$$

Consequently, the differential pressure $dp = \rho c_p dT$ (2.2), corresponding to a fake heat equation with a heat capacity coefficient at constant pressure is also fake.

The falsity of equations (2.1) is proven again.

Proved inequality $\rho \frac{dh}{dt} \neq \frac{dp}{dt}$!

From fake equality $\rho \frac{dh}{dt} = \frac{dp}{dt}$, the Poisson adiabat [1] is derived, consequently, the Poisson adiabat is also fake !!!

As is known, the Poisson adiabat is widely used in gas dynamics, for example, when calculating the propagation velocity of small perturbations, i.e. speed of sound.

3. Falsification of the speed of sound of Laplace

On the basis of the equation of Clapeyron –Mendeleeva Newton derived the isothermal speed of sound

$$a = \sqrt{\frac{\partial p}{\partial \rho}} = \sqrt{\frac{\partial(\rho RT)}{\partial \rho}} = \sqrt{RT}, \; a = \sqrt{\frac{p}{\rho}}$$

Laplace proposed to use the Poisson adiabat $p = p_0 (\frac{\rho}{\rho_0})^k$:

$$a = \sqrt{\frac{\partial p}{\partial \rho}} = \sqrt{\frac{\partial}{\partial \rho}(p_0 (\frac{\rho}{\rho_0})^k)} = \sqrt{k\frac{p}{\rho}}, \; a = \sqrt{kRT} \tag{3.1}$$

Connection $R = c_p - c_v$ takes place only for constant pressure $p = const$, therefore, the Laplace formula (3.1) is not only adiabatic, but also isobaric sound speed.

Consequently, due to the falsity of the Poisson adiabat, it is logical to consider the formula (3.1) to be the adiabatic and isobaric Laplace sound velocity as fake.

Using a fake link $\rho c_p dT = dp$ and the equation of state Clapeyron-Mendeleev, we organize the calculations:

$$\frac{dp}{\rho} = c_p dT = \frac{c_p}{R} d(RT) = \frac{c_p}{R} d(\frac{p}{\rho}), \; \frac{c_p}{R} d(\frac{p}{\rho}) = \frac{dp}{\rho}, \; \frac{c_p}{R} \cdot \frac{\rho dp - p d\rho}{\rho^2} = \frac{dp}{\rho},$$

$$\frac{c_p}{R} dp - \frac{c_p}{R} \cdot p \frac{d\rho}{\rho} = dp, \; (\frac{c_p}{R} - 1) dp = \frac{c_p}{R} \cdot p \frac{d\rho}{\rho}, \; (\frac{c_p}{R} - 1)\frac{dp}{p} = \frac{c_p}{R}\frac{d\rho}{\rho},$$

$$\frac{c_p - R}{R} d\ln p = \frac{c_p}{R} d\ln \rho, \; d\ln p - \frac{c_p}{c_p - R} d\ln \rho = 0,$$

$$\ln \frac{p}{\rho^\chi} = const, \; \frac{p}{p_0} = (\frac{\rho}{\rho_0})^\chi, \; \chi = \frac{c_p}{c_p - R}$$

So, from the false connection $\rho c_p dT = dp$ we get the adiabat

$$\frac{p}{p_0} = (\frac{\rho}{\rho_0})^\chi, \; \chi = \frac{c_p}{c_p - R}, \tag{3.2}$$

which for $R = c_p - c_v$ goes to the Poisson adiabat.

Calculate the speed of sound:

$$a=\sqrt{\frac{\partial p}{\partial\rho}}=\sqrt{\frac{\partial}{\partial\rho}(p_0(\frac{\rho}{\rho_0})^{\chi})}=\sqrt{\frac{p_0}{\rho_0{}^{\chi}}\chi\rho^{\chi-1}}=$$

$$=\sqrt{\frac{p_0}{\rho}\chi(\frac{\rho}{\rho_0})^{\chi}}=\sqrt{\frac{c_p}{c_p-R}\frac{p}{\rho}}$$

So, for the speed of sound, the formula is obtained (also fake, as in Laplace)

$$a=\sqrt{\frac{c_p}{c_p-R}\frac{p}{\rho}},\ a=\sqrt{\frac{c_p}{c_p-R}RT},$$

which for $R=c_p-c_v$ goes to the Laplace formula (3.1).

4. Universal adiabatic sound speed

The 1st law of thermodynamics $d'Q=dE+pd(\frac{1}{\rho})$ in an adiabatic gas (heat is not removed and not supplied $d'Q=0$):

$$0=dE+pd(\frac{1}{\rho}),\quad dE=c_v dT \tag{4.1}$$

According to the equation of state of Clapeyron-Mendeleev we find:

$$0=c_v dT+pd(\frac{1}{\rho}),\ 0=c_v d(\frac{p}{R\rho})-p\frac{d\rho}{\rho^2}$$

Next are the necessary conversions:

$$0=\frac{c_v}{R}\cdot\frac{\rho dp-pd\rho}{\rho^2}-p\frac{d\rho}{\rho^2},\ 0=\frac{c_v}{R}\cdot(\rho dp-pd\rho)-pd\rho,$$

$$0=\frac{c_v}{R}\cdot(\frac{dp}{p}-\frac{d\rho}{\rho})-\frac{d\rho}{\rho},\ \frac{c_v}{R}\cdot\frac{dp}{p}=(\frac{c_v}{R}+1)\frac{d\rho}{\rho},\ \frac{dp}{p}=(\frac{R}{c_v}+1)\frac{d\rho}{\rho}$$

From the last equality follows adiabata (Jakupov)*:

$$\frac{p}{p_0}=(\frac{\rho}{\rho_0})^{\zeta},\ \zeta=\frac{R}{c_v}+1$$

which for $R=c_p-c_v$, i.e. for constant pressure too goes to the Poisson adiabat.

So, the logic for the speed of sound is the formula (Jakupov)*

$$a=\sqrt{\frac{\partial p}{\partial \rho}}=\sqrt{(\frac{R}{c_v}+1)\frac{p}{\rho}},\ \ a=\sqrt{(\frac{R}{c_v}+1)RT},$$

which, for a constant pressure, when performing $R=c_p-c_v$, goes to the

Laplace formula (3.1).

Note. The barometric formula [7] $p=p_0\exp(-\frac{Mgz}{RT})$ confirms the fact that even in a stationary atmosphere V = 0 pressure is a variable function.

* These adiabatic names and the universal formula for the speed of sound are necessary to emphasize novelty and differences from the Poisson and Laplace formulas.

К. Б. Жақып-тегі

ҚР БҒМ Математика және математикалық моделдеу институты, Алматы, Қазақстан
Аль-Фараби атындағы Қазақ Ұлттық Университеті, Алматы, Қазақстан

ПУАССОННЫҢ АДИАБАТАСЫНЫҢ, ЛАПЛАСТЫҢ ДЫБЫС ЖЫЛДАМДЫҒЫНЫҢ ЖӘНЕ ЭНЕРГИЯЛАР БАЛАНСЫНЫҢ ТЕҢДЕУІНІҢ ЖАЛҒАНДЫҚТАРЫ

Аннотация. Қысым тұрақтылықтығы, жылусыйымдылық еселеуіші бар энергиялар балансының жалғандығы, сонымен қатар Пуассонның адиабатысының және Лапластың дыбыс жылдамдығының кейіте-мелерінің қателіктері нақты дәлелделінген. Идеалдық газдардың адиабатасының кейіптемесі орнатылған, оған байланысты дыбыс жылдам- дығының жаңадан универсальдық тұрпаты негізделген. Библ.10.

Түйін сөздер: теңдеу, жылусыйымдылық, адиабата, изобарлық.

УДК 532.533

К.Б. Джакупов

Институт математики и математического моделирования МОН РК, Алматы, Казахстан
Казахский Национальный Университет им.Аль-Фараби, Алматы, Казахстан

ФАЛЬСИФИКАЦИИ УРАВНЕНИЯ БАЛАНСА ЭНЕРГИЙ, АДИАБАТЫ ПУАССОНА И СКОРОСТИ ЗВУКА ЛАПЛАСА

Аннотация. Установлены фальшивость уравнения баланса энергий с удельным коэффициентом теплоемкости при постоянном давлении, фальшивость адиабаты Пуассона и фальшивость формулы Лапласа адиабатической скорости звука. Предложены и обоснованы универсальные формулы адиабаты идеального газа и скорости звука. Библ.10.

Ключевые слова: уравнение, звук, теплоемкость, адиабата, изобарический.

Information about the author:

Jakupov Kenes Bazhkenovitch - Doctor of Physical and Mathematical Sciences Professor, Academician of the Russian Academy of Natural Sciences. Service Address: RSE Institute of Mathematics and Mathematical modeling of the CM MES RK, 050010, Pushkin St., 125, Almaty, Kazakhstan, Telefone: 8 727 305 92 44, +7 701 667 88 59, jakupovKB@mail.ru, https://orcid.org/0000-0003-1097-2893

REFERENCES

[1] Loitsyansky L.G. Fluid and gas mechanics. M.: “Science”, 1973.

[2] Sedov L.I. Continuum mechanics. T.1. M.: “Science”, 1973.

[3] Lykov A.V. Thermal Mass Transfer. M .: "Energy", 1972. P.560.

[4] George E. Mase. Theory and Problems of Continium Mechanics. Schaum’s Outline Series. MCGRAW-HILL BOOK COMPANI. NewYork, St. Louis, San Francisco, London 1970.

[5] Batchelor J. Introduction to fluid dynamics. M .: Mir, 1973

[6] Landau L. D., Lifshchits E.M. Hydrodynamics. M .: “Science”, 1973.

[7] Saveliev IV. The course of general physics. Vol. 1. M .: “Science”, 1977.

[8] Schlichting G. Theory of the boundary layer. M.: “Science”, 1974.

[9] Jakupov K.B. RHEOLOGICAL LAWS OF VISCOUS FLUID DYNAMICS // NEWS of the National Academy of Sciences of the Republic of Kazakhstan, physico-mathematical Series, 1(293), 2014г.с.51-55. I SSN 1991-346X.

[10] Jakupov K.B. Elimination of falsifications and modernization of the foundations of mechanics Continuous environment - Almaty: Publishing house "The White Orders", 2017. С.435. ISBN 978-601-280-859-9

[11] Jakupov K.B. NATURAL FILTRATION EQUATIONS. FIASCO “OF DARCY’S LAW” //NEWS of the National Academy of Sciences of the Republic of Kazakhstan, physico-mathematical Series, 6(322), 2018, p.54-70. ISSN 2518-1726(Online), ISSN 1991 346X (Print), DOI https://doi.org/10.32014/2018.2518-1726.18

[12] Jakupov K.B. NONLINEAR LAW OF HONEY IN THE THEORY OF ELASTICITY OF INHOMOGENEOUS AND ANISOTROPIC BODIES//NEWS of the National Academy of Sciences of the Republic of Kazakhstan, physico-mathematical Series, 1(317), 2018, p.63-74. ISSN 1991 346X (Print), ISSN 2518-1726(Online)

N E W S
OF THE NATIONAL ACADEMY OF SCIENCES OF THE REPUBLIC OF KAZAKHSTAN
PHYSICO-MATHEMATICAL SERIES
ISSN 1991-346X **https://doi.org/10.32014/2019.2518-1726.59**
Volume 5, Number 327 (2019), 59 – 69

UDK 517.9

A.Sh. Shaldanbayev[1] , A.A. Shaldanbayeva[2] , B.A. Shaldanbay[3]

[1]Silkway International University, Shymkent, Kazakhstan;
[2]Regional social-innovative University, Shymkent, Kazakhstan;
[3]South Kazakhstan State University M.O.Auezov, Shymkent, Kazakhstan shaldanbaev51@mail.ru, altima_a@mail.ru, baglan.shaldanbayev@bk.ru

INVERSE PROBLEM OF A STURM-LIOUVILLE OPERATOR WITH NON-SEPARATED BOUNDARY VALUE CONDITIONS AND SYMMETRIC POTENTIAL

Abstract. In this paper we prove a uniqueness theorem, in a single spectrum, for the Sturm-Liouville operator with non-separated boundary value conditions and real continuous and symmetric potential. The research method is different from all known methods, and based on internal symmetry of the operator generated by invariant subspaces.

Keywords: Sturm - Liouville operator, spectrum, Sturm - Liouville inverse problem, Borg theorem, Ambartsumian theorem, Levinson theorem, non-separated boundary value conditions, symmetric potential, invariant subspaces.

1. Introduction. By inverse problems of spectral analysis, we understand the tasks of restoring a linear operator according to its one or other spectral characteristics.

The first significant result in this direction was obtained in 1929 by V.A. Ambartsumyan [1]. He proved the following theorem.

We denote eigenvalues of the following Sturm - Liouville operator by $\lambda_0 < \lambda_1 < \lambda_2 < \cdots$:

$$-y'' + q(x)y = \lambda y, \tag{1.1}$$

$$y'(0) = 0, y'(\pi) = 0; \tag{1.2}$$

where $q(x)$ is a real continuous function. If $\lambda_n = n^2$ $(n = 0,1,2,\dots)$, then $q(x) \equiv 0$.

The first mathematician who drew attention to importance of this Ambartsumian result was the Swedish mathematician Borg. He also performed the first systematic research of one of the important inverse problems, namely, the inverse problem for the classical Sturm – Liouville operator of the form (1.1) by the spectra [2]. Borg showed that, in the general case, one spectrum of the Sturm-Liouville operator does not define it, so Ambartsumian's result is an exception to the general rule. In the same paper [2], Borg shows that two spectra of the Sturm – Liouville operator (with different boundary conditions) uniquely determine it. More precisely, Borg proved the following theorem.

Borg Theorem.

Let the equation

$$-y'' + q(x)y = \lambda y, \tag{1.1}$$
$$-z'' + p(x)z = \lambda z, \tag{1.3}$$

have the same spectrum under the following boundary conditions

$$\begin{cases} \alpha y(0) + \beta y'(0) = 0, \\ \gamma y(\pi) + \delta y'(\pi) = 0; \end{cases} \tag{1.4}$$

and under the following boundary value conditions

$$\begin{cases} \alpha y(0) + \beta y'(0) = 0, \\ \gamma' y(\pi) + \delta' y'(\pi) = 0. \end{cases}$$

Then $q(x) = p(x)$ almost everywhere on the segment $[0, \pi]$, if

$$\delta \cdot \delta' = 0, |\delta| + |\delta'| > 0.$$

Shortly after the Borg's work important studies on the theory of inverse problems were performed by Levinson [3], in particular, he proved that if $q(\pi - x) = q(x)$, then the Sturm – Liouville operator

$$-y'' + q(x)y = \lambda y, \tag{1.1}$$

$$\begin{cases} y'(0) - hy(0) = 0, \\ y'(\pi) + hy(\pi) = 0 \end{cases} \tag{1.5}$$

restored by one spectrum. Ambartsumian and Levinson theorems were developed in [4] - [6].

Inverse spectral analysis problems for Sturm – Liouville operators with non-separated boundary conditions

A number of works B.M. Levitan [7] - [8] are devoted to reconstructing the Sturm-Liouville operator from one and two spectra.

Note that inverse problems of spectral analysis for Sturm – Liouville operators with non-separated boundary conditions were studied in [9] - [10] by other methods, with the results obtained being expressed through conformal mappings, and difficult to verify.

From later works in this direction, we note [11] - [13].

This paper is devoted to the generalization of Ambartsumian [1] and Levinson [3] theorems to non-decaying boundary conditions, in particular, our results contain results of these authors. Method of this paper appeared i development of spectral methods for solving ill-posed problems of mathematical physics [14] - [25].

2. Research Method.

Idea of this paper is very simple. Carefully studying the content of [1, 3], we realized that both of these operators have an invariant subspace. If for the linear operator L the following formulas hold:

$$LP = PL^*, QL = L^*Q,$$

where P, Q are orthogonal projectors, satisfying the condition $P + Q = I$, then the operators L and L^* have invariant subspaces, sometimes restriction of these operators to these invariant subspaces, with certain conditions, form a Borg pair.

3. Research Results.

In Hilbert space $H = L^2(0, \pi)$ we consider the Sturm – Liouville operator

$$Ly = -y'' + q(x)y, x \in (0, \pi); \tag{3.1}$$

$$\begin{cases} a_{11}y(0) + a_{12}y'(0) + a_{13}y(\pi) + a_{14}y'(\pi) = 0, \\ a_{21}y(0) + a_{22}y'(0) + a_{23}y(\pi) + a_{24}y'(\pi) = 0 \end{cases} \tag{3.2}$$

where $q(x)$ is a continuous complex function, a_{ij} $(i = 1,2;\ j = 1,2,3,4)$ are arbitrary complex coefficients, and by Δ_{ij} $(i = 1,2;\ j = 1,2,3,4)$ we denote minors of the boundary matrix:

$$A = \begin{pmatrix} a_{11} & a_{12} & a_{13} & a_{14} \\ a_{21} & a_{22} & a_{23} & a_{24} \end{pmatrix}.$$

We suppose that $\Delta_{24} \neq 0$, then the Sturm – Liouville operator (3.1) – (3.2) takes the following form

$$Ly = -y'' + q(x)y, x \in (0, \pi); \tag{3.1}$$

$$\begin{cases} \Delta_{14}y(0) + \Delta_{24}y'(0) + \Delta_{34}y(\pi) = 0, \\ \Delta_{12}y(0) + \Delta_{32}y(\pi) - \Delta_{24}y'(\pi) = 0 \end{cases} \tag{3.3}$$

and its conjugate operator L^{+} takes the form

$$L^{+}z = -z'' + q(x)z, x \in (0,\pi); \qquad (3.1)^{+}$$

$$\begin{cases} \overline{\Delta_{14}}z(0) + \overline{\Delta_{24}}z'(0) + \overline{\Delta_{12}}z(\pi) = 0, \\ \overline{\Delta_{34}}z(0) + \overline{\Delta_{32}}z(\pi) - \overline{\Delta_{24}}z'(\pi) = 0. \end{cases} \qquad (3.3)^{+}$$

Let P and Q be orthogonal projectors, defined by the formulas

$$Pu(x) = \frac{u(x)+u(\pi-x)}{2}, Qv(x) = \frac{v(x)-v(\pi-x)}{2} \qquad (3.4)$$

The main result of this paper is the following theorem.

Theorem 3.1. If $\Delta_{24} \neq 0$, and

1) $LP = PL^{+}$;
2) $QL = L^{+}Q$;
3) $\Delta_{12} = -\Delta_{12}$;

then the Sturm – Liouville operator (3.1) – (3.3) is restored by one spectrum.

4. Discussion.

In this section we prove the theorem and discuss the obtained results. The following Lemma 4.1 and Lemma 4.2 can have independent values.

Lemma 4.1. If for a linear and discrete operator L we have:

1) $LP = PL^{*}$;
2) $QL = L^{*}Q$;
3) $P + Q = I$;

where P, Q are orthogonal projectors, and I is a unique operator, then all its eigenvalues are real.

Proof.

Let $LP = PL^{*}$, $QL = L^{*}Q$; then

$$(LP)^{*} = P^{*}L^{*} = PL^{*} = LP;$$
$$(QL)^{*} = L^{*}Q^{*} = L^{*}Q = QL;$$

i.e. operators LP and QL are self-adjoint, therefore their eigenvalues are real.

If $Ly = \lambda y, y \neq 0$, then $QLy = \lambda Qy$, $L^{+}Qy = \lambda Qy$, $L^{+}Q(Qy) = \lambda Qy$, $QL(Qy) = \lambda Qy$ if $Qy \neq 0$, then λ is a real quantity; if $Qy = 0$, then $y = Py \neq 0$, and $LPy = \lambda Py, LP(Py) = \lambda Py$. Consequently, λ is again real quantity.

The following lemmas shows that the spectrum $\sigma(L)$ of the operator L is divided into two parts, therefore the operator L, apparently, is also divided into two parts. Later we will see that this is exactly what happens, and more precisely, these parts form a Borg pair under a certain condition.

Lemma 4.2. If L is a linear discrete operator satisfying the conditions:

1) $LP = PL^{*}$;
2) $QL = L^{*}Q$;
3) $P + Q = I$;

where P, Q are orthogonal projectors, and I is identity operator, then we get

$$\sigma(L) = \sigma(L_1) \cup \sigma(L_2).$$

where $L_1 = LP, L_2 = QL, \sigma(L)$ is a spectrum of the operator L.

Proof.

If $Ly = \lambda y, y \neq 0$, then $QLy = \lambda Qy, L^{+}Qy = \lambda Qy$, $L^{+}Q(Qy) = \lambda Qy$, $L_2Qy = \lambda Qy$. If $Qy \neq 0$, hence $\lambda \in \sigma(L_2)$. If $Qy = 0$, then we get $y = Py \neq 0$ and $LPy = \lambda Py$, $LP(Py) = \lambda Py, L_1Py = \lambda Py$. Consequently, $\lambda \in \sigma(L_1)$.

Thus, $\sigma(L) \subset \sigma(L_1) \cup \sigma(L_2)$.

If $\lambda \neq 0$, and $\lambda \in \sigma(L_1) \cup \sigma(L_2)$, then

a) If $\lambda \in \sigma(L_1)$, then $\exists u \neq 0$, such that $u \in H_1, L_1u = \lambda u, LPu = \lambda u, \rightarrow Lu = \lambda u$. Consequently, $\lambda \in \sigma(L)$.

б) If $\lambda \in \sigma(L_2)$, then $\exists v \in H_2$, $v \neq 0$ such that $L_2v = \lambda v$, $QLv = \lambda v$, $L^{+}Qv = \lambda v, L^{+}v = \lambda v$. Consequently, $\lambda \in \sigma(L^{+}) = \sigma(L)$.

в) If $0 \in \sigma(L_1) \cup \sigma(L_2)$, then If $0 \in \sigma(L_1)$, therefore $L_1 u = 0, u \in H_1$, $LPu = 0, => Lu = 0, => 0 \in \sigma(L)$. If $0 \in \sigma(L_2)$, then $L_2 v = 0$, $v \in H_2$, $QLv = 0, => L^+ Qv = 0, L^+ v = 0, => 0 \in \sigma(L^+) = \sigma(L)$.

The following Lemma 4.3 nad Lemma 4.4 clarify the boundary conditions of Sturm-Liouville operators with invariant subspaces.

Lemma 4.3. If

а) $\Delta_{24} \neq 0$;

б) $LP = PL^+$;

then we have

1) $\overline{\left(\frac{\Delta_{12}+\Delta_{32}}{\Delta_{24}}\right)} = \frac{\Delta_{12}+\Delta_{32}}{\Delta_{24}} = \frac{\Delta_{14}+\Delta_{34}}{\Delta_{24}}$;

2) $q(\pi - x) = q(x)$;

3) $\overline{q(x)} = q(x)$;

and the operators L and L^+ take the following forms:

$Ly = -y'' + q(x)y, x \in (0, \pi)$;

$$\begin{cases} \frac{\Delta_{12}-\Delta_{14}}{\Delta_{24}}[y(0) - y(\pi)] - y'(0) - y'(\pi) = 0, \\ \Delta_{12} y(0) + \Delta_{32} y(\pi) - \Delta_{24} y'(\pi) = 0. \end{cases}$$

$L^+ z = -z'' + q(x)z, x \in (0, \pi)$;

$$\begin{cases} \frac{\Delta_{12}+\Delta_{32}}{\Delta_{24}}[z(0) + z(\pi)] + z'(0) + z'(\pi) = 0, \\ \overline{\Delta_{14}} z(0) + \overline{\Delta_{24}} z'(0) + \overline{\Delta_{12}} z(\pi) = 0. \end{cases}$$

Proof.

Let $a_{24} \neq 0$, then the Sturm-Liouville operator has the form

$$Ly = -y'' + q(x)y, x \in (0, \pi); \tag{4.1}$$

$$\begin{cases} \Delta_{14} y(0) + \Delta_{24} y'(0) + \Delta_{34} y(\pi) = 0, \\ \Delta_{12} y(0) + \Delta_{32} y(\pi) - \Delta_{24} y'(\pi) = 0, \end{cases} \tag{4.2}$$

and its conjugate operator L^+ takes the form

$L^+ z = -z'' + \overline{q(x)} z, x \in (0, \pi)$; $(4.1)^+$

$$\begin{cases} \overline{\Delta_{14}} z(0) + \overline{\Delta_{24}} z'(0) + \overline{\Delta_{12}} z(\pi) = 0, \\ \overline{\Delta_{34}} z(0) + \overline{\Delta_{32}} z(\pi) - \overline{\Delta_{24}} z'(\pi) = 0. \end{cases} \tag{4.2$^+$}$$

By P and Q we denote the following orthogonal projectors

$$Pu(x) = \frac{u(x)+u(\pi-x)}{2}, Qv(x) = \frac{v(x)-v(\pi-x)}{2}. \tag{4.3}$$

If $LP = PL^+$, then $y = Pz \in D(L)$, where $z \in D(L^+)$, therefore

$$y(x) = \frac{z(x) + z(\pi - x)}{2}, y'(x) = \frac{z'(x) - z'(\pi - x)}{2};$$

$$\begin{cases} \Delta_{14} \frac{z(0) + z(\pi)}{2} + \Delta_{24} \frac{z'(0) - z'(\pi)}{2} + \Delta_{34} \frac{z(0) + z(\pi)}{2} = 0, \\ \Delta_{12} \frac{z(0) + z(\pi)}{2} + \Delta_{32} \frac{z(0) + z(\pi)}{2} - \Delta_{24} \frac{z'(\pi) - z'(0)}{2} = 0; \end{cases}$$

$$\begin{cases} (\Delta_{14} + \Delta_{34}) \frac{z(0) + z(\pi)}{2} + \Delta_{24} \frac{z'(0) - z'(\pi)}{2} = 0, \\ (\Delta_{12} + \Delta_{32}) \frac{z(0) + z(\pi)}{2} + \Delta_{24} \frac{z'(0) - z'(\pi)}{2} = 0; \end{cases}$$

From $LP = PL^{+}$ we get that $\Delta_{12} + \Delta_{32} = \Delta_{14} + \Delta_{34}$, hence these boundary conditions melt into one boundary condition:

$$(\Delta_{12} + \Delta_{32})\frac{z(0)+z(\pi)}{2} + \Delta_{24}\frac{z'(0)+z'(\pi)}{2} = 0. \quad (4.4)$$

Summing up these boundary conditions $(4.2)^{+}$, we have

$$(\overline{\Delta_{14}} + \overline{\Delta_{34}})z(0) + (\overline{\Delta_{12}} + \overline{\Delta_{32}})z(\pi) + \overline{\Delta_{24}}[z'(0) - z'(\pi)] = 0,$$

$$(\overline{\Delta_{12}} + \overline{\Delta_{32}})\frac{z(0)+z(\pi)}{2} + \overline{\Delta_{24}}[z'(0) - z'(\pi)] = 0. \quad (4.5)$$

Combining (4.4) with (4.5), we get the following system of equations:

$$\begin{cases} (\Delta_{12} + \Delta_{32})\dfrac{z(0) + z(\pi)}{2} + \Delta_{24}\dfrac{z'(0) - z'(\pi)}{2} = 0. \\ (\overline{\Delta_{12}} + \overline{\Delta_{32}})\dfrac{z(0) + z(\pi)}{2} + \overline{\Delta_{24}}\dfrac{z'(0) - z'(\pi)}{2} = 0. \end{cases}$$

This system of equations has a non-trivial solution, thus

$$\begin{vmatrix} \Delta_{12} + \Delta_{32} & \Delta_{24} \\ \overline{\Delta_{12}} + \overline{\Delta_{32}} & \overline{\Delta_{24}} \end{vmatrix} = 0,$$

or

$$\overline{\left(\frac{\Delta_{12} + \Delta_{32}}{\Delta_{24}}\right)} = \frac{\Delta_{12} + \Delta_{32}}{\Delta_{24}} = \frac{\Delta_{14} + \Delta_{34}}{\Delta_{24}}.$$

Therefore, operator L^{+} has the form:

$$L^{+}z = -z'' + q(x)z, x \in (0, \pi);$$

$$\begin{cases} \dfrac{\Delta_{12} + \Delta_{32}}{\Delta_{24}}[z(0) + z(\pi)] + z'(0) + z'(\pi) = 0, \\ \overline{\Delta_{14}}z(0) + \overline{\Delta_{24}}z'(0) + \overline{\Delta_{12}}z(\pi) = 0; \end{cases}$$

where

$$\overline{\left(\frac{\Delta_{12} + \Delta_{32}}{\Delta_{24}}\right)} = \frac{\Delta_{12} + \Delta_{32}}{\Delta_{24}} = \frac{\Delta_{14} + \Delta_{34}}{\Delta_{24}}.$$

Now we find the operator L, subtracting the second row of the formula (4.2) from the first row, we obtain

$$(\Delta_{12} - \Delta_{14})y(0) + (\Delta_{32} - \Delta_{34})y(\pi) - \Delta_{24}[y'(0) + y'(\pi)] = 0,$$

$$(\Delta_{12} - \Delta_{14})y(0) + (\Delta_{14} - \Delta_{12})y(\pi) - \Delta_{24}[y'(0) + y'(\pi)] = 0,$$

$$(\Delta_{12} - \Delta_{14})[y(0) - y(\pi)] - \Delta_{24}[y'(0) + y'(\pi)] = 0.$$

Consequently, operator L has the form

$$\begin{cases} \dfrac{\Delta_{12} - \Delta_{14}}{\Delta_{24}}[y(0) - y(\pi)] - y'(0) - y'(\pi) = 0, \\ \Delta_{12}y(0) + \Delta_{32}y(\pi) - \Delta_{24}y'(\pi) = 0. \end{cases}$$

Further, from the formula $LP = PL^{+}$ we get

$$LPz = PL^{+}z, \forall z \in D(L^{+}),$$

$$LPz = L^{\circ}\frac{z(x) + z(\pi - x)}{2} = -\frac{z''(x) + z''(\pi - x)}{2} + q(x)\frac{z(x) + z(\pi - x)}{2};$$

$$PL^{+}z = P^{\circ}\left[-z'' + \overline{q(x)}z\right] = -\frac{z''(x) + z''(\pi - x)}{2} +$$

$$+\frac{\bar{q}(x)z(x) + \bar{q}(\pi - x)z(\pi - x)}{2};$$

$$q(x)z(x) + q(x)z(\pi - x) = \bar{q}(x)z(x) + \bar{q}(\pi - x)z(\pi - x),$$

$$[q(x) - \bar{q}(x)]z(x) + [q(x) - \bar{q}(\pi - x)]z(\pi - x) = 0, \ (4.6)$$

$$[q(\pi - x) - \bar{q}(\pi - x)]z(\pi - x) + [q(\pi - x) - \bar{q}(x)]z(x) = 0;$$

$$\begin{vmatrix} q(x) - \bar{q}(x) & q(x) - \bar{q}(\pi - x) \\ q(\pi - x) - \bar{q}(x) & q(\pi - x) - \bar{q}(\pi - x) \end{vmatrix} = 0;$$

$$[q(x) - \bar{q}(x)] \cdot [q(\pi - x) - \bar{q}(\pi - x)] = [q(x) - \bar{q}(\pi - x)] \cdot [q(\pi - x) - \bar{q}(x)]$$

$$q(x)q(\pi - x) - q(x)\bar{q}(\pi - x) - \bar{q}(x)q(\pi - x) + \bar{q}(x)\bar{q}(\pi - x) =$$

$$= q(x)q(\pi - x) - q(x)\bar{q}(x) - \bar{q}(\pi - x)q(\pi - x) + \bar{q}(\pi - x)\bar{q}(x);$$

$$q(x)\bar{q}(\pi - x) + \bar{q}(x)q(\pi - x) = q(x)\bar{q}(x) + \bar{q}(\pi - x)q(\pi - x),$$

$$q(x)[\bar{q}(\pi - x) - \bar{q}(x)] + q(\pi - x)[\bar{q}(x) - \bar{q}(\pi - x)] = 0,$$

$$[\bar{q}(x) - \bar{q}(\pi - x)] \cdot [q(\pi - x) - q(x)] = 0,$$

$$|q(x) - q(\pi - x)|^2 = 0, \Rightarrow \ q(x) = q(\pi - x). \qquad (4.7)$$

From (4.6) and (4.7) it follows that

$$[q(x) - \bar{q}(x)]z(x) + [q(x) - \bar{q}(x)]z(\pi - x) = 0,$$

$$[q(x) - \bar{q}(x)][z(x) + z(\pi - x)] = 0, \Rightarrow q(x) - \bar{q}(x) = 0.$$

Lemma 4.4. If

a) $\Delta_{24} \neq 0$;

b) $QL = L^{+}Q$,

then

1) $\overline{\left(\frac{\Delta_{14} - \Delta_{12}}{\Delta_{24}}\right)} = \frac{\Delta_{14} - \Delta_{12}}{\Delta_{24}} = \frac{\Delta_{32} - \Delta_{34}}{\Delta_{24}}$;

2) $q(\pi - x) = q(x)$;

3) $\bar{q}(x) = q(x)$,

and the operators L and L^{+} take the forms:

$$Ly = -y'' + q(x)y, x \in (0, \pi);$$

$$\begin{cases} \frac{\Delta_{12} - \Delta_{14}}{\Delta_{24}}[y(0) - y(\pi)] - y'(0) - y'(\pi) = 0, \\ \Delta_{12}y(0) + \Delta_{32}y(\pi) - \Delta_{24}y'(\pi) = 0. \end{cases}$$

$$L^{+}z = -z'' + q(x)z, x \in (0, \pi);$$

$$\begin{cases} \overline{\left(\frac{\Delta_{12} + \Delta_{32}}{\Delta_{24}}\right)}[z(0) + z(\pi)] + z'(0) - z'(\pi) = 0, \\ \overline{\Delta_{14}}z(0) + \overline{\Delta_{24}}z'(0) + \overline{\Delta_{12}}z(\pi) = 0. \end{cases}$$

Proof.

If $QL = L^{+}Q$ and $y \in D(L)$, тthen $z = Qy \in D(L^{+})$, thus we get

$$z(x) = \frac{y(x) - y(\pi - x)}{2}, z'(x) = \frac{y'(x) + y'(\pi - x)}{2};$$

$$\begin{cases} \overline{\Delta_{14}}\dfrac{y(0)-y(\pi)}{2}+\overline{\Delta_{24}}\dfrac{y'(0)+y'(\pi)}{2}+\overline{\Delta_{12}}\dfrac{y(\pi)-y(0)}{2}=0, \\ \overline{\Delta_{34}}\dfrac{y(0)-y(\pi)}{2}+\overline{\Delta_{32}}\dfrac{y(\pi)-y(0)}{2}-\overline{\Delta_{24}}\dfrac{y'(\pi)+y'(0)}{2}=0; \end{cases}$$

$$\begin{cases} (\Delta_{14}-\Delta_{12})\dfrac{y(0)-y(\pi)}{2}+\overline{\Delta_{24}}\dfrac{y'(0)+y'(\pi)}{2}=0, \\ (\overline{\Delta_{34}}-\overline{\Delta_{32}})\dfrac{y(0)-y(\pi)}{2}-\Delta_{24}\dfrac{y'(0)+y'(\pi)}{2}=0. \end{cases}$$

Due to the formula $\Delta_{14}-\Delta_{12}=\Delta_{32}-\Delta_{34}$ these boundary conditions melt into one boundary condition

$$(\overline{\Delta_{14}}-\overline{\Delta_{12}})\frac{y(0)-y(\pi)}{2}+\overline{\Delta_{24}}\frac{y'(0)+y'(\pi)}{2}=0. \quad (4.8)$$

Subtracting the second row of the formula (4.2) from its first row, we have

$$(\Delta_{14}-\Delta_{12})y(0)+(\Delta_{34}-\Delta_{32})y(\pi)+\Delta_{24}[y'(0)+y'(\pi)]=0,$$

$$(\Delta_{14}-\Delta_{12})[y(0)-y(\pi)]+\Delta_{24}[y'(0)+y'(\pi)]=0,$$

$$(\Delta_{14}-\Delta_{12})\frac{[y(0)-y(\pi)]}{2}+\Delta_{24}\frac{[y'(0)+y'(\pi)]}{2}=0. \quad (4.9)$$

Combining (4.8) with (4.9), we get the system of equations

$$\begin{cases} (\overline{\Delta_{14}}-\overline{\Delta_{12}})\dfrac{y(0)-y(\pi)}{2}+\overline{\Delta_{24}}\dfrac{y'(0)+y'(\pi)}{2}=0, \\ (\Delta_{14}-\Delta_{12})\dfrac{y(0)-y(\pi)}{2}+\Delta_{24}\dfrac{y'(0)+y'(\pi)}{2}=0. \end{cases}$$

This system has a non-trivial solution, therefore

$$\begin{vmatrix} \overline{\Delta_{14}}-\overline{\Delta_{12}} & \overline{\Delta_{24}} \\ \Delta_{14}-\Delta_{12} & \Delta_{24} \end{vmatrix}=0, => \overline{\left(\frac{\Delta_{14}-\Delta_{12}}{\Delta_{24}}\right)}=\frac{\Delta_{14}-\Delta_{12}}{\Delta_{24}}=\frac{\Delta_{32}-\Delta_{34}}{\Delta_{24}}.$$

Thus, operator L has the form

$$Ly=-y''+q(x)y, x\in(0,\pi);$$

$$\begin{cases} \frac{\Delta_{14}-\Delta_{12}}{\Delta_{24}}[y(0)-y(\pi)]+y'(0)+y'(\pi)=0, \\ \Delta_{12}y(0)+\Delta_{32}y(\pi)-\Delta_{24}y'(\pi)=0; \end{cases}$$

where

$$\overline{\left(\frac{\Delta_{14}-\Delta_{12}}{\Delta_{24}}\right)}=\frac{\Delta_{14}-\Delta_{12}}{\Delta_{24}}=\frac{\Delta_{32}-\Delta_{34}}{\Delta_{24}}.$$

Combining boundary conditions $(4.2)^{+}$, we receive:

$$(\overline{\Delta_{14}}+\overline{\Delta_{34}})z(0)+(\overline{\Delta_{12}}+\overline{\Delta_{32}})z(\pi)+\overline{\Delta_{24}}[z'(0)-z'(\pi)]=0,$$

$$(\overline{\Delta_{12}}+\overline{\Delta_{32}})[z(0)+z(\pi)]+\overline{\Delta_{24}}[z'(0)-z'(\pi)]=0,$$

$$\frac{\overline{\Delta_{12}}+\overline{\Delta_{32}}}{\overline{\Delta_{24}}}[z(0)+z(\pi)]+z'(0)-z'(\pi)=0.$$

Consequently,

$$L^{+}z=-z''+q(x)z, x\in(0,\pi);$$

$$\overline{\left(\frac{\Delta_{12}+\Delta_{32}}{\Delta_{24}}\right)}[z(0)+z(\pi)]+z'(0)-z'(\pi)=0,$$

$$\overline{\Delta_{14}}z(0)+\overline{\Delta_{24}}z'(0)+\overline{\Delta_{12}}z(\pi)=0.$$

Further, from the formula $QL = L^{+}Q$, we have

$$QLy = Q^{\circ}[-y''+q(x)y] = -\frac{y''(x)-y''(\pi-x)}{2}+$$

$$+\frac{q(x)y(x)-q(\pi-x)y(\pi-x)}{2};$$

$$L^{+}Qy = L^{+}\left[\frac{y(x)-y(\pi-x)}{2}\right]=$$

$$=-\frac{y''(x)-y''(\pi-x)}{2}+\bar{q}(x)\frac{y(x)-y(\pi-x)}{2};$$

$$q(x)y(x)-q(\pi-x)y(\pi-x)=\bar{q}(x)y(x)-\bar{q}(x)y(\pi-x),$$

$[q(x)-\bar{q}(x)]y(x)+[\bar{q}(x)-q(\pi-x)]y(\pi-x)=0,$ (4.10)

$$[q(\pi-x)-\bar{q}(\pi-x)]y(\pi-x)+[\bar{q}(\pi-x)-q(x)]y(x)=0;$$

$$\begin{vmatrix} q(x)-\bar{q}(x) & \bar{q}(x)-q(\pi-x) \\ \bar{q}(\pi-x)-q(x) & q(\pi-x)-\bar{q}(\pi-x) \end{vmatrix}=0,$$

$$[q(x)-\bar{q}(x)]\cdot[q(\pi-x)-\bar{q}(\pi-x)]-$$

$$-[\bar{q}(x)-q(\pi-x)][\bar{q}(\pi-x)-q(x)]=0,$$

$$q(x)q(\pi-x)-q(x)\bar{q}(\pi-x)-\bar{q}(x)q(\pi-x)+\bar{q}(x)\bar{q}(\pi-x)=$$

$$=\bar{q}(x)\bar{q}(\pi-x)-\bar{q}(x)q(x)-q(\pi-x)\bar{q}(\pi-x)+q(\pi-x)q(x),$$

$$q(x)\bar{q}(\pi-x)+\bar{q}(x)q(\pi-x)=\bar{q}(x)q(x)+q(\pi-x)\bar{q}(\pi-x),$$

$$q(x)[\bar{q}(\pi-x)-\bar{q}(x)]+q(\pi-x)[\bar{q}(x)-\bar{q}(\pi-x)]=0,$$

$$[\bar{q}(x)-\bar{q}(\pi-x)][q(\pi-x)-q(x)]=$$

$$=-|q(x)-q(\pi-x)|^{2}=0, \Rightarrow\ q(x)=q(\pi-x). \tag{4.7}$$

From (4.7) and (4.10), we have

$$[q(x)-\bar{q}(x)]y(x)+[\bar{q}(x)-q(x)]y(\pi-x)=0,$$

$$[q(x)-\bar{q}(x)][y(x)-y(\pi-x)]=0, \Rightarrow\ q(x)-\bar{q}(x)=0.$$

Comparing the results of Lemma 4.3 and Lemma 4.4, we obtain the following theorem

Theorem 4.1. If

а) $\Delta_{24}\neq 0$;

б) $LP = PL^{+}$;

в) $QL = L^{+}Q$,

then restriction of the operator L to the subspace $H_1 = PH$ has the form

$$L_1 u = -u''+q(x)u, x\in\left(0,\frac{\pi}{2}\right),$$

$$\frac{\Delta_{12}+\Delta_{32}}{\Delta_{24}}u(0)+u'(0)=0, u'\left(\frac{\pi}{2}\right)=0; \tag{4.11}$$

and restriction of the operator L^+ to the subspace $H_2 = QH$ has the form

$$L_2 v = -v'' + q(x)v, x \in \left(0, \frac{\pi}{2}\right),$$
$$\frac{\Delta_{14}-\Delta_{12}}{\Delta_{24}} v(0) + v'(0) = 0, v\left(\frac{\pi}{2}\right) = 0; \tag{4.12}$$

where

1) $\overline{\left(\frac{\Delta_{12}+\Delta_{32}}{\Delta_{24}}\right)} = \frac{\Delta_{12}+\Delta_{32}}{\Delta_{24}} = \frac{\Delta_{14}+\Delta_{34}}{\Delta_{24}}$;
2) $\overline{\left(\frac{\Delta_{14}-\Delta_{12}}{\Delta_{24}}\right)} = \frac{\Delta_{14}-\Delta_{12}}{\Delta_{24}} = \frac{\Delta_{32}-\Delta_{34}}{\Delta_{24}}$;
3) $q(\pi - x) = q(x)$;
4) $\bar{q}(x) = q(x)$.

Equating the coefficients of the boundary conditions (4.11) and (4.12), we have

$$\Delta_{12} + \Delta_{32} = \Delta_{14} - \Delta_{12}, => \Delta_{12} = \Delta_{14} - \Delta_{12} - \Delta_{32} =$$
$$= -(\Delta_{12} + \Delta_{32} - \Delta_{14}) = -\Delta_{34}.$$

Then operators L_1 and L_2 have the following forms

$$L_1 u = -u'' + q(x)u, x \in \left(0, \frac{\pi}{2}\right),$$
$$(\Delta_{14} - \Delta_{12})u(0) + \Delta_{24}u'(0) = 0, u'\left(\frac{\pi}{2}\right) = 0;$$
$$L_2 v = -v'' + q(x)v, x \in \left(0, \frac{\pi}{2}\right),$$
$$(\Delta_{14} - \Delta_{12})v(0) + \Delta_{24}v'(0) = 0, v\left(\frac{\pi}{2}\right) = 0.$$

If spectrum of the operator L is known, then by Lemma 4.2 spectra of the operators L_1 and L_2, considered on the segment $\left[0, \frac{\pi}{2}\right]$, are known. Then, by the Borg theorem, the operator L is defined uniquely on the interval $\left[0, \frac{\pi}{2}\right]$, and due to the evenness and periodicity of the functions $q(x)$, on the whole interval $[0, \pi]$.

ӘОЖ 517.9

А.Ш. Шалданбаев[1], А.А. Шалданбаева[2] , Б.А. Шалданбай[3]

[1]Халықаралық Silkway университеті, Шымкент қ., Казақстан;
[2]Аймақтық әлеуметтік-инновациялық университеті, Шымкент қ., Казақстан;
[3]М.О.Ауезов атындағы Оңтүстік Қазақстан мемлекеттік университеті, Шымкент қ., Казақстан

ПОТЕНЦИАЛЫ СИММЕТРИЯЛЫ, АЛ ШЕКАРАЛЫҚ ШАРТТАРЫ АЖЫРАМАЙТЫН ШТУРМ-ЛИУВИЛЛ ОПЕРАТОРЫНЫҢ КЕРІ ЕСЕБІ ТУРАЛЫ

Аннотация. Бұл еңбекте потенциалы симметриялы,нақты әрі үзіксіз, ал шекаралық шарттары ажырамайтын Штурм-Лиувилл операторын бір спектр арқылы анықтауға болатыны көрсетілді. Зерттеу әдісі бұрынғы әдістердің ешбіріне ұқсамайды, және ол оператордың ішкі симметриясына негізделген, ал ол өз кезегінде инвариантты кеңістіктердің салдары.

Түйін сөздер: Штурм-Лиувиллдің операторы, спектр, Штурм-Лиувиллдің кері есебі, Боргтың теоремасы, Амбарцумянның теоремасы, Левинсонның теоремасы, ажырамайтын шекаралық шарттар, симметриялы потенциал,инвариантты кеңістіктер.

УДК 517.9

А.Ш.Шалданбаев[1], А.А.Шалданбаева[2], Б.А.Шалданбай[3]

[1]Международный университет Silkway, г. Шымкент, Казахстан;
[2]Региональный социально-инновационный университет, г. Шымкент, Казахстан;
[3]Южно-Казахстанский Государственный университет им.М.Ауезова, г. Шымкент, Казахстан

ОБРАТНАЯ ЗАДАЧА ОПЕРАТОРА ШТУРМА-ЛИУВИЛЛЯ С НЕРАЗДЕЛЕННЫМИ КРАЕВЫМИ УСЛОВИЯМИ И СИММЕТРИЧНЫМ ПОТЕНЦИАЛОМ

Аннотация. В данной работе доказана теорема единственности по одному спектру для оператора Штурма-Лиувилля с неразделенными краевыми условиями и вещественным непрерывным и симметричным потенциалом. Метод исследования отличается от всех известных методов и основан на внутреннюю симметрию оператора, порожденного инвариантными подпространствами.

Ключевые слова: оператор Штурма-Лиувилля, спектр, обратная задача Штурма-Лиувилля, теорема Борга, теорема Амбарцумяна, теорема Левинсона, неразделенные краевые условия, симметричный потенциал, инвариантные подпространства.

Information about authors:

Shaldanbayev A.Sh. – doctor of physico-mathematical Sciences, associate Professor, head of the center for mathematical modeling, «Silkway» International University, Shymkent; http://orcid.org/0000-0002-7577-8402;

Shaldanbayeva A.A. - "Regional Social-Innovative University", Shymkent; https://orcid.org/0000-0003-2667-3097;

Shaldanbay B.A. - M.Auezov South Kazakhstan State University, Shymkent; https://orcid.org/0000-0003-2323-0119.

REFERENCES

[1] Ambartsumyan V.A. Uber eine Frage der Eigenwert-theorie, Zsch.f.Physik, 53(1929), 690-695.

[2] Borg G. Eine Umbehrung der Sturm – Liovillschen Eigenwertaufgabe, Acta Math., 78, №2(1946)

[3] Levinson N. The inverse Sturm – Lioville problem, Math.Tidsskr. B., 1949, 25-30.

[4] Hald O.H. The Inverse Sturm-Liouville Problem with symmetric Potentials, Acta mathematica 1978,141:1,263 .

[5] Isaakson E. L., Trubowitz - Pure Appl. Math. 1983. V. 36. N 6. P. 763-783.

[6] Isaakson E. L., McKean H. P., Trubowitz - Pure Appl. Math. 1984. V. 37. N 1. P. 1-12.

[7] Levitan B.M. On definition of the Sturm-Liouville operator by two spectra. News of the AS USSR, ser. Math., 28(1964), 63-78.

[8] Levitan B.M. On definition of the Sturm-Liouville operator by one and two spectra. News of the AS USSR, ser. Math., 42. №1. 1964.

[9] Plaksina O.A., Inverse problems of spectral analysis for Sturm – Liouville operators with non-separated boundary conditions, Math. Sb., 1986, Vol. 131 (173), Number 1(9), 3–26.

[10] Plaksina O.A., Inverse problems of spectral analysis for Sturm – Liouville operators with non-separated boundary conditions. II, Math. Sat, 1988, vol. 136 (178), Number 1(5), 140–159.

[11] Esin Inan Eskitascioglu, Mehmet Acil. An inverse sturm-liouville problem with a generalized symmetric potential., Electronic Journal of Differential Equations, Vol. 2017 (2017), No. 41, pp. 1-7. ISSN: 1072-6691. URL: http://ejde.math.txstate.edu or http://ejde.math.unt.edu.

[12] Martin Bohnera, Hikmet Koyunbakanb.Inverse Problems for Sturm–Liouville Difference Equations. Filomat 30:5 (2016), 1297–1304 DOI 10.2298/FIL1605297B.

[13] Münevver Tuz.On inverse sturm- liouville problems with symmetric potentials., ITM Web of Conferences 13, 01035 (2017) DOI: 10.1051/itmconf/20171301035.

[14] Akylbayev M.I., Beysebayeva A., Shaldanbayev A. Sh., On the Periodic Solution of the Goursat Problem for a Wave Equation of a Special Form with Variable Coefficients. News of the National Academy of Sciences of the republic of Kazakhstan. Volume 1, Number 317 (2018), 34 – 50.

[15] Shaldanbaeva A. A., Akylbayev M.I., Shaldanbaev A. Sh., Beisebaeva A.Zh., The Spectral Decomposition of Cauchy Problem's Solution for Laplace Equation. News of the National Academy of Sciences of the republic of Kazakhstan. Volume 5, Number 321 (2018), 75 – 87. https://doi.org/10.32014/2018.2518-1726.10

[16] T.Sh. Kal'menov, A.Sh. Shaldanbaev, On a criterion of solvability of the inverse problem of heat conduction. Journal of Inverse and Ill-posed Problems. 18:5, (2010). 471_492.

[17] Shaldanbayev A., Shomanbayeva M., Kopzhassarova A., Solution of a singularly perturbed Cauchy problem for linear systems of ordinary differential equations by the method of spectral decomposition, International Conference on Analysis and Applied Mathematics (ICAAM 2016) Серия книг: AIP Conference Proceedings Том:1759 Номер статьи: 020090 DOI: 10.1063/1.4959704, 2016.

[18] Orazov I., Shaldanbayev A., Shomanbayeva M., Solution of a singularly perturbed Cauchy problem using a method of a deviating argument, Advancements in Mathematical Sciences (AMS 2015) Серия книг: AIP Conference Proceedings Том: 1676

Номер статьи: 020072 DOI:10.1063/1.4930498, 2015, WOS:000371818700072, International Conference on Advancements in Mathematical Sciences (AMS),NOV 05-07, 2015, Antalya, Turkey.

[19] Shaldanbayev A., Orazov I., Shomanbayeva M., On the restoration of an operator of Sturm-Liouville by one spectrum, International Conference on Analysis and Applied Mathematics (ICAAM 2014). Серия книг: AIP Conference Proceedings Том: 1611 Стр. 53-57, DOI: 10.1063/1.4893803, 2014, WOS:000343720600010, 2-nd International Conference on Analysis and Applied Mathematics (ICAAM), SEP 11-13, 2014,Shymkent, Kazakhstan.

[20] Orazov I., Shaldanbayev A., Shomanbayeva M., About the Nature of the Spectrum of the Periodic Problem for the Heat Equation with a Deviating Argument, Abstract and Applied Analysis Номер статьи: 128363 DOI: 10.1155/2013/128363. Опубликовано: 2013,WOS:000325557100001.

[21] Imanbaeva, A.B., Kopzhasarova, A.A. and Shaldanbaev, A.Sh. Asymptotic expansion of solution of a singularly perturbed Cauchy problem for a system of ordinary differential equations with constant coefficients. “News of NAS RK. Physics and Mathematics Series”, 2017, No. 5, 112-127.

[22] Kopzhasarova A.A., Shaldanbaev A.Sh., Imanbaeva A.B. Solution of singularly perturbed Cauchy problem by the similarity method. “News of NAS RK. Physics and Mathematics Series”, 2017, no 5,127-134.

[23] Amir Sh. Shaldanbayev, Manat T. Shomanbayeva , Solution of singularly perturbed Cauchy problem for ordinary differential equation of second order with constant coefficients by Fourier method ,Citation: AIP Conference Proceedings 1880, 040017 (2017); doi: 10.1063/1.5000633 View online: http://dx.doi.org/10.1063/1.5000633 View Table of Contents: http://aip.scitation.org/toc/apc/1880/1 Published by the American Institute of Physics.

[24] Shaldanbayev A.Sh., Shaldanbayeva A.A., Shaldanbay B.A., On projectional orthogonal basis of a linear non-self - adjoint operator. N e w s of the national academy of sciences of the republic of Kazakhstan Physic - mathematical series 7, Issn 1991-346X https://doi.org/10.32014/2019.2518-1726.15, Volume 2, Number 324 (2019), 79 – 89.

[25] Akylbayev M.I., Shaldanbayev A.Sh., Orazov I., Beysebayeva A., About single operator method of solution of a singularly perturbed Cauchy problem for an ordinary differential equation n – order. N e w s of the national academy of sciences of the republic of Kazakhstan Physico-mathematical series, Issn 1991-346X https://doi.org/10.32014/2019.2518-1726.8, Volume 2, Number 324 (2019), 17 – 36.

N E W S
OF THE NATIONAL ACADEMY OF SCIENCES OF THE REPUBLIC OF KAZAKHSTAN
PHYSICO-MATHEMATICAL SERIES
ISSN 1991-346X **https://doi.org/10.32014/2019.2518-1726.60**
Volume 5, Number 327 (2019), 70 – 77

УДК 517.9: 515.16
МРНТИ 27.31.21

A.A. Zhadyranova

Eurasian International Center for Theoretical Physics and Department
of General & Theoretical Physics, Eurasian National University, Astana 010008, Kazakhstan.
a.a.zhadyranova@gmail.com

HIERARCY OF WDVV ASSOCIATIVITY EQUATIONS FOR $n=3$ AND $N=2$ CASE WHEN $V_0=0$ WITH NEW SYSTEM a_t, b_t, c_t

Abstract. We investigate solutions of Witten-Dijkgraaf-E.Verlinde-H.Verlinde (WDVV) equations. The article discusses nonlinear equations of the third order for a function f = f(x,t)) of two independent variables x,t. The equations of associativity reduce to the nonlinear equations of the third order for a function f = f(x,t)) when prepotential F dependet of the metric η. In this work we consider the WDVV equation for n = 3 case with an antidiagonal metric η. The solution of some cases of hierarchy equations of associativity illustrated. Lax pairs for the system of three equations, that contains the equation of associativity are written to find the hierarchy of associativity equation. Using the compatibility condition are found the relations between the matrices U, V_2, V_1. The elements of matrix V_2 are found with the expression of z_{ij} and independent and dependent variables for the matrix V_2. Also solving elements of matrix V_1 expressed through y_{ij} and independent and dependent variables for the matrix V_1. We accepted that elements of matrix V_0 are zero. In the physical setting the solutions of WDVV describe moduli space of topological conformal field theories [1, 2]. Let us introduce new variables a, b, c. In the above variables the nonlinear equations of the third order for a function f = f(x,t)) we rewritten as a new system of three equations. Expressed are variables a_t ,b_t ,c_t of three equations are written with the help of matrix elements z_{ij} ,y_{ij}.

Key words: equations of Witten-Dijkgraaf-E.Verlinde-H.Verlinde, the equations of associativity, nonlinear equations of the third order, antidiagonal metric, the Lax pair, the compatibility condition, independent elements, dependent variables, system with equations.

Introduction. The WDVV equations, in general, have the following form [1, 2, 3]:

$$\frac{\partial^3 F}{\partial t^i \partial t^j \partial t^p}\eta^{pq}\frac{\partial^3 F}{\partial t^q \partial t^k \partial t^r} = \frac{\partial^3 F}{\partial t^j \partial t^k \partial t^p}\eta^{pq}\frac{\partial^3 F}{\partial t^i \partial t^q \partial t^r}, \quad \forall i,j,k,r \in \{1,...,n\},$$

where F is a prepotential, η is a metric. The coordinates t^i can be linearly rearranged so that the metric, η, is antidiagonal [1], i.e.

$$\eta = \begin{pmatrix} 0 & 0 & 1 \\ 0 & 1 & 0 \\ 1 & 0 & 0 \end{pmatrix}.$$

In this work we consider the WDVV equation for $n=3$ case with an antidiagonal metric η [2]. In this case, two types of dependence of the function F on the fixed variable t^1 were found by Dubrovin [2, 3, 4] which are

$$F = \frac{1}{2}(t^1)^2 t^3 + \frac{1}{2}t^1 (t^2)^2 + f(t^2, t^3) \tag{1}$$

and

$$F = \frac{1}{6}(t^1)^3 + t^1 t^2 t^3 + f(t^2, t^3).$$

For these cases the equations of associativity reduce to the following two nonlinear equations of the third order for a function $f = f(x,t)$) of two independent variables ($x = t^2, t = t^3$):

$$f_{ttt} = f_{xxt}^2 - f_{xxx} f_{xtt} \tag{2}$$

and

$$f_{xxx} f_{ttt} - f_{xxt} f_{xtt} = 1,$$

correspondingly.

The function F in equation (1) has the form from the law of multiplication in the three-dimensional algebra A_t with the basis $e_1 = 1$, e_2 ,e_3 [3]. Every basis is a complete uniformly minimal system [2].

In this work, we consider the solution (1). Let us introduce new variables a,b,c as follows [2, 3]:

$$a = f_{xxx}, \quad b = f_{xxt}, \quad c = f_{xtt}.$$

In the above variables the equation (2) can be rewritten as a system of three equations as follows:

$$\begin{aligned} a_t &= b_x, \\ b_t &= c_x, \\ c_t &= (b^2 - ac)_x. \end{aligned} \tag{3}$$

The Lax pair for the system (3) is given by [8]

$$\begin{aligned} \Psi_x &= \lambda U \Psi, \\ \Psi_t &= \lambda V \Psi, \end{aligned} \tag{4}$$

where U is given by

$$U = \begin{pmatrix} 0 & 1 & 0 \\ b & a & 1 \\ c & b & 0 \end{pmatrix}$$

and V is given by

$$V = \begin{pmatrix} 0 & 0 & 1 \\ c & b & 0 \\ (b^2 - ac) & c & 0 \end{pmatrix}.$$

The compatibility condition for the system (4) is given by

$$\begin{aligned} U_t &= V_x, \\ [U,V] &= 0. \end{aligned}$$

In the following sections we work with the new system (3).

Methods. The solution to a hierarchy for $N = 1$ case corresponds to the system of equations (3). Hierarchy for $N = 2$ case when $V_0 \neq 0$ is given in the work [2]

In this section we consider a hierarchy for $N = 2$ case when $V_0 = 0$ and the following system

$$\begin{aligned} a_t &= \varepsilon_1 b_x + \varepsilon_2 F_x, \\ b_t &= \varepsilon_1 c_x + \varepsilon_2 H_x, \\ c_t &= \varepsilon_1 (b^2 - ac)_x + \varepsilon_2 G_x. \end{aligned} \tag{5}$$

The Lax representation of the above system is same as before in the work [13].
In particular, for $N = 2$ case when $V_0 = 0$ we have

$$\begin{aligned} \Psi_x &= \lambda U \Psi, \\ \Psi_t &= (\lambda^2 V_2 + \lambda V_1)\Psi = V\Psi \end{aligned}$$

The compatibility condition of (4) is given by

$$\lambda U_t - V_x + \lambda [U, V] = 0.$$

The compatibility condition of the Lax representation is given by the system

$$[U, V_2] = 0, \tag{6}$$

$$U_t = V_{1x}, \tag{7}$$

$$V_{2x} = [U, V_1]. \tag{8}$$

Statement of problem. We first consider the second equation of the system and let V_1 to be given by

$$V_1 = \begin{pmatrix} y_{11} & y_{12} & y_{13} \\ y_{21} & y_{22} & y_{23} \\ y_{31} & y_{32} & y_{33} \end{pmatrix}.$$

From the above system it follows that $y_{11}, y_{12}, y_{13}, y_{23}, y_{33}$ are constants w.r.t. x. Writing a system with equations for a_t, b_t, c_t only yields

$$\begin{aligned} a_t &= y_{22x}, \\ b_t &= y_{21x}, \\ b_t &= y_{32x}, \\ c_t &= y_{31x}. \end{aligned} \tag{9}$$

Now we equate similar terms in the systems (5) and (9), i.e. we have a system

$$\begin{aligned} a_t &= y_{22x} = \varepsilon_1 b_x + \varepsilon_2 F_x, \\ b_t &= y_{21x} = \varepsilon_1 c_x + \varepsilon_2 H_x, \\ b_t &= y_{32x} = \varepsilon_1 c_x + \varepsilon_2 H_x, \\ c_t &= y_{31x} = \varepsilon_1 (b^2 - ac)_x + \varepsilon_2 G_x. \end{aligned} \tag{10}$$

Scheme of the method and reduction to equivalent problem. From the above system (10) we find the following

$$\begin{aligned} y_{22} &= \varepsilon_1 b + \varepsilon_2 F, \\ y_{21} &= \varepsilon_1 c + \varepsilon_2 H, \\ y_{32} &= \varepsilon_1 c + \varepsilon_2 H, \\ y_{31} &= \varepsilon_1 (b^2 - ac) + \varepsilon_2 G. \end{aligned}$$

Thus the matrix V_1 has the form

$$V_1 = \begin{pmatrix} y_{11} & y_{12} & y_{13} \\ \varepsilon_1 c + \varepsilon_2 H & \varepsilon_1 b + \varepsilon_2 F & y_{23} \\ \varepsilon_1 (b^2 - ac) + \varepsilon_2 G & \varepsilon_1 c + \varepsilon_2 H & y_{33} \end{pmatrix}. \tag{11}$$

Now we solve the equation (6). Denote V_2 as follows:

$$V_2 = \begin{pmatrix} z_{11} & z_{12} & z_{13} \\ z_{21} & z_{22} & z_{23} \\ z_{31} & z_{32} & z_{33} \end{pmatrix},$$

Plugging U , V_2 into (6) we obtain the following relations:

$$\begin{aligned} z_{23} &= z_{12}, \\ z_{32} &= z_{21}, \\ z_{33} &= z_{11}. \end{aligned}$$

Hence, we are left with the equations

$$\begin{aligned} z_{21} &= b z_{12} + c z_{13}, \\ z_{22} &= z_{11} + a z_{12} + b z_{13}, \\ z_{31} &= c z_{12} + (b^2 - ac) z_{13}. \end{aligned}$$

Thus the matrix V_2 has the form

$$V_2 = \begin{pmatrix} z_{11} & z_{12} & z_{13} \\ b z_{12} + c z_{13} & z_{11} + a z_{12} + b z_{13} & z_{12} \\ c z_{12} + (b^2 - ac) z_{13} & b z_{12} + c z_{13} & z_{11} \end{pmatrix}.$$

Hence, only z_{11}, z_{12}, z_{13} are independent elements of V_2, and the other elements can be written in terms of them.

Now let us find the elements of V_1 in (11). To do so we use the equation (8). First we evaluate $[U, V_1]$.

We have elementwise yields the following system:

11: $z_{11x} = \varepsilon_1 c + \varepsilon_2 H - by_{12} - cy_{13}$,

12: $z_{12x} = \varepsilon_1 b + \varepsilon_2 F - y_{11} - ay_{12} - by_{13}$,

13: $z_{13x} = y_{23} - y_{12}$,

21: $b_x z_{12} + bz_{12x} + c_x z_{13} + cz_{13x} = by_{11} + a(\varepsilon_1 c + \varepsilon_2 H) + (\varepsilon_1(b^2 - ac) + \varepsilon_2 G) - b(\varepsilon_1 b + \varepsilon_2 F) - cy_{23}$,

22: $z_{11x} + a_x z_{12} + az_{12x} + b_x z_{13} + bz_{13x} = by_{12} - by_{23}$,

23: $z_{12x} = by_{13} + ay_{23} + y_{33} - (\varepsilon_1 b + \varepsilon_2 F)$,

31: $c_x z_{12} + cz_{12x} + (b^2 - ac)_x z_{13} + (b^2 - ac)z_{13x} = cy_{11} - cy_{33}$,

32: $b_x z_{12} + bz_{12x} + c_x z_{13} + cz_{13x} = cy_{12} + b(\varepsilon_1 b + \varepsilon_2 F) - (\varepsilon_1(b^2 - ac) + \varepsilon_2 G) - a(\varepsilon_1 c + \varepsilon_2 H) - by_{33}$,

33: $z_{11x} = cy_{13} + by_{23} - (\varepsilon_1 c + \varepsilon_2 H)$.

Now let us express $\varepsilon_1 c + \varepsilon_2 H$, $\varepsilon_1 b + \varepsilon_2 F$, y_{23} in the element 11, 12, 13 of the above system.

$$\begin{aligned} \varepsilon_1 c + \varepsilon_2 H &= z_{11x} + by_{12} + cy_{13}, \\ \varepsilon_1 b + \varepsilon_2 F &= z_{12x} + y_{11} + ay_{12} + by_{13}, \\ y_{23} &= z_{13x} + y_{12}. \end{aligned}$$

Now let us express $\varepsilon_1(b^2 - ac) + \varepsilon_2 G$ in the element 21 and substitute the values for $\varepsilon_1 c + \varepsilon_2 H$, $\varepsilon_1 b + \varepsilon_2 F$, y_{23}

$$\varepsilon_1(b^2 - ac) + \varepsilon_2 G = b_x z_{12} + bz_{12x} + c_x z_{13} + 2cz_{13x} - az_{11x} + bz_{12x} + (b^2 - ac)y_{13} + cy_{12}$$

Now let us express y_{33} in the element 23 and substitute the values for $\varepsilon_1 b + \varepsilon_2 F$, y_{23}

$$y_{33} = 2z_{12x} - az_{13x} + y_{11}$$

Hence, dependent elements of V_1 are given by:

$$\begin{aligned} &\varepsilon_1(b^2 - ac) + \varepsilon_2 G = b_x z_{12} + bz_{12x} + c_x z_{13} + 2cz_{13x} - az_{11x} + bz_{12x} + (b^2 - ac)y_{13} + cy_{12}, \\ &\varepsilon_1 c + \varepsilon_2 H = z_{11x} + by_{12} + cy_{13}, \\ &\varepsilon_1 b + \varepsilon_2 F = z_{12x} + y_{11} + ay_{12} + by_{13}, \\ &y_{23} = z_{13x} + y_{12}, \\ &y_{33} = 2z_{12x} - az_{13x} + y_{11}. \end{aligned} \tag{12}$$

Now let us rewrite the element 22 by substituting the values for y_{23}. So we have

$$z_{11x} + 2bz_{13x} + a_x z_{12} + az_{12x} + b_x z_{13} = 0$$

Now let us rewrite the element 31 by substituting the values for y_{33}. So we have

$$c_x z_{12} + 3cz_{12x} + (b^2 - ac)_x z_{13} + (b^2 - 2ac)z_{13x} = 0$$

Now let us rewrite the element 32 by substituting the values for $\varepsilon_1 b + \varepsilon_2 F$, $\varepsilon_1(b^2 - ac) + \varepsilon_2 G$, $\varepsilon_1 c + \varepsilon_2 H$, y_{33}. So we have

$$2b_x z_{12} + 4bz_{12x} + 2c_x z_{13} + (3c - ab)z_{13x} = 0$$

Now let us rewrite the element 33 by substituting the values for y_{23}, $\varepsilon_1 c + \varepsilon_2 H$

$$2z_{11x} - bz_{13x} = 0$$

Also, the independent variables z_{11}, z_{12}, z_{13} of the matrix V_2 have to satisfy the following system of equations:

$$\begin{aligned} z_{11x} + 2bz_{13x} + a_x z_{12} + az_{12x} + b_x z_{13} &= 0, \\ c_x z_{12} + 3cz_{12x} + (b^2 - ac)_x z_{13} + (b^2 - 2ac)z_{13x} &= 0, \\ 2b_x z_{12} + 4bz_{12x} + 2c_x z_{13} + (3c - ab)z_{13x} &= 0, \\ 2z_{11x} - bz_{13x} &= 0. \end{aligned} \tag{13}$$

From the above system (13) it follows that

$$z_{13x} = \left(\frac{4a_x b - 2ab_x}{3ac - a^2 b - 10b^2} \right) z_{12} + \left(\frac{4bb_x - 2ac_x}{3ac - a^2 b - 10b^2} \right) z_{13} \tag{14}$$

$$\begin{aligned} z_{12x} = &\left(-\frac{c_x}{3c} - \frac{b^2 - 2ac}{3c} \cdot \frac{4a_x b - 2ab_x}{3ac - a^2 b - 10b^2} \right) z_{12} + \\ &+ \left(-\frac{b^2 - 2ac}{3c} \cdot \frac{4bb_x - 2ac_x}{3ac - a^2 b - 10b^2} - \frac{(b^2 - ac)_x}{3c} \right) z_{13} \end{aligned} \tag{15}$$

Results. Using necessary terms in the system (12) in (10), we obtain

$$\begin{aligned} a_t &= \frac{a_x z_{13x}}{2} + a_x y_{12} + b_x y_{13}, \\ b_t &= \frac{b_x z_{13x}}{2} + b_x y_{12} + c_x y_{13}, \\ c_t &= b_{xx} z_{12} + 3b_x z_{12x} + c_{xx} z_{13} + (a_x b + 3c_x - \frac{ab_x}{2}) z_{13x} - a_x z_{11x} + (b^2 - ac)_x y_{13} + c_x y_{12} \end{aligned} \tag{16}$$

We plug $z_{11x}, z_{12x}, z_{13x}$ in (13), (15), (14) into (16) and obtain the following equation

$$\begin{aligned} a_t &= \left(\frac{2ba_x^2 - aa_x b_x}{3ac - a^2 b - 10b^2} \right) z_{12} + \left(\frac{2ba_x b_x - aa_x c_x}{3ac - a^2 b - 10b^2} \right) z_{13} + a_x y_{12} + b_x y_{13}, \\ b_t &= \left(\frac{2ba_x b_x - ab_x^2}{3ac - a^2 b - 10b^2} \right) z_{12} + \left(\frac{2bb_x^2 - ab_x c_x}{3ac - a^2 b - 10b^2} \right) z_{13} + b_x y_{12} + c_x y_{13}, \\ c_t &= \left(b_{xx} - \frac{b_x c_x}{c} + \frac{5abca_x b_x - 4b^3 a_x b_x + 2ab^2 b_x^2 - 3a^2 cb_x^2 + 2b^2 ca_x^2 + 12bca_x c_x - 6acb_x c_x}{3ac^2 - a^2 bc - 10b^2 c} \right) z_{12} \\ &+ \left(c_{xx} - \frac{b_x (b^2 - ac)_x}{c} + \frac{6abcb_x^2 - 4b^3 b_x^2 + 2ab^2 b_x c_x - 3a^2 cb_x c_x + 2b^2 ca_x b_x + 12bcb_x c_x - abca_x c_x - 6acc_x^2}{3ac^2 - a^2 bc - 10b^2 c} \right) z_{13} \\ &+ (b^2 - ac)_x y_{13} + c_x y_{12} \end{aligned} \tag{17}$$

Conclusion. The solution to a hierarchy for $N = 2$ case when system is given by (5) corresponds to the system of equations (17).

So, we considered of some cases of hierarchy of WDVV associativity equations. Lax pairs for the system of three equations, that contained the equation of associativity written to find the hierarchy of associativity equation. Using the compatibility condition are found the relations between the matrices U, V_2, V_1. Thus, we obtained the elements of the matrices V_2, V_1 for case N = 2 when V_0=0 and the above system a_t, b_t, c_t. It was found, that only z_{11} ,z_{12} ,z_{13} are independent elements of V_2, and the other elements can be written in terms of them. From the above system it follows that $y_{11}, y_{12}, y_{13}, y_{23}, y_{33}$ are constants w.r.t. x . It is found, that y_{11}, y_{12}, y_{13} are independent elements of V_1, and the other elements can be written in terms of them and z_{11}, z_{12}, z_{13}. Expressed are variables a_t,b_t,c_t of three equations are written with the help of matrix elements z_{ij},y_{ij}.

Acknowledgments. I express gratitude to Professor R. Myrzakulov for useful discussions and advices. The work is performed under the financial support of the scientific and technical program BR05236277 "Investigation of some problems of astrophysics and cosmology in the framework of the Einstein and non-Einstein theories of gravity", 2018.

УДК 517.9: 515.16
МРНТИ 27.31.21

А.А. Жадыранова

Кафедра общей и теоретической физики Евразийского
национального университета имени Л.Н.Гумилева, Астана, Казахстан

ИЕРАРХИЯ УРАВНЕНИЙ АССОЦИАТИВНОСТИ WDVV ДЛЯ СЛУЧАЯ n = 3 И N = 2 ПРИ V_0= 0 С НОВОЙ СИСТЕМОЙ a_t, b_t, c_t

Аннотация. В данной статье исследуются уравнения Виттена-Диджкграфа-Е.Верлинде-Г.Верлинде (ВДВВ). В работе обсуждаются нелинейные уравнения третьего порядка для функции f = f(x,t) двух независимых переменных x,t. Уравнения ассоциативности сводятся к нелинейным уравнениям третьего порядка для функции f = f(x,t), когда потенциал фунции F связан с метрикой η. В этой работе рассматривается уравнение WDVV для случая n = 3 с антидиагональной метрикой η. Описано решение некоторых случаев иерархии уравнений ассоциативности. Для нахождения иерархии уравнений ассоциативности были записаны пары Лакса для системы из трех уравнений, которая содержит уравнения ассоциативности. С применением условия совместности найдены соотношения между матрицами U, V_2, V_1. Были вычислены элементы матрицы V_2, выраженные через z_{ij}, независимые и зависимые переменные матрицы V_2. Также были найдены элементы матрицы V_1, выраженные через y_{ij} , независимые и зависимые переменные матрицы V_1. Элементы матрицы V_0 равны 0. В физическом приложении решение уравнения ассоциативности WDVV описывает пространство модулей топологических конформных теорий поля. Введены новые переменные a, b, c. В новых переменных нелинейные уравнения третьего порядка для функции f = f(x,t) записаны через новую систему трёх уравнений. Выраженные переменные a_t, b_t, c_t системы из трех уравнений были записаны через матричные элементы z_{ij}, y_{ij}.

Ключевые слова: уравнения Виттена-Дижграфа-Е.Верлинде-Г.Верлинде, уравнения ассоциативности, нелинейные уравнения третьего порядка, антидиагональная метрика, пары Лакса, условие совместности, независимые элементы, зависимые переменные, система с уравнениями.

УДК 517.9: 515.16
МРНТИ 27.31.21

А.А. Жадыранова

Л.Н.Гумилев атындағы Еуразия ұлттық университетінің
жалпы және теориялық физика кафедрасы, Астана, Қазақстан

n = 3 ЖӘНЕ N = 2 ЖАҒДАЙЛАРЫ ҮШІН ЕНГІЗГІЗІЛГЕН ЖАҢА ЖҮЙЕ a_t, b_t, c_t V_0 = 0 БОЛҒАНДАҒЫ WDVV АССОЦИАТИВТІЛІК ТЕҢДЕУІНІҢ ИЕРАРХИЯСЫ

Аннотация. Берілген мақалада Виттен – Диджкграф - Е.Верлинде - Г.Верлинде (ВДВВ) теңдеулері зерттеледі. Бұл жұмыста x, t тәуелсіз айнымалыларынан тұратын f = f(x,t) функциясы үшін үшінші ретті сызықты емес теңдеулер талқыланады. Тәуелсіз x, t айнымалыларынан тұратын f = f(x,t) функциясы үшін үшінші ретті сызықты емес теңдеулер F потенциалы η метрикасымен байланысты болғанда келтіріледі. Сонымен қатар ассоциативтілік теңдеулер иерархиясының бірнеше шешімдері сипатталады. Ассоциативтілік теңдеулерінің иерархиясын табу мақсатында ассоциативтілік теңдеулерінен құралған теңдеулер жүйесі үшін Лакс жұптары жазылды. Сәйкестік шартының қолдану арқылы U, V_2, V_1 матрицалары арасындағы қатынастар анықталды. z_{ij} арқылы өрнектелген V_2 матрицасының элементтері мен V_2 матрицасының тәуелді және тәуелсіз айнымалылары

есептелінді. y_{ij} арқылы өрнектелген V_1 матрицасының элементтері мен V_1 матрицасының тәуелді және тәуелсіз айнымалылары табылды. Сонымен қатар V_0 матрицасының элементтері нөлге тең деп алынды. Физикалық қолданылуда WDVV ассоциативтілік теңдеуінің шешімі өрістің топологиялық конформдық теориясының модульдерінің кеңістігін сипаттайды. Жаңа айнымалылар енгізілген. Жаңа айнымалыларда f = f(x,t) функциясы үшін үшінші ретті сызықты емес теңдеулер жаңа жүйе арқылы жазылған. Теңдеулер жүйесінен тұратын a_t, b_t, c_t айнымалылары z_{ij}, y_{ij} матрицалық елементтері арқылы өрнектеліп жазылды.

Түйін сөздер: Виттен-Диджграф-Е.Верлинде-Г.Верлинде теңдеулері, ассоциативтілік теңдеуі, үшінші ретті сызықты емес теңдеулер, антидиагональ метрика, Лакс жұптары, үйлесімділік шарты, тәуелсіз элементтер, тәуелді айнымалылар, теңдеулер жүйесі.

Information about authors:

Zhadyranova A.A. - PhD student of the department of general and theoretical physics, L.N. Gumilyov Eurasian National University, Satpayev str., Astana, Kazakhstan. E-mail: a.a.zhadyranova@gmail.com

REFERENCES

[1] Kontsevich M., Manin Yu., Gromov-Witten classes, quantum cohomology and enumerative geometry, Mirror symmetry, II, 607-653, AMS/IP Stud. Adv. Math., 1, Amer. Math. Soc., Providence, RI, (1997).

[2] Kontsevich M., Manin Yu., Relations between the correlators of the topological sigma-model coupled to gravity, Comm. Math. Phys., 196 (1998), no. 2, 385-398.

[3] Dubrovin B.A. Geometry of 2D topological field theories, Springer Lecture Notes in Math. 1620, 120-348, 1996. [arXiv:hep-th/9407018]

[4] Dijkgraaf R., Verlinde E., Verlinde H., Notes on topological string theory and 2D quantum gravity, Nucl. Phys. B 352 (1991) 59.

[5] Witten E., On the structure of the topological phase of two-dimensional gravity, Nucl. Phys.B 340 (1990) 281-332.

[6] Hertling C., Frobenius manifolds and moduli spaces for singularities, Cambridge University Press, Cambridge (UK), 2002.

[7] Hertling C., Manin Y., Weak Frobenius manifolds, Internat. Math. Res. Notices, no. 6 (1999), 277-286.

[8] Mokhov O.I., Ferapontov Y.V. Equations of Associativity in Two-Dimensional Topological Field Theory as Integrable Hamiltonian Nondiagonalizable Systems of Hydrodynamic Type, Functional analysis and its applications 30(3), 1995. [arXiv:hep-th/9505180]

[9] Dubrovin B.A., Novikov S.P., Hydrodynamics of weakly deformed soliton lattices. Differential geometry and Hamiltonian theory, Uspekhi Mat.Nauk. 44 (1989), 29-98. English translation in Russ. Math. Surveys 44 (1989), 35-124.

[10] Dubrovin B.A., On almost duality for Frobenius manifolds, Amer. Math. Soc. Transl. 212 (2004) 75-132.

[11] A.Sh. Shaldanbayev , A.A. Shaldanbayeva , B.A. Shaldanbay (**2019**) On projectional orthogonal basis of a linear non-self -adjoint operator. News of the National Academy of Sciences of the Republic of Kazakhstan. Physical-mathematical series. Volume 2, Number 324 (2019), PP, 79–89. ISSN 2518-1726 (Online), ISSN 1991-346X (Print). https://doi.org/10.32014/2019.2518-1726.15

[12] Mokhov O.I. Symplectic and poisson geometry on loop spaces of manifolds and nonlinear equations, Translations of the American Mathematical Society-Series 2 170, 121-152, 1995. [arXiv:hep-th/9503076]

[13] Ferapontov E.V., Mokhov O.I., Nonlocal Hamiltonian operators of hydrodynamic type that are connected with metrics of constant curvature, Russ. Math. Surv. 45 (1990), no. 3, 218-219.

[14] Zhadyranova A.A., Myrzakul Zh.R., Anuarbekova Y.Ye. Hierarchy of WDVV associativity equations for n = 3 case and N = 2 when V0≠0 [Ierarchiya WDVV uravneniya dlya n = 3 i N = 2 sluchaya, kogda V0≠0] Bulletin of L.N. Gumilyov Eurasian National University [Vestnik Evrazijskogo nacional’nogo universiteta imeni L.N. Gumileva]. 4(125), 60-66, 2018.

N E W S
OF THE NATIONAL ACADEMY OF SCIENCES OF THE REPUBLIC OF KAZAKHSTAN
PHYSICO-MATHEMATICAL SERIES
ISSN 1991-346X **https://doi.org/10.32014/2019.2518-1726.61**
Volume 5, Number 327 (2019), 78 – 88

МРНТИ: 41.29.21; 41.29.25
UDK 524

D. Kairatkyzy[1, 2]

[1]Al-Farabi Kazakh National University,
[2]"V.G. Fesenkov Astrophysical Institute", JSC "national Center of Space Research and Technology",
Aerospace Committee of the MDAI of the Republic of Kazakhstan
kairatkyzy_dina90@mail.ru

THE EVOLUTION OF DARK MATTER AND THE FORMATION BASIC THEORY OF STRUCTURAL GROWTH OF THE STANDARD UNIVERSE MODEL

Abstract. The formation and evolution of dark matter and galaxies is one of the basic topics in cosmological research. This thesis uses numerical simulation to study the evolution of the universe under the cold dark matter model. The first chapter introduces the relevant background, including the theory of cosmology and structure formation, the evolution of dark matter levels and the physical processes of galaxy formation, and the numerical simulation tools we use: N-body simulation and semi-analytical galaxies formation models.The second part solves the local cavity crisis by using high-precision numerical simulation combined with semi-analytical model. The local void is considered to be the crisis of the standard cosmological model because the density of the galaxies is too low, and some of the predecessors believe that such low density cannot exist in the cosmic structure predicted by standard cosmology. We look for a system similar to the local space in the numerical simulation of standard cosmology, and then look for a structure similar to the local void to verify whether the local void exists in standard cosmology. Our work found that 77 similar local space systems can be found in the simulation, with a 14% chance of finding local voids nearby, indicating that local voids can exist entirely in the cold dark matter model. The reason for the extremely low density of local hollow galaxies is that it is mainly due to the low density of dark matter halos, and the influence of the environment on the formation of galaxies also reduces the number of galaxies by 25%.

Key words: Standard cosmological model, dark matter halo, local cavity crisis.

1. Basic theory of structural growth of the Universe

Since the universe is expanding, the universe must be smaller than it is in the past, and it will continue to go back to the past. The universe collapsed into a state of extremely high density and extremely high temperature. The current structure is formed by the "big bang" and subsequent surges. Hubble's Law finally introduces the now widely accepted "Big Bang" universe model. At the beginning of the "Big Bang", most astronomers considered it a joke, but since 1964, the discovery of microwave background radiation [1] has made the "Big Bang" cosmological model gradually mainstream.

From the theoretical point of view, the same expanded universe. In 1917, Einstein used the general theory of relativity to study the universe and found that the universe was not static, so he introduced cosmological constants to try to keep the universe stable. Subsequently, in 1922, Friedman combined the Robertson-Walker metric [2] to obtain the Friedman equation: assuming that the universe is homogeneously isotropic, then Robertson-Walker can be used at any point in the universe. Gauge representation

$$ds^2 = (cdt)^2 - a^2(t)\left[\frac{dr^2}{1-kr^2} + r^2\left(d\theta^2 + sin^2\theta d\phi^2\right)\right] \quad (1)$$

Where c is the speed of light, it can also be written as 1, $(r,\ \theta,\ \varphi)$ is the spatial co-polar polar system, t is the time, $a(t)$ is the scale factor, today is equal to 1, k is a constant, only the three values 1,0,1 represent the open, flat, and closed Universe. Using this metric, the Einstein field equation can be reduced to the Friedman equation:

$$\ddot{a} = -\frac{4\pi G}{3}a(\rho + \frac{3p}{c^2}) + [\frac{1}{3}\Lambda ac^2], \quad (2)$$

$$\dot{a}^2 = -\frac{8\pi G\rho}{3}a^2 - kc^2 + [\frac{1}{3}\Lambda a^2c^2], \quad (3)$$

Here G is the gravitational constant, ρ is the average density of the universe, and Λ is the cosmological constant. Define the basic parameters: Hubble constant $H = \dot{a}/a$, cosmic density $\Omega_m = 8\pi G\rho/3H^2$ and cosmological constant density $\Omega_\Lambda = \Lambda c^2/3H^2$, and assume that the cosmic curvature density is $\Omega_\kappa = -k/(aH)^2$. This formulacan be simplified to:

$$\Omega_m + \Omega_\Lambda + \Omega_k = 1 \quad (4)$$

This formula simply gives the three energies in the universe: the relationship between matter, curvature, and dark energy. $\Omega_{m,0}$, $\Omega_{\Lambda,0}$, $\Omega_{k,0}$ represent the average material density, cosmological constant density and curvature density of the current universe. Then the variation of the density of the universe with the scale factor is $\Omega_m = \Omega_{m,0}/a^3$, $\Omega_\Lambda = \Omega_{\Lambda,0}$ and $\Omega_k = \Omega_{k,0}/a^2$. Moreover, the relationship between the redshift and expansion factors of cosmology is:

$$1 + z = \frac{a(t_0)}{a(t)} = \frac{\lambda_{obs}}{\lambda} \quad (5)$$

Then, Equation 4 can be written as:

$$\frac{H^2(z)}{H_0^2} = \Omega_{m,0}(1 + z)^3 + \Omega_{k,0}(1 + z)^2 + \Omega_{\Lambda,0} \quad (6)$$

Where $\Omega_{m,0}$, $\Omega_{\Lambda,0}$, H_0 are the three basic cosmological constants. The curvature of the universe Ω_k is confirmed to be very close to $k \approx 0$ [3]. Cosmological constants can be measured by supernovae, large-scale structures, and microwave background radiation, as shown in Figure 1. As can be seen from the figure, the observations show that our universe is a flat, dark energy-dominated, constantly expanding universe. The latest PLANCK (Planck Collaboration et al., 2013) of the microwave background survey is given by the satellite: $H_0 = 67.3 \pm 1.2\ km/s/\ Mpc$, $\Omega_m = 0.315 \pm 0.017$, $\Omega_\Lambda = 0.685$, $\sigma_8 = 0.828$.

After knowing the three cosmological constants, you can integrate the backtracking time for a given redshift according to Equation 6:

$$t_0 - t_z = \frac{1}{H_0}\int_0^z \frac{dz}{\sqrt{\Omega_{m,0}(1+z)^5 + \Omega_{\Lambda,0}(1+z)^3}} \tag{7}$$

or use a scale factor to represent:

$$t_0 - t_z = \frac{1}{H_0}\int_{a(z)}^1 \frac{ada}{\sqrt{\Omega_{m,0}a + \Omega_{\Lambda,0}a^4}} \tag{8}$$

when $z = \infty$, the result is the age of the universe.

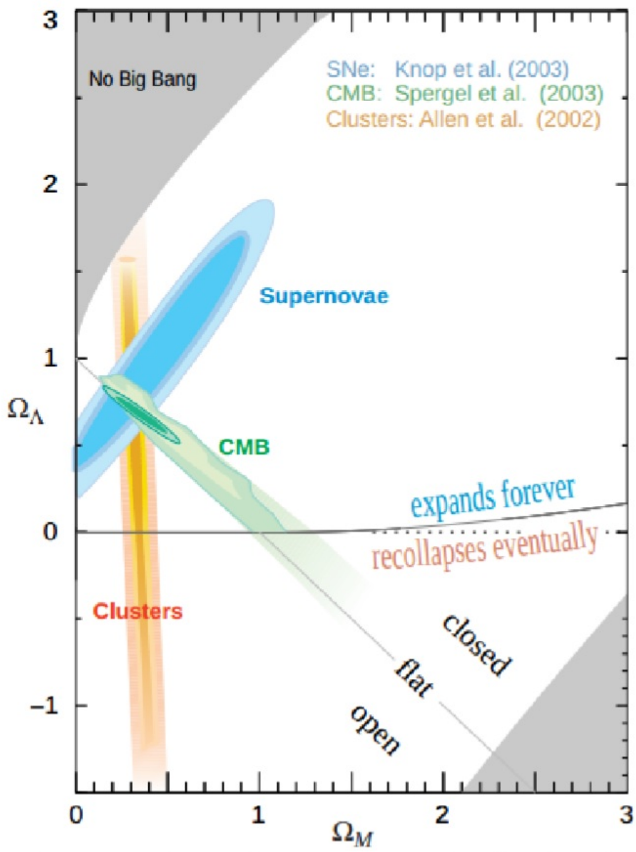

Figure 1 - CMB, supernova, and large galaxies are observed for $\Omega_{m,0}$ and $\Omega_{\Lambda,0}$ [4]

Existing observations and theories all herald a flat, accelerated expansion universe. According to the study of the structure of the universe, our universe is dominated by cold dark matter. This flat cosmological model dominated by cold and dark matter is what we usually call the standard cosmological model. The standard cosmological model can explain many of the major observations today, such as the large-scale distribution of galaxies [5], and the baryonic oscillations [6]. The small-scale clustering model of the cold-dark matter prophecy is also consistent with the observations, so the standard cosmological model is widely accepted. Our next work is carried out under the framework of standard cosmology. As observations and theoretical results advance, some observations seem to be unexplained using standard cosmological models, such as loss of satellite galaxies [7], density contours at dark centers [8]. . Some of these problems can be explained by galaxies forming models, and some may require new physical processes or alter the nature of dark matter. Looking forward to more deeper and broader observations in the future, it may bring us conceptual changes.

2. Basic properties of dark matter halo

The dark matter halo is the cornerstone of the cosmic structure. It is a system of Vary equilibrium, often defined as the area where the average density is 200 times the critical density of the universe. Of course there are other definitions of density, and we will not explain them one by one here. A very important parameter of dark matter halos is its mass distribution. From theoretical and numerical simulations, it is found that the density profile of dark matter conforms to the NFW profile:

$$\frac{\rho(r)}{\rho_{crit}} = \frac{\delta_c}{(r/r_s)(1+r/r_s)^2} \tag{9}$$

Here r_s is the characteristic scale of the dark matter halo, δ_c is the feature density, and $\rho_{crit} = 3H/8\pi G$ is the critical density of the universe. From the center to the edge of the dark matter halo, the density profile is excessive from r^{-1} to r^{-3}, and $\rho \propto r^{-2}$ at r_s. This density profile has been confirmed by many numerical simulations [9].

Through the density profile, you can define the compaction coefficient of the dark matter halo:

$$c = r_h / r_s \tag{10}$$

where r_h is the radius of the dark matter halo. In this paper, the radius of the dark matter halo is generally r_{200}, that is, when the density of the region is 200 times the critical density of the universe. The radius. The compacting factor is an important feature of the dark matter halo. It gives the degree of convergence of the material distribution in the dark matter halo. The larger the compacting factor, the darker material halo density distribution to the center, and vice versa. High-precision numerical simulations show that the compaction factor depends on the mass of the dark matter halo. For a given mass, the compaction factor depends on the formation time of the dark halo. The density profile of the dark matter halo determines its rotational velocity profile. After introducing the compaction factor, Navarro et al. (1997) also gave a rotational velocity profile at the NFW density profile:

$$\left[\frac{V_c(r)}{V_{200}}\right]^2 = \frac{1}{x}\frac{ln(1+cx) - \frac{cx}{1+cx}}{ln(1+c) - \frac{c}{1+c}} \tag{11}$$

Here V_{200} is the rotational speed at dark matter halo r_{200}, $x = r / R_{200}$. When $x \approx 2.16/c$, the rotation speed reaches the maximum V_{max}:

$$\left[\frac{V_{\max}}{V_{200}}\right]^2 = \frac{0.216c}{ln(1+c) - \frac{c}{1+c}} \tag{12}$$

Therefore, the clamping factor can also be solved with V_{max} / V_{200}.

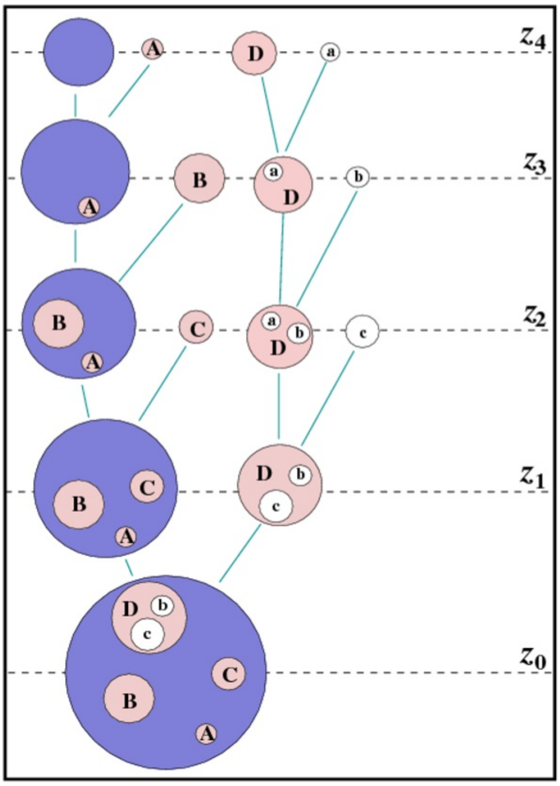

Figure 2 - Convergence tree of dark matter halos, you can see the structure of the dark halo after the combination

3. Dispels the Local Cavity Crisis of the Standard Cosmological Model

The neighboring galaxy survey found a hole around the cluster of galaxies, which does not contain galaxies, accounting for about 1/3 of the volume of the local space ($1Mpc < D < 8Mpc$ around the Milky Way). As the performance of the telescope increases, we can observe darker galaxies, and the samples are more complete, but with integrated optics and HI surveys, local voids still contain few galaxies [10].

Peebles and Nusser published an article in the American Journal of Nature in 2012 [11] claiming that the extremely low density of local voids cannot exist in standard cosmological theory. They combined the neighboring galaxy's catalogues at the time and found that there were 562 galaxies in the local space, and only three galaxies were in the local voids. However, in dark matter simulations, the dark matter halo density in the cavity is $1/10$ of the average density [12]. Combined with the HOD model [13], the luminosity function of the galaxy is monotonically related to the mass function of the dark matter halo. Peebles and Nusser believe that the standard cosmological numerical simulation predicts that there should be about 19 galaxies in the local cavity ($562 \times 1/10 \times 1/3$), 6 times higher than observation. Therefore, they believe that the extremely low density in the local void reality is a threat to the theory of the formation of cold dark matter structure. Maybe dark matter can't be cold, or you need to modify the intervention of gravitational theory to get this very low density cavity.

This view is limited by two factors. First, they only used a numerical simulation [14]. The scale of this simulation is not large. Using only one model to study local voids will make the results have large deviations and lose statistical significance. More numerical simulations are needed to statistically analyze the dark matter density in the cavity. Second, this work assumes that the HOD method applies the same law to dark matter halos in different environments. The effect of assembly bias is not considered. Dark matter halos, especially small mass dark halos, can be significantly different in different environments [15]. The galaxies in the local voids are very dark, and there are dark halos in the small mass, so the influence of the aggregation bias is large. Galaxies form a process of aggregation that depends on the dark matter halos of their host. So whether the HOD is directly used with a small mass of dark halo is still unknown.

Paper [16] used another method to detect whether the low density of local voids is consistent with standard cosmology. They also believe that local voids are a crisis. They assume that there are HI galaxies that can be observed in the dark halo with a wraparound speed greater than $25km \cdot s^{-1}$. They found that the number density of this dark halo in the cavity is an order of magnitude higher than the number density of the observed dwarf galaxies. But the correctness of their hypothesis remains to be discussed.

As mentioned earlier, the physical processes formed by galaxies and the evolution of dark matter halos are not exactly the same, and the dependence on the environment is not exactly the same. The above two work on local voids did not take this difference into account. In this paper, we use Millennium Simulation II [17], a large-scale high-precision simulation, combined with the formation of a semi-analytical model of the galaxy. The following question: Can the current understanding of standard cosmology and galaxies physics explain the existence of local voids; or whether new physical processes need to be invoked to explain observations.

4. Local voids in observations

The projected distribution of neighboring galaxies given in the work of [18] (Fig. 3). They used the neighboring galaxy catalog of Karachentsev [19] (K04) to select more accurately 337 galaxies from SDSS [20] and HIParkes All Sky Survey (HIPASS) [21], 172 and 53 galaxies were selected as supplements. It can be seen that about 1/3 of the area in the projection of the left figure in Figure 3 is a void with obvious boundaries, including only three galaxies.

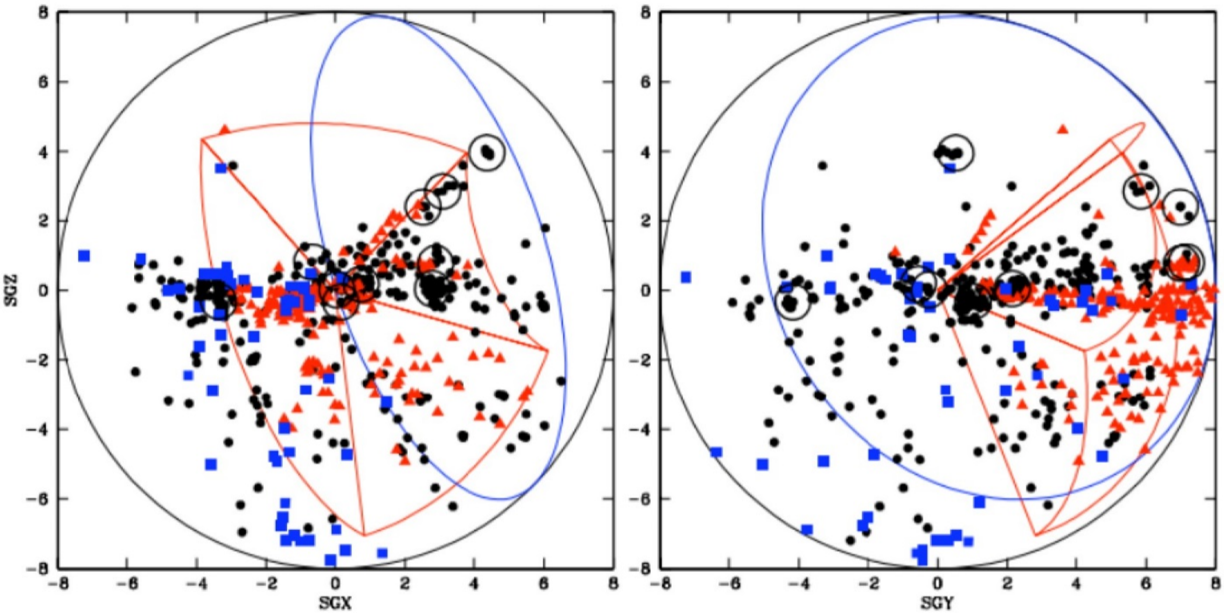

Figure 3 - Local space galaxy projections in Peebles and Nusser work. Each symbol in the figure is a neighboring galaxies within $1Mpc < D < 8Mpc$ around the Milky Way, and the left and right figures are the two projection directions in the super-galaxies coordinate system. The black dots in the picture are from K04, the red triangles are from the Sloan Digital Sky Survey, and the blue squares are from the HIPASS Sky Survey. Lines of the same color correspond to the coverage angles of these surveys

With the increase of observation accuracy, the observation samples of local space have been more complete in recent years. Karachentsev published the latest Neighbor Galaxy catalogue, newly added optical bands for the latest observations and HL surveyed galaxies, including SDSS [20] and HIPASS [21] data. The new catalogue measures the distance and luminosity of the galaxy more accurately; and removes some illuminating objects that are not galaxies. In this catalogue, the completeness of a galaxy with a $m_B < 17.5$, such as a star, is 70%−80%. In the new catalogue, within the range of $1Mpc < D < 8Mpc$ from the Milky Way, there are 486 galaxies that are brighter than $m_B < 17.5$, adding more than a hundred galaxies to K04. Peebles and Nusser also added SDSS and HIPASS galaxies to their work, but the distance measurements they added to the galaxy were not accurate, and some illuminating objects were misjudged as galaxies in the HIPASS patrol. So some of the galaxies they use don't exist in the latest catalogs we use, and there are many galaxies that change position on the projected map. We use the new star catalog to make the same projection of the neighboring galaxies in Figure 4. We only painted galaxies that are brighter than $m_B < 17.5$ and $1Mpc < D < 8Mpc$ from the Milky Way. Comparing Figure 4 with Figure 3, it can be seen that some of the galaxies in Figure 3 disappeared in Figure 4, and the three empty galaxies on the SGZ-SGX projection in Peebles work "disappear" in our diagram (Figure 4 in the blue dotted circle), one of the three missing galaxies is projected elsewhere, two galaxies that are judged to be false are not included in the new catalog, and some are scattered in the void projected in Figure 4 on.

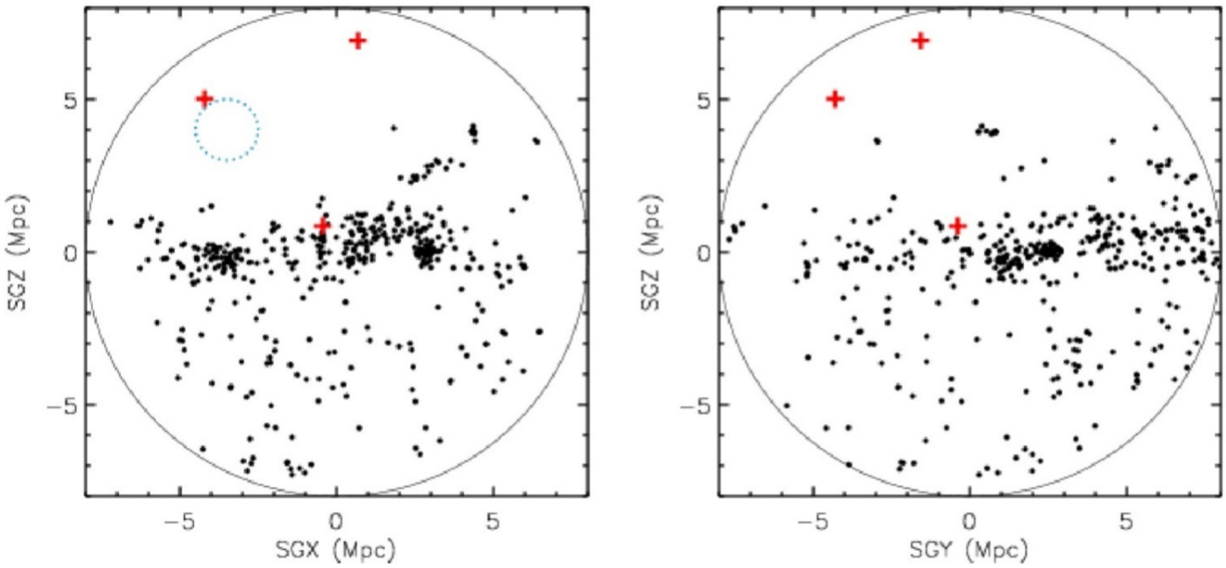

Figure 4 - Projection distribution of neighboring galaxies brighter than $m_B < 17.5$ in the nearest Galaxy K13 from the Milky Way $1Mpc < D < 8Mpc$. The left and right images are the projection directions in the two superclustered cluster coordinate systems. The red cross represents a galaxy that exists in a three-dimensional local void. The blue dotted circle gives the location of the three empty galaxies given in the Peebles and Nusser articles. But in the new catalog, the three galaxies "disappeared" because of the more accurate calculation of the distance

The size of the local hole depends on its definition. In the work of Peebles and Nusser, the volume of the cavity is calculated to be 1/3 of the total volume. It is worth noting that they are calculated from projections, and such voids are not real. In order to more accurately assess the degree of voiding in a local void, it is necessary to calculate the volume of the void in three dimensions. We use a cleaner and more accurate K13 to calculate the 3D volume of the local void, so that the resulting void is more realistic.

Because the local void is fan-shaped and has dense boundaries on the projected image, we suspect that the local void is similar to a cone in three dimensions. When determining local voids, we use a cone scan. Specifically, all of the neighboring galaxies are in a spherical shell of $1\,Mpc < R < 8\,Mpc$, and the center of the sphere is the Milky Way. We will have a cone representing the cavity, and the apex of the cone is the Milky Way. The orientation of the cone is determined by adjusting the orientation of the cone along the φ and θ of the spherical coordinates and calculating the number of galaxies falling into the cone. Because the void usually consists of a distinct boundary, the density of the star coefficients in the cone at the hole will plummet, so the shortest position we find is the local void. After finding the hole location, we experimented with different cone deflection angles and calculated the number of galaxies in the cavity to test the size of the hole. By this method, we get a cavity size of about π solid angle, which is 1/4 of the total volume, and contains three galaxies. These three galaxies are marked with a red cross in Figure 4.

5. Comparing simulated voids and observational voids

The actual hole size and star coefficient density are determined. Next, numerical simulations are needed to find out whether such holes exist in the numerical simulation of standard cosmology. First look for similar spaces in standard cosmological simulations based on the observed local space. The characteristics of the local space in the observation are: 1) The local galaxies in the observation contain a pair of giant galaxies: the Milky Way and M31, which are $0.77\ Mpc$ apart; 2) The Milky Way is a spiral galaxy with a mass of $6.4\times10^{10}\ M_{\odot}$ [22]; 3) The host dark halo mass of M31 is slightly smaller than that of the Milky Way host, but the mass of the star is larger, with $(10-15)\times10^{10} M_{\odot}$ [23]; 4) local galaxies There are no large clusters of galaxies in the surrounding $10Mpc$. In order to make the comparison between simulation and observation more authentic, we use the following constraints to find the local space from the numerical simulation.

First, we select galaxies like the Milky Way from the simulated star catalogues by stellar mass and morphology. The specific conditions are as follows: 1) The candidate galaxies must be disc-dominant, the nuclear sphere mass ratio is lower than $M_{bulge} / M_{*} < 0.5$; 2) the mass is similar to that of the Milky Way, $5.4\times10^{10} M_{\odot} < M_{*} < 7.4\times10^{10} M_{\odot}$. Then we find a system similar to the local galaxies from the candidate simulated galactic system by M31. The specific conditions are as follows: 3) Within 1Mpc around the candidate of the galactic system, at least one galaxies have a mass of $0.5\times M_{MW} < M_{*} < 2\times M_{MW}$ between. Because the Milky Way and M31 are the brightest galaxies in the galaxies, we require: 4) There are no galaxies in the $1Mpc$ space around the Milky Way that are twice as large as the Milky Way. Finally, because the nearest Virgo Cluster of Galaxy is about $12.8\ Mpc$ around the Milky Way, we require: 5) There is no dark halo in the $10\ Mpc$ around the simulated Milky Way with a mass greater than $10^{14}\ M_{\odot}$ to ensure that the local space in the simulation is also in a real situation. The same relatively isolated environment. Under these conditions, we have a total of 77 systems similar to local space in the MS-II numerical simulation.

Before finding a hole in a numerical simulation, in order to determine that our numerical simulation is believable, it is necessary to check whether the photometric function in our simulated local space is comparable to the observation. We use the distance to the Milky Way to calculate the visual star of the galaxy in the simulation. The black line gives the count of the galaxies in the observation K13, and the error bar is the Poisson error. The solid red line gives the median of 77 simulated local spaces and the dashed line is the 1 standard deviation range. It is clear that the star coefficient density of the simulated star catalog we used is very consistent with the observations. Note that in the figure, we have not corrected the completeness. In the observation, the completeness of the K13 galaxies is 70−90% at the apparent star $m_B = 17.5$. Therefore, the number of galaxies in the observation is evenly distributed at the dark end, while the number of galaxies in the simulation is continuously increasing at the dark end. We expect that higher-resolution observations in the future should complement more dark galaxies.

We use the method of finding local voids as described above to find holes in the simulated local space. We use a cone of the same size as the observed local hole, ie the solid angle is π scanned in the simulated local cavity, the position with the lowest density is defined as the void, and the number of empty galaxies is recorded N_{void}. Here, as with observations, the statistics are all galaxies that are brighter than $m_B < 17.5$. In our simulation, the shortest local void contains only one galaxy, even more empty than the local void in the observation. Considering the Poisson error, we have a sample with a number of empty galaxies less than 5 that are similar to local voids. Then, among our 77 simulated local spaces, there are local holes in 11 systems with a probability of 14%. Explain that the degree of voiding of local voids in the observation is not special.

A projection of the local void in the simulation is given in Figure 5. The figure shows the local space where the number of six empty galaxies is less than 5. Each figure shows all the galaxies in the $1Mpc < D < 8Mpc$ space around the simulated Milky Way, and the red cross represents the actual hollow galaxies (in three dimensions, not in the projected image that looks like voids). The local space of these simulations looks very similar to the actual observed local space (Figure 4).

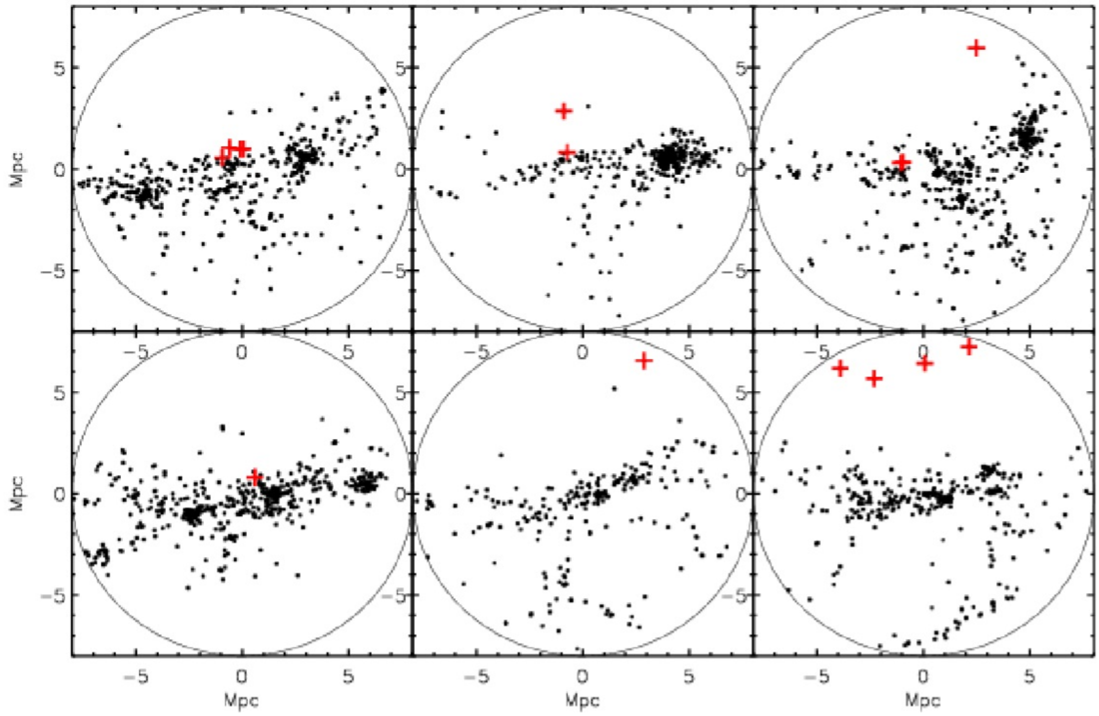

Figure 5 - Local voids in the simulation. Each black dot in the figure represents a galaxy, and all galaxies are brighter than mB< 17.5, within 1Mpc < D < 8Mpc of the simulated Milky Way. The red cross indicates the galaxy in the cavity

6. Summary

We use large-scale, high-precision dark matter numerical simulations of MSII,add the latest semi-analytical galaxy formation model [24], to study darker galaxies in local space. We focus on the problem of the degree of voiding in local voids. Prior to this, the local void problem was thought to be considered a threat to the theory of standard cosmological structure formation [25].

We use the latest star catalogue of neighboring galaxies [26] to recalculate the density of galaxies in local voids in 3D space. The star catalog we used and the star-to-surface ratio used by [25] added a large number of new galaxies and made more accurate measurements of distance. This catalogue has a completeness of 70−80% at a star level of $m_B = 17.5$. We use a cone to simulate the shape of a three-dimensional cavity, use a three-dimensional cone scan to find a three-dimensional local cavity in a new star table, and then adjust the size of the cone to measure the volume of the cavity. We found that the local void in the observations accounted for approximately 1/4 of the local space and contained three galaxies. We use the same approach in the simulated local space for systems of the same size and similar cavities. We found that 14% of the simulated local space contains structures similar in size and hole to local voids. These simulated local voids are not only similar in number to galaxies, but their projections are also very similar to the observed local voids. This shows that local voids are not a threat to standard cosmological theory, but exist in the predictions of standard cosmology. In other words, local voids are the success of standard cosmology.

In the local voids we simulated, the low density of galaxies was mainly due to the low density of dark matter halos in the voids. At the same time, the environmental convergence caused by the dark matter halo during the formation process will affect the formation process of the cavity galaxies, resulting in a 25% lower mass function of the galaxies in the same mass dark matter halo.

The work was carried out within the framework of Project No. AP05134454 "Evolution of the perturbations in the density of dark matter in a very early Universe", financed by the JSC "National Center for Space Research and Technology", Aerospace Committee of the MDAI of the Republic of Kazakhstan.

Author express their gratitude to professorYougang Wang from National Astronomical Observatories of Chinese Academy of Sciences for the problem forwarding and the permanent supporting for its solving.

Д. Қайратқызы

Әл-Фарабиатындағы ҚазҰУ, «В.Г. Фесенковатындағы Астрофизика Институты»,
«Ұлттық ғарыштық зерттеулер мен технологиялар орталығы »АҚ,
Қазақстан Республикасы ММАИ аэроғарыштық комитеті

ҚАРАҢҒЫ МАТЕРИЯНЫҢ ЭВОЛЮЦИЯСЫ ЖӘНЕ СТАНДАРТТЫ ӘЛЕМДІК МОДЕЛЬДІҢ ҚҰРЫЛЫМДЫҚ ӨСУІНІҢ НЕГІЗГІ ТЕОРИЯСЫ

Аннотация. Қараңғы материямен галактикалардың пайда болуы және эволюциясы – космологиялық зерттеулердегі негізгі тақырыптардың бірі. Бұл мақалада қараңғы материяның суық моделі бойынша ғаламның эволюциясын зерттеу үшін сандық модельдеу қолданылады. Бірінші бөлімде космология мен құрылымның қалыптасу теориясы, қараңғы материя деңгейінің эволюциясы және галактиканың қалыптасуының физикалық процестері, сондай-ақ біз қолданатын сандық құралдар: N-денені модельдеу және жартылай аналитикалық галактикалардың қалыптасу теориялары сияқты тиісті мәліметтер келтірілген.

Екінші бөлім жартылай аналитикалық модельмен біріктірілген жоғары дәлдікті сандық модельдеуді қолдану арқылы жергілікті қуыстың дағдарысын шешеді. Жергілікті бос орын стандартты космологиялық модельдің дағдарысы деп саналады, өйткені галактикалардың тығыздығы тым төмен, ал кейбір болжамдар мұндай төмен тығыздық стандартты космология тұжырымдамасында ғарыштық құрылымда бола алмайды деп санайды.

Біз стандартты космологияны сандық модельдеуде жергілікті кеңістікке ұқсас жүйені іздейміз, содан кейін стандартты космологияда жергілікті қуыстың бар-жоғын тексеру үшін жергілікті қуысқа ұқсас құрылымды іздейміз. Біздің жұмысымызда 77 ұқсас жергілікті ғарыштық жүйелерді модельде табуға болатындығы, жергілікті бос жерлердің 14% мүмкіндігі бар екендігі анықталды, бұл жергілікті бос орындар толығымен суық қара материя моделінде өмір сүре алатындығын көрсетеді. Жергілікті қуыс галактикалардың өте төмен тығыздығының себебі, бұл негізінен қараңғы материялар галосының тығыздығының төмендігі мен байланысты және галактикалардың пайда болуына қоршаған ортаның әсері де галактикалар санын 25% төмендетеді.

Түйін сөздер: стандартты космологиялық модель, қара матералды гало, қуыстың жергілікті дағдарысы.

Д. Кайраткызы

Казахский национальный университет им. Аль-Фараби, «В.Г. Фесенковский астрофизический институт», АО «Национальный центр космических исследований и технологий», Аэрокосмический комитет МДАИ Республики Казахстан

ЭВОЛЮЦИЯ ТЕМНОЙ МАТЕРИИ И ФОРМИРОВАНИЕ БАЗОВОЙ ТЕОРИИ СТРУКТУРНОГО РОСТА СТАНДАРТНОЙ МОДЕЛИ ВСЕЛЕННОЙ

Аннотация. Формирование и эволюция темной материи и галактик является одной из основных тем в космологических исследованиях. Этот тезис использует численное моделирование для изучения эволюции Вселенной в рамках модели холодной темной материи. В первой части представлен соответствующий фон, включая теорию космологии и формирования структуры, эволюцию уровней темной материи и физические процессы образования галактик, а также инструменты численного моделирования, которые мы используем: моделирование N-тел и полуаналитические модели формирования галактик. Вторая часть решает локальный кризис полости с помощью высокоточного численного моделирования в сочетании с полуаналитической моделью. Локальная пустота считается кризисом стандартной космологической модели, потому что плотность галактик слишком мала, и некоторые предшественники считают, что такая низкая плотность не может существовать в космической структуре, предсказываемой стандартной космологией. Мы ищем систему, подобную локальному пространству, в численном моделировании стандартной космологии, а затем ищем структуру, подобную локальной пустоте, чтобы проверить, существует ли локальная пустота в стандартной космологии. Наша работа показала, что в симуляции можно найти 77 подобных локальных космических систем с 14% -ной вероятностью нахождения локальных пустот поблизости, что указывает на то, что локальные пустоты могут существовать полностью в модели холодной темной материи. Причина чрезвычайно низкой плотности локальных полых галактик заключается в том, что это происходит главным образом из-за низкой плотности гало темной материи, а влияние окружающей среды на образование галактик также уменьшает количество галактик на 25%.

Ключевые слова: стандартная космологическая модель, гало темной материи, локальный кризис полости.

Information about the author

Kairatkyzy D. - Master of Natural Science in “Astronomy”, PhD - doctoral student in the specialty "Physics and Astronomy". Senior Lecturer of the Department of Solid State Physics and Nonlinear Physics of the Physical-Technical Faculty of the al-Farabi Kazakh National University. An expert in the field of modern cosmology, specializing in the problems of formation and evolution of the Universe. She has more than 20 publications, including articles in the journal “Reports of the National Academy of Sciences of Kazakhstan”, made 8 reports at republican conferences. Orcid code: 0000-0002-9543-8464

REFERENCES

[1] Penzias A.A., Wilson R.W. (1965). Measurement of the Flux Density of CAS a at 4080 Mc/s. ApJ, 142:1149.

[2] Robertson H.P. (1935). Kinematics and World-Structure. ApJ, 82:284.

[3] Larson D., Dunkley J., Hinshaw G., Komatsu E., Nolta M. R., Bennett C. L., et al. (2011). Seven-yearWilkinson Microwave Anisotropy Probe (WMAP) Observations: Power Spectra and WMAP-derived Parameters. ApJS, 192:16.

[4] Lahav O., Liddle A. R. (2006). The Cosmological Parameters 2006. ArXiv e-prints.

[5] Tegmark M., Strauss M.A., Blanton M.R., et al., 2004. CosmologicalparametersfromSDSSandWMAP. Phys.Rev.D,69(10):103501.

[6] Percival W.J., Reid B.A., Eisenstein D.J., Bahcall N.A., et al. (2010). Baryon acoustic oscillations in the Sloan Digital Sky Survey Data Release 7 galaxy sample. MNRAS, 401:2148–2168.

[7] Klypin A., Kravtsov A.V., Valenzuela O., Prada F. (1999). Where Are the Missing Galactic Satellites? ApJ, 522:82–92.

[8] Ogiya G., Mori M. (2014). The Core-Cusp Problem in Cold Dark Matter Halos and Supernova Feedback: Effects of Oscillation. ApJ, 793:46.

[9] JingY.P., SutoY.(2002). Triaxial Modeling of Halo Density Profiles with High-Resolution N-Body Simulations. ApJ, 574:538–553.

[10] Karachentsev I.D., Karachentseva V.E., Huchtmeier W.K., Makarov D.I. (2004). A Catalog of Neighboring Galaxies. AJ, 127:2031–2068.

[11] Peebles P.J.E., Nusser A. (2010). Nearby galaxies as pointers to a better theory of cosmic evolution. Nature, 465:565–569.

[12] Gottlöber S., Łokas E.L., Klypin A., Hoffman Y. (2003). The structure of voids. MNRAS, 344:715–724.

[13] Tinker J.L., Conroy C. (2009). The Void Phenomenon Explained. ApJ, 691:633–639.

[14] Gottlöber S., Łokas E.L., Klypin A., Hoffman Y. (2003). The structure of voids. MNRAS, 344:715–724.

[15] Gao L., Springel V., White S.D.M. (2005). The age dependence of halo clustering. MNRAS, 363:L66–L70.

[16] Tikhonov A.V., Klypin A. (2009). The emptiness of voids: yet another overabundance problem for the Λ cold dark matter model. MNRAS, 395:1915– 1924

[17] Boylan-Kolchin M., Springel V., White S.D.M., Jenkins A., Lemson G. (2009b). Resolving cosmic structure formation with the Millennium-II Simulation. MNRAS, 398:1150–1164.

[18] Peebles P.J.E.,Nusser A. (2010). Nearby galaxies as pointers to a better theory of cosmic evolution. Nature, 465:565–569.

[19] Karachentsev I.D., Karachentseva V.E., Huchtmeier W.K., Makarov D.I. (2004). A Catalog of Neighboring Galaxies. AJ, 127:2031–2068.

[20] Abazajian K.N., Adelman-McCarthy J.K., Agüeros M.A., Allam S.S., Allende Prieto C., An D., Anderson K.S.J., Anderson S.F., Annis J., Bahcall N.A., et al. (2009). The Seventh Data Release of the Sloan Digital Sky Survey. ApJS, 182:543–558.

[21] Wong O.I., Ryan-Weber E.V., Garcia-Appadoo D.A. et al. (2006). The Northern HIPASS catalogue - data presentation, completeness and reliability measures. MNRAS, 371:1855–1864.

[22] McMillan P.J. (2011). Mass models of the Milky Way. MNRAS, 414:2446– 2457.

[23] Tamm A., Tempel E., Tenjes P., Tihhonova O., Tuvikene T. (2012). Stellar mass map and dark matter distribution in M 31. A&A, 546:A4.

[24] GuoQ., White S.(2013).Numericalresolutionlimitsonsubhaloabundance matching. MNRAS.

[25] Peebles P. J. E., Nusser A. (2010). Nearby galaxies as pointers to a better theory of cosmic evolution. Nature, 465:565–569.

[26] Karachentsev I.D., Makarov D.I., Kaisina E.I.(2013). UpdatedNearby Galaxy Catalog. AJ, 145:101.

N E W S
OF THE NATIONAL ACADEMY OF SCIENCES OF THE REPUBLIC OF KAZAKHSTAN
PHYSICO-MATHEMATICAL SERIES
ISSN 1991-346X **https://doi.org/10.32014/2019.2518-1726.62**
Volume 5, Number 327 (2019), 89 – 97

UDC 517.956
MRNTI 27.31.15

S.A. Aldashev, M.N.Maikotov

[1] Kazakh National Pedagogical University named after Abai, Almaty, Kazakhstan
aldash51@mail.ru, mukhit777@mail.ru

DIRICHLET PROBLEM IN A CYLINDRICAL AREA FOR ONE CLASS OF MULTIDIMENSIONAL ELLIPTIC-PARABOLIC EQUATIONS

Abstract. Boundary-value problems for degenerate elliptic-parabolic equations on the plane are studied quite well ([1]). The correctness of the Dirichlet problem for degenerate multidimensional elliptic-parabolic equations with degeneration of type and order was established in [3]. In the work for multidimensional elliptic-parabolic equations with degeneration of type and order, the solvability is shown and an explicit form of the classical solution of the Dirichlet problem is obtained.
Keywords: solvability, mixed problem, multidimensional elliptic-parabolic equations, Bessel function.

Problem statement and result

Let $\Omega_{\alpha\beta}$ – the cylindrical area of the Euclidean space of E_{m+1} points $(x_1,...,x_m,t)$ bounded by a cylinder $\Gamma=\{(x,t):|x|=1\}$, planes $t=\alpha>0$ and $t=\beta<0$,where $|x|-$ is the length of a vector $x=(x_1,...,x_m)$.

Denote by Ω_α and Ω_β parts $\Omega_{\alpha\beta}$ – of the area and $\Gamma_\alpha,\Gamma_\beta$ – through parts of the surface Γ, lying in the half-spaces $t>0$ and $t<0$, σ_α – the upper and σ_β – lower base area $\Omega_{\alpha\beta}$.

Let $S-$ further the common part of the borders of the areas Ω_α and Ω_β representing the $\{t=0,\ 0<|x|<1\}$ set in E_m.

In the area $\Omega_{\alpha\beta}$, we consider degenerate multidimensional hyperbolic-parabolic equations

$$0=\begin{cases} p_1(t)\Delta_x u - p_2(t)u_{tt}+\sum_{i=1}^{m} a_i(x,t)u_{x_i}+b(x,t)u_t+c(x,t)u=0,\ t>0, \\ g(t)\Delta_x u - u_t+\sum_{i=1}^{m} d_i(x,t)u_{x_i}+e(x,t)u,t<0, \end{cases} \tag{1}$$

where $p_i(t)>0$ at $t>0, p_i(0)=0, p_i(t)\in C([0,\alpha])g\ (t)>0$ at $t<0$, and may vanish when $t=0$, $g(t)\in C[\beta,0])$, a Δ_x – Laplace operator with variables $x_1,\dots,x_m$, $m\ge 2$.

In the future, it is convenient for us to move from the Cartesian coordinates $x_1,\dots,x_m$,t to spherical $r,\theta_1,\dots,\theta_{m-1},t,r\ge 0,0\le\theta_{m-1}<2\pi,\ 0\le\theta_i\le\pi, i=1,2,\dots,m-2,\ \theta=(\theta_1,\dots,\theta_{m-1})$.

Problem 1 (Dirichlet). Find a solution to the equation (1) in the area of $\Omega_{\alpha\beta}$ at $t\ne 0$, from the class $C^1(\overline{\Omega}_{\alpha\beta})\cap C^2(\Omega_\alpha\cup\Omega_\beta)$, satisfying boundary conditions

$$u|_{\sigma_\alpha}=\varphi_1(r,\theta),\quad u|_{\Gamma_\alpha}=\psi_1(t,\theta), \tag{2}$$

$$u|_{\Gamma_\beta}=\psi_2(t,0),\ \ u|_{\sigma_\beta}=\varphi_2(t,\theta). \quad (3)$$

wherein $\varphi_1(1,\theta)=\psi_1(\alpha,\theta),\psi_1(0,\theta)=\psi_2(0,\theta),\psi_2(\beta,\theta)=\varphi_2(1,\theta).$

Let $\{Y^k_{n,m}(\theta)\}$ - system of linearly independent spherical functions of order n, $1\le k\le k_n$, $(m-2)!n!k_n=(n+m-3)!(2n+m-2), W_2^l(S), l=0,1,...$ - Sobolev space. Takes place ([4]).

Lemma 1. Let $f(r,\theta)\in W_2^l(S)$. If $l\ge m-1$, that row

$$f(r,\theta)=\sum_{n=0}^{\infty}\sum_{k=1}^{k_n}f_n^k(r)Y^k_{n,m}(\theta), \quad (4)$$

as well as series derived from it by order differentiation $p\le l-m+1$, converge absolutely and evenly.

Lemma 2. In order to $f(r,\theta)\in W_2^l(S)$, it is necessary and sufficient that the coefficients of the series (4) satisfy the inequalities.

$$\left|f_0^1(r)\right|\le c_1, \sum_{n=1}^{\infty}\sum_{k=1}^{k_n}n^{2l}\left|f_n^k(r)\right|^2\le c_2,\ c_1,c_2=const.$$

Through $\tilde{d}^k_{in}(r,t),\ d^k_{in}(r,t),\ \tilde{e}^k_n(r,t),\ \tilde{d}^k_n(r,t), \rho^k_n, \overline{\varphi}^k_{1n}(r), \overline{\varphi}^k_{2n}(r), \psi^k_{1n}(t), \psi^k_{2n}(t),$ denote the coefficients of the series (4), respectively functions $d_i(r,\theta,t)\rho(\theta),\ d_i\dfrac{x_i}{r}\rho,$ $e(r,\theta,t)\rho, d(r,\theta,t)\rho,\ \rho(\theta), i=1,...,m, \varphi_1(r,\theta), \varphi_2(r,\theta), \psi_1(t,\theta), \psi_2(t,\theta),$ and $\rho(\theta)\in C^\infty(H)$, H- unit sphere in E_m.

Let $\dfrac{a_i(r,\theta,t)}{g_2(t)}, \dfrac{b(r,\theta,t)}{g_2(t)}, \dfrac{c(r,\theta,t)}{g_2(t)}\in W_2^l(\Omega_\alpha)\subset C(\bar{\Omega}_\alpha), d_i(r,\theta,t),$

$c(r,\theta,t)\in W_2^l(\Omega_\beta), i=1,...,m, l\ge m+1, c(r,\theta,t)\le 0, \forall(r,\theta,t)\in\Omega_\alpha, e(r,\theta,t)\in\Omega_\beta.$

Then fair

Theorem.

If $\varphi_1(r,\theta),\varphi_2(r,\theta)\in W_2^l(S),\ \psi_1(t,\theta)\in W_2^p(\Gamma_\alpha), \psi_2(t,\theta)\in W_2^l(\Gamma_\beta), l>\dfrac{3m}{2}$, then problem 1 is solvable.

Proof of the theorem. First, let us rock the solvability of problem (1), (3). In spherical coordinates of equation (1) in the area Ω_β has the appearance

$$Lu\equiv g(t)(u_{rr}+\frac{m-1}{r}u_r-\frac{1}{r^2}\delta u)-u_{tt}+\sum_{i=1}^{m}d_i(r,\theta,t)u_{x_i}+e(r,\theta,t)u=0, \quad (5)$$

$$\delta\equiv-\sum_{j=1}^{m-1}\frac{1}{g_j\sin^{m-j-1}\theta_j}\frac{\partial}{\partial\theta_j}(\sin^{m-j-1}\frac{\partial}{\partial\theta_j}), g_1=1, g_j=(\sin\theta_1...\sin\theta_{j-1})^2, j>1.$$

It is known [4] that the spectrum of the operator δ consists of own numbers $\lambda_n=n(n+m-2), n=0,1,...$ each of which corresponds k_n orthonormal functions $Y^k_{n,m}(\theta)$.

The desired solution to problem 1 in the field Ω_β we will look in the form

$$u(r,\theta,t)=\sum_{n=0}^{\infty}\sum_{k=1}^{k_n}\overline{u}_n^k(r,t)Y_{n,m}^k(\theta), \tag{6}$$

where $\overline{u}_n^k(r,t)$ - functions to be defined.

Substituting (6) в (5), then multiplying the resulting expression by $\rho(\theta)\neq 0,$ and integrating over a single sphere H, for $\overline{u}_n^k$ will get [5-7]

$$\begin{gathered} g(t)\rho_0^1\overline{u}_{0rr}^1+\rho_0^1\overline{u}_{0tt}^1+(\frac{m-1}{r}g(t)\rho_0^1+\sum_{i=1}^{m}d_{i0}^1)u_{0r}^1+ \\ +\sum_{n=1}^{\infty}\sum_{k=1}^{k_n}\{g(t)\rho_n^k\overline{u}_{nrr}^k+\rho_n^k\overline{u}_{ntt}^k+(\frac{m-1}{r}g(t)\rho_n^k+\sum_{i=1}^{m}d_{in}^k)\overline{u}_{nr}^k \\ +[\tilde{c}_n^k-\lambda_n\frac{\rho_n^k}{r^2}g(t)+\sum_{i=1}^{m}(\tilde{d}_{in-1}^k-nd_{in}^k)]\overline{u}_n^k\}=0. \end{gathered} \tag{7}$$

Now consider the infinite system of differential equations

$$g(t)\rho_0^1\overline{u}_{0rr}^1+\rho_0^1u_{ott}^1+\frac{m-1}{r}g(t)\rho_0^1\overline{u}_{0r}^1=0, \tag{8}$$

$$\begin{gathered} g(t)\rho_1^k\overline{u}_{1rr}^k-\rho_1^k\overline{u}_{1t}^k+\frac{m-1}{r}g(t)\rho_1^k\overline{u}_{1r}^k-\frac{\lambda_1}{r^2}g(t)\rho_1^k\overline{u}_1^k= \\ =-\frac{1}{k_1}(\sum_{i=1}^{m}d_{i0}^1\overline{u}_{0r}^1+\tilde{e}_0^1\overline{u}_o^1),\ n=1,\ k=\overline{1,k_1}, \end{gathered} \tag{9}$$

$$\begin{gathered} g(t)\rho_n^k\overline{u}_{nrr}^k-\rho_n^k\overline{u}_{nt}^k+\frac{m-1}{r}g(t)\rho_n^k\overline{u}_{nr}^k-\frac{\lambda_n}{r^2}g(t)\rho_n^k\overline{u}_n^k= \\ =-\frac{1}{k_n}\sum_{k=1}^{k_{n-1}}\{\sum_{i=1}^{m}d_{in-1}^k\overline{u}_{n-1r}^k+[\tilde{e}_{n-1}^k+\sum_{i=1}^{m}(\tilde{d}_{in-2}^k-(n-1)d_{in-1}^k)]\overline{u}_{n-1}^k\}, \\ k=\overline{1,k_n}.\quad n=2,3,\ldots . \end{gathered} \tag{10}$$

Summing up the equation (8) from 1 before k_1, and the equation (9)- from 1 before k_n, and then adding the resulting expressions together with (7), come to the equation (6).

It follows that if $\{\overline{u}_n^k\}, k=\overline{1,k_n}, n=0,1,\ldots$ system solution (7)-(9), then it is a solution to the equation (6).

It is easy to see that each equation of system (7) - (9) can be represented as

$$g(t)(\overline{u}_{nrr}^k+\frac{m-1}{r}\overline{u}_{nr}^k-\frac{\lambda_n}{r^2}\overline{u}_n^k)-u_{nt}^k=\overline{f}_n^k(r,t), \tag{11}$$

where $\overline{f}_n^k(r,t)$ are determined from the previous equations of this system, while $\overline{f}_0^1(r,t)\equiv 0.$

Further, from the boundary condition (3), by virtue of (6), we will have

$$\overline{u}_n^k(r,\beta)=\overline{\varphi}_{2n}^k(r),\ \overline{u}_n^k(1,t)=\psi_{2n}^k(t),\ k=\overline{1,k_n},\ n=0,1,\ldots . \tag{12}$$

In (11), (12) replacing $\overline{\vartheta}_n^k(r,t)=\overline{u}_n^k(r,t)-\psi_{2n}^k(t),$ will get

$$g(t)(\overline{\vartheta}_{nrr}^k+\frac{m-1}{r}\overline{\vartheta}_{nr}^k-\frac{\lambda_n}{r^2}\overline{\vartheta}_n^k)-\overline{\vartheta}_{ntt}^k=\overline{f}_n^k(r,t), \tag{13}$$

$$\overline{\vartheta}_n^k(r,\beta)=\varphi_{2n}^k(r),\ \overline{\vartheta}_n^k(1,t)=0,\quad k=\overline{1.k_n},\ n=0,1,.... \tag{14}$$

$$f_n^k(r,t)=\overline{f}_n^k(r,t)+\psi_{2nt}^k+\frac{\lambda_n g(t)}{r^2}\psi_{2n}^k,\varphi_{2n}^k(r)=\overline{\varphi}_{2n}^k(r)-\psi_{2n}^k(\beta).$$

Replacing the variable $\overline{\vartheta}_n^k(r,t)=r^{\frac{(1-m)}{2}}\vartheta_n^k(r,t)$ задачу (13), (14) we will lead to the following problem

$$L\vartheta_n^k=g(t)(\vartheta_{nrr}^k+\frac{\overline{\lambda}_n}{r^2}\vartheta_n^k)-\vartheta_{nt}^k=\tilde{f}_n^k(r,t), \tag{15}$$

$$\vartheta_n^k(r,\beta)=\overline{\varphi}_{2n}^k(r),\ \vartheta_n^k(1,t)=0,\ \vartheta_n^k(1,t)=0, \tag{16}$$

$$\overline{\lambda}_n=\frac{[(m-1)(3-m)-4\lambda_n]}{4},\ \ \tilde{f}_n^k(r,t)=r^{\frac{(m-1)}{2}}f_n^k(r,t),$$

$$\tilde{\varphi}_{2n}^k(r)=r^{\frac{(m-1)}{2}}\varphi_{2n}^k(r).$$

The solution of the problem (15), (16) is sought in the form

$$\vartheta_n^k(r,t)=\vartheta_{1n}^k(r,t)+\vartheta_{2n}^k(r,t), \tag{17}$$

where $\vartheta_{1n}^k(r,t)$ the solution of the problem

$$L\vartheta_{1n}^k=\tilde{f}_n^k(r,t), \tag{18}$$

$$\vartheta_{1n}^k(r,\beta)=0,\ \vartheta_{1n}^k(1,t)=0, \tag{19}$$

where $\vartheta_{2n}^k(r,t)$ the solution of the problem

$$L\vartheta_{1n}^k=0, \tag{20}$$

$$\vartheta_{2n}^k(r,\beta)=\tilde{\varphi}_{2n}^k(r)0,\ \vartheta_{2n}^k(1,t)=0, \tag{21}$$

The solution to the above problems, we consider in the form

$$\vartheta_n^k(r,t)=\sum_{s=1}^{\infty}R_s(r)T_s(t), \tag{22}$$

at the same time let

$$\tilde{f}_n^k(r,t)=\sum_{s=1}^{\infty}a_{ns}^k(t)R_s(r),\ \tilde{\varphi}_{2n}^k(r)=\sum_{s=1}^{\infty}b_{ns}^kR_s(r). \tag{23}$$

Substituting (22) into (18), (19), taking into account (23), we obtain

$$R_{srr}+\frac{\overline{\lambda}_n}{r^2}R_s+\mu_{s,n}R_s=0,\ 0<r<1, \tag{24}$$

$$R_s(1)=0,\ |R_s(0)|<\infty, \tag{25}$$

$$T_{st}-\mu_{s,n}\,g(t)T_s(t)=-a_{ns}^k(t),\ \beta<t<0, \tag{26}$$

$$T_s(\beta)=0. \tag{27}$$

A limited solution to problem (24), (25) is ([8])

$$R_s(r)=\sqrt{r}J_v(\mu_{s,n}r), \tag{28}$$

where $v=\dfrac{n+(m-2)}{2}$, $\mu_{s,n}$ - zeros of the Bessel function of the first kind $J_v(z)$, $\mu=\mu_{s,n}^2$.

The solution to problem (26), (27) is

$$T_{s,n}(t)=(\exp(-\mu_{s,n}^2\int_0^t g(\xi)d\xi))\int_t^\beta g(\xi)(\exp\mu_{s,n}^2\int_0^\xi g(\xi_1)d\xi_1)d\xi). \tag{29}$$

Substituting (28) into (23) we get

$$r^{-\frac{1}{2}}\tilde{f}_n^k(r,t)=\sum_{s=1}^\infty a_{ns}^k(t)J_v(\mu_{s,n}r),\ r^{-\frac{1}{2}}\tilde{\varphi}_{1n}^k(r)=\sum_{s=1}^\infty b_{ns}^k J_v(\mu_{s,n}r), 0<r<1. \tag{30}$$

Rows (30) - Fourier-Bessel series expansions ([9]), if

$$a_{ns}^k(t)=2[J_{v+1}(\mu_{s,n})]^{-2}\int_0^1\sqrt{\xi}\tilde{f}_n^k(\xi,t)J_v(\mu_{s,n}\xi)d\xi. \tag{31}$$

$$b_{ns}^k=2[J_{v+1}(\mu_{s,n})]^{-2}\int_0^1\sqrt{\xi}\tilde{\varphi}_{2n}^k(\xi)J_v(\mu_{s,n}\xi)d\xi, \tag{32}$$

where $\mu_{s,n}$ $s=1,2,...$ - positive zeros of the Bessel function $J_v(z)$, located in ascending order of magnitude.

Of (22), (28), (29) get the solution to the problem (18), (19)

$$\vartheta_{1n}^k(r,t)=\sum_{s=1}^\infty\sqrt{r}T_{s,n}(t)J_v(\mu_{s.n}r), \tag{33}$$

where $a_{ns}^k(t)$ determined from (31).

Next, substituting (22) в (20), (21), taking into account (23), will have

$$T_{st}-\mu_{s,n}^2 g(t)T_s=0,\ \beta<t<0, T_s(\beta)=b_{ns}^k,$$

which solution is

$$T_{s,n}(t)=b_{ns}^k\exp(\mu_{s,n}^2\int_t^\beta g(\xi)d\xi. \tag{34}$$

From (28), (34) we get

$$\vartheta_{2n}^k(r,t)=\sum_{s=1}^\infty b_{ns}^k\sqrt{r}(\exp\mu_{s,n}^2\int_t^\beta g(\xi)d\xi)J_v(\mu_{s,n}r), \tag{35}$$

where b_{ns}^k are from (32).

Therefore, first solving the problem (8), (12) (n=0), and then (9) ,(12) (n=1) etc. let's find everything $\vartheta_n^k(r,t)$ of (17), where $\vartheta_{2n}^k(r,t)$ are determined from (33),(35).

So, in the area D_α, takes place

$$\int_H\rho(\theta)L_1udH=0. \tag{36}$$

Let $f(r,\theta,t)=R(r)\rho(\theta)T(t)$, and $R(r)\in V_0, V_0-$ tight in $L_2((0,1))$, $\rho(\theta)\in C^\infty(H)-$ tight in в $L_2(H)$, $T(t)\in V_1, V_1-$ tight in $L_2((\beta,0))$. Then $f(r,\theta,t)\in V, V=V_0\otimes H\otimes V_1-$ tight in $L_2(\Omega_\beta)$ [10].

From here and from (36), it follows that

$$\int_{\Omega_\beta} f(r,\theta,t)L_1 u d\Omega_\beta = 0$$

and

$$L_1 u = 0,\ \forall (r,\theta,t) \in \Omega_\beta.$$

Thus, by solving the problem (1), (3) in the field Ω_β is the function

$$u(r,\theta,t) = \sum_{n=0}^{\infty}\sum_{k=1}^{k_n}\{\psi_{2n}^k(t) + r^{\frac{(1-m)}{2}}[\vartheta_{1n}^k(r,t) + \vartheta_{2n}^k(r,t)]\}Y_{n,m}^k(\theta), \tag{37}$$

where $\vartheta_{1n}^k(r,t), \vartheta_{2n}^k(r,t)$ are from (33), (35).

Given the formula ([9]):

$$2J_v^{'}(z) = J_{v-1}(z) - J_{v+1}(z),\ \text{ratings [11,4]}$$

$$J_v(z) = \sqrt{\frac{2}{\pi z}}\cos(z - \frac{\pi}{2}v - \frac{\pi}{4}) + 0(\frac{1}{z^{3/2}}),\ v \ge 0,$$

$$|k_n| \le c_1 n^{m-2},\ \left|\frac{\partial^l}{\partial\theta_j^l}Y_{n,m}^k(\theta)\right| \le c_2 n^{\frac{m}{2}-1+l},\ j = \overline{1,m-1}, l = 0,1,\dots, \tag{38}$$

as well as lemmas, restrictions on the coefficients of equation (1) and on given functions $\varphi_1(r,\theta), \varphi_2(r,\theta),\ \psi_1(t,\theta), \psi_2(t,\theta)$ can be shown that received solution (37) belongs to the class $C^1(\bar{\Omega}_\beta) \cap C^2(\Omega_\beta)$.

$$u(r,\theta,0) = \tau(r,\theta) = \sum_{n=0}^{\infty}\sum_{k=1}^{k_n}\tau_n^k(r)Y_{n,m}^k(\theta), \tag{39}$$

$$\tau_n^k(r) = \psi_{2n}^k(0) + \sum_{s=1}^{\infty} r^{\frac{(2-m)}{2}}[\int_0^\beta a_{ns}^k(\xi)(\exp\mu_{s,n}^2\int_0^\xi g(\xi_1)d\xi_1)d\xi + b_{ns}^k\exp(\mu_{s,n}^2\int_0^\beta g(\xi)d\xi]J_v(\mu_{s,n}r).$$

From (30) - (33), (35), and also from the lemmas, it follows that $\tau(r,\theta) \in W_2^l(S),\ l > \frac{3m}{2}.$

Thus, taking into account the boundary conditions (2) and (39), we arrive at Ω_β to the Dirichlet problem for an elliptic equation.

$$L_2 u \equiv p_1(t)\Delta_x u + p_2(t)u_{tt} + \sum_{i=1}^{m} a_i(r,\theta,t)u_{x_i} + b(r,\theta,t)u_t + c(r,\theta,t)u = 0, \tag{40}$$

with data

$$u\Big|_{S_0} = \tau(r,\theta),\ u\Big|_{\Gamma_\alpha} = \psi_1(t,\theta),\ u\Big|_{\sigma_\alpha} = \varphi_1(r,\theta), \tag{41}$$

having a solution ([12]).

Hence the solvability of the problem 1 is established.

The uniqueness of the solution to problem 1. First, we consider problem (1), (3) in the area Ω_β and prove its uniqueness of the solution. To do this, we first construct the solution of the first boundary value problem for the equation

$$L_1^* \vartheta \equiv g(t)\Delta_x \vartheta + \vartheta_t - \sum_{i=1}^{m} d_i \vartheta_{x_i} + d\vartheta = 0, \qquad (5^*)$$

with data

$$\vartheta\Big|_s = \tau(r,\theta)\sum_{n=0}^{\infty}\sum_{k=1}^{k_n} \overline{\tau}_n^k(r) Y_{n,m}^k(\theta), \ \ \vartheta\Big|_{\Gamma_\beta} = 0, \qquad (42)$$

where $d(x,t) = e - \sum_{i=1}^{m} d_{ix_i}$, $\overline{\tau}_n^k(r) \in G, G$ - many functions $\tau(r)$ from the class $C([0,1]) \cap C^1(0,1))$. Lots of G tight everywhere in $L_2((0,1))$ [10]. The solution to the problem (5 *), (42) will be sought in the form (6), where the functions $\vartheta_n^k(r,t)$ will be defined below. Then, similarly to item 2. functions $\overline{\vartheta}_n^k(r,t)$ satisfy the system of equations (8)-(10), where $\overline{d}_{in}^k, d_{in}^k$ replaced respectively by $-\tilde{d}_{in}^k, -d_{in}^k$, a $\tilde{e}_n^k$ on $\tilde{d}_n^k$, $i = 1,...,m$, $k = \overline{1,k_n}$, $n = 0,1,...$.

Further, from the boundary condition (42), by virtue of (6), we obtain

$$\overline{\vartheta}_n^k(r,\theta) = \overline{\tau}_n^k(r), \ \overline{\vartheta}_n^k(1,t) = 0, \ k = \overline{1,k_n}, \ n = 0,1,... . \qquad (43)$$

As previously noted, each equation of system (8) - (10) is represented as (11). Problem (11), (43) we will result in the following problem.

$$L\vartheta_n^k = g(t)(\vartheta_{nrr}^k + \frac{\overline{\lambda}_n}{r^2}\vartheta_n^k) + \vartheta_{nt}^k = \tilde{f}_n^k(r,t), \qquad (15')$$

$$\vartheta_n^k(r,0) = \tau_n^k(r), \quad \vartheta_n^k(1,t) = 0, \qquad (44)$$

$$\vartheta_n^k(r) = r^{\frac{(m-1)}{2}}\overline{\vartheta}_n^k(r,t), \ \ \tilde{f}_n^k(r,t) = r^{\frac{(m-1)}{2}}\overline{f}_n^k(r,t), \ \ \tau_n^k(r) = r^{\frac{(m-1)}{2}}\overline{\tau}_n^k(r).$$

The solution to problem (15), (44) will be sought in the form (17), where $\vartheta_n^k(1,t)$ - solution of the problem for equation (18) with the data $\vartheta_{2n}^k(r,t)$

$$\vartheta_{1n}^k(r,0) = 0, \ \vartheta_{1n}^k(1,t) = 0, \qquad (45)$$

a - $\vartheta_{2n}^k(r,t)$ solution of the problem for equation (20) with the condition

$$\vartheta_{2n}^k(r,0) = 0, \ \ \vartheta_{2n}^k(1,t) = 0, \qquad (46)$$

The solution of problems (18), (45) and (20), (46) respectively I have the form

$$\vartheta_{1n}^k(r,t) = \sum_{s=1}^{\infty}\sqrt{r}(\exp(+\mu_{s,n}^2\int_0^t g(\xi)d\xi))(\int_0^t a_{ns}^k(\xi)(\exp(\mu_{s,n}^2\int_0^{\xi} g(\xi_1)d\xi_1)J_v(\mu_{s,n}r),$$

where

$$\tau_{s,n} = 2[J_{v+1}(\mu_{s,n})]^{-2}\int_0^1 \sqrt{\xi}\tau_n^k(\xi)J_v(\mu_{s,n}\xi)d\xi, \quad v = \frac{n+(m-2)}{2}.$$

Thus, solving the problem (5 *), (42) in the form of a series

$$u(r,\theta,t) = \sum_{n=0}^{\infty}\sum_{k=1}^{k_n} r^{\frac{(1-m)}{2}}[\vartheta_{1n}^k(r,t) + \vartheta_{2n}^k(r,t)]Y_{n,m}^k(0),$$

built, which by virtue of estimates (38) belongs to the class $C(\overline{\Omega}_\beta) \cap C^2(\Omega_\beta)$.

As a result of integration by area Ω_β identity [13]

$$\vartheta L_1 u - u L_1^* \vartheta = -\vartheta P(u) + u P(\vartheta) - u\vartheta Q,$$

where

$$P(u) = g(t)\sum_{i=1}^{m} u_{x_i} \cos(N^\perp, x_i),\ Q = \cos(N^\perp, t) - \sum_{i=1}^{m} d_i \cos(N^\perp, x_i),$$

but $N^\perp$ - internal normal to the border $\partial\Omega_\beta$, according to the Green formula we get

$$\int_S \tau(r,\theta) u(r,\theta,0) ds = 0. \qquad (47)$$

Since the linear span of a system of functions $\{\overline{\tau}_n^k(r) Y_{n,m}^k(\theta)\}$ tight $L_2(S)$ ([10]), hen from (47) we conclude that $u(r,\theta,0) = 0,\ \forall (r,\theta) \in S.$. So on the principle of extremum for a parabolic equation (5) [14] $u \equiv 0$ в $\overline{\Omega}_\beta$.

Next, from the Hopf principle ([15]) $u \equiv 0$ в $\overline{\Omega}_\beta$.

The theorem is proven completely.

УДК 517.956
МРНТИ 27.31.15

С.А. Алдашев, М.Н. Майкотов

[1] Абай атындағы Қазақ Ұлттық Педагогикалық Университеті, Алматы, Қазақстан
[2] Абай атындағы Қазақ Ұлттық Педагогикалық Университеті, Алматы, Қазақстан

КӨП-ӨЛШЕМДІ ЭЛЛИПТИКО-ПАРАБОЛАЛЫҚ ТЕҢДЕУЛЕРІНІҢ БІР КЛАСЫ БОЙЫНША ЦИЛИНДРЛІК ОБЛЫСЫНДА ДИРИХЛЕ ЕСЕБІ

Аннотация. Жазықтықтағы эллиптико-параболикалық теңдеулер үшін шеттік есептер өте жақсы зерттелген ([1]). Дирихле есебінің корректілігі түрі мен ретті алып тұратын көп өлшемді эллиптико-параболалық теңдеулер үшін орнатылған [3]. Көп-өлшемді эллиптико-параболалық теңдеулер үшін жұмыс істеу түрі мен ретті өзгертумен рұқсат етілген және Дирихле есебін классикалық шешудің айқын түрі алынған.

Түйін сөздер: шешімділігі, аралас есеп, көп өлшемді эллиптико-параболалық теңдеулер, Бессель функциясы.

УДК 517.956
МРНТИ 27.31.15

С.А. Алдашев, М.Н. Майкотов

Казахский Национальный Педагогический Университет имени Абая, Алматы, Казахстан

ЗАДАЧА ДИРИХЛЕ В ЦИЛИНДРИЧЕСКОЙ ОБЛАСТИ ДЛЯ ОДНОГО КЛАССА МНОГОМЕРНЫХ ЭЛЛИПТИКО-ПАРАБОЛИЧЕСКИХ УРАВНЕНИЙ

Аннотация. Краевые задачи для вырождающихся эллиптико-параболических уравнений на плоскости достаточно хорошо изучены ([1]). Корректность задачи Дирихле для вырожденных многомерных эллиптико-параболических уравнений с вырождением типа и порядка была установлена в [3]. В работе для многомерных эллиптико-параболических уравнений с вырождением типа и порядка показана разрешимость и получен явный вид классического решения задачи Дирихле.

Ключевые слова: разрешимость, смешанная задача, многомерные эллиптико-параболические уравнения, функция Бесселя.

Information about authors:

Aldashev Serik Aimurzaevich, Kazakh National Pedagogical University named after Abay, professor, doctor of physico-mathematical sciences., aldash51@mail.ru, https://orcid.org/0000-0002-8223-6900;

Maikotov Mukhit Nurdauletovich, Kazakh National Pedagogical University named after Abay, doctoral student, specialty 6D060100-Mathematics, mukhit777@mail.ru, https://orcid.org/0000-0002-9739-5672;

REFERENCES

[1] Picker G. To a unified theory of boundary value problems for second order elliptic-parabolic equations: Coll. translations. Mathematics, 1963, v.7, No. 6, pp. 99-121.

[2] Oleinik O.A. Radkevich E.V. Equations with a nonnegative characteristic form, Moscow: Moscow University Press, 2010-360c.

[3] Aldashev S.A. The correctness of the Dirichlet problem for degenerate multidimensional elliptic-parabolic equations // Mathematical Journal, Almaty, 2018, v. 18, No. 3 p. 5-17.

[4] Mikhlin S.G. Multidimensional singular integrals and integral equations, Moscow: Fizmatgiz, 1962 - 254 p.

[5] Aldashev S.A. Boundary value problems for multidimensional hyperbolic and mixed equations. Almaty: Gylym, 1994. 170s.

[6] Aldashev S.A. Darboux-Protter problems for degenerate multidimensional hyperbolic equations // News of universities. Mathematics, 2006, №9 (532) -p.3-9.

[7] Aldashev S.A. Degenerate multidimensional hyperbolic equations, Oral: ZKATU, 2007.139p.

[8] E. Kamke. Reference book on ordinary differential equations, M .: Science, 1965. 703 p.

[9] G. Bateman, A. Erdein. Higher Transcendental Functions, V. 2, Moscow: Science, 1974. 297s.

[10] Kolmogorov A.N., Fomin S.V. Elements of the theory of functions and functional analysis, M.: Science, 1976. 543 p.

[11] Tikhonov A.N., Samara A.A. Equations of mathematical physics: M: Science, 1966-724c.

[12] Aldashev S.A., Mikotov M.N. The correctness of the Dirichlet problem in a cylindrical domain for multidimensional elliptic equations with degeneration of type and order. Proceedings of the V International Scientific Conference "Non-local boundary value problems and related problems of mathematical biology, computer science and physics." December 4-7, 2018 Nalchik, Kabardino-Balkaria. p.27.

[13] Smirnov V.I. The course of higher mathematics, Vol.4, d.2, M.: Science, 1981. 550 p.

[14] Friedman A. Partial differential equations of parabolic type. M.: Mir, 1968. 527 p.

[15] L. Bers, John F., Schechter M. Partial differential equations. M.: Mir, 1966. 351s.

[16] Assanova A.T., Alikhanova B.Zh., Nazarova K.Zh. Well-posedness of a nonlocal problem with integral conditions for third order system of the partial differential equations, News of the National Academy of Sciences of the Republic of Kazakhstan. Physico-Mathematical Series.5:321(2018),33–41. https://doi.org/10.32014/2018.2518-1726.5

N E W S
OF THE NATIONAL ACADEMY OF SCIENCES OF THE REPUBLIC OF KAZAKHSTAN
PHYSICO-MATHEMATICAL SERIES
ISSN 1991-346X **https://doi.org/10.32014/2019.2518-1726.63**
Volume 5, Number 327 (2019), 98 – 104

UDC 531, 53(075). 622.732.62-9. 53.072
IRSTI 29.03.77

K.A.Kabylbekov[1], Kh.K.Abdrakhmanova[2], B.Sh.Kedelbaev[1], Ye.B. Issayev[1]

[1]M.Auezov South-Kazakhstan State University, Shymkent, Kazakhstan;
[2]South-Kazakhstan State Pedagogical University, Shymkent, Kazakhstan
kenkab@mail.ru, khadi_kab@mail.ru, b.sh.kedelbaev@mail.ru, erzhanisaev@mail.ru

MODELING OF THE NORMAL MAGNETIZATION CURVE OF FERROMAGNETIC

Abstract. The normal magnetization curve is used in technical calculations of magnetic circuits when it is required to investigate (to model) nonlinear inductive elements. Modeling of the normal magnetization curve by the use of an analytical function allows describing with a high precision a real magnetization curve along all characteristic sections and defining the magnetization curve by the continuous function. This procedure allows avoiding breaks and discontinuities of the extreme dependences obtained as a result of differentiation. There are a lot of ways of approximating the table function by the analytical function which with a particular degree of accuracy models an initial function at the given points. Modeling of the normal magnetization curve of the ferromagnetic is done by using the *arctangent* function for approximation of the curve and the Matlab software. The *arctangent* function is chosen because this function and its derivative are easily calculated and also because this function describes the normal magnetization curve with an adequate accuracy. There are also the experimental data of magnetic field induction dependence on magnetizing field intensity and the approximating magnetization curve. The obtained diagrams show that the table function is approximated by the analytical function of *arctangent* which with a sufficient accuracy models the table function at the given points.

Key words: ferromagnetic, magnetization curve, experimental data, approximation, arctangent function.

Introduction. Modeling of the normal magnetization curve of the ferromagnetic is done by using the Matlab software [1-7]. The Matlab software is based not only on the best practices of development and computer realization of numerical methods build up for the last three decades but also on all experience of formation of mathematics throughout all history of mankind. About one million legally registered users already apply this software. The top universities and scientific centers of the world willingly use it in their scientific projects. It is important that the Matlab software can be integrated with such popular software as Mathcad, Maple and Mathematica. Thus, the Matlab system can become the excellent assistant in scientific research.

Unfortunately, the numerical calculations which are carried out by students often are done by means of the calculator that is almost manually. Modern computers are frequently used only for presentation of the work. Actually students should be able not only to solve these or other engineering problems, but also do them by using modern methods, that is, using personal computers.

The use of the computer simulation allows: to individualize and differentiate tutoring process; to exercise control with diagnostics of mistakes and with a feed-back; to carry out self-testing and self-correction of educational activity; to avoid during indoor classes the laborious routine calculations due to performing them by computers; to visualize an educational information; to simulate and imitate the studied processes or phenomena; to carry out the virtual version of the real laboratory works and experiments by simulating them on the computer; to develop imaginary and theoretical thinking; to enhance learning motivation; to form the culture of cognitive activity, etc.

In M.Auezov South Kazakhstan State University computers are used on Physics classes for the following activities: statistical processing of results of a laboratory experiment and plotting the diagrams of the studied relationship; demonstration and study of processes which for various reasons can't be observed in reality.

Application of Matlab software on Physics classes allows simulating and researching various physical processes, saves time for practical classes, promotes deeper understanding the phenomena, increases interest in studying physics; develops creativity of students.

In our early works [8-28] we have shown the potentials of the Matlab software for modeling and visualization of physical processes in mechanics, molecular physics, electromagnetism and quantum physics.

The normal magnetization curve is used in technical calculations of magnetic circuits when it is required to investigate (to model) nonlinear inductive elements. The normal magnetization curve is presented by the diagram of the magnetic field induction versus magnetic field intensity or reverse functional dependence H(B). The normal magnetization curve has three segments: the initial segment corresponding to lower part of the curve, the second segment corresponding to the swift increase of the induction and the third segment corresponding to the saturation of the steel core of the inductor.

As an example in the table we have given the data for the magnetization curve of the **steel 2312.**

Source: © simenergy.ru

№	1	2	3	4	5	6	7	8	
H, A/m	**0**	**68**	**76**	**86**	**96**	**140**	**190**	**240**	
B, T	**0**	**0.4**	**0.5**	**0.6**	**0.7**	**0.8**	**0.9**	**1.0**	
№	**9**	**10**	**11**	**12**	**13**	**14**	**15**	**16**	**17**
H, A/m	**300**	**400**	**550**	**1000**	**1600**	**3400**	**7700**	**13400**	**19400**
B, T	**1.1**	**1.2**	**1.3**	**1.4**	**1.5**	**1.6**	**1.7**	**1.8**	**1.9**

There are many ways of approximation of table function by analytical function which with a particular degree of accuracy models the initial function at the given points. These mathematical ways of description of the table function are based on application of various mathematical functions. Modeling of the normal magnetization curve by using analytic function allows with a high precision describing a real magnetization curve along all characteristic segments, defining the magnetization curve by the continuous function. This procedure allows avoiding breaks and discontinuities of the extreme dependences obtained as a result of differentiation. In general, power functions are widely used since they allow carrying out calculations of magnetic circuits with alternating magnetic fields. The accuracy of approximation of a real curve by power polynomial is proportional to the determination number of its coefficients. Hyperbolic sine and tangent at their expansion in a series turn into power polynomial. The results of approximation by a hyperbolic sine and tangent are close to approximation by a power polynomial, and in many cases they almost exactly coincide with data of natural experiments.

The *arctangent* function is widely used nowadays for approximation of the magnetization curve because this function and its derivative are easily calculated and also because this function with an adequate accuracy describes the normal magnetization curve.

Formulation of the problem. Let us consider the approximation of the normal magnetization curve by the function containing *arctangent* and three adjustable coefficients

$$B(H) = p1 \cdot arctg(p2 \cdot H) + p3 \cdot H$$

The unknown coefficients (*p1, p2, p3*) may be determined by using least square technique. According to this technique the approximating function is determined as the minimum of the sum of squares of the calculated approximating function deviation from experimental points. This criterion of the least square technique is written as the following expression:

$$\sum_{i=1}^{N} \delta^2 = \sum_{i=1}^{N} \left(p1 \cdot arctg(p2 \cdot H_i) + p3 \cdot H_i - B_i \right)^2 \to \min$$

The necessary condition for existence of the function minimum is the equality to zero of its partial derivatives with respect to unknown variables *p1, p2* and *p3*. As a result we obtain the following system of equations:

$$\frac{\partial}{\partial p_1}\sum_{i=1}^{N}\delta^2=0;\sum_{i=1}^{N}2\cdot\left(p1\cdot arctg\left(p2\cdot H_i\right)+p3\cdot H_i-B_i\right)\cdot arctg\left(p2\cdot H_i\right)=0$$

$$\frac{\partial}{\partial p_2}\sum_{i=1}^{N}\delta^2=0;\sum_{i=1}^{N}2\cdot\left(p1\cdot arctg\left(p2\cdot H_i\right)+p3\cdot H_i-B_i\right)\cdot\frac{p1\cdot H_i}{1+p_2^2\cdot H_i^2}=0$$

$$\frac{\partial}{\partial p_3}\sum_{i=1}^{N}\delta^2=0;\sum_{i=1}^{N}2\cdot\left(p1\cdot arctg\left(p2\cdot H_i\right)+p3\cdot H_i-B_i\right)\cdot H_i=0$$

The solution of this system of nonlinear equations allows determining the coefficients of the approximating function.

There is the listing of the program for approximation at small magnitudes of the magnetizing field:

```
>> H=[0 68 76 86 96 140 190 240]; % in A/m
>>  B=[0 0.4 0.5 0.6 0.7 0.8 0.9 1]; % in T
>> plot(H,B,'o')
>>grid on
>> p1=0.984;
>>p2=7.273*10.^-3;
>>p3=1.935*10.^-5;
>>hold on
>>B=p1*atan(p2*H)+p3*H;
>>plot(H,B,'-');
```

The result is presented in the fig.1

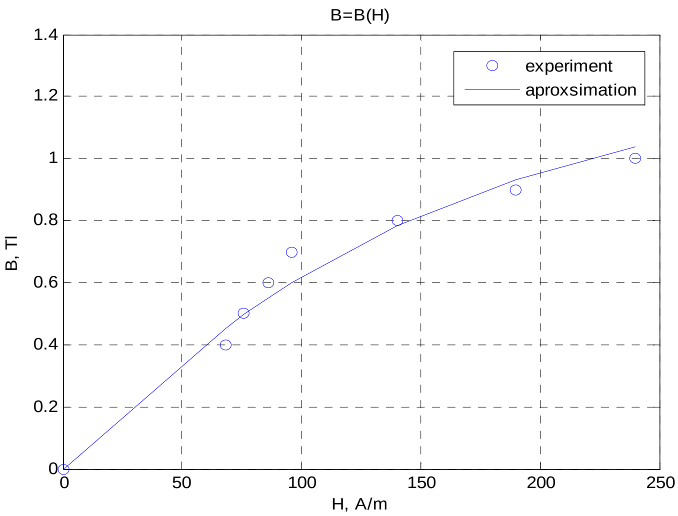

Figure 1 - Approximation of the magnetization curve by *arctangent* function at small magnitudes of the magnetizing field

The listing of the program for approximation at large magnitudes of the magnetizing field:

```
>> H=[300 400 550 1000 1600 3400 7700 13400 19400];% in A/m
>> B=[1.1 1.2 1.3 1.4 1.5 1.6 1.7 1.8 1.9]; % in T
>> plot(H,B,'o')
```

```
>> grid on
>> p1=0.984;
>> p2=7.273*10.^-3;
>> p3=1.935*10.^-5;
>> hold on
>> B=p1*atan(p2*H)+p3*H;
>> plot(H,B,'-');
```

The result is presented in the fig.2

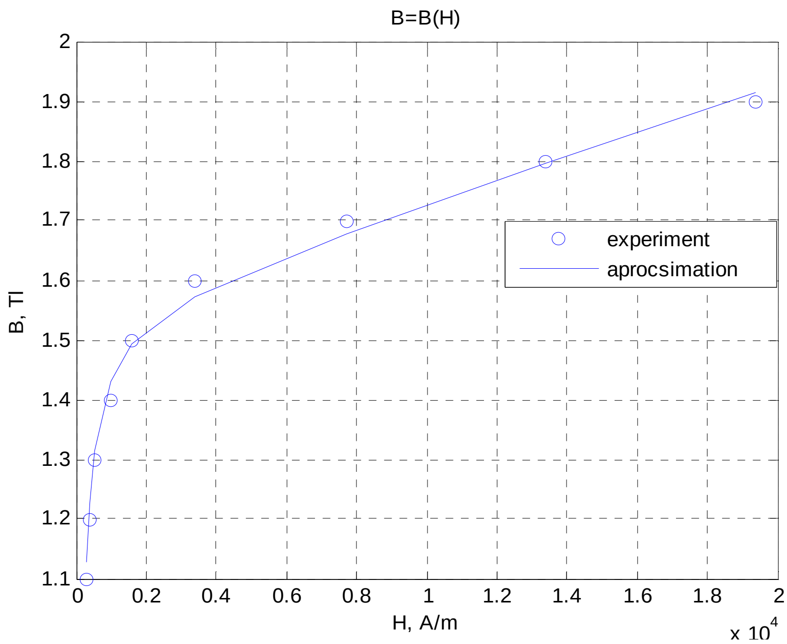

Figure 2 - Approximation of the magnetization curve by *arctangent* function at large magnitudes of the magnetizing field

This approximation is odd and may be applied for calculation of magnetic circuits with stationary as well as with alternating fields.

The listing of the program for approximation at magnitudes of the magnetizing field from zero up to 7700 A/m:

```
>> H=[0 68 76 86 96 140 190 240 300 400 550 1000 1600 3400 7700];
>>  B=[0 0.4 0.5 0.6 0.7 0.8 0.9 1 1.1 1.2 1.3 1.4 1.5 1.6 1.7];
>> plot(H,B,'o');
>> plot(H,B,'o');
>> grid on
>> p1=0.984;
>>p2=7.273*10.^-3;
>>p3=1.935*10.^-5;
>>hold on
>>B=p1*atan(p2*H)+p3*H;
>>plot(H,B,'-');
```

The result is presented in the fig.3

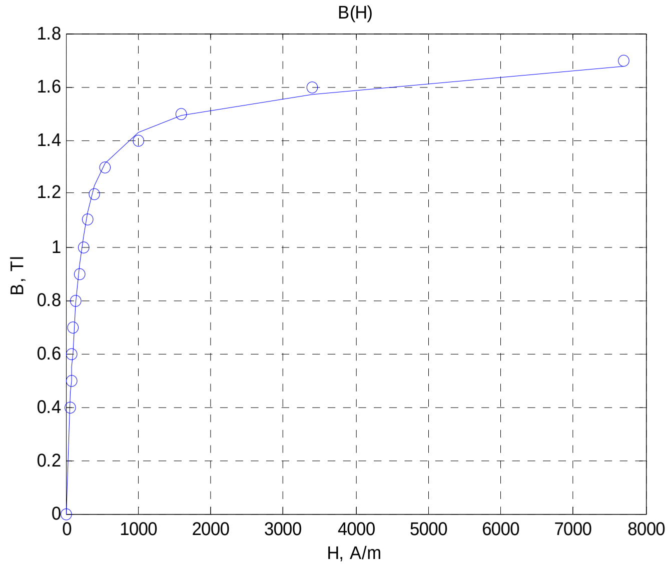

Figure 3 - Approximation of the magnetization curve by *arctangent* function at magnitudes of the magnetizing field from zero up to 7700 A/m

Conclusion: Modeling of the normal magnetization curve of the ferromagnetic is done by using the *arctangent* function for approximation of the curve and the Matlab software. The *arctangent* function is chosen because this function and its derivative are easily calculated and also because this function describes the normal magnetization curve with an adequate accuracy. There are also the experimental data of magnetic field induction dependence on magnetizing field intensity and the approximating magnetization curve. The obtained diagrams show that the table function is approximated by the analytical function of *arctangent* which with a sufficient accuracy models the table function at the given points.

К.А.Қабылбеков[1], Х.К.Абдрахманова[2], Б.Ш. Кеделбаев[1], Е.Б. Исаев[1]

[1]М.Әуезов атындағы Оңтүстік Қазақстан мемлекеттік университеті, Шымкент, Қазақстан
[2]Оңтүстік Қазақстан мемлекеттік педагогикалық университеті,
Шымкент, Қазақстан
kenkab@mail.ru, khadi_kab@mail.ru, b.sh.kedelbaev@mail.ru, erzhanisaev@mail.ru

ФЕРРОМАГНЕТИКТІҢ НЕГІЗГІ МАГНИТТЕЛУ ҚИСЫҒЫН МОДЕЛДЕУ

Аннотация. Магниттік тізбектерді техникалық есептеулерде сызықтық емес индуктивті элементтерді зерттегенде (моделдеуде) негізгі магнттелу қисығы қолданылады. Магниттелудің негізгі қисығын аналитикалық функция көмегімен модельдеу барлық сипаттамалық бөлімдерде нақты магниттелу қисығын жоғары дәлдікпен сипаттауға, дифференциалдау нәтижесінде пайда болатын экстремалды тәуелділіктердегі үзілістерді болдырмайтын үздіксіз функциямен магниттелу қисығын орнатуға мүмкіндік береді. Белгілі бір дәлдікпен берілген нүктелердегі бастапқы функцияны модельдейтін аналитикалық функциямен кестелік функцияны жақындастырудың көптеген әдістері бар. Ферромагнетиктің негізгі магниттелу қисығын модельдеу үшін біз Matlab жүйесін және магниттелу қисық сызығын аппроксимациялау үшін, функцияның өзі мен оның туындысын есептеу қарапайымдылығына, сондай-ақ тәжірибелік магниттелу қисығын жеткілікті дәлдікпен сипаттайтына байланысты, арктангенс функциясын таңдадық. Нақты ферромагнетик үшін магниттік индукцияның магниттеуші өрістен тәуелдігінің эксперименттік мәліметтері мен олардың аппроксимацияланған қисық келтірілген. Келтірілген суреттен (кесте бойынша) нүктелермен берілген функцияны жеткілікті дәлдікпен арктангенс фукциясымен аппроксимацияланған, яғни бастапқы функцияны модельдейтін арктангенс фукциясы арқылы алынған магниттелу қисығы көрсетілген.

Түйін сөздер. Ферроманетик, магниттелу қисығы, тәжірибелік берілгендер, аппроксимация, арктангенс функциясы.

К.А. Кабылбеков[1], Х.К. Абдрахманова[2], Б.Ш.Кеделбаев[1], Е.Б.Исаев[1]

[1]Южно-Казахстанский государственный университет им. М.Ауэзова, Шымкент, Казахстан;
[2]Южно-Казахстанский государственный педагогический университет, Шымкент, Казахстан

МОДЕЛИРОВАНИЕ ОСНОВНОЙ КРИВОЙ НАМАГНИЧЕНИЯ ФЕРРОМАГНЕТИКОВ

Аннотация. Основная кривая намагничивания используется при технических расчетах магнитных цепей, когда требуется исследовать (моделировать) нелинейные индуктивные элементы. Моделирование основной кривой намагничивания с помощью аналитической функции позволяет с высокой точностью описать реальную кривую намагничивания на всех характерных участках, задать кривую намагничивания непрерывной функцией, что позволяет избежать изломов и разрывов экстремальных зависимостей, получаемых в результате дифференцирования. Существуют множество способов аппроксимации таблично заданной функции аналитической функцией, которая с определенной степенью точности моделирует исходную функцию в заданных точках. Для моделирования основной кривой намагничивания ферромагнетика нами выбрана система Matlab и арктангенсная функция аппроксимации кривой намагничивания из-за простоты вычислений самой функции и ее производной, а также достаточной точности отображения оригинальной кривой намагничивания. Представлены экспериментальные данные зависимости индукции магнитного поля от напряженности намагничивающего поля с аппроксимационой кривой намагничивания. Из представленной картины видно, что таблично заданная функция аппроксимируется аналитической функцией арктангенса, которая с достаточной степенью точности моделирует исходную функцию в заданных точках.

Ключевые слова. Ферромагнетики, кривая намагничивания, экспериментальные данные, аппроксимация, функция арктангенса.

Information about authors

Kabylbekov K.A. – cand.ph-math.sc., associate professor of the chair of Physics, M.Auezov South-Kazakhstan State University, kenkab@mail.ru;

Abdrakhmanova Kh.K. - cand.chem.sc., associate professor of the chair of Physics, South-Kazakhstan State Pedagogical University, khadi_kab@mail.ru;

Kedelbaev B.Sh. - doc. eng. sciences, professor of the chair of “Microbiology”, M. Auezov South-Kazakhstan State University, b.sh.kedelbaev@mail.ru;

Issaev E.B. - cand.techn.sciences, associate professor of the department “Biology” of M. Auezov SKSU, erzhanisaev@mail.ru

REFERENCES

[1] Porsev S. V. Computer simulation of physical processes in the package MATLAB. M.: Hot Line-Telecom, 2003. 592 p.

[2] Kotkin G.A., Cherkassky V.S. Computer modeling of physical processes using MATLAB: Tutorial. / Novosibirsk University.

[3] Lurie M. S., Lurie O. M. Application of the MATLAB program in the study of course of electrical engineering. For students of all specialties and forms of educatio. Krasnoyarsk: SibSTU, 2006208 p.

[4] Potemkin V. system of engineering and scientific calculations MATLAB 5.x (in 2 volumes). Moscow: Dialog-MIFI, 1999.

[5] Averyanov G. P., Budkin, Dmitrieva V. V. Design automation. Computer workshop. Part 1. Solving problems of Electrophysics in MATLAB: tutorial. Moscow: MEPhI, 2009. 111 p.

[6] Dyakonov V. p. MATLAB. Complete tutorial. M: DMK Press, 2012. 768 p.

[7] Ryndin E. A., Lysenko I. E. Solving problems of mathematical physics in Matlab. Taganrog: TRTU. 2005. 62 p.

[8] Kabylbekov K.A., Abdrakhmanova Kh.K., Abekova J., Abdraimov R.T., Ualikhanova B.S. Calculation and visualization of a system-an electron in a deep square potential well, with use of the software package of MATLAB. Proceeding of the III International Scientific and Practical Conference «Topical researches of the World Science» (Iune 28, 2017,Dubai, UAE). №7(23). Vol.I, July 2017, P 7-13.

[9] Kabylbekov K., Saidullaeva N., Spabekova R., Omashova G, Tagaev N., Bitemirova A., Berdieva M. Model of a blank form for computer laboratory work on research of the speed selector. Journal of Theoretical and Applied Information Technology15th July 2017. Vol. 95. No 13, P. 2999-3009, c 2005 – ongoing JATIT & LLS. Indexada en Scopus.

[10] Kabylbekov K.A., Omashova G.,Spabekova R., Saidullaeva N., Saidakhmetuv P., Junusbekova S. Management and organization of computer laboratory work in physics education. Espacios. Vol. 38 (Nº 45) Año 2017. Pág. 35. Indexada en Scopus.

[11] Kabylbekov K., Omashova G, Spabekova R, Saidullaeva N, Saidakhmetuv P. Junusbtkova S., Management and organization of computer laboratory work in physics education. Espacios. Vol. 38 (Nº 45) Año 2017. Pág. 35. Indexada en Scopus, Google Schollar.

[12] Kabylbekov K.A., Ashirbaev Kh.A., Arysbaeva A.S., Jumagaliyeva A.M. Model of the form of the organization of computer laboratory work in the study of physical phenomena. Modern high technologies, №4, Moscow, 2015, P 40-43.

[13] Kabylbekov K.A., Madiyarov N.K., Saidakhmetov P.A. Independent design of research tasks of computer laboratory works on thermodynamics. Proceedings of the IX International Scientific and Methodological Conference. Teaching natural sciences (biology, physics, chemistry) mathematics and computer science. Tomsk-2016, P. 93-99.

[14] Kabylbekov K.A, Omashova G. Sh, Spabekova R.S, Saidakhmetov P.A, Serikbaeva G.S, Aktureeva G. Organization of computer laboratory works on study the turn-on and turn-off current of the power supply by using MATLAB software package. News of the National Academy of Sciences of the Republic of Kazakhstan, Series of Physics and Mathematics, Almaty, Volume 3, Number 313 2017, P. 139-146.

[15] Kabylbekov K.A, Omashova G. Sh, Spabekova R.S, Saidakhmetov P.A, Serikbaeva G.S , Aktureeva G. Organization of computer labs for the study of velocity and height distribution of molecules from the Earth's surface by using MATLAB software package. Bulletin of NAS RK, Almaty, Volume 3, Number 367, 2017, P 111-119.

[16] Kabylbekov K.A, Ashirbayev H.A, Abdrakhmanova Kh.K, Dzhumagalieva A.I., Kydyrbekova J.B. Organization of laboratory work on study of electric and magnetic fields by using MATLAB software package. Proceedings of the National Academy of Sciences of the Republic of Kazakhstan, Series of Physics and Mathematics, Almaty, Volume 3, Number 313, 2017, P 206-213.

[17] Kabylbekov K. A., Spabekova R. S., Omashova G.Sh., Abzhapparov A.A., Polatbek A, Serkebayeva S. G. The use of the software package MATLAB for solving problems on bifurcated electrical circuits. Bulletin of NAS RK, Almaty 2017, Volume 4, Number 368, P 101-108.

[18] Kabylbekov K. A., Ashirbaev H. A., Abdrakhmanova Kh.K., Dzhumagalieva A. I., Kadyrbekova J. B. Organization of the performance of the laboratory work "Modeling the electric field of a system consisting of a dielectric square and a long charged conductor" by using MATLAB software package. News of the National Academy of Sciences of the Republic of Kazakhstan, Series of Physics and Mathematics, Almaty 2017, Volume 4, Number 314, P 252-259.

[19] Kabylbekov K. A., Abdrakhmanova Kh.K., Ermakhanov M.N., Urmashev B.A., Jaтkanbayev E.T. Calculation and visualization of a body motion in a gravitational field. NEWS of the National Academy of Sciences of the Republic of Kazakhstan. Series of geology and technical sciences.Volume 4, Number 430 (2018), P 87-98.

[20] Kabylbekov K. A., Abdrakhmanova Kh.K., Omashova G.Sh., Lakhanova K.M., Abekova Zh.A. Organization of computer laboratory work “Calculation and visualization of small forced oscillations” N E W S of the National Academy of Sciences of the Republic of Kazakhstan, Series of geology and technical sciences. Volume 3, Number 430 (2018), P 145-155.

[21] Kabylbekov K. A., Abdrakhmanova Kh.K., Omashova G.Sh., Kedelbaev B., Abekova Zh.A. Calculation and visualization of electric field of a space –charged sphere. N E W S of the National Academy of Sciences of the Republic of Kazakhstan. Series of geology and technical sciences. Volume 5, Number 431 (2018), P 201 – 209. doi.org/10.32014/2018.2518-170X.26

[22] K. A. Kabylbekov, Kh. K. Abdrakhmanova, P. A. Saidakhmetov, T. S. Sultanbek, B. Sh. Kedelbaev. Calcuiation and visualization of isotopes separation process using MATLAB program. N E W S of the National Academy of Sciences of the Republic of Kazakhstan. Series of geology and technical sciences. Volume 5, Number 431 (2018), P 218– 225. doi.org/10.32014/2018.2518-170X.28

[23] Kabylbekov K. A., Abdrakhmanova Kh.K., Saidakhmetov P.A., Musaev J.M., Issayev Ye.B., Ashirbaev Kh.A. Calculation and visualization of a body motion under the gravity force and the and the opposing drag. N E W S of the National Academy of Sciences of the Republic of Kazakhstan Series of geology and technical sciences. Volume 6, Number 432 (2018), P 85– 95. doi.org/10.32014/2018.2518-170X.38

[24] Kabylbekov K. A., Abdrakhmanova Kh.K., Saidakhmetov P.A., Kedelbaev B.Sh., Abdraimov R. T., Ualikhanova Б.S. Calculation and visualization of the field coaxial cable carrying steady current. N E W S of the National Academy of Sciences of the Republic of Kazakhstan Series of geology and technical sciences. Volume 6, Number 432 (2018), P 55 – 65. doi.org/10.32014/2018.2518-170X.35

[25] Kabylbekov K. A., A.D.Dasibekov, Abdrakhmanova Kh.K., Saidakhmetov P.A., Issayev E.B., Urmashev B.A. Calculation and visualization of oscillating systems. N E W S of the National Academy of Sciences of the Republic of Kazakhstan Series of geology and technical sciences. Volume 6, Number 432 (2018), P 110 – 120. doi.org/10.32014/2018.2518-170X.41

[26] Kenzhekhan Kabylbekov, Khadisha Abdrakhmanova, Gaukhar Omashova, Pulat Saidakhmetov, Turlan Sultanbek, Nurzhamal Dausheyeva. A Laboratory on visualization of Electrostatic and Magnetic Fields. Acta Polytechnica Hungarica Vol. 15, No. 7, 2018, P49-70. DOI: 10.12700/APH.15.7.2018.7.3

[27] Kabylbekov K. A., Dasibekov A.D., Abdrakhmanova Kh.K., Saidakhmetov P.A. Calculation and visualization of quantum-mechanical tunnel effect. News of the National Academy of Sciences of the Republic of Kazakhstan, Series of Physics and Mathematics, Volume 2, Number 324 (2019), P 60-68 . doi.org/10.32014/2019.2518-1726.13

[28] Kabylbekov K. A., Dasibekov A.D., Abdrakhmanova Kh.K., Saidakhmetov P.A. Calculation and visualization of small oscillations of a double plane pendulum. News of the National Academy of Sciences of the Republic of Kazakhstan, Series of Physics and Mathematics, Volume 2, Number 324 (2019), P 69-79. doi.org/10.32014/2018.2518-1726.14

N E W S
OF THE NATIONAL ACADEMY OF SCIENCES OF THE REPUBLIC OF KAZAKHSTAN
PHYSICO-MATHEMATICAL SERIES
ISSN 1991-346X **https://doi.org/10.32014/2019.2518-1726.64**
Volume 5, Number 327 (2019), 105 – 110

UDC 531, 53(075). 622.732.62-9. 53.072
IRSTI 29.03.77

K.A.Kabylbekov[1], Kh.K.Abdrakhmanova[2],
P.A.Saidakhmetov[1], B.Sh.Kedelbayev[1], Ye.B. Issayev[1]

[1]M.Auezov South-Kazakhstan State University, Shymkent, Kazakhstan;
[2]South-Kazakhstan State Pedagogical University, Shymkent, Kazakhstan
kenkab@mail.ru, khadi_kab@mail.ru, timpf_ukgu@mail.ru, b.sh.kedelbaev@mail.ru, erzhanisaev@mail.ru

PERFORMANCE OF THE LABORATORY WORK "OSCILLATIONS IN L-R-C SERIES CIRCUIT" BY USING MATLAB SOFTWARE PACKAGE

Abstract. The article suggests the calculation and visualization of oscillations that occur in the L-R-C series circuit. It contains the formulation of the problem, the physical analog and mathematical model of the process and the Matlab software program codes describing the process. There are graphs of the current through the circuit versus time, of the voltage across the inductor and across the resistor versus time. Because of the resistance the electromagnetic energy in the circuit is dissipated and converted to internal energy of circuit materials. The article also contains the assignments for students' individual work which require them to make comparative conclusions about various oscillations that occur when parameters of the circuit change.

Keywords. L-R-C series circuit, inductance, capacitor, resistor, power source, voltage, current.

Introduction

Nowadays all educational institutions of Kazakhstan are provided with computer hardware and software, interactive boards and internet. Almost all teachers have completed language and computer courses for professional development. Hence the educational institutions have all conditions for using computer training programs and models for performing computer laboratory works. In recent years the new computer system Matlab for performing mathematical and engineering calculations is widely used in university and engineering researches throughout the world [1-7]. Unfortunately, the numerical calculations which are carried out by students often are done by means of the calculator that is almost manually. Modern computers are frequently used only for presentation of the work. Actually students should be able not only to solve these or other engineering problems, but also do them by using modern methods, that is, using personal computers.

Students of the physics specialties 5B060400 and 5B011000 successfully master the discipline "Computer modeling of physical phenomena" which is the logical continuation of the disciplines "Information technologies in teaching physics" and "Use of electronic textbooks in teaching physics". The aim of this discipline is to study and learn the MATLAB program language, acquaintance with its huge opportunities for modeling and visualization of physical processes.

In our early works [8-28] we have shown the potentials of the Matlab software for modeling and visualization of physical processes in mechanics, molecular physics, electromagnetism and quantum physics where it have been used for solving the ordinary differential equations (ODE), for visualization of the equipotential lines of the systems of charged conductors and of the motion of charged particles in electric, magnetic and gravitational fields.

The present article is devoted to calculation and visualization of oscillations in the L-R-C series circuit by using the MATLAB software.

Formulation of the problem. The L-R-C circuit contains an inductor with inductance L, a capacitor with capacitance C, a resistor with resistance R and a power source. Let's consider electromagnetic processes that occur in the L-R-C series circuit.

Physical analog. Let's consider the L-R-C circuit with definite parameters (Fig. 1). The resistor has only ohmic resistance, the inductor has only inductive resistance, the capacitor has only capacitive resistance. The source generates a sinusoidal emf (electromotive force), the internal resistance of the source is negligibly small compared with the circuit resistance. The circuit doesn't radiate.

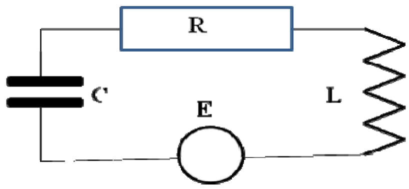

Figure 1 - The diagram of the L-R-C circuit

Parameters of the modeling. The capacitance of the capacitor, the inductance of the inductor, the ohmic resistance of the resistor, the amplitude and frequency of the source's emf.

Mathematical model. According to Kirchhoff rules, the algebraic sum of voltage drops across all elements of the circuit is equal to the source's emf. Therefore, the mathematical model of the circuit is:

$$L\frac{dI}{dt} + RI + \frac{1}{C}\int Idt = E,$$

$$L\frac{dI}{dt} + RI + \frac{1}{C}\int Idt = E_0 \cos \omega t$$

To get rid of integration, we will differentiate the left-side and right-side of the above equation with respect to time:

$$\frac{d^2I}{dt^2} + \frac{R}{L}\frac{dI}{dt} + \frac{1}{LC}I = -E_0\frac{\omega}{L}sin\omega t. \qquad (1)$$

Here R is ohmic resistance of the resistor with SI unit Ohm (Ω), L is the inductance of the inductor with SI unit Henry (H), C is the capacitance of the capacitor with SI unit Farad (F), I is the current through the circuit with SI unit Ampere (A) and $E = E_0 cos\,\omega t$ is the source's emf which as a function of time changes with frequency ω and amplitude E_0.

By changing variables

$$I = z_1,\ \frac{dI}{dt} = \frac{dz_1}{dt} = z_2,\ \frac{d^2I}{dt^2} = \frac{dz_2}{dt} = -\frac{R}{L}\frac{dI}{dt} - \frac{1}{LC}I + E_0\frac{\omega}{L}\sin \omega t$$

We will reduce the equation (1) to the system of two differential equations of the first order

$$\frac{dz_1}{dt} = z_2,\ \frac{dz_2}{dt} = -\frac{R}{L}z_2 - \frac{1}{LC}I + E_0\frac{\omega}{L}\sin \omega t \qquad (2)$$

For calculation of the right-sides of the system of the differential equations (2) we create m-file titled "contur.m".

```
function dzdt=contur(t,z)
global  R C L E0 w
dzdt=[z(2); -R/L*z(2) – 1/(L*C)*z(1)+wE0*sin(w*t)/L];
```

In the command line we write the codes of the program Matlab

```
global  R C L E0 w
>> R=0.3;
>> L=1;
```

```
>> C=0.25;
>> z0=[1;0];
>> t0=0;
>> w0=1/sqrt(L*C);
>> T=2*pi/w0;
>> E0=0;
>> w=1;
>> tmax=5*T;
>> dt=[t0 tmax];
>> [t z]=ode45(@contur,dt,z0);
>> subplot(3,1,1);
>>  plot(t,z(:,1),'LineWidth',2);
>>  title('current through the circuit','FontName','Arial Unicode MS')
>> ylabel(‘I,A’, ‘FontName’, ‘Arial Unicode MS’)
>> grid on
>> subplot(3,1,2);
>> UL=z(:,2)*L;
>> plot(t,UL,’LineWidth’,2)
>> title(‘Voltage across the inductor’, ‘FontName’,’Arial Unicode MS’)
>> ylabel(‘UL,B’, ‘FontName’, ‘Arial Unicode MS’)
>> xlabel(‘время,c’, ‘FontName’,’Arial Unicode MS’)
>> grid on
>> subplot(3,1,3);
>> UC=z(:,1)*R;
>> plot(t,UC,’LineWidth’,2)
>> title(‘Voltage across the resistor,’FontName’,’Arial Unicode MS’)
>>  ylabel(‘UR,B’, ‘FontName’, ‘Arial Unicode MS’)
>> xlabel(‘время,c’, ‘FontName’,’Arial Unicode MS’)
>> grid on
```

Results are presented in the fig.2

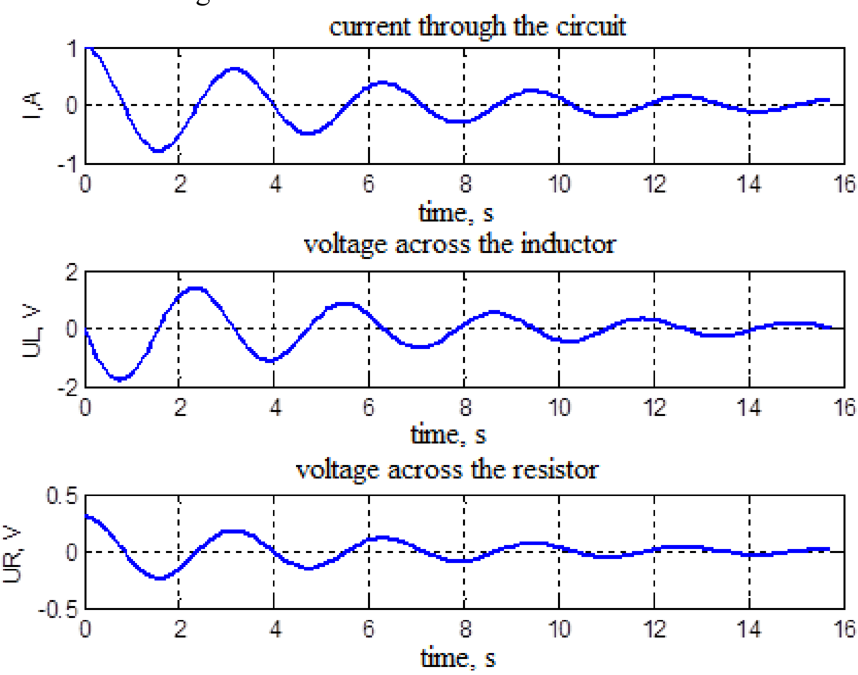

Figure 2 -The graphs of the current through the circuit and voltage across the inductor versus time; the graph of the voltage across the resistor versus time

At the ohmic resistance of the resistor of R = 0.3 Ω the oscillations are damping because of conversion of electric energy to internal energy of the resistor. The voltage across the resistor is in phase with the current in the resistor, while the voltage across the inductor leads the current by 90^o.

Assignments for individual work:

1. Specify the value of ohmic resistance of the resistor to be R=0. Obtain the graphs and make a conclusion about influence of resistance of the resistor on the nature of oscillations.
2. Increase the resistance of the resistor and make a conclusion about the degree of damping as a function of the ohmic resistance.
3. Increase the magnitude of the inductance in the circuit by 4 times. How did the oscillation frequency change? Conduct similar researches with the capacitance.
4. Specify the resistance of the resistor to be greater than its critical magnitude $R_c = 2\sqrt{L/C}$ and observe the transformation of the damping process to aperiodic one.
5. Connect the circuit to the source (E_0 > 0). Observe transition processes in the circuit. By gradually increasing the time of the experiment t_{max}, try to obtain the stationary oscillations.
6. By gradually changing the frequency ω of emf specify its magnitude to be equal to the natural frequency of the circuit $\omega_0 = 1/\sqrt{LC}$. Observe the increase in the amplitude of the oscillation (resonance). Compare the magnitude of emf with the magnitude of the voltage amplitude across the inductor.
7. Draw the graph of the voltage across the capacitor. For this purpose make changes in the code of the program. The voltage across the capacitor is defined by the expression $U_C = \frac{1}{C}\int Idt$.
8. Draw the graph of the magnetic field energy, produced by the current through the inductor $W_m = \frac{1}{2}LI^2$. Compare the frequencies of oscillations of the magnetic field energy and the voltage across the inductor.

Conclusion: The calculation and visualization of oscillations that occur in the L-R-C series circuit with definite parameters is performed using Matlab software. The article contains the formulation of the problem, the physical analog and mathematical model of the process and the Matlab software program codes describing the process. There are graphs of the current through the circuit versus time, of the voltage across the inductor and across the resistor versus time. Because of the resistance the electromagnetic energy in the circuit is dissipated and converted to internal energy of circuit materials. The article also contains the assignments for students' individual work which require them to make comparative conclusions about various oscillations that occur when parameters of the circuit change.

К.А.Қабылбеков[1], Х.К.Абдрахманова[2],
П.А.Саидахметов[1], Б.Ш. Кеделбаев[1], Е.Б. Исаев[1]

[1]М.Әуезов атындағы Оңтүстік Қазақстан мемлекеттік университеті, Шымкент, Қазақстан;
[2]Оңтүстік Қазақстан мемлекеттік педагогикалық университеті, Шымкент, Қазақстан

«ТЕРБЕЛМЕЛІ КОНТУРДАҒЫ ТЕРБЕЛІСТЕРДІ СИПАТТАУҒА» АРНАЛҒАН КОМПЬЮТЕРЛІК ЗЕРТХАНАЛЫҚ ЖҰМЫСТЫ ОРЫНДАУДЫ ҰЙЫМДАСТЫРУ

Аннотация. Тербелмелі контурдағы тербелістерді сипаттауға арналған компьютерлік зертханалық жұмысты орындауды ұйымдастыру ұсынылады. Мәселені тұжырымдау, контурда жүретін процестердің физикалық және математикалық моделдері, оларды Matlab жүйесінде іске асыратын бағдарлама кодтары келтірілген. Контурдағы токтың, индуктивтік катушкадағы және резистордегі кернеу түсуінің уақытқа тәуелділік графиктері берілген. Резистрдің кедергісі болған жағдайда тербелістер өшпелі сипатта болатыны байқалады. Үйткені резисторда энергия жұтылады. Өз бетінше орындауға арналған тапсырмалар ұсынылып, контур элементтерінің кейбір параметрлерін өзгерткен жағдайлардағы тербеліс сипаттары туралы қорытынды жасау ұсынылады.

Түйін сөздер. Тербелмелі контур, индуктивтілік, конденсатор, резистор, ток көзі, кернеу, ток.

К.А.Кабылбеков[1], Х.К.Абдрахманова[2], П.А.Саидахметов[1], Б.Ш.Кеделбаев[1], Е.Б. Исаев[1]

[1]Южно-Казахстанский государственный университет им. М.Ауэзова, Шымкент, Казахстан;
[2]Южно-Казахстанский государственный педагогический университет, Шымкент, Казахстан

ОРГАНИЗАЦИЯ ВЫПОЛНЕНИЯ КОМПЬЮТЕРНОЙ ЛАБОРАТОРНОЙ РАБОТЫ «ПРОЦЕССЫ, ПРОИСХОДЯЩИЕ В КОЛЕБАТЕЛЬНОМ КОНТУРЕ»

Аннотация. Предлагается расчет и визуализация характера колебаний, происходящие в последовательном колебательном контуре. Приведены формулировка задачи, физическая и математическая модели процесса, коды программы, реализующие процессы в программной среде Matlab. Построены графики зависимостей силы тока в контуре, напряжений на катушке индуктивности и падения напряжения на резисторе от времени. При наличии сопротивления резистора колебания являются затухающими, что связано с поглощением энергии резистором. Предложены задания для самостоятельной работы и проведение сравнительных выводов о характере колебаний при изменений отдельных параметров элементов контура.

Ключевые слова. Колебательный контур, индуктивность, конденсатор, резистор, источник, напряжение, ток.

Information about authors

Kabylbekov K.A. – cand.ph-math.sc., associate professor of the chair of Physics, M.Auezov South-Kazakhstan State University, kenkab@mail.ru, https://orcid.org/0000-0001-8347-4153,;

Abdrakhmanova Kh.K.- cand.chem.sc., associate professor of the chair of Physics, South-Kazakhstan State Pedagogical University, khadi_kab@mail.ru, https://orcid.org//0000-0002-6110-970X;

Saidakhmetov P.A.- cand.ph-math.sc., associate professor of the chair of Physics, M.Auezov South-Kazakhstan State University, timpf_ukgu@mail.ru, https://orcid.org/0000-0002-9146-047X;

Kedelbaev B.Sh.- doc. eng. sciences, professor of the chair of “Microbiology”, M. Auezov South-Kazakhstan State University, b.sh.kedelbaev@mail.ru, .- https://orcid.org/0000-0001-7158-1488;

Issaev E.B.- cand.techn.sciences, associate professor of the department “Biology” of M. Auezov SKSU, erzhanisaev@mail.ru, https://orcid.org/0000-0001-7536-5643

REFERENCES

[1] Porsev S. V. Computer simulation of physical processes in the package MATLAB. M.: Hot Line-Telecom, 2003. 592 p.

[2] Kotkin G.A., Cherkassky V.S. Computer modeling of physical processes using MATLAB: Tutorial. / Novosibirsk University.

[3] Lurie M. S., Lurie O. M. Application of the MATLAB program in the study of course of electrical engineering. For students of all specialties and forms of educatio. Krasnoyarsk: SibSTU, 2006208 p.

[4] Potemkin V. system of engineering and scientific calculations MATLAB 5.x (in 2 volumes). Moscow: Dialog-MIFI, 1999.

[5] Averyanov G. P., Budkin, Dmitrieva V. V. Design automation. Computer workshop. Part 1. Solving problems of Electrophysics in MATLAB: tutorial. Moscow: MEPhI, 2009. 111 p.

[6] Dyakonov V. p. MATLAB. Complete tutorial. M: DMK Press, 2012. 768 p.

[7] Ryndin E. A., Lysenko I. E. Solving problems of mathematical physics in Matlab. - Taganrog: TRTU. 2005. 62 p.

[8] Kabylbekov K.A., Abdrakhmanova Kh.K., Abekova J., Abdraimov R.T., Ualikhanova B.S. Calculation and visualization of a system-an electron in a deep square potential well, with use of the software package of MATLAB. Proceeding of the III International Scientific and Practical Conference «Topical researches of the World Science» (Iune 28, 2017,Dubai, UAE). №7(23). Vol.I, July 2017, P 7-13.

[9] Kabylbekov K., Saidullaeva N., Spabekova R., Omashova G, Tagaev N., Bitemirova A., Berdieva M. Model of a blank form for computer laboratory work on research of the speed selector. Journal of Theoretical and Applied Information Technology15th July 2017. Vol.95. No 13, P 2999-3009, c 2005 – ongoing JATIT & LLS. Indexada en Scopus.

[10] Kabylbekov K.A., Omashova G.,Spabekova R., Saidullaeva N., Saidakhmetuv P., Junusbekova S. Management and organization of computer laboratory work in physics education. Espacios. Vol. 38 (Nº 45) Año 2017. Pág. 35. Indexada en Scopus.

[11] Kabylbekov K., Omashova G, Spabekova R, Saidullaeva N, Saidakhmetuv P. Junusbtkova S., Management and organization of computer laboratory work in physics education. Espacios. Vol. 38 (Nº 45) Año 2017. Pág. 35. Indexada en Scopus, Google Schollar.

[12] Kabylbekov K.A., Ashirbaev Kh.A., Arysbaeva A.S., Jumagaliyeva A.M. Model of the form of the organization of computer laboratory work in the study of physical phenomena. Modern high technologies, №4, Moscow, 2015, P. 40-43.

[13] Kabylbekov K.A., Madiyarov N.K., Saidakhmetov P.A. Independent design of research tasks of computer laboratory works on thermodynamics. Proceedings of the IX International Scientific and Methodological Conference. Teaching natural sciences (biology, physics, chemistry) mathematics and computer science. Tomsk-2016, P. 93-99.

[14] Kabylbekov K.A, Omashova G. Sh, Spabekova R.S, Saidakhmetov P.A, Serikbaeva G.S, Aktureeva G. Organization of computer laboratory works on study the turn-on and turn-off current of the power supply by using MATLAB software package.

News of the National Academy of Sciences of the Republic of Kazakhstan, Series of Physics and Mathematics, Almaty, Volume 3, Number 313 2017, P. 139-146**.**

[15] Kabylbekov K.A, Omashova G. Sh, Spabekova R.S, Saidakhmetov P.A, Serikbaeva G.S , Aktureeva G. Organization of computer labs for the study of velocity and height distribution of molecules from the Earth's surface by using MATLAB software package. Bulletin of NAS RK, Almaty, Volume 3, Number 367, 2017, P. 111-119.

[16] Kabylbekov K.A, Ashirbayev H.A, Abdrakhmanova Kh.K, Dzhumagalieva A.I., Kydyrbekova J.B. Organization of laboratory work on study of electric and magnetic fields by using MATLAB software package. Proceedings of the National Academy of Sciences of the Republic of Kazakhstan, Series of Physics and Mathematics, Almaty, Volume 3, Number 313, 2017, P. 206-213.

[17] Kabylbekov K. A., Spabekova R. S., Omashova G.Sh., Abzhapparov A.A., Polatbek A, Serkebayeva S. G. The use of the software package MATLAB for solving problems on bifurcated electrical circuits. Bulletin of NAS RK, Almaty 2017, Volume 4, Number 368, P. 101-108.

[18] Kabylbekov K. A., Ashirbaev H. A., Abdrakhmanova Kh.K., Dzhumagalieva A. I., Kadyrbekova J. B. Organization of the performance of the laboratory work "Modeling the electric field of a system consisting of a dielectric square and a long charged conductor" by using MATLAB software package. News of the National Academy of Sciences of the Republic of Kazakhstan, Series of Physics and Mathematics, Almaty 2017, Volume 4, Number 314, P. 252-259.

[19] Kabylbekov K. A., Abdrakhmanova Kh.K., Ermakhanov M.N., Urmashev B.A., Jaткanbayev E.T. Calculation and visualization of a body motion in a gravitational field. NEWS of the National Academy of Sciences of the Republic of Kazakhstan. Series of geology and technical sciences. Volume 3, Number 430 (2018), P. 87-98.

[20] Kabylbekov K. A., Abdrakhmanova Kh.K., Omashova G.Sh., Lakhanova K.M., Abekova Zh.A. Organization of computer laboratory work “Calculation and visualization of small forced oscillations” NEWS of the National Academy of Sciences of the Republic of Kazakhstan, Series of geology and technical sciences. Volume 3, Number 430 (2018), P. 145-155.

[21] Kabylbekov K. A., Abdrakhmanova Kh.K., Omashova G.Sh., Kedelbaev B., Abekova Zh.A. Calculation and visualization of electric field of a space –charged sphere. N E W S of the National Academy of Sciences of the Republic of Kazakhstan. Series of geology and technical sciences. Volume 5, Number 431 (2018), P. 201–209. doi.org/10.32014/2018.2518-170X.26

[22] K. A. Kabylbekov, Kh. K. Abdrakhmanova, P. A. Saidakhmetov, T. S. Sultanbek, B. Sh. Kedelbaev. Calcuiation and visualization of isotopes separation process using MATLAB program. NEWS of the National Academy of Sciences of the Republic of Kazakhstan. Series of geology and technical sciences. Volume 5, Number 431 (2018), P. 218–225. doi.org/10.32014/2018.2518-170X.28

[23] Kabylbekov K. A., Abdrakhmanova Kh.K., Saidakhmetov P.A., Musaev J.M., Issayev Ye.B., Ashirbaev Kh.A. Calculation and visualization of a body motion under the gravity force and the opposing drag. NEWS of the National Academy of Sciences of the Republic of Kazakhstan Series of geology and technical sciences. Volume 6, Number 432 (2018), P. 85– 95. doi.org/10.32014/2018.2518-170X.38

[24] Kabylbekov K. A., Abdrakhmanova Kh.K., Saidakhmetov P.A., Kedelbaev B.Sh., Abdraimov R. T., Ualikhanova Б.S. Calculation and visualization of the field coaxial cable carrying steady current. NEWS of the National Academy of Sciences of the Republic of Kazakhstan Series of geology and technical sciences. Volume 6, Number 432 (2018), P. 55 – 65. doi.org/10.32014/2018.2518-170X.35

[25] Kabylbekov K. A., A.D.Dasibekov, Abdrakhmanova Kh.K., Saidakhmetov P.A., Issayev E.B., Urmashev B.A. Calculation and visualization of oscillating systems. N E W S of the National Academy of Sciences of the Republic of Kazakhstan Series of geology and technical sciences. Volume 6, Number 432 (2018), P. 110 – 120. doi.org/10.32014/2018.2518-170X.41

[26]Kenzhekhan Kabylbekov, Khadisha Abdrakhmanova, Gaukhar Omashova, Pulat Saidakhmetov, Turlan Sultanbek, Nurzhamal Dausheyeva. A Laboratory on visualization of Electrostatic and Magnetic Fields. Acta Polytechnica Hungarica Vol. 15, No. 7, 2018, P.49-70. DOI: 10.12700/APH.15.7.2018.7.3

[27] Kabylbekov K. A., Dasibekov A.D., Abdrakhmanova Kh.K., Saidakhmetov P.A. Calculation and visualization of quantum-mechanical tunnel effect. News of the National Academy of Sciences of the Republic of Kazakhstan, Series of Physics and Mathematics, Volume 2, Number 324 (2019), P. 60-68 . doi.org/10.32014/2019.2518-1726.13

[28] Kabylbekov K. A., Dasibekov A.D., Abdrakhmanova Kh.K., Saidakhmetov P.A. Calculation and visualization of small oscillations of a double plane pendulum. News of the National Academy of Sciences of the Republic of Kazakhstan, Series of Physics and Mathematics, Volume 2, Number 324 (2019), P. 69-79 . doi.org/10.32014/2018.2518-1726.14

N E W S
OF THE NATIONAL ACADEMY OF SCIENCES OF THE REPUBLIC OF KAZAKHSTAN
PHYSICO-MATHEMATICAL SERIES
ISSN 1991-346X **https://doi.org/10.32014/2019.2518-1726.65**
Volume 5, Number 327 (2019), 111 – 119

UDC 531, 53(075). 622.732.62-9. 53.072
IRSTI 29.03.77

K.A.Kabylbekov[1], Kh.K.Abdrakhmanova[2], P.A.Saidakhmetov[1], Ye.B. Issayev[1], B.Sh.Kedelbayev[1]

[1]M.Auezov South-Kazakhstan State University, Shymkent, Kazakhstan;
[2]South-Kazakhstan State Pedagogical University, Shymkent, Kazakhstan
kenkab@mail.ru, khadi_kab@mail.ru, timpf_ukgu@mail.ru, erzhanisaev@mail.ru, b.sh.kedelbaev@mail.ru

RESEARCH OF A CAR COLLISION WITH AN OBSTACLE

Abstract. The article considers the calculation and visualization of collision of a car with an obstacle by using the Matlab software. It contains the formulation of the problem, car and obstacle models, modeling parameters (the mass of the car, the speed of the car, parameters of the suspension: width, height, profile) and mathematical model of the collision profile. There are the calculation and visualization of the profile of the road roughness. The *m*-file titled "polizei.m" is created for calculation and visualization of the car's motion. Calculation results are presented in graphs of displacement around a vertical axis and speed along the vertical axis at a various mass of the car, coefficients of elasticity and damping of the suspension. There is also the discussion of the results of the calculation and visualization. The program allows making experiments with a change of width and height of roughness of the road, of the mass of the car, of suspension parameters.

Keywords. Car, mass, suspension, profile of the obstacle, width and height, displacement around and along the vertical axis.

Introduction

Nowadays all educational institutions of Kazakhstan are provided with computer hardware and software, interactive boards and internet. Almost all teachers have completed language and computer courses for professional development. Hence the educational institutions have all conditions for using computer training programs and models for performing computer laboratory works. In recent years the new computer system Matlab for performing mathematical and engineering calculations is widely used in university and engineering researches throughout the world [1-7]. Unfortunately, the numerical calculations which are carried out by students often are done by means of the calculator that is almost manually. Modern computers are frequently used only for presentation of the work. Actually, students should be able not only to solve these or other engineering problems, but also do them by using modern methods, that is, using personal computers.

Students of the physics specialties 5B060400 and 5B011000 successfully master the discipline "Computer modeling of physical phenomena" which is the logical continuation of the disciplines "Information technologies in teaching physics" and "Use of electronic textbooks in teaching physics". The aim of this discipline is to study and learn the MATLAB program language, acquaintance with its huge opportunities for modeling and visualization of physical processes.

In our early works [8-28] we have shown the potentials of the Matlab software for modeling and visualization of physical processes in mechanics, molecular physics, electromagnetism and quantum physics where it have been used for solving the ordinary differential equations (ODE), for visualization of the equipotential lines of the systems of charged conductors and of the motion of charged particles in electric, magnetic and gravitational fields.

The present article is devoted to calculation and visualization of the car's collision with the obstacle by using the MATLAB software.

Formulation of the problem. The car (fig.1) moves on the flat road and collides with an artificial obstacle, the so called “sleeping policeman” or “speed bump”. Let us consider the kinematics and dynamics of the car’s motion.

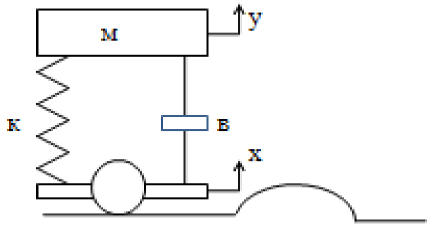

Figure 1 - The car collides with an artificial obstacle

The car model. Let's consider the collision only of one wheel of the car with The horizontal component of the car’s velocity doesn’t change. The action of the obstacle causes only the production of the vertical motion of the car. The wheel when driving completely repeats the obstacle’s profile. The suspension consists of an elastic spring (K) and a damper (B).

Parameters of the modeling. The mass of the car, the velocity of the car. The parameters of the suspension: the coefficient of elasticity and the damping coefficient. The parameters of the obstacle: its width, height and profile, elastic properties and the damping parameters.

Mathematical model. When the wheel collides with the obstacle the wheel moves along the vertical direction. This displacement is described by a variable *x*. The action of the road is transferred to the car body by the aid of suspension (the spring with rigidity *k* and the damper with damping coefficient *B*). Power action by means of spring is defined by the relative motion of the car body described by the displacements *x* and *y*. Power action of the damper is defined by the relative velocities of these displacements *dx/dt* and *dy/dt*. In the equation of motion we will neglect the continuous action on the car body which is compensated by equal in magnitude and oppositely directed elastic force of the spring $Mg = k\Delta x$. By taking into account the above made suggestions and using the Newton’s second law we get the following equation describing the motion of the car:

$$M\frac{d^2y}{dt^2} = B\left(\frac{dx}{dt} - \frac{dy}{dt}\right) + k\left(x - y\right) \qquad (1)$$

$$\frac{d^2y}{dt^2} + \frac{B}{M}\frac{dy}{dt} = \frac{B}{M}\frac{dx}{dt} + \frac{k}{M} \qquad (2)$$

The vertical component of the car acceleration $\frac{d^2y}{dt^2}$ is the function of the car horizontal velocity. At the same time the profile of the road makes a significant contribution to this acceleration. Let us take the following function as the mathematical model of the road roughness:

$$x\left(s\right) = \frac{H}{2}\left(1 - \cos\left(\frac{2\pi s}{L}\right)\right) \quad 0 \le s \le L$$

Visualization of the profile of the road roughness at H = 10 cm and L = 100 cm.

```
>> clc
>> H=10;
>> L=100; s=0:1:L;
>> plot(s,H)
>> x=(H/2)*(1-cos(2*pi*s/L));
>> plot(s,x)
```

>> grid on
>> xlabel('s, sm')
>> ylabel('H,sm')
>> title('x(s)')

The diagram of this function for H = 10 cm and L = 100cm is presented in the fig.2

It should be noted that the radius of the wheel mustn't be greater than the radius of the curvature fitting to each point of the trajectory.

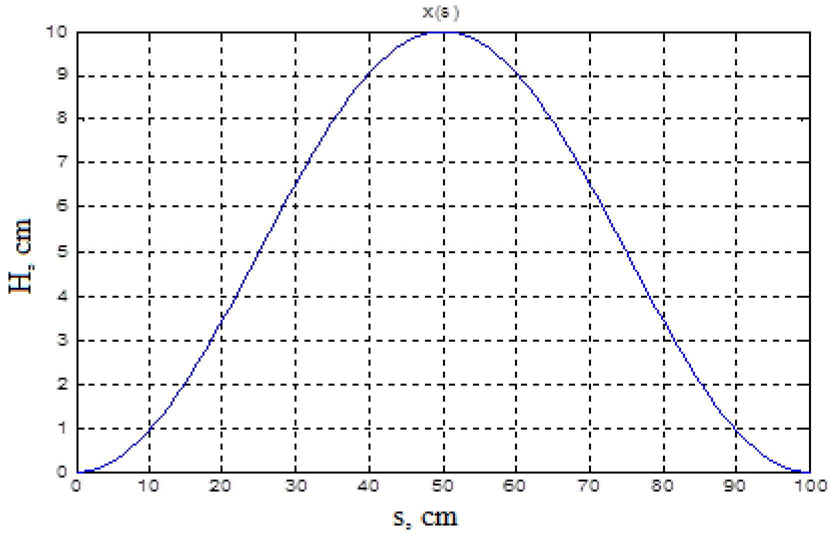

Figure 2 - The model of the road roughness

At the constant horizontal component of the car velocity $S = \upsilon_0 \cdot t$ the function determining the road roughness and its derivative are given by the expressions:

$$x(s) = \frac{H}{2}\left(1 - \cos\left(\frac{2\pi\upsilon_0 t}{L}\right)\right)$$

$$\frac{dx}{dt} = \frac{H}{L}\pi\upsilon_0 \sin\left(\frac{2\pi\upsilon_0 t}{L}\right)$$

By using the change of variables

$$y = z_1; \quad \frac{dy}{dt} = \frac{dz_1}{dt} = z_2; \quad \frac{d^2 y}{dt^2} = \frac{dz_2}{dt} = -\frac{B}{M}\frac{dy}{dt} - \frac{k}{M}y + \frac{B}{M}\frac{dx}{dt} + \frac{k}{M}x$$

we reduce the equation of motion to the expression easy for integration with the help of procedure ode45.

For calculation and visualization of the car motion we create the m-file titled "polizei.m":

```
function dzdt=polizei(t,z)
global M K B V0 H L
g=9.81; % free fall acceleration
dzdt=zeros (2,1); % vector column
s=V0*t;
x=H/2*(1-cos(2*pi*s/L));
xdot=H/L*pi*V0*sin(2*pi*V0*t/L);
% the roughness of the road is in the range of 0 ≤ S ≤ L
if s> L
x=0;
```

```
xdot=0;
end
dzdt(1)=z(2);
dzdt(2)=-B/M*z(2)-K/M*z(1)+B/M*xdot+K/M*x;
```

In the command line we write

```
clc
global M K B V0 H L
M=450;
K=35000;
B=7300;
z10=0;
z20=0;
accel=zeros(1000);
i=1;
V0=20;
H=0.05;
L=0.8;
% L/V0 –the time of motion on the roughness
tmax=2*L/V0;
z0=[z10; z20];
dt=[0 tmax];
dt=0:tmax/500:tmax;
ii=0;
aa=zeros(1000,1);
>> opt=odeset('RelTol', 1e-8);
[t,z]=ode45(@polizei, dt,z0, opt);
subplot(2,2,1); plot(t,z(:,1))
title('displacement')
grid on
subplot(2,2,2); plot(t,z(:2))
grid on
subplot(2,2,3); plot(t,aa(1:size(t)))
grid on
```

The result is presented in the fig.3

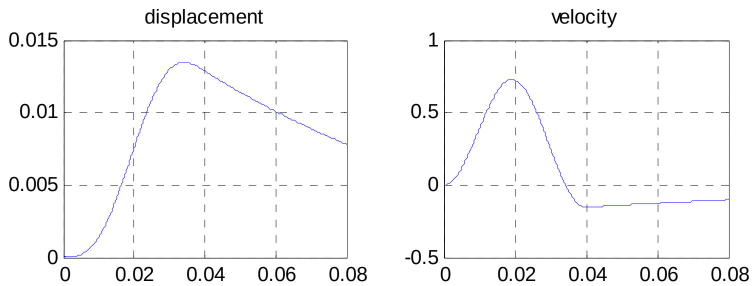

Figure 3 - Displacement round the vertical axis (left graph) and velocity along the vertical axis at the mass of the car of M = 450 kg

Now we change the mass of the car and in the command line we write:

```
clc
global M K B V0 H L
M=958;
K=35000;
B=7300;
```

```
z10=0;
z20=0;
accel=zeros(1000);
i=1;
V0=20;
H=0.05;
L=0.8;
% L/V0 - the time of motion on the roughness
tmax=2*L/V0;
z0=[z10; z20];
dt=[0 tmax];
dt=0:tmax/500:tmax;
ii=0;
aa=zeros(1000,1);
>> opt=odeset('RelTol', 1e-8);
[t,z]=ode45(@polizei, dt,z0, opt);
subplot(2,2,1); plot(t,z(:,1))
title('displacement')
grid on
subplot(2,2,2); plot(t,z(:,2))
title('velocity')
grid on
```

The result is presented in the fig.4

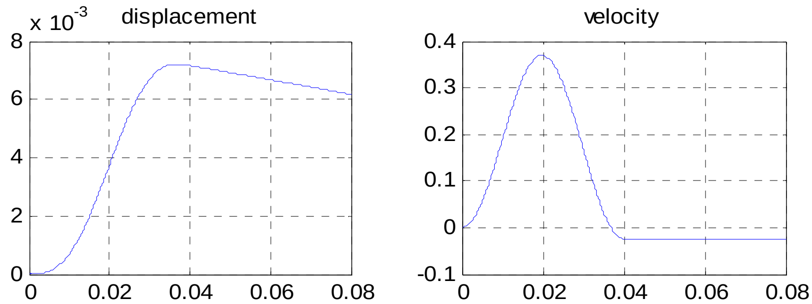

Figure 4 - Displacement round the vertical axis (left graph) and velocity along the vertical axis at the mass of the car of M = 958 kg

At the decrease of the spring rigidity till K = 20 000 the graph of the displacement round the vertical axis (left graph) and velocity along the vertical axis at the mass of the car of M = 658 kg doesn’t change (compare the fig.4 and 5). Here we give only the results in fig.5.

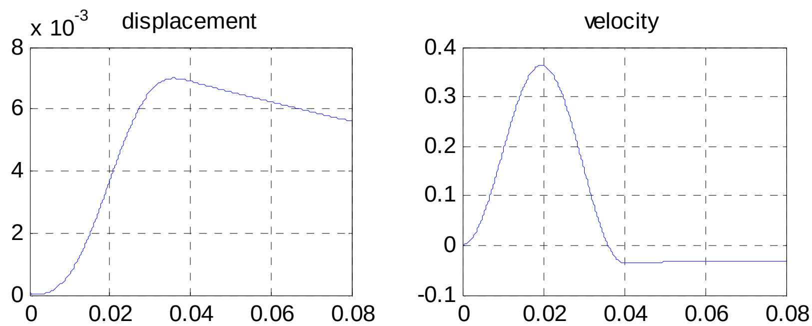

Figure 5 - Displacement round the vertical axis (left graph) and velocity along the vertical axis at the mass of the car of M = 658 kg

Then we increase the damping coefficient up to K = 20 000 (the mass of the car is 958 kg)

```
clc
global M K B V0 H L
M=958;
K=20000;
B=21900;
z10=0;
z20=0;
accel=zeros(1000);
i=1;
V0=20;
H=0.05;
L=0.8;
%  L/V0 - the time of motion on the roughness
tmax=2*L/V0;
z0=[z10; z20];
dt=[0 tmax];
dt=0:tmax/500:tmax;
ii=0;
aa=zeros(1000,1);
opt=odeset('RelTol', 1e-8);
[t,z]=ode45(@polizei, dt,z0, opt);
subplot(2,2,1); plot(t,z(:,1))
title('displacement')
grid on
subplot(2,2,2); plot(t,z(:,2))
title('velocity')
grid on
```

The result is presented in the fig.6.

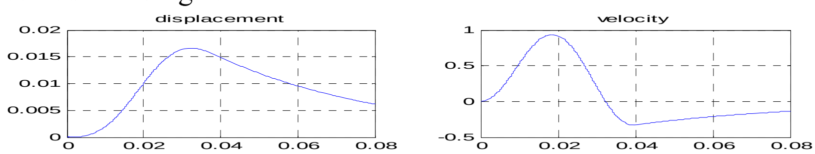

Figure 6 - Displacement round the vertical axis (left graph) and velocity along the vertical axis at the mass of the car of M = 958 kg

The figure 6 shows that the change of the damping coefficient significantly affects the displacement round the vertical axis and the velocity along this axis (compare figures 4 and 6).

Assignments for individual work:

9. Decrease the damping coefficient by 3 times till zero. How did the process change during the motion along the obstacle? After overcoming the obstacle?

10. Change the parameters of the obstacle. Consider the options of the narrow and low obstacle (the height and width are 10 cm and 40 cm, 10 cm and 100 cm, 4 cm and 100 cm)

Conclusion. The article considers the calculation and visualization of the car collision with an obstacle by using the Matlab software. It contains the formulation of the problem, car and obstacle models, modeling parameters (the mass of the car, the speed of the car, parameters of the suspension: the width, height, profile) and the mathematical model of the collision profile. There are the calculation and

visualization of the profile of the road roughness. The *m*-file titled "polizei.m" is created for calculation and visualization of the car's motion. Calculation results are presented in graphs of displacement around a vertical axis and velocity along the vertical axis at a various mass of the car, coefficients of elasticity and damping of the suspension. There is also the discussion of the results of the calculation and visualization. The program allows making experiments with a change of width and height of roughness of the road, of the mass of the car, of suspension parameters.

К.А.Қабылбеков[1], Х.К.Абдрахманова[2],
П.А.Саидахметов[1], Е.Б. Исаев[1], Б.Ш. Кеделбаев[1]

[1]М.Әуезов атындағы Оңтүстік Қазақстан мемлекеттік университеті, Шымкент, Қазақстан;
[2]Оңтүстік Қазақстан мемлекеттік педагогикалық университеті, Шымкент, Қазақстан

АВТОМОБИЛЬДІҢ КЕДЕРГІДЕН ӨТУІН ЗЕРТТЕУ

Аннотация. Matlab жүйесінде автомобилдің кедергіден өтуін есептеу мен бейнелеу ұсынылады. Проблеманы тұжырымдау, автомобил мен кедергінің көрініс моделі, моделдеудің параметрлері (автомобилдің массасы мен жылдамдығы, аспаның серпімділік және демпферлік коэффициенттері, кедергі параметрлері: ені мен биіктігі) және кедергіден өту процесінің математикалық моделі келтірілген. Жолдың тегіс еместігінің параметрлері есептеліп, бейнеленген. Автомобилдің кедергіден өту қозғалысын есептеу мен бейнелеу үшін polizei.m атты m-файл құрастырылған. Есептеу нәтижелері автомобилдің массалары, аспаның серпімділік жіне демпферлік коэффициенттері әртүрлі жағдайларындағы вертикал өс бойындағы және осы өсті айнала қозғалысының жылдамдықтарының графиктері берілген. Есептеу мен бейнелеу нәтижелері талқыланған. Бағдарлама автомобиль массасын, кедергі параметрлерін, жолдың тегіс еместікгінің биіктігін өзгертіп эксперименттер жасауға мүмкіншілік береді.

Түйін сөздер. Автомобил, масса, аспа (подвеска), кедергі параметрі- ені және биіктігі, вертикаль өс бойында және оны айнала қозғалуы.

К.А.Кабылбеков[1], Х.К.Абдрахманова[2],
П.А.Саидахметов[1], Е.Б. Исаев[1], Б.Ш.Кеделбаев[1]

[1]Южно-Казахстанский государственный университет им. М.Ауэзова, Шымкент, Казахстан;
[2]Южно–-Казахстанский государственный педагогический университет, Шымкент, Казахстан

ИССЛЕДОВАНИЕ НАЕЗДА АВТОМОБИЛЯ НА ПРЕПЯТСТВИЕ

Аннотация. Предлагается программа расчета и визуализации наезда автомобиля на препятствие в системе Matlab. Приведены формулировка проблемы, модели автомобиля и препятствия, параметры моделирования (масса автомобиля; скорость автомобиля, параметры подвески: коэффициент упругости и коэффициент демфпирования, параметры препятствия: ширина, высота, профиль) и математическая модель процесса наезда. Проведен расчет и визуализация профиля неровности дороги Для расчета и визуализации движения автомобиля создан m-файл под названием polizei.m. Результаты расчетов представлены в графиках перемещения вокруг вертикальной оси и скорости вдоль вертикальной оси при различных массах автомобиля и коэффициентов упругости и демпфирования подвески. Обсуждены результаты расчетов и визуализации.

Программа позволяет проводить эксперименты с изменением ширины и высоты неровности дороги, массу автомобиля, параметров подвески.

Ключевые слова. Автомобиль, масса, подвеска, профиль препятствия- ширина и высота, перемещение вокруг и вдоль вертикальной оси.

Information about authors

Kabylbekov K.A. – cand.ph-math.sc., associate professor of the chair of Physics, M.Auezov South-Kazakhstan State University, kenkab@mail.ru, https://orcid.org/0000-0001-8347-4153,;

Abdrakhmanova Kh.K.- cand.chem.sc., associate professor of the chair of Physics, South-Kazakhstan State Pedagogical University, khadi_kab@mail.ru, https://orcid.org//0000-0002-6110-970X;

Saidakhmetov P.A.- cand.ph-math.sc., associate professor of the chair of Physics, M.Auezov South-Kazakhstan State University, timpf_ukgu@mail.ru, https://orcid.org/0000-0002-9146-047X;
Kedelbaev B.Sh.- doc. eng. sciences, professor of the chair of “Microbiology”, M. Auezov South-Kazakhstan State University, b.sh.kedelbaev@mail.ru, .- https://orcid.org/0000-0001-7158-1488;
Issaev E.B.- cand.techn.sciences, associate professor of the department “Biology” of M. Auezov SKSU, erzhanisaev@mail.ru, https://orcid.org/0000-0001-7536-5643

REFERENCES

[1] Porsev S. V. Computer simulation of physical processes in the package MATLAB. M.: Hot Line-Telecom, 2003.592 p.

[2] Kotkin G.A., Cherkassky V.S. Computer modeling of physical processes using MATLAB: Tutorial. / Novosibirsk University.

[3] Lurie M. S., Lurie O. M. Application of the MATLAB program in the study of course of electrical engineering. For students of all specialties and forms of educatio. Krasnoyarsk: SibSTU, 2006208 p.

[4] Potemkin V. system of engineering and scientific calculations MATLAB 5.x (in 2 volumes). Moscow: Dialog-MIFI, 1999.

[5] Averyanov G. P., Budkin, Dmitrieva V. V. Design automation. Computer workshop. Part 1. Solving problems of Electrophysics in MATLAB: tutorial. Moscow: MEPhI, 2009. 111 p.

[6] Dyakonov V. p. MATLAB. Complete tutorial. M: DMK Press, 2012. 768 p.

[7] Ryndin E. A., Lysenko I. E. Solving problems of mathematical physics in Matlab. Taganrog: TRTU. 2005. 62 p.

[8] Kabylbekov K.A., Abdrakhmanova Kh.K., Abekova J., Abdraimov R.T., Ualikhanova B.S. Calculation and visualization of a system-an electron in a deep square potential well, with use of the software package of MATLAB. Proceeding of the III International Scientific and Practical Conference «Topical researches of the World Science» (Iune 28, 2017,Dubai, UAE). №7(23). Vol.I, July 2017, P. 7-13.

[9] Kabylbekov K., Saidullaeva N., Spabekova R., Omashova G, Tagaev N., Bitemirova A., Berdieva M. Model of a blank form for computer laboratory work on research of the speed selector. Journal of Theoretical and Applied Information Technology15th July 2017. Vol.95. No 13, P 2999-3009, c 2005 – ongoing JATIT & LLS. Indexada en Scopus.

[10] Kabylbekov K.A., Omashova G.,Spabekova R., Saidullaeva N., Saidakhmetuv P., Junusbekova S. Management and organization of computer laboratory work in physics education. Espacios. Vol. 38 (Nº 45) Año 2017. Pág. 35. Indexada en Scopus.

[11] Kabylbekov K., Omashova G, Spabekova R, Saidullaeva N, Saidakhmetuv P. Junusbtkova S., Management and organization of computer laboratory work in physics education. Espacios. Vol. 38 (Nº 45) Año 2017. Pág. 35. Indexada en Scopus, Google Schollar.

[12] Kabylbekov K.A., Ashirbaev Kh.A., Arysbaeva A.S., Jumagaliyeva A.M. Model of the form of the organization of computer laboratory work in the study of physical phenomena. Modern high technologies, №4, Moscow, 2015, P. 40-43.

[13] Kabylbekov K.A., Madiyarov N.K., Saidakhmetov P.A. Independent design of research tasks of computer laboratory works on thermodynamics. Proceedings of the IX International Scientific and Methodological Conference. Teaching natural sciences (biology, physics, chemistry) mathematics and computer science. Tomsk-2016, P. 93-99.

[14] Kabylbekov K.A, Omashova G. Sh, Spabekova R.S, Saidakhmetov P.A, Serikbaeva G.S, Aktureeva G. Organization of computer laboratory works on study the turn-on and turn-off current of the power supply by using MATLAB software package. News of the National Academy of Sciences of the Republic of Kazakhstan, Series of Physics and Mathematics, Almaty, Volume 3, Number 313 2017, P. 139-146**.**

[15] Kabylbekov K.A, Omashova G. Sh, Spabekova R.S, Saidakhmetov P.A, Serikbaeva G.S , Aktureeva G. Organization of computer labs for the study of velocity and height distribution of molecules from the Earth's surface by using MATLAB software package. Bulletin of NAS RK, Almaty, Volume 3, Number 367, 2017, P. 111-119.

[16] Kabylbekov K.A, Ashirbayev H.A, Abdrakhmanova Kh.K, Dzhumagalieva A.I., Kydyrbekova J.B. Organization of laboratory work on study of electric and magnetic fields by using MATLAB software package. Proceedings of the National Academy of Sciences of the Republic of Kazakhstan, Series of Physics and Mathematics, Almaty, Volume 3, Number 313, 2017, P. 206-213.

[17] Kabylbekov K. A., Spabekova R. S., Omashova G.Sh., Abzhapparov A.A., Polatbek A, Serkebayeva S. G. The use of the software package MATLAB for solving problems on bifurcated electrical circuits. Bulletin of NAS RK, Almaty 2017, Volume 4, Number 368, P. 101-108.

[18] Kabylbekov K. A., Ashirbaev H. A., Abdrakhmanova Kh.K., Dzhumagalieva A. I., Kadyrbekova J. B. Organization of the performance of the laboratory work "Modeling the electric field of a system consisting of a dielectric square and a long charged conductor" by using MATLAB software package. News of the National Academy of Sciences of the Republic of Kazakhstan, Series of Physics and Mathematics, Almaty 2017, Volume 4, Number 314, P. 252-259.

[19] Kabylbekov K. A., Abdrakhmanova Kh.K., Ermakhanov M.N., Urmashev B.A., Jaтkanbayev E.T. Calculation and visualization of a body motion in a gravitational field. NEWS of the National Academy of Sciences of the Republic of Kazakhstan. Series of geology and technical sciences.Volume 4, Number 430 (2018), P. 87-98.

[20] Kabylbekov K. A., Abdrakhmanova Kh.K., Omashova G.Sh., Lakhanova K.M., Abekova Zh.A. Organization of computer laboratory work "Calculation and visualization of small forced oscillations" N E W S of the National Academy of Sciences of the Republic of Kazakhstan, Series of geology and technical sciences. Volume 3, Number 430 (2018), P. 145-155.

[21] Kabylbekov K. A., Abdrakhmanova Kh.K., Omashova G.Sh., Kedelbaev B., Abekova Zh.A. Calculation and visualization of electric field of a space –charged sphere. N E W S of the National Academy of Sciences of the Republic of Kazakhstan. Series of geology and technical sciences. Volume 5, Number 431 (2018), P. 201–209. doi.org/10.32014/2018.2518-170X.26

[22] Kabylbekov K. A., Abdrakhmanova Kh. K., Saidakhmetov P. A., Sultanbek T. S., Kedelbaev B. Sh. Calcuiation and visualization of isotopes separation process using MATLAB program. N E W S of the National Academy of Sciences of the Republic of Kazakhstan. Series of geology and technical sciences. Volume 5, Number 431 (2018), P. 218–225. doi.org/10.32014/2018.2518-170X.28

[23] Kabylbekov K. A., Abdrakhmanova Kh.K., Saidakhmetov P.A., Musaev J.M., Issayev Ye.B., Ashirbaev Kh.A. Calculation and visualization of a body motion under the gravity force and the and the opposing drag. N E W S of the National Academy of Sciences of the Republic of Kazakhstan Series of geology and technical sciences. Volume 6, Number 432 (2018), P. 85– 95. doi.org/10.32014/2018.2518-170X.38

[24] Kabylbekov K. A., Abdrakhmanova Kh.K., Saidakhmetov P.A., Kedelbaev B.Sh., Abdraimov R. T., Ualikhanova Б.S. Calculation and visualization of the field coaxial cable carrying steady current. N E W S of the National Academy of Sciences of the Republic of Kazakhstan Series of geology and technical sciences. Volume 6, Number 432 (2018), P. 55 – 65. doi.org/10.32014/2018.2518-170X.35

[25] Kabylbekov K. A., A.D.Dasibekov, Abdrakhmanova Kh.K., Saidakhmetov P.A., Issayev E.B., Urmashev B.A. Calculation and visualization of oscillating systems. N E W S of the National Academy of Sciences of the Republic of Kazakhstan Series of geology and technical sciences. Volume 6, Number 432 (2018), P. 110 – 120. doi.org/10.32014/2018.2518-170X.41

[26] Kenzhekhan Kabylbekov, Khadisha Abdrakhmanova, Gaukhar Omashova, Pulat Saidakhmetov, Turlan Sultanbek, Nurzhamal Dausheyeva. A Laboratory on visualization of Electrostatic and Magnetic Fields. Acta Polytechnica Hungarica Vol. 15, No. 7, 2018, P49-70.

DOI: 10.12700/APH.15.7.2018.7.3

[27] Kabylbekov K. A., Dasibekov A.D., Abdrakhmanova Kh.K., Saidakhmetov P.A. Calculation and visualization of quantum-mechanical tunnel effect. News of the National Academy of Sciences of the Republic of Kazakhstan, Series of Physics and Mathematics, Volume 2, Number 324 (2019), P. 60-68 . doi.org/10.32014/2019.2518-1726.13

[28] Kabylbekov K. A., Dasibekov A.D., Abdrakhmanova Kh.K., Saidakhmetov P.A. Calculation and visualization of small oscillations of a double plane pendulum. News of the National Academy of Sciences of the Republic of Kazakhstan, Series of Physics and Mathematics, Volume 2, Number 324 (2019), P. 69-79 . doi.org/10.32014/2018.2518-1726.14

N E W S
OF THE NATIONAL ACADEMY OF SCIENCES OF THE REPUBLIC OF KAZAKHSTAN
PHYSICO-MATHEMATICAL SERIES
ISSN 1991-346X **https://doi.org/10.32014/2019.2518-1726.66**
Volume 5, Number 327 (2019), 120 – 125

UDC 517.929.4
IRSTI 27.29.17, 27.29.23

K.B. Bapaev[1], G.K. Vassilina[1,2]

[1]Institute of Mathematics and Mathematical Modeling, Almaty, Kazakhstan;
[2]Almaty University of Energy and Communications, Almaty, Kazakhstan
bapaev41@bk.ru, v_gulmira@mail.ru

ON LAGRANGE STABILITY AND POISSON STABILITY OF THE DIFFERENTIAL-DYNAMIC SYSTEMS

Abstract. The real difference-dynamic system is considered. The case of unlimited continuity of solutions is investigated for this difference-dynamic system. Unlimited continuity to the right of solutions of the difference-dynamic system is a necessary condition for Lyapunov stability of solutions of this system. Using functions similar to Lyapunov functions, sufficient conditions for the unlimited continuity of solutions of the difference-dynamical system are obtained. The concepts of Lagrange stability and Poisson stability are introduced. Relations between Lyapunov functions and Lagrange stability are investigated. Using the discrete analogue of the second Lyapunov method, the necessary and sufficient conditions for Lagrange stability of the solution of the difference-dynamical system are obtained. A dynamic-difference system is considered for which a discrete operator is constructed, with the help of which the Poisson stability of the system solutions is investigated.

Key Words: difference-dynamic system, continuity, Lyapunov functions, Lagrange stability, Poisson stability.

Introduction

Concepts of Lagrange stability and Poisson stability play an important role for studying the qualitative behavior of the trajectories and of the motion of dynamical system given in an arbitrary metric space.

By the Lyapunov functions method necessary and sufficient conditions for the Lagrange stability of systems of ordinary differential equations are obtained in the Ioshizawa work [1]. Poisson stability was investigated from the position of the topological theory of dynamical systems in [2,3]. In these papers a differential operator is constructed in the class of ordinary differential equations. Using this differential operator Poisson stability of solutions of the ordinary differential equations is studied. In [4] the problem of stability of a program manifold with respect to the given vector-function of non-autonomous basic control systems with stationary nonlinearity is investigated.

In this paper the concepts of stability according to Lagrange and Poisson are considered in the class of difference-dynamic systems.

Lagrange stability of the difference dynamic systems

Unlimited continuity of the solutions of the difference-dynamic systems.

Consider the real difference-dynamic systems

$$x_{n+1} = X(n, x_n),\ n \geq 0. \tag{1}$$

There are two possibilities for arbitrary solution $x_n = x(n, n_0, x_0), n_0 \in N^+$:

1) x_n makes sense on the infinite set $N_{n_0} = \{n_0, n_0+1, \dots, n, \dots\}$. Then it will continue to the right.;

2) x_n is defined only on some finite interval $\{n_0, n_0+1, \dots, m-1\}$, here $m < \infty$.

Lemma 1. If the solution x_n has a finite time to determine $\{n_0, n_0+1, \dots, m-1\}, m < \infty$, then

$$\|x_n\| \to \infty \text{ при } n \to m-0.$$

Proof is obvious, see [5].

Consequence 1. If the solution $x_n = x(n, n_0, x_0)$ is limited on its maximum existence interval $x_n = x(n, n_0, x_0)$, then it remains infinitely continued to the right, i.e. $m = \infty$.

Unlimited continuity to the right of solutions (1) of the difference-dynamic systems is necessary condition for stability according to Lyapunov of solutions of the difference-dynamic systems. Using functions similar to Lyapunov functions, one can obtain sufficient conditions for unbounded continuability of the solutions of the difference-dynamic systems (1) for $n \to +\infty$.

Let us consider the difference-dynamic systems (1). Let x_n be solution with initial condition $x_{n_0} = x^0$. It's clear that

1) This solution can be continued for all $n_0 \le n$. Then the solution x_n can be extended indefinitely.

2) There is $m > n_0$ such that $\|x_n\| \to \infty$ for $n \to m$. Then the solution x_n has a finite definition time.

3) The solution x_n is bounded.

The boundedness of all solutions is stability in a manner. In this case there is Lagrange stability [1,6,7].

In this paper relationships between Lyapunov functions and Lagrange stability (boundedness of solutions) are studied.

Using the discrete analogue of the second Lyapunov method necessary and sufficient conditions for Lagrange stability of the solution of the difference-dynamic system are obtained [1].

Definition 1. Difference-dynamic system (1) is called Lagrange stable if

1) ∃ solutions $x\left(n, n_{0,} x_{n_0}\right)$ for $n \in Z^+$, here $n_0 \in Z^+$;

2) $\|x_n\|$ is bounded on Z^+.

For example, if the difference-dynamic system (1) has a bounded solution that is asymptotically stable in general. Then difference-dynamic system (1) is Lagrange stable.

Using Lyapunov functions, it is easy to formulate necessary and sufficient conditions for the Lagrange stability of the difference-dynamic systems (1).

Theorem 1. Difference-dynamic systems (1) is Lagrange stable if and only if there exists the function $V(n, x_n)$ on $Z^+ \times R^k$ such that

1) $V(n, x_n) \ge W(x_n)$, here $\lim\limits_{x_n \to \infty} W\left(x_{n_1}\right) = \infty$;

2) the function $V(n, x_n)$ is not increasing for all solution x_n.

Proof. Sufficiency. Let there is a function $V(n, x_n)$ with properties 1) and 2) for the difference-dynamic system (1). For all solution $x\left(n; n_0, x_{n_0}\right)$ $\left(n_0 \in Z^+; \left\|x_{n_0}\right\| < \infty\right)$.

By virtue of condition 2), we have $V(n, x_n) \le V\left(n_0, x_{n_0}\right)$ for $n \ge n_0$.

Using 1) we get

$$W\left(x\left(n; n_0, x_{n_0}\right)\right) \le V\left(n; x\left(n; n_0, x_{n_0}\right)\right) \le V\left(n_0, x_{n_0}\right) \quad \text{for } n \ge n_0 . \tag{2}$$

From the inequality (2) it follows that the solution $x\left(n; n_{0,} x_{n_0}\right)$ is bounded.

Indeed, if this is not the case, then there would be a sequence of moments $n_l \to \infty$ $\left(l = 1,2....; n_1 > n_0\right)$ such that $\lim\limits_{l\to\infty}\left\|x_{n_l}\right\| = \infty$. Hence $\lim\limits_{l\to\infty} Wx_{n_l} = \infty$.

This would contradict inequality (2), which is impossible.

Necessity. Let arbitrary solution $x_n = x\left(n; n_0; x_{n_0}\right)$ exists and bounded on Z^+ for the difference-dynamic systems (1).

Set

$$V\left(n, x_n\right) = \sup_{v>0}\left\|x_{n+v}\right\| = \sup_{v>0}\left\|x\left(n+v; n, x_n\right)\right\|^2, \tag{3}$$

here $\left\|x_n\right\| < \infty, n > n_0 \in Z^+$. From the formula (3) we have $V_n \geq \left\|x\left(n+v; n, x_n\right)\right\|^2 = \left\|x_n\right\|^2 = W\left(x_n\right)$.

And, obviously $\lim\limits_{\|x_n\|\to\infty} W\left(x_n\right) = \infty$. That is, condition 1) is fulfilled.

Further, considering that due to the uniqueness of the solution, $x_n = x\left(n; n_2; x_{n_2}\right)$ is a continuation of the solution $x_n = x\left(n; n_1; x_{n_1}\right)$ for $n_0 < n_1 < n_2$, we have

$$V\left(n, x_{n_1}\right) = \sup_{v>0}\left\|x\left(n_1 + v; n_1, x_n\right)\right\|^2 \geq \sup_{v>0}\left\|x\left(n_2 + v; n_2; x\left(n_2; n_0; x_{n_0}\right)\right)\right\|^2 =$$
$$= V\left(n_2; x\left(n_2; n_0; x_{n_0}\right)\right).$$

Thus, condition 2) is also satisfied.

Poisson stability of the difference dynamic systems

The concept of Poisson stability introduced by A. Poincaré [7] originated in celestial mechanics. This concept represents the broadest concept of periodicity and is characterized by a property called recurrence. Poisson stability is considered as a general concept of the oscillatory regime [6,7].

The problem of Poisson stability was studied from the position of the topological theory of dynamical systems, the main purpose of which, as noted by J. Birkhoff [9], is the classification of movements and the establishment of a connection between them. Such classes include periodicity, almost periodicity in the sense of G. Baire [10], recurrence in the sense of J. Birkhoff [8], almost recurrence in the sense of M.V. Bebutov [11]. The common property of all these classes is the recurrence property, and each individual Poisson stability class is determined by a certain peculiarity of the recurrence character specific for this class. The problem of strong stability and a change in the stability of difference-dynamic system was studied in [12]. Here we consider the difference-dynamic system for which the discrete operator is constructed [2,3], with the help of which the Poisson stability of the solutions of the difference-dynamic system is investigated.

Let us consider the difference-dynamic system

$$x_{n+1} = F(n, x_n). \tag{4}$$

Here $x_n \in R^m$, $n \in Z$, f is vector function, defined and continuous with its partial derivatives $\frac{\partial f}{\partial x_n}$, $k, j = 1, \dots, m$ on $Z \times D$.

The fulfillment of the indicated conditions means that the conditions of the following existence and uniqueness theorem are satisfied for system (4).

Theorem 2. Let

$$(n_0,\ \xi_0) \tag{5}$$

be some point of the set $Z \times D$. Then for all point (5) there is a solution ξ (n) of the difference-dynamic system (4) with the initial condition

$$\xi(n_0) = \xi_0, \tag{6}$$

defined on some interval containing the point n_0. Moreover, if there are two solutions with the same initial condition (6), each of which is defined on its set containing the point n_0, then these solutions coincide in the common area of their definition.

Let

$$x_n = \varphi(n), \tag{7}$$

be solution of the difference-dynamic system (4), defined on $(k, k+1, \dots, k+\tau)$. Let

$$x_n = \psi(n) \tag{8}$$

solution of the same system, but defined on some other interval $(l, l+1, \dots, l+\theta)$. We will say that solution (8) is a continuation of the solution (7), if interval $(l, l+1, \dots, l+\theta)$ contains interval $(k, k+1, \dots, k+\tau)$. Solution (8) coincides with solution (7) on the interval $(k, k+1, \dots, k+\tau)$. In particular, it is considered that solution (8) is a continuation of solution (7) if the interval $(l, l+1, \dots, l+\theta)$ contains interval $(k, k+1, \dots, k+\tau)$. And solution (8) coincides with the solution (7) on $(k, k+1, \dots, k+\tau)$. Solution (8) is a continuation of solution (7) even in the case when the intervals $(l, l+1, \dots, l+\theta)$ and $(k, k+1, \dots, k+\tau)$ coincide, as solutions (7) and (8) completely coincide.

Solution (7) is called noncontinuable if there is no solution different from it, which is its continuation. It is easy to show that each solution can be continued to a non-continuable solution. And there is the only way to do it. Therefore, in the future, only non-continuing solutions will be considered. To emphasize that some solution $\xi(n)$ of the difference-dynamic system (4) is solution with initial condition (6), further we will write this solution in the form

$$\xi(n, n_0, n_0, \xi_0). \tag{9}$$

Then it is easy to see that

1) For each point (5) of the set $Z \times D$, there is a noncontinuable solution of the difference-dynamic system (4) with the initial condition (6).

2) If some noncontinuable solution of the difference-dynamic system (4) coincides with some other noncontinuable solution of this system with at least one value of n, then it is a continuation of this solution.

3) If the two continued solutions of the difference-dynamic system (4) coincide with each other for at least one value of n, then they completely coincide. I.e. they have the same definition interval and they are equal on it.

Let (9) be some non-continuable solution of the difference-dynamic system (4) with the initial condition (7) defined on the interval

$$(k_1(n_0, \xi_0); k_2(n_0, \xi_0)), \tag{10}$$

depending on the initial values (5). Set S is the set of all points (n, n_0, ξ_0) of the space $Z \times Z \times D$ for which solution (9) is defined and satisfies the obvious conditions: point (5) belongs to the set $Z \times D$ and number n to interval (10). Then the following theorem holds, which is well known as the theorem on the continuous dependence of solutions on initial values.

Theorem 3. Set S of all points (n, n_0, ξ_0)) is the open set in the space $Z \times Z \times D$. On the set S the function $\xi(n, n_0, \xi_0)$ is defined. This function is the continued solution (9) of the difference-dynamic system (4) with the initial values (5). At the same time, the function $\xi(n, n_0, \xi_0)$ is continuous across all arguments on S.

We now note that along with the concept of the difference-dynamic system (4) solution, it is often more convenient to use an object very close to it, which we call motion.

Let (9) be a not continued solution defined for all values of $n \in Z$ and let φ be a function given by

$$\varphi(\ n_0, n, \xi_0) = \xi(n_0 + n, n_0, \xi_0). \tag{11}$$

Suppose that under the action of some law mathematically described by the difference-dynamic system (4), the physical system will go into a new state ξ_1 in time $n \in Z^+$. From a mathematical point of view, seems appropriate to determine ξ_1 through the solution of the difference-dynamic system (4) using the formula $\xi_1 = \xi(n_0 + n, n_0, \xi_0)$. From a physical point of view, the record $\xi = \varphi(n_0, n, \xi_0)$ is more appropriate. In this case, obviously, the concept of solution of the difference-dynamic system (4) and the concept of the function φ, corresponding to it, are equivalent.

Definition 2. Let $\varphi(l, n, p)$ be the mapping of the set $Z \times Z^+ \times D$ on the space D. Set $\varphi(l, n, p) = O(l, n)p$ and we will assume that

1) mapping $\varphi(l, n, p)$ is continuous on set of variables l, n, p on $Z \times Z^+ \times D$;
2) there is $O(l, 0)p = p$ for all $(l, p) = Z \times D$;
3) $O(l + s, n)O(l, s) = O(l, n + s)$ takes place for all $(l, n, s) \in Z \times Z^+ \times Z^+$.

Then we say that $\varphi(l, n, p)$ is a motion of a non-autonomous difference-dynamic system [7] if the pair $(l, p) \in Z \times D$ is fixed.

From the above definition it can be seen that the concept of motion is broader than the concept of the solution of difference-dynamic system (4). Thus, in particular, the mapping $\varphi(l, n, p)$ does not have to be differentiable with respect to n, not to mention l, p. At the same time, if in the domain of definition of the solution $x_n = \xi(n, l, p)$ of the difference-dynamic system (4), defined for $n \epsilon N^+$, we take $\varphi(l, n, p) = \xi(l + n, l, p)$, then it is easy to see that the above definitions of motion and solution are very close. Moreover, the motion turns into a solution if $l = 0$. Finally, we call the operator $O(l, n)$ the shift operator along the motion $\varphi(l, n, p)$. It should also be noted here that the form of the shift operator $O(l, n)$ along motions corresponding to the solutions of the difference-dynamic system (1) is determined by the right-hand side of the difference-dynamic system.

Definition 3. A point $p \in D$ is called Poisson positively stable if for each neighborhood A_p and for each positive number T one can specify such number $n \geq T$ that $\varphi(n, p) \in A_p$. Similarly, a point $p \in D$ is called Poisson negatively stable if for each neighborhoods A_p and for every positive number T one can specify such number $n \leq -T$ such that $\varphi(n, p) \in A_p$. And, finally, the Poisson stable point, both positively and negatively, is called Poisson stable [2,5,13]. This is equivalent to the fact that the motion $\varphi(n, p)$ intersects an arbitrary neighborhood A_p for infinitely large n.

Theorem 4. If a point $p \in D$ is positively Poisson stable, then each point of the trajectory, described by the motion $\varphi(n, p)$, is also positively Poisson stable. A similar statement holds for points that are negatively Poisson stable.

Proof. First of all, we note that a point p is positively Poisson stable if and only if there exists such a sequence $n_1, n_2, \dots, n_k, \dots$, $\lim_{k\to\infty} n_k = +\infty$

$$\lim_{k\to\infty} \varphi(n_k, p) = p. \tag{12}$$

Indeed, the definition of positive stability follows immediately from the equality (12). Conversely, if positive stability holds, there exists a sequence of positive numbers $\varepsilon_1, \varepsilon_2, \dots, \varepsilon_k, \dots$, $\lim_{k\to\infty} \varepsilon_k = 0$ and positive integers $n_k > k$, что $d\big(p, \varphi(n_k, p)\big) < \varepsilon_k$, whence follows (12).

Suppose now that p is the arbitrary point of trajectory of the function $\varphi(n, p)$. Then, by virtue of property 1) of definition 2, the equality $\lim\limits_{k\to\infty} \varphi(n + n_k, p) = \varphi(n, p)$ takes place for all values $n \in Z$.

By virtue of Theorem 4, it is easy to see that in the future it makes sense to speak of positive stability and negative stability and Poisson stability not of individual points, but of motions and trajectories of dynamical systems.

К.Б. Бапаев[1], Г.Қ. Василина[1,2]

[1]Математика және математикалық моделдеу институты, Алматы, Қазақстан;
[2]Алматы энергетика және байланыс университеті, Алматы, Қазақстан

ДИНАМИКАЛЫҚ-АЙЫРЫМДЫҚ ЖҮЙЕЛЕРДІҢ ЛАГРАНЖ ЖӘНЕ ПУАССОН БОЙЫНША ОРНЫҚТЫЛЫҒЫ ТУРАЛЫ

Аннотация. Нақты динамикалық-айырымдық жүйе қарастырылды. Оның шешімдерінің шексіз кеңеюі жағдайы зерттелді. Динамикалық-айырымдық жүйенің шешімдерінің оңға қарай шексіз кеңеюі осы жүйенің шешімінің Ляпунов бойынша орнықтылығы үшін қажетті шарты болып табылады. Ляпуновтың функциясына ұқсас функцияларды қолдану арқылы біз динамикалық-айырымдық жүйенің шешімдерінің шексіз кеңеюі үшін жеткілікті шарттары алынды. Лагранж бойынша орнықтылығының және Пуассон бойынша орнықтылығының ұғымдары енгізілді. Ляпуновтың функциялары мен Лагранж бойынша орнықтылығы арасындағы қатынастар зерттелді. Ляпуновтың екінші әдісінің дискретті аналогын қолдану арқылы динамикалық-айырымдық жүйенің шешімінің Лагранж бойынша орнықтылығы үшін қажетті және жеткілікті шарттар алынды. Дискретті оператор құрылатын динамикалық-айырымдық жүйе қарастырылды. Құрылған оператордың көмегімен жүйенің шешімдерінің Пуассон бойынша орнықтылығы зерттелді.

Түйін сөздер: динамикалық-айырымдық жүйе, шексіз кеңею, Ляпуновтың функциялары, Лагранж бойынша орнықтылық, Пуассон бойынша орнықтылық.

К.Б. Бапаев[1], Г.К. Василина[1,2]

[1]Институт математики и математического моделирования, Алматы, Казахстан
[2]Алматинский университет энергетики и связи, Алматы, Казахстан

ОБ УСТОЙЧИВОСТИ РАЗНОСТНО-ДИНАМИЧЕСКИХ СИСТЕМ ПО ЛАГРАНЖУ И ПО ПУАССОНУ

Аннотация. Рассматривается действительная разностно-динамическая система для которой исследуется случай неограниченной продолжаемости решений. Неограниченная продолжаемость вправо решений разностно-динамической системы является необходимым условием устойчивости в смысле Ляпунова решений этой системы. Используя функции, аналогичные функциям Ляпунова, получены достаточные условия неограниченной продолжаемости решений разностно-динамической системы. Введены понятия устойчивости по Лагранжу и устойчивости по Пуассону. Исследуются соотношения между функциями Ляпунова и устойчивостью по Лагранжу (ограниченностью решений). С помощью дискретного аналога второго метода Ляпунова получены необходимые и достаточные условия устойчивости решения по Лагранжу разностно-динамической системы. Рассматривается разностно-динамическая система для которой строится дискретный оператор, с помощью которой исследуется устойчивость по Пуассону решений системы.

Ключевые слова: разностно-динамическая система, неограниченная продолжаемость, функции Ляпунова, устойчивость по Лагранжу, устойчивость по Пуассону.

Information about authors.

Bapaev K.B. - Institute of Mathematics and Mathematical Modeling, Almaty, Kazakhstan, https://orcid.org/0000-0002-7931-6985, bapaev41@bk.ru;

Vassilina G.K. - Institute of Mathematics and Mathematical Modeling, Almaty University of Energy and Communications, Almaty, Kazakhstan, https://orcid.org/0000-0003-2504-9620, v_gulmira@mail.ru.

REFERENCES

[1] Stepanov V.V. Course of differential equations. - Moscow: Fizmatgiz, 1959. 468 p.

[2] Nemytsky V.V., Stepanov V.V. Qualitative theory of differential equations. Moscow-Leningrad: State publishing house of technical and theoretical literature, 1949. - 545 p.

[3] Results of science and technology. Modern problems of mathematics. Dynamic systems. Vol. 1,2. 1985.

[4] Zhumatov S.S. Absolute stability of a program manifold of non-autonomous basic control systems // News of the National academy of sciences of the Republic of Kazakhstan. Series physic-mathematical. ISSN 1991-346X. Volume 6, Number 322 (2018). – P. 37-43. https://doi.org/10.32014/2018.2518-1726.15

[5]Yoshizava T. Lyapunovs function and boundedness of solutions. 1959. P. 95-142.

[6] Poincaré A. Selected Works. Vol.1. Moscow: Nauka, 1971.

[7] Birkhoff J. Dynamic Systems. Moscow-Leningrad, 1941.

[8] Baer G. Almost periodic functions. Moscow: Gostekhizdat, 1934.

[9] Bebutov M.V. On dynamic systems in the space of continuous functions // Bulletin of Moscow University. Mathematics. 1941. Vol. 2, № 5. P. 1-52.

[10] Krasnoselsky M.A. Shift operator along trajectories of differential equations. Moscow: Nauka, 1966.

[11] Sibirskiy K.S. Introduction to topological dynamics. Kishinev, 1970.

[12] Bapaev K.B., Slamzhanova S.S. On stability and bifurcation of resonant difference-dynamic system // News of the national academy of sciences of the republic of Kazakhstan. Series physico-mathematical. 2015. № 4. P. 250-255.

[13] Aleksandrov PS Introduction to the general theory of sets and functions. - Moscow-Leningrad: State publishing house of technical and theoretical literature, 1948.

N E W S
OF THE NATIONAL ACADEMY OF SCIENCES OF THE REPUBLIC OF KAZAKHSTAN
PHYSICO-MATHEMATICAL SERIES
ISSN 1991-346X **https://doi.org/10.32014/2019.2518-1726.67**
Volume 5, Number 327 (2019), 126 – 132

UDC 538.972

G.A. Kaptagay[1], N.O. Koilyk[2], A.M. Tatenov[1], N.A. Sandibaeva[1], A.A. Dutbayeva[1]

[1]Kazakh national women's teacher training university, Almaty, Kazakhstan;
[2]National center of development of qualification «Orleu», Almaty, Kazakhstan
gulbanu.kaptagay@gmail.ru, nurgali.koilyk@mail.ru, tatenov_adambek@mail.ru,
nazira.s@mail.ru, 5678arda@gmail.com

EVALUATION OF ENERGY EFFICIENCY OF THE NITROGEN-DOPED Co_3O_4 (100) SURFACE FOR WATER DISSOCIATION

Abstract: Co_3O_4 is easily available and thermodynamic stable oxide in a wide interval of temperatures and conditions with rich concentration of oxygen. Also Co_3O_4 among oxides of transition metals – useful materials for gas sensors, storage systems of energy and materials of anodes of lithium - ion batteries, zink-air batteriesand other energy applications.

For enhancing energy efficiency of decomposition of water molecules on cobalt oxide surfaces was studied effect of various dopants. One of the promising doping materials for Co_3O_4 is nitrogen.

In paper we report the results of theoretical investigations of water adsorption on undoped and nitrogen-doped Co_3O_4 (100) surface by means of the plane-wave periodic density functional theory (DFT) calculations combined with the Hubbard-*U* approach and statistical thermodynamics.

We discuss the effect of nitrogen-doping of the Co_3O_4 (100) surface and calculated oxygen evolution reaction overpotential based on the Gibbs free-energy diagram of undoped and N-doped surfaces. Results of calculations of the overpotentials of water molecule decomposition on the nitrogen-doped (100) surface of cobaltum oxide demonstrate generally the decreased values in comparison withundoped surface with some deviation on considered steps of decomposition.

Keywords: Co_3O_4, spinel oxide, water sorption, free-energy diagram, surface.

1. Introduction

Nowadays, we know that transition to "green" energy perspectival in ecological and economical view. Advantages of technologies of renewable energy make these problems priority for the scientifically research. So, its lead to intensive development of researches for alternative energy resources.

Today, all the talk about hydrogen energy or even a hydrogen economy is the use of hydrogen as the main energy source for various devices.

One of the methods for producing hydrogen is electrolysis. This is a much more expensive way than getting from hydrocarbons, but it is without thermal pollution.

Consuming growth not - renewable fossil energy resources of which "thermal pollution", bursts in the atmosphere of products of burning and fast exhaustion of power sources is result do perspective creation of highly effective technologies of use of renewables that first of all includes development of methods of conversion of solar energy.

Reaction of dissociation ofwater takes place with energy absorption as a result of which the free energy of Gibbs increases by 237 kJ of mole^{-1}. This additional energy necessary for photocatalytic and photoelectrochemical decomposition of water is provided by means of energy of sunlight. For this purpose forelectrode material of electrolyze process used different materials.

Co_3O_4 is easily available and thermodynamic stable oxide in a wide interval of temperatures and conditions with rich concentration of oxygen. Crystal Co_3O_4 has structure of spinel (spatial group) with the semi-filled sites in an octahedral environment of Co^{3+}, and cobalt ions in a tetrahedral environment of Co^{2+}.

Also Co_3O_4among oxides of transition metals – useful materials for gas sensors [1,2], storage systems of energy and materials of anodes of lithium - ion batteries [3],zink-air batteries [4] and other energy applications.

For enhancing energy efficiency of decomposition of water molecules oncobalt oxidesurfaces studied effect of various dopants. One of the promising doping materials for Co_3O_4 is nitrogen. Xu et.al in their experimental work discuss production of N-doped Co_3O_4 nanosheets [5].

2. Method and Surface Model

2.1 Computational Methodology and Thermodynamic Description

The calculations have been performed using the *ab initio* plane wave computer code VASP [6] using the the projector-augmented plane-wave (PAW) method [7] in conjunction with PBE (Perdew – Burke - Ernzerhof) GGA exchange-correlation functional [8]. The standard Monkhorst-Pack grid with the $4 \times 4 \times 4$ sampling mesh for the bulk calculations and the $2 \times 2 \times 2$ for the slab calculations was used [9] along with the cutoff energy of 550eV and the Methfessel-Paxton [10] smearing with σ=0.1 eV. In performed calculations for the periodic slab model (infinite in two dimensions) the positions of all ions were fully relaxed, to render the net forces acting upon the ions smaller than 1×10^{-2}eV ·$Å^{-1}$. In order to avoid the interaction between periodically translated images along the direction normal to the surface, we used vacuum gap of 12 Å. As known from our theoretical researches [11] (100) plane was modeled as shown in figure 1.

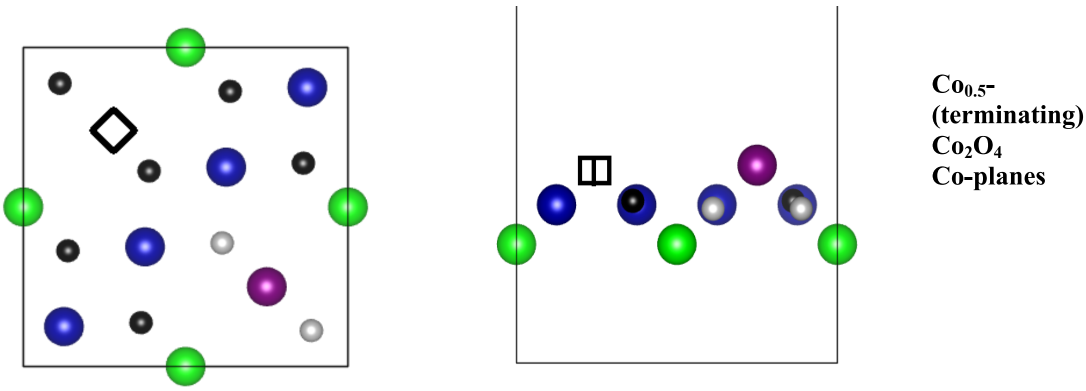

a b

Figure 1 - Co_3O_4 (100) $Co_{0.5}$-terminated surface top view (a) and side view (b). Color coding: Co^{o}_{5c}, blue;Co^{T}_{4c}, green;Co^{T}_{2c} ,purple;O_{3c} ,black O_{4c}, grey; The empty cube indicates Co site.

There are four coordinatively unsaturated 5-fold Co^{o}_{5c}, two recessed, fully coordinated 4-fold Co^{T}_{4c}, and two protruding 2-fold Co^{T}_{2c}. The distance between the nearest Co^{o} ions in a slab is 2.91 Å and the Co^{T} ions are separated by 7.63 Å . There are observed two types of oxygen ions: the 4-fold O_{4c} and 3-fold O_{3c}.

Results.

Water adsorption

In the present study, we studied water dissociation and adsorption process on the top of $Co^{T}_{2c}$and Co^{O}_{5c} sites on the pure and N-doped Co_3O_4(100) surface.

The adsorption and dissociation energy of water molecules are calculated as

$\Delta E_{ads} = E_{adsorbate/surface} - (E_{adsorbate} + E_{surface})$ (1)

where$E_{adsorbate/surface}$, $E_{adsorbate}$ and $E_{surface}$ correspond to the total energies of a system formed by the adsorbate at the surface, the isolated adsorbate molecule in gas phase and the bare surface, respectively.Oxygen atoms substituted with nitrogen atoms in four concentrations. There are four concentrations – 1, 2, 4 and 8 N per 32(O+N) atoms. Respectively, nitrogen-doped Co_3O_4(100) $Co_{0.5}$-terminated surfaces with four concentration of nitrogen denoted as Configuration 1 (configuration with 12,5% concentration), Configuration 2 (configuration with 25% concentration), Configuration 3 (configuration with 50% concentration), Configuration 4 (nanorod).

In table 1 given basic characteristics of water adsorption process on undoped and nitrogen–doped Co_3O_4(100) $Co_{0.5}$-terminated surface.

Table 1 - Basic characteristics of water adsorption process on undoped and doped Co_3O_4(100) $Co_{0.5}$-terminated surfaces with different concentration of nitrogen.$\Delta E_{ads}$is adsorption energy; *d* dissociative mode; *a* associative mode; $d_{Co-O(H2)}$-bond length in angstroms

	Adsorption Center Co_{2c}^{T}			**Adsorption Center Co_{5c}^{o}**		
	$\Delta E_{ads}/eV$	Adsorption type	$d_{Co-O(H_2O)}$	$\Delta E_{ads}/eV$	Adsorption Type	$d_{Co-O(H_2O)}$
perfect	-0.43	d	1.84	-0.47	a	2.1
Conf.1	-0.58	a	2.07	-0.83	a	2.04
Conf.2	-0.39	a	2.02	-0.45	a	2.03
Conf.3	-1.12	d	1.90	-0.28	a	1.98
Conf.4	-0.75	d	1.98	-1.41	d	1.95

The binding energies of O, OH and OOH (ΔE_O, ΔE_{OH}, ΔE_{OOH}) and the bond lengths on the pure and N-doped Co_3O_4(100) $Co_{0.5}$-terminated surface are given in table 2. We observed that the binding energies of O*, OH* and OOH* on the cobalt oxide surface, calculated with PBE+*U*, scale according to the relation $\Delta E_{OOH*} = \Delta E_{OH*} + 3.2$ within $\pm$0.4 eV as was shown in ref.[12,13]. In table 2 given the binding energies of O, OH and OOH and bond length on the undoped and N-doped Co_3O_4(100) surface.

Table 2 -The binding energies of O, OH and OOH ($\Delta E_O, \Delta E_{OH}, \Delta E_{OOH}$ in eV) and bond length on the undoped and N-doped Co_3O_4(100) $Co_{0.5}$-terminated surfaces.$\boldsymbol{d_x}$-is bond length in Å, * denotes adsorbate atom.

	ΔE_O	d_{Co-O}	ΔE_{OH}	$d_{Co-O(H)}$ $d_{O(*)-H(*)}$	ΔE_{OOH}	d_{Co-O} $d_{O(*)-H(*)}$ $d_{O(*)-O(*)}$	ΔE_O	d_{Co-O}	ΔE_{OH}	$d_{Co-O(H)}$ $d_{O(*)-H(*)}$	ΔE_{OOH}	d_{Co-O} $d_{O(*)-H(*)}$ $d_{O(*)-O(*)}$
	Adsorption Center Co_{2c}^{T}						**Adsorption Center Co_{5c}^{o}**					
Un-doped	2.23	1.59	-0.11	1.78 0.97	3.03	1.81 0.98 1.47	2.29	1.86	- 0.09	1.79 0.97	3.26	2.08 0.98 1.45
Conf.1	1.65	1.6	0.25	1.77 0.97	2.69	1.79 0.96 1.48	2.69	1.85	0.15	1.80 0.97	3.33	2.09 0.98 1.47
Conf.2	1.90	1.58	0.42	1.76 0.90	3.26	1.76 0.94 1.52	2.98	1.83	0.29	1.76 0.93	3.90	2.03 0.92 1.41
Conf.3	1.56	1.48	0.41	1.70 0.92	2.76	1.79 0.90 1.43	2.87	1.78	0.40	1.82 0.91	2.55	1.98 0.93 1.39
Conf.4	1.94	1.50	1.08	1.68 0.89	2.61	1.72 0.87 1.35	2.82	1.75	1.08	1.75 0.93	2.71	2.07 0.91 1.47

Calculated values of theoverpotentials for each step of water molecule decomposition along the reaction pathway using the computational standard hydrogen electrode (SHE) allowing us to replace a proton and an electron with the half a hydrogen molecule at V=0 V vs SHE according to theory [12,13]for five configurations presented in table 3. The theoretical overpotentialis found according to the standard relation

$$\boldsymbol{\eta}=\max[\Delta G_i]/e - 1.23[V] \tag{2}$$

Fig.3 presents the free energy changes of reactions of adsorption of water molecule and intermediate products of dissociation based on DFT+*U* calculations of adsorbed intermediates on the perfect and fluorine-doped Co_3O_4(100) surface at 0.2ML water coverage.

Undoped surface

a) Co^{T}_{2c}site

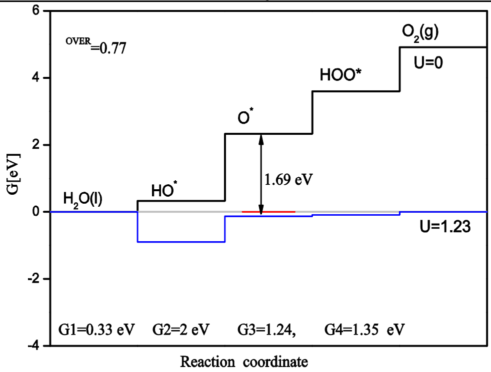

b) Co^{O}_{5c} site

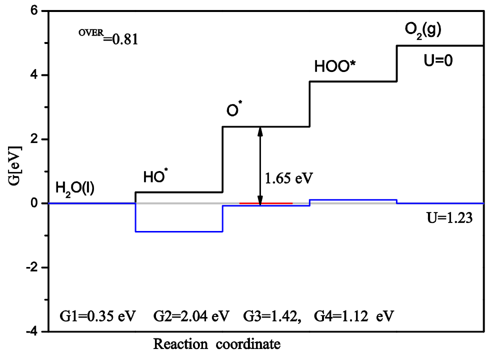

Configuration 1

c) Co^{T}_{2c}site

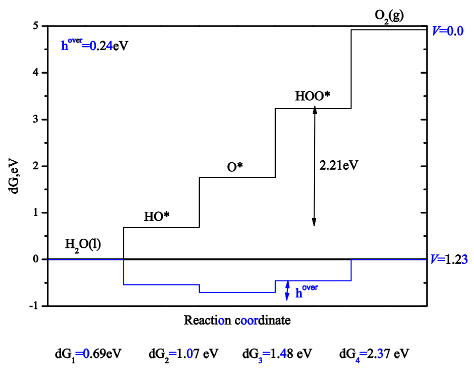

d)Co^{O}_{5c} site

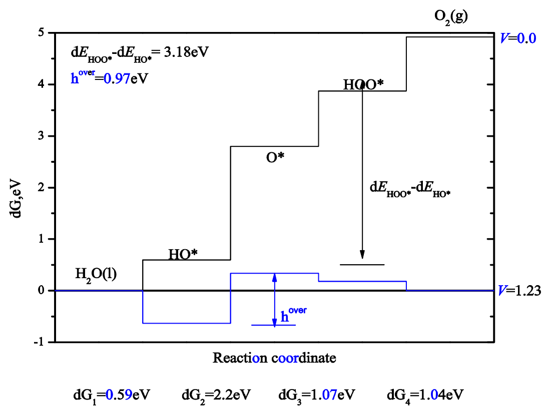

Configuration 2

e) Co^{T}_{2c}site

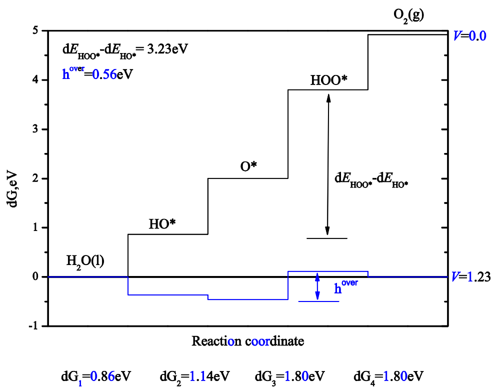

f)Co^{O}_{5c} site

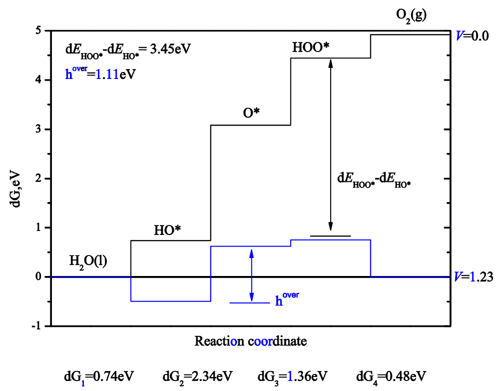

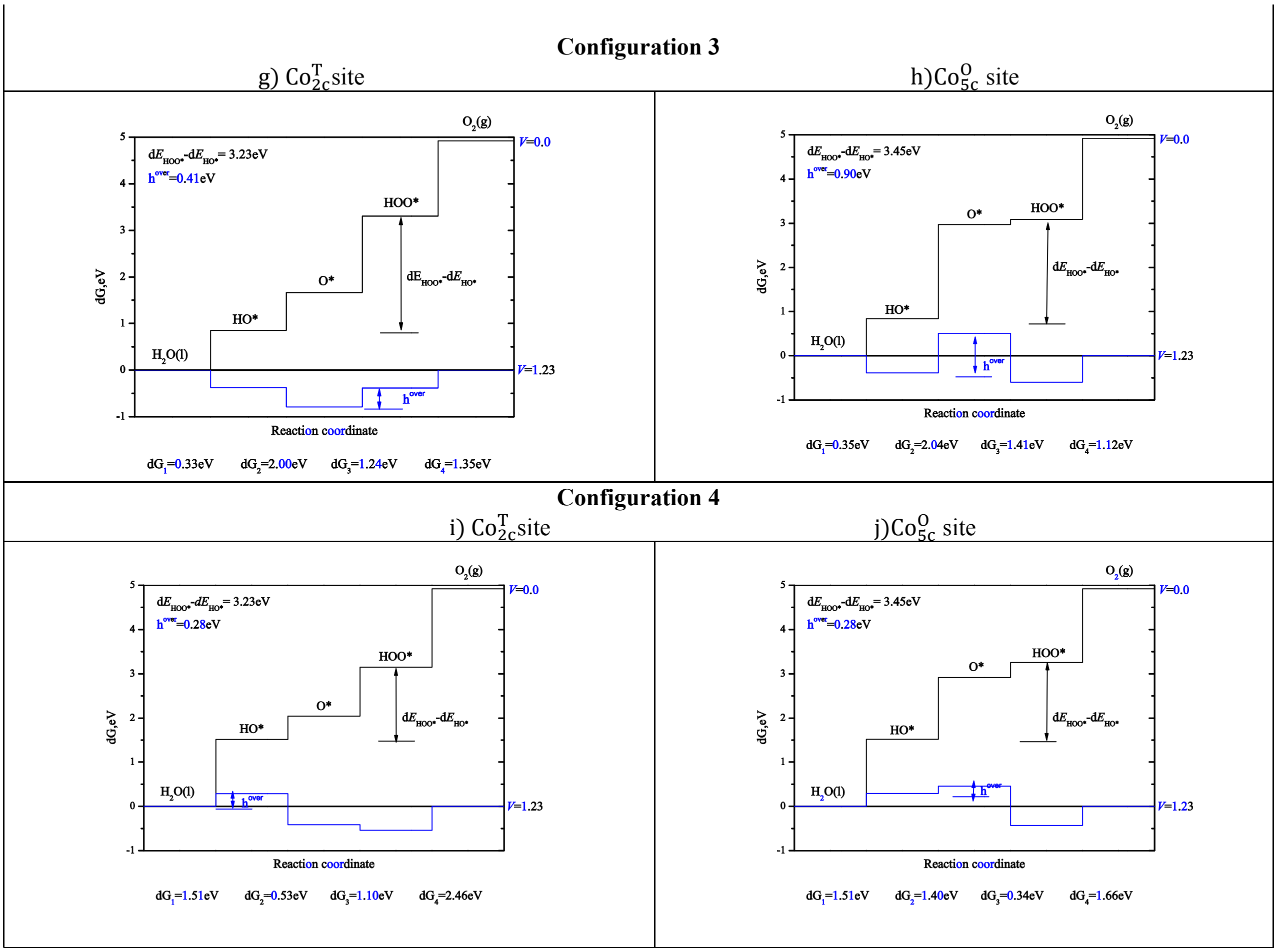

Figure 3 - Free-energy diagram at pH=0 and T=298 K for the four steps of the OER at V=0 and V=1.23 V. Results for theCo_{2c}^{T} and Co_{5c}^{O} sites at 0.2ML water coverage for undoped and 4 Configurations of N-doped surfaces shown; For each case the highest free-energy change is indicated

The calculations suggest that the theoretical overpotentials for water adsorption on the pure surface 0.77 and 0.81 V, respectively Co_{2c}^{T} and Co_{5c}^{O}sites. N-doped surfaces demonstrate at Co_{2c}^{T} site decreasing of overpotential (0.56-0.24 V)in comparisonCo_{2c}^{T}site inundoped Co_3O_4surface. For Co_{5c}^{O} site on doped surface values of overpotentialexihibited are nearly the same values as on clean surface (0.90-1.11 V) except for Configuration 4 (0.28 V). In this case of Co_{2c}^{T} site on doped surface reduced values observed with the OOH^* formation as the determining step except Configuration 4.

Conclusion

It is seen from the figures 3 that an electron charge accumulation lead to strongly reducing overpotentials for Co_{2c}^{T} site in connection with the redistribution of the electron charge in the local environment of the impurity nitrogen atoms. When nitrogenis introduced, most of the charge is distributed to neighboring cobalt ions. In addition, the introduction of nitrogen leads to the polarization of neighboring ions.

The analyzing electron redistribution on the surface by the introducing nitrogen dopants will be described in our forthcoming paper.

Г.Ә.Қаптағай[1], Н.О.Қойлық[2], А.М.Татенов[1], Н.А.Сандибаева[1], А.А.Дутбаева[1]

[1]Қазақ ұлттық қыздар педагогикалық университеті, Алматы, Қазақстан;
[2]«Өрлеу» ұлттық біліктілік көтеру орталығы, Алматы, Қазақстан

АЗОТПЕН ҚОСПАЛАНҒАН Co_3O_4 (100) БЕТІНІҢ СУДЫҢ ДИССОЦИЯЛАНУЫНА ЭНЕРГЕТИКАЛЫҚ ТИІМДІЛІГІН БАҒАЛАУ

Аннотация: Мақалада Хаббард-U жуықтауымен және статистикалық термодинамикамен кіріктірілген тығыздық функционалы теориясының (ТФП) шеңберінде таза және азот қоспаланған Co_3O_4 (100) бетіндегі судың адсорбциясын теориялық зерттеудің нәтижелері берілген. Азот қоспасы есебінен пайда болатын беттің каталитикалық қасиеттерінің өзгеру әсерлері талқыланды және таза және қоспаланған пластинадағы азотқа Гиббсеркін энергиясының схемасы негізінде асқын потенциал есептелген.

Co_3O_4 оксиді температурамен оттегінің бай концентрациясы жағдайындағы кең интервалда қол жетімді және термодинамикалық тұрақты. Сондай-ақ, Co_3O_4 ауыспалы металдар оксидтерінің арасында – газ сенсорларына, энергия сақтау жүйелеріне арналған тиімді материал және литий-ионды аккумуляторларда, мырыш батареяларынан және басқада энергетикалық қолданыстағы анодтық материалдар ретінде кеңінен қолданылады.

Кобальт оксидінің бетінде су молекулаларының ыдырауының энергетикалық тиімділігі нарттыру үшін әртүрлі қоспалардың әсері зерттелген. Co_3O_4 үшін перспективалы қоспалаушы материалдардың бірі-азот.

Мақалада Хаббард-U тәсілі мен және статистикалық термодинамика мен үйлескен тығыздық функционалының жазық толқындық теориясын (DFT) есептеу көмегімен таза және азотпен қоспаланған Co_3O_4 (100) беттеріндегі су адсорбциясын теориялық зерттеулердің нәтижелері келтіріледі.

Co_3O_4 (100) бетін азотпен қоспалаудың және қоспаланған беттердің Гиббсеркін энергия диаграммасының негізінде оттегінің бөліну реакциясының есепті касқын кернеуінің әсері талқыланады. Кобальт оксидінің азотпен легирленге (100) бетінде су молекулаларының ыдырауының асқын кернеулерін есептеу нәтижелері талданатын ыдырау сатыларында кейбір ауытқулармен қоспаланған беттермен салыстырғанда жалпы төмен мәндерді көрсетеді.

Түйін сөздер: Co_3O_4, оксидшпинелі, суадсорбциясы, еркінэнергиядиаграммасы, бет

Г.А.Каптагай[1], Н.О.Койлык[2], А.М.Татенов[1], Н.А.Сандибаева[1], А.А.Дутбаева[1]

[1]Казахский национальный женский педагогический университет, Алматы, Казахстан;
[2]Национальный центр повышения квалификаций «Орлеу», Алматы, Казахстан

ОЦЕНКА ЭНЕРГЕТИЧЕСКОЙ ЭФФЕКТИВНОСТИ АЗОТ ДОПИРОВАННОЙ ПОВЕРХНОСТИ (100) Co_3O_4 ДЛЯ РАСЩЕПЛЕНИЯ ВОДЫ

Аннотация: В статье представлены результаты теоретического исследования адсорбции воды на чистой и азотдопированной пластине Co_3O_4 (100) в рамках теории функционала плотности (ТФП) комбинированной с приближением Хаббарда-U и статистической термодинамикой. Обсуждены эффекты изменения каталитических свойств пластины, возникающие за счет примеси азота и рассчитаны избыточные потенциалы на основе схемы свободной энергии Гиббса на чистой и азот допированной пластине.

Co_3O_4 является легко доступным и термодинамически стабильным оксидом в широком интервале температур и условий с богатой концентрацией кислорода. Также Co_3O_4 среди оксидов переходных металлов - полезные материалы для газовых сенсоров, систем хранения энергии и материалы анодов из литий-ионных аккумуляторов, цинковых батарей и других энергетических применений.

Для повышения энергетической эффективности разложения молекул воды на поверхности оксида кобальта было изучено влияние различных легирующих примесей. Одним из перспективных легирующих материалов для Co_3O_4 является азот.

В статье приводятся результаты теоретических исследований адсорбции воды на нелегированной и легированной азотом поверхности Co_3O_4 (100) с помощью расчетов плоской волновой теории функционала плотности (DFT) в сочетании с подходом Хаббарда-U и статистической термодинамикой.

Обсуждается влияние легирования азотом поверхности Co_3O_4 (100) и расчетного перенапряжения реакции выделения кислорода на основе диаграммы свободной энергии Гиббса нелегированных и N-допированных поверхностей. Результаты расчетов перенапряжений разложения молекул воды на легированной азотом (100) поверхности оксида кобальта демонстрируют в целом пониженные значения по сравнению с нелегированной поверхностью с некоторым отклонением на анализируемых стадиях разложения.

Ключевые слова: Co_3O_4, шпинель оксида, водная адсорбция, диаграмма свободной энергии, поверхность

ACKNOWLEDGEMENTS

The project Nr. AP05131211 "First Principles Investigation on Catalytic Properties of N-doped Co3O4" is supported by the Ministry of Education and Science of the Republic of Kazakhstan within the framework of the grant funding for scientific and (or) scientific and technical research for 2018-2020. The authors thank Y.Mastrikov for fruitful discussions and valuable suggestions.

REFERENCES

[1] Batzill M., Diebold U. Surface studies of gas sensing metal oxides // Phys. Chem. Chem. Phys. Vol.9, №19. 2007. P.2307-2318. https://doi.org/10.1039/B617710G

[2] Sassykova L.R., Nalibayeva A. Technology of synthesis of effective catalysts for neutralization of waste gases of the vehiciles and industry // News of NAS RK. Series chemistry-technology. Vol.1, №421. 2017. P.9-15. ISSN 2224-5286.

[3] Zhigang Z., Lianlian G.,Yanfeng D., Jinping Z., Wu Z. Embedding Co_3O_4 nanoparticles into graphene nanoscrolls as anode for lithium ion batteries with superior capacity and outstanding cycling stability // Progress in Natural Science: Materials International. Vol.28, №2. 2018. P.212-217. https://doi.org/10.1016/j.pnsc.2018.02.005

[4] Tomon C., Sarawutanukul S., DuangdangchoteS., Krittayavathananon A., Sawangphruk M. Photoactive Zn–air batteries using spinel-type cobalt oxide as a bifunctional photocatalyst at the air cathode //Chem. Commun.,Vol.55. 2019. P.5855-5858. https://doi.org/10.1039/C9CC01876J

[5] Xu, L., Wang, Z., Wang, J., Xiao, Z., Huang, X., Liu, Z., & Wang, S. N-doped nanoporous Co_3O_4nanosheets with oxygen vacancies as oxygen evolving electrocatalysts // Nanotechnology, Vol.28. №16. 2017. P.165402-165409.https://doi.org/10.1088/1361-6528/aa6381

[6] Kresse G., Furthmüller Efficient iterative schemes for ab initio total-energy calculations using a plane-wave basis set // Physical Review B - Condensed Matter and Materials Physics, Vol.54. №16. 1996. P.11169-11186.https://doi.org/ 10.1103/PhysRevB.54.11169

[7] P.E. Bloch, Projector augmented-wave method // Phys. Rev., Vol.50. №24. 1994. P.17953-17959. https://doi.org/10.1103/PhysRevB.50.17953

[8] J.P. Perdew, K. Burke, M. Ernzerhof, Generalized Gradient Approximation Made Simple //Phys. Rev. Lett., Vol.77. №18. 1996. P.3865-3868.https://doi.org/10.1103/PhysRevLett.77.3865

[9] H.J.Monkhorst, J. D. Pack,Special points for Brillouin-zone integrations // Phys. Rev. B Vol.13. №12. 1976. P.5188-5192.https://doi.org/10.1103/PhysRevB.13.5188

[10] M. Methfessel, A. T. Paxton, High-precision sampling for Brillouin-zone integration in metals // Phys. Rev. Vol.40. №6. 1989. P.3616-3621.https://doi.org/10.1103/PhysRevB.40.3616

[11] Kaptagay G.A., Inerbaev T.M., MastrikovYu.A., Kotomin E.A.,Akilbekov A.T. Water interaction with perfect and fluorine-doped Co_3O_4 (100) surface // Solid State Ionics. Vol.277. 2015. P.77-82.https://doi.org/10.1016/j.ssi.2015.03.012

[12] M.Garcia-Mota, M.Bajdich, V.Viswanathan, A.Vojvodic, A.T. Bell and Jens K. Norskov, J. Importance of Correlation in Determining Electrocatalytic Oxygen Evolution Activity on Cobalt Oxides // Phys. Chem. C. Vol.116. №32. 2012. P.21077-21082. https://doi.org/10.1021/jp306303y

[13] I. C. Man, H.-Y. Su, F. Calle-Vallejo, H. A. Hansen, J. I. Martínez, N. G. Inoglu, J. Kitchin, T. F. Jaramillo, Jens K. Nørskov, and J. Rossmeisl,Universality in Oxygen Evolution Electrocatalysis on Oxide Surfaces // Chem. Cat. Chem. Vol.3. №7. –2011. –P.1159-1165.https://doi.org/10.1002/cctc.201000397

[14] Mamyrbayev O. Zh., Shayakhmetova A. S., Seisenbekova P. B. The methodology of creating an intellectual environment of increasing the competence of students based on a bayesian approach//News of the National academy of sciences of the Republic of Kazakhstan. Series physico-mathematical. 2019. №4 (326). P. 50-58. https://doi.org/10.32014/2019.2518-1726.43

МАЗМҰНЫ

СОДЕРЖАНИЕ

CONTENTS

Publication Ethics and Publication Malpractice in the journals of the National Academy of Sciences of the Republic of Kazakhstan

For information on Ethics in publishing and Ethical guidelines for journal publication see http://www.elsevier.com/publishingethics and http://www.elsevier.com/journal-authors/ethics.

Submission of an article to the National Academy of Sciences of the Republic of Kazakhstan implies that the described work has not been published previously (except in the form of an abstract or as part of a published lecture or academic thesis or as an electronic preprint, see http://www.elsevier.com/postingpolicy), that it is not under consideration for publication elsewhere, that its publication is approved by all authors and tacitly or explicitly by the responsible authorities where the work was carried out, and that, if accepted, it will not be published elsewhere in the same form, in English or in any other language, including electronically without the written consent of the copyright-holder. In particular, translations into English of papers already published in another language are not accepted.

No other forms of scientific misconduct are allowed, such as plagiarism, falsification, fraudulent data, incorrect interpretation of other works, incorrect citations, etc. The National Academy of Sciences of the Republic of Kazakhstan follows the Code of Conduct of the Committee on Publication Ethics (COPE), and follows the COPE Flowcharts for Resolving Cases of Suspected Misconduct (http://publicationethics.org/files/u2/New_Code.pdf). To verify originality, your article may be checked by the Cross Check originality detection service http://www.elsevier.com/editors/plagdetect.

The authors are obliged to participate in peer review process and be ready to provide corrections, clarifications, retractions and apologies when needed. All authors of a paper should have significantly contributed to the research.

The reviewers should provide objective judgments and should point out relevant published works which are not yet cited. Reviewed articles should be treated confidentially. The reviewers will be chosen in such a way that there is no conflict of interests with respect to the research, the authors and/or the research funders.

The editors have complete responsibility and authority to reject or accept a paper, and they will only accept a paper when reasonably certain. They will preserve anonymity of reviewers and promote publication of corrections, clarifications, retractions and apologies when needed. The acceptance of a paper automatically implies the copyright transfer to the National Academy of Sciences of the Republic of Kazakhstan.

The Editorial Board of the National Academy of Sciences of the Republic of Kazakhstan will monitor and safeguard publishing ethics.

Правила оформления статьи для публикации в журнале смотреть на сайтах:

www:nauka-nanrk.kz

http://physics-mathematics.kz/index.php/en/archive

ISSN 2518-1726 (Online), ISSN 1991-346X (Print)

Редакторы *М. С. Ахметова, Т.А. Апендиев, Д.С. Аленов*
Верстка на компьютере *А.М. Кульгинбаевой*

Подписано в печать 10.10.2019.
Формат 60x881/8. Бумага офсетная. Печать – ризограф.
9,6 п.л. Тираж 300. Заказ 5.

Национальная академия наук РК
050010, Алматы, ул. Шевченко, 28, т. 272-13-18, 272-13-19